

*THERMODYNAMIC AND ENVIRONMENTAL
COMPARISON OF R744 BOOSTER
SUPERMARKET REFRIGERATION SYSTEMS
OPERATING IN SOUTHERN EUROPE*



Paride Gullo

Polytechnic Department of Engineering and Architecture

University of Udine

This dissertation is submitted for the degree of Doctor of Philosophy (Title of
“DOCTOR EUROPÆUS”) in

Environmental and Energy Engineering Science - XXIX Cycle

December 2016

Ph.D. Board

Prof. Judith Evans	REFEREE
Dr. Yunting T. Ge	REFEREE
Prof. Giulio Croce	MEMBER OF FINAL COMMISSION
Dr. Samer Sawalha	MEMBER OF FINAL COMMISSION
Prof. Claudio Zilio	MEMBER OF FINAL COMMISSION

To my family

In memory of Valeria Solesin and Giulio Regeni

“...esser stronzi è dono di pochi
farlo apposta è roba da idioti...”

Author's email addresses: rockinpeace86@gmail.com

Author's web page: www.researchgate.net/profile/Paride_Gullo2

*“...maledetto il giorno in cui mi son fidato di questo paese
lurido, sperduto, imbarazzato, freddo, grigio, solitario, disastro...
...e poi ho visto solo mare, mare, mare, tanto mare
solo acqua tanta nei polmoni che fa male e non riesci a respirare
che ti chiedi i pesci come fanno
ma non lo diranno mai, lo sai...
...ma il sole risorge ogni giorno e ogni giorno che passa diventa un ricordo
giù da questo scoglio, giù nel mare in verticale
giù e poi nuotare, non c'è altro da fare, senza bestemmiare, zitto e non fiatare
tanto l'anima non conta...”*

*“If it cannot be measured, it does not exist;
if it can be measured, it can be improved.”*

*“Understand me. I'm not like an ordinary world.
I have my madness, I live in another dimension and I do not have time for things that
have no soul.”*

DECLARATION

This dissertation is the result of my own work and it was submitted as a partial fulfilment of the requirements for the Ph.D. (Title of “DOCTOR EUROPÆUS”) in Environmental and Energy Engineering Science at University of Udine.

The present study ensues from:

- three-year Ph.D. project carried out from the 1st of January 2014 to the 31st of December 2016 at University of Udine (Polytechnic Department of Engineering and Architecture);
- eight-month external research stay conducted from November 2014 to June 2015 at DTU Technical University of Denmark (Department of Mechanical Engineering) under the supervision of Prof. Brian Elmegaard;
- three-month external research stay fulfilled from January to March 2016 at SINTEF Energy Research (Department of Thermal Energy) under the supervision of Prof. Armin Hafner.

This project was partly funded by the “Fondo Sociale Europeo (FSE) in Friuli Venezia Giulia”.

Paride Gullo

Udine, 22nd of December 2016

ABSTRACT

Supermarket applications are characterized by enormous direct and indirect greenhouse gas emissions. In an attempt to substantially reduce the carbon footprint associated with the food retail industry, carbon dioxide (or R744) seems to be the most suitable long-term working fluid. In fact, R744 possesses a negligible Global Warming Potential (GWP) and advantageous thermo-physical properties, besides being non-toxic, non-flammable, inexpensive and readily available. However, the energy efficiency of the pure R744 (i.e. transcritical R744 or “CO₂ only”) systems still needs to be considerably enhanced when it comes to units featuring the basic architecture and operating in warm regions. The reason for this lies in the occurrence of transcritical operating conditions at which very poor performance can be ascribed to the aforementioned solutions. The full deployment on the part of the commercial refrigeration sector in high ambient temperature countries towards “CO₂ only” systems is also strongly related to the presence of some remaining non-technological barriers.

In this study, the performance of the state-of-the-art arrangements for pure CO₂ supermarket applications was theoretically compared with that of the most currently used solutions (i.e. HFC-based systems). The comparison was based on both energy and environmental assessments. Also, the actual improvement potential achievable by a conventional R744 booster refrigeration configuration, as well as some enhancement strategies were evaluated by applying the advanced exergy analysis. All these assessments were carried out by opting for the typical running modes of retail stores located in Southern Europe. In relation to the studies available in the open literature, this work involved at least four relevant and peculiar scientific merits, such as the application of the multi-ejector concept, the evaluation of the performance of CO₂ refrigeration systems integrated with the air-conditioning (AC) unit, the selection of various warm climate cities and the implementation of the advanced exergy analysis.

It could be concluded that nowadays transcritical R744 ejector supported parallel systems are the most highly efficient and eco-friendly technologies for food retail industry in Mediterranean Europe, being able to successfully replace HFC-based solutions.

Keywords: Advanced exergy analysis, Air-conditioning, CO₂, Multi-ejector, Overfed evaporator, Parallel compression, Transition zone, Warm climates.

SOMMARIO

Le applicazioni commerciali, quali supermercati e centri commerciali, si caratterizzano per notevoli impatti ambientali. La sempre più crescente attenzione nei confronti dell'ambiente, nonché l'adozione di normative sempre più stringenti atte a contrastare i cambiamenti climatici in corso, favoriscono l'utilizzo dell'anidride carbonica (o R744) come unico refrigerante in tali applicazioni. Tale fluido di lavoro rappresenta la più promettente alternativa a lungo termine ai refrigeranti sintetici attualmente largamente usati. Ciò è dovuto al fatto che la CO₂ presenta proprietà termo-fisiche ed ambientali favorevoli, oltre ad essere non tossica, ininfiammabile, economica e facilmente reperibile. D'altro canto, l'efficienza energetica della configurazione base a R744 viene fortemente compromessa ad alte temperature esterne a causa del verificarsi delle condizioni operative transcritiche. Ciò, insieme ad alcune barriere non-tecnologiche ancora persistenti, hanno notevolmente sfavorito la diffusione di tale refrigerante nei supermercati localizzati in climi caldi.

In questo studio le prestazioni delle tecnologie più promettenti per quanto concerne le macchine frigorifere a CO₂ sono state confrontate teoricamente con quelle dei sistemi ad idrofluorocarburi (HFC) attualmente più utilizzati. Tale comparazione ha coinvolto sia gli aspetti energetici che ambientali. Inoltre, il reale potenziale di miglioramento di una soluzione booster a CO₂ è stato investigato per mezzo dell'analisi exergetica avanzata. Tutte le valutazioni sono state implementate considerando le tipiche condizioni operative di un supermercato localizzato nell'Europa mediterranea. In confronto ai lavori attualmente disponibili in letteratura, il seguente studio si caratterizza per almeno quattro rilevanti meriti scientifici, quali: l'applicazione del concetto di multi-eiettori, la valutazione delle prestazioni di un sistema di refrigerazione a CO₂ integrato con l'unità di condizionamento dell'aria (AC), la scelta di località caratterizzate da un clima caldo e l'implementazione dell'analisi exergetica avanzata.

Il presente lavoro ha dimostrato che i sistemi a CO₂ equipaggiati con la tecnologia dei multi-eiettori rappresentano in assoluto la migliore soluzione, sia dal punto di vista energetico che ambientale, per il settore della refrigerazione commerciale dell'Europa Mediterranea.

Keyword: Analisi exergetica avanzata, Climi caldi, CO₂, Compressione parallela, Condizionamento dell'aria, Evaporatori sovralimentati, Multi-eiettori.

ACKNOWLEDGEMENTS

First of all, I need to express my deepest gratitude to my family for supporting and accepting all my decisions. I promise that a day...in the future...I'll be back home!

Special thanks to:

- Alessio and Nicola because the pleasant moments we spent together helped me to go through with/survive against this (mis)adventure;
- Prof. Brian Elmegaard for the fantastic hospitality at DTU Technical University of Denmark, as well as to all the marvellous people met in Denmark!!;
- Prof. Armin Hafner for the magnificent hospitality at SINTEF Energy Research, for the valuable suggestions and especially for having given me the opportunity to continue doing the work that I love.

Last but not least, I will forever be beholden to my “old” friends from Florence!

CONTENTS

1 INTRODUCTION.....	1
1.1 AIM OF THE STUDY	5
1.2 METHODOLOGY.....	6
1.3 CONTRIBUTION TO THE KNOWLEDGE.....	7
1.4 PUBLICATIONS.....	7
1.4.1 <i>Papers for international conferences.....</i>	8
1.4.2 <i>Papers for national journals.....</i>	9
1.4.2 <i>Papers for international journals.....</i>	9
1.5 DISPOSITION OF THE THESIS.....	10
2 CO₂ AS A REFRIGERANT.....	11
2.1 PROPERTIES OF R744.....	11
2.2 EFFECT OF HEAT REJECTION PRESSURE ON PERFORMANCE OF R744 REFRIGERATION SYSTEMS IN TRANSCRITICAL RUNNING MODES	20
2.3 REFERENCE THERMODYNAMIC CYCLE FOR TRANSCRITICAL R744 REFRIGERATION SYSTEMS.....	23
3 SUPERMARKET REFRIGERATION SYSTEMS.....	25
3.1 CURRENT TREND FOR SUPERMARKET APPLICATIONS	27
3.2 TRANSCRITICAL R744 CONFIGURATIONS	32
3.2.1 <i>Conventional transcritical booster system.....</i>	33
3.2.2 <i>Transcritical booster system with dedicated mechanical subcooling.....</i>	35
3.2.3 <i>Transcritical booster system with parallel compression</i>	38
3.2.4 <i>Transcritical booster system with overfed evaporators.....</i>	41
3.2.5 <i>Combined transcritical booster systems</i>	44
3.2.6 <i>Transcritical booster systems with multi-ejector rack.....</i>	47
3.2.7 <i>Fundamental aspects for diffusion of transcritical booster systems in warm regions.....</i>	58
3.3 HIGH GWP-BASED CONFIGURATIONS	60
3.3.1 <i>Cascade system</i>	60
3.3.2 <i>R404A multiplex direct expansion system.....</i>	64
4 METHODS AND MATERIALS	65
4.1 CASE STUDIES.....	65
4.1.1 <i>Operating conditions of conventional booster solutions</i>	65
4.1.2 <i>Operating conditions of solution with dedicated mechanical subcooling</i>	66

4.1.3	<i>Operating conditions of solutions equipped with parallel compression</i>	67
4.1.4	<i>Operating conditions of solutions equipped with overfed evaporators</i>	67
4.1.5	<i>Operating conditions of solutions equipped with multi-ejector</i>	67
4.1.6	<i>Operating conditions of HFC-based systems</i>	69
4.1.7	<i>Common operating conditions</i>	70
4.1.8	<i>Integration with the air conditioning unit</i>	71
4.2	SIMULATION MODELS	72
4.3	THERMODYNAMIC ANALYSES	76
4.3.1	<i>Energy analysis</i>	76
4.3.2	<i>Exergy analysis</i>	77
4.3.3	<i>Advanced exergy analysis</i>	78
4.3.3.1	<i>Endogenous and exogenous exergy destruction</i>	79
4.3.3.2	<i>Avoidable and unavoidable exergy destruction</i>	81
4.3.3.3	<i>Combining of the two splitting approaches</i>	83
4.3.3.4	<i>Interaction among the components</i>	84
4.4	ENVIRONMENTAL ANALYSIS	85
5	RESULTS AND DISCUSSION	87
5.1	RESULTS OF THERMODYNAMIC ANALYSES	87
5.1.1	<i>Results of energy analysis</i>	87
5.1.1.1	<i>Optimal heat rejection pressure for a typical supermarket</i>	88
5.1.1.2	<i>Comparison in terms of COP for a typical supermarket</i>	89
5.1.1.3	<i>Annual energy consumption for a typical supermarket</i>	96
5.1.1.4	<i>Effect of the MT on the annual energy consumption of the booster systems with overfed evaporators</i>	104
5.1.1.5	<i>Effect of the adoption of the de-superheater on the annual energy consumption of some booster systems</i>	105
5.1.1.6	<i>Annual energy consumption of the integrated solution for a typical supermarket</i>	106
5.1.1.7	<i>Influence of size of AC unit, global efficiency of auxiliary compressors and size of supermarket on the annual energy consumption</i>	109
5.1.2	<i>Results of exergy analyses</i>	114
5.1.2.1	<i>Conventional exergy analysis</i>	114
5.1.2.2	<i>Improvement strategy for conventional booster solution</i>	120
5.1.2.3	<i>Proposed layout: multi-ejector based solution</i>	122
5.2	RESULTS OF ENVIRONMENTAL ANALYSIS	123

5.2.1 Results of TEWI for a typical supermarket	123
5.2.2 Results of TEWI of the integrated solution	127
5.3 DISCUSSION	128
6 CONCLUSIONS AND FUTURE WORK	133
6.1 CONCLUSIONS	133
6.2 FUTURE WORK.....	137
REFERENCES	139
APPENDICES	157

LIST OF TABLES

TABLE 2.1 PHYSICAL, ENVIRONMENTAL AND SAFETY PROPERTIES OF THE SELECTED REFRIGERANTS.	13
TABLE 2.2 PERFORMANCE COMPARISON OF VAPOUR COMPRESSION REFRIGERATION SYSTEMS USING R22 AND R744.	14
TABLE 3.1 CONTRIBUTIONS OF EACH COMPONENT TO TOTAL IRREVERSIBILITIES (I.E. EFFICIENCY DEFECT) OCCURRING IN A VAPOUR COMPRESSION REFRIGERATION SYSTEM USING R22 AND R744.	48
TABLE 3.2 ADVANTAGES AND DISADVANTAGES OF TRANSCRITICAL CO ₂ BOOSTER CONFIGURATIONS.	59
TABLE 4.1 INDEPENDENT VARIABLES FOR THE OPTIMIZATION PROCEDURES OF THE R744 BOOSTER REFRIGERATION SYSTEMS UNDER INVESTIGATION.	72
TABLE 4.2 OPERATING ZONES FOR CB.	75
TABLE 4.3 OPERATING ZONES FOR THE OTHER INVESTIGATED BOOSTER SOLUTIONS.	75
TABLE 4.4 ASSUMPTIONS MADE TO IMPLEMENT THE ADVANCED EXERGY ANALYSIS.	80
TABLE 5.1 ANNUAL ENERGY CONSUMPTION [MWH·Y ⁻¹] OF THE INVESTIGATED SYSTEMS IN FIVE WARM CLIMATES IN SOUTHERN EUROPE ($\dot{Q}_{MT,design} = 120$ kW, $\dot{Q}_{LT,design} = 25$ kW).	97
TABLE 5.2 ANNUAL ENERGY CONSUMPTION [MWH·Y ⁻¹] OF DXS+AC AND EJ_OV_AC ($\dot{Q}_{MT,design} = 120$ kW, $\dot{Q}_{LT,design} = 25$ kW).	107
TABLE 5.3 ANNUAL ENERGY CONSUMPTION [MWH·Y ⁻¹] OF DXS+AC, EJ_OV_AC AND “IMPROVED” EJ_OV_AC FOR LF ~ 2.5 AS A FUNCTION OF AC SIZE.	111
TABLE 5.4 ANNUAL ENERGY CONSUMPTION [MWH·Y ⁻¹] OF DXS+AC, EJ_OV_AC AND “IMPROVED” EJ_OV_AC FOR LF ~ 5 AS A FUNCTION OF AC SIZE.	112
TABLE 5.5 ANNUAL ENERGY CONSUMPTION [MWH·Y ⁻¹] OF DXS+AC, EJ_OV_AC AND “IMPROVED” EJ_OV_AC FOR LF = 8 AS A FUNCTION OF AC SIZE.	113
TABLE 5.6 SPLITTING OF THE EXOGENOUS EXERGY DESTRUCTION OF THE MAIN COMPONENTS BELONGING TO CB AT THE DESIGN OUTDOOR TEMPERATURE OF 40 °C.	117

TABLE 5.7 TEWI [TONNES] AND PERCENT DIFFERENCE [%] IN COMPARISON WITH DXS.
..... 125

TABLE 5.8 TEWI [TONNES] AND PERCENT DIFFERENCE [%] IN COMPARISON WITH DXS+AC
FOR THE SMALLEST AND THE LARGEST AC UNIT SIZE INVESTIGATED IN THIS STUDY.
..... 128

LIST OF FIGURES

FIGURE 1.1: HFC PHASE-OUT SCHEDULE	1
FIGURE 1.2: REFRIGERATION EQUIPMENT AFFECTED BY EU F-GAS REGULATION 517/2014, COMMONLY EMPLOYED REFRIGERANTS AND POSSIBLE REPLACEMENTS.....	2
FIGURE 1.3: THE HISTORY OF THE CARBON DIOXIDE AS A REFRIGERANT.....	4
FIGURE 2.1: PHASE DIAGRAM OF CO ₂	12
FIGURE 2.2: COMPARISON OF A SUBCRITICAL (R134A) AND A TRANSCRITICAL (R744) THERMODYNAMIC CYCLE IN LOG(P)-H DIAGRAM.....	14
FIGURE 2.3: TEMPERATURE PROFILE IN A R134A (SUBCRITICAL) CONDENSER AND THAT IN A CO ₂ (TRANSCRITICAL) GAS COOLER.....	16
FIGURE 2.4: VAPOUR PRESSURE FOR DIFFERENT REFRIGERANTS	16
FIGURE 2.5: SLOPE OF SATURATION CURVE FOR DIFFERENT REFRIGERANTS	17
FIGURE 2.6: VOLUMETRIC REFRIGERATING CAPACITY FOR DIFFERENT REFRIGERANTS	17
FIGURE 2.7: SPECIFIC HEAT CAPACITY AT CONSTANT PRESSURE OF CO ₂	18
FIGURE 2.8: PSEUDOCRITICAL TEMPERATURE AND MAXIMUM SPECIFIC HEAT CAPACITY AT CONSTANT PRESSURE OF CO ₂	18
FIGURE 2.9: COMPARISON OF THE HEAT TRANSFER COEFFICIENTS FOR R22, R134A AND R744.....	19
FIGURE 2.10: EFFECT OF THE GAS COOLER PRESSURE ON THE OVERALL SYSTEM PERFORMANCE IN TRANSCRITICAL RUNNING MODES	20
FIGURE 2.11: OPTIMAL HEAT REJECTION PRESSURE AT DIFFERENT GAS COOLER EXIT TEMPERATURES.....	21
FIGURE 2.12: EFFECT OF THE HEAT REJECTION PRESSURE ON THE COOLING CAPACITY AND THE COP.....	22
FIGURE 2.13: MODIFIED LORENTZ CYCLE IN A T-S DIAGRAM	23
FIGURE 2.14: REAL TRANSCRITICAL CO ₂ CYCLE IN T-H AND P-H DIAGRAMS	24
FIGURE 3.1: GROWTH IN BOTH NUMBER (LEFT) AND TOTAL AREA (RIGHT IN THOUSANDS M ²) OF RETAIL STORES IN EUROPE FROM 2000 TO 2011	26

FIGURE 3.2: MARKET TREND FROM 2011 TO 2013 OF R744 BOOSTER REFRIGERATION SYSTEMS IN EUROPEAN SUPERMARKET APPLICATIONS.....	28
FIGURE 3.3: GROWTH IN EUROPEAN SUPERMARKETS EMPLOYING TRANSCRITICAL R744 REFRIGERATION SYSTEMS FROM 2013 TO 2016	29
FIGURE 3.4: EFFECT OF THE EXTERNAL TEMPERATURE ON COP OF BOTH A TRANSCRITICAL CO ₂ REFRIGERATION SYSTEM AND A HFC-BASED REFRIGERATING PLANT.....	30
FIGURE 3.5: ENERGY SAVING OF A SINGLE-STAGE R744 REFRIGERATION SYSTEM OVER A R404A DIRECT EXPANSION SOLUTION IN DIFFERENT LOCATIONS.....	31
FIGURE 3.6: CONVENTIONAL R744 BOOSTER REFRIGERATION SYSTEM IMPLEMENTING HEAT RECOVERY AND CORRESPONDING P-H DIAGRAM	33
FIGURE 3.7: SCHEMATIC OF A R744 BOOSTER REFRIGERATION SYSTEM WITH DEDICATED MECHANICAL SUBCOOLING	36
FIGURE 3.8: LOG(P)-H DIAGRAM OF R744 BOOSTER REFRIGERATION SYSTEMS WITH AND WITHOUT DEDICATED MECHANICAL SUBCOOLING.....	36
FIGURE 3.9: TOTAL MASS FLOW RATE AND FLASH GAS MASS FLOW RATE OF A TRANSCRITICAL R744 BOOSTER REFRIGERATION SYSTEM ($T_{MT} = -10\text{ }^{\circ}\text{C}$, $T_{LT} = -35\text{ }^{\circ}\text{C}$)	38
FIGURE 3.10: SCHEMATIC OF A R744 BOOSTER REFRIGERATION SYSTEM WITH PARALLEL COMPRESSION.....	39
FIGURE 3.11: LOG(P)-H DIAGRAM OF A R744 BOOSTER REFRIGERATION SYSTEM WITH PARALLEL COMPRESSION.....	39
FIGURE 3.12: SCHEMATIC OF A R744 BOOSTER REFRIGERATION SYSTEM WITH MT OVERFED EVAPORATORS BASED ON THE ADOPTION OF LIQUID EJECTORS	42
FIGURE 3.13: SCHEMATIC OF A R744 BOOSTER REFRIGERATION SYSTEM WITH MT OVERFED EVAPORATORS BASED ON THE ADOPTION OF A PUMP.....	43
FIGURE 3.14: TYPICAL OPERATING CONDITIONS FOR A DRY-EXPANSION EVAPORATOR (A) AND FOR AN OVERFED EVAPORATOR (B)	44
FIGURE 3.15: SCHEMATIC OF A R744 BOOSTER REFRIGERATION SYSTEM WITH DEDICATED MECHANICAL SUBCOOLING AND PARALLEL COMPRESSION.....	45

FIGURE 3.16: SCHEMATIC OF A R744 BOOSTER REFRIGERATION SYSTEM WITH MT OVERFED EVAPORATORS AND PARALLEL COMPRESSION	46
FIGURE 3.17: EFFECT OF THE OVERFEEDING OF THE MT EVAPORATORS ON A R744 BOOSTER REFRIGERATION SYSTEM WITH PARALLEL COMPRESSION IN THE LOG(P)-H DIAGRAM	46
FIGURE 3.18: T-S DIAGRAM FOR R134A AND R744.....	47
FIGURE 3.19: WORKING PRINCIPLE OF AN EJECTOR.....	49
FIGURE 3.20: EXPANSION AND COMPRESSION OF DRIVING AND DRIVEN FLOWS IN A R744 EJECTOR FOR EXPANSION WORK RECOVERY	51
FIGURE 3.21: SCHEMATIC (A) AND CORRESPONDING P-H DIAGRAM (B) OF A TRANSCRITICAL R744 REFRIGERATION SYSTEM USING AN EJECTOR TO RECOVER SOME EXPANSION WORK	52
FIGURE 3.22: MULTI-EJECTOR BLOCK AND ITS MAIN COMPONENTS	53
FIGURE 3.23: SCHEMATIC OF A R744 BOOSTER REFRIGERATION SYSTEM WITH PARALLEL COMPRESSION, MT OVERFED EVAPORATORS AND MULTI-EJECTOR RACK	55
FIGURE 3.24: SCHEMATIC OF A R744 BOOSTER REFRIGERATION SYSTEM WITH PARALLEL COMPRESSION, LT AND MT OVERFED EVAPORATORS AND MULTI-EJECTOR RACK ...	56
FIGURE 3.25: EFFECT OF THE OVERFEEDING OF THE LT EVAPORATORS ON A R744 BOOSTER REFRIGERATION SYSTEM EQUIPPED WITH MULTI-EJECTOR RACK IN THE LOG(P)-H DIAGRAM	56
FIGURE 3.26: LEFT-HAND SIDE: 2 PARALLEL COMPRESSORS, 4 HS AND 4 LS COMPRESSORS; RIGHT-HAND SIDE: 1 LIQUID EJECTOR AT THE BOTTOM, 2 VAPOUR EJECTORS AT THE TOP.....	57
FIGURE 3.27: SCHEMATIC OF A CASCADE REFRIGERATION SYSTEM FOR SUPERMARKET APPLICATIONS	60
FIGURE 3.28: T-S DIAGRAM OF A R134A/R744 CASCADE REFRIGERATION SYSTEM	61
FIGURE 3.29: TOTAL PRODUCTION AND ATMOSPHERIC RELEASE OF HFC-134A	63
FIGURE 3.30: (A) HFC CONSUMPTION IN EUROPE; (B) MARKET SECTORS NEEDING HFCs	63
FIGURE 3.31: SCHEMATIC OF A MULTIPLEX DIRECT EXPANSION SYSTEM	64

FIGURE 4.1: SCHEMATIC OF AN “ALL-IN-ONE” R744 BOOSTER REFRIGERATION SYSTEM WITH PARALLEL COMPRESSION, LT AND MT OVERFED EVAPORATORS AND MULTI-EJECTOR RACK.....	71
FIGURE 4.2: DEFINITION OF THE OPERATING ZONES FOR THE R744 BOOSTER REFRIGERATION SYSTEMS UNDER INVESTIGATION.....	74
FIGURE 4.3: NUMBER OF HOURS PER YEAR AT DIFFERENT OUTDOOR TEMPERATURES IN THE SELECTED LOCATIONS	76
FIGURE 4.4: THERMODYNAMIC CYCLES IN ENDOGENOUS OPERATION CONDITIONS FOR A CONVENTIONAL VAPOUR COMPRESSION REFRIGERATION SYSTEM.....	81
FIGURE 4.5: REAL AND THEORETICAL THERMODYNAMIC CYCLES FOR A CONVENTIONAL VAPOUR COMPRESSION REFRIGERATION SYSTEM	82
FIGURE 4.6: FLOW CHART FOR THE ADVANCED EXERGY ANALYSIS.....	84
FIGURE 4.7: SKETCH OF THE SPLITTING OF THE EXERGY DESTRUCTION ASSOCIATED WITH THE K -TH COMPONENT FOR THE ADVANCED EXERGY ANALYSIS	85
FIGURE 5.1: OPTIMAL HEAT REJECTION PRESSURE FOR ALL THE INVESTIGATION R744 BOOSTER REFRIGERATING SOLUTIONS AS A FUNCTION OF THE OUTDOOR TEMPERATURE	88
FIGURE 5.2: COMPARISON IN TERMS OF COP AMONG ALL THE INVESTIGATION SOLUTIONS AS A FUNCTION OF THE OUTDOOR TEMPERATURE.....	94
FIGURE 5.3: COOLING CAPACITY REQUIRED BY THE SUBCOOLING LOOP BELONGING TO MS+PC AS A FUNCTION OF THE OUTDOOR TEMPERATURE	95
FIGURE 5.4: OPTIMAL INTERMEDIATE PRESSURE FOR PC AND PC_VAR AS A FUNCTION OF THE OUTDOOR TEMPERATURE	95
FIGURE 5.5: ENERGY SAVING OVER CS OF SOME OF THE INVESTIGATED SOLUTIONS IN DIFFERENT EUROPEAN LOCATIONS.....	98
FIGURE 5.6: ENERGY SAVING OVER IB OF SOME OF THE INVESTIGATED SOLUTIONS IN DIFFERENT EUROPEAN LOCATIONS.....	100
FIGURE 5.7: ENERGY SAVING OVER PC OF SOME OF THE INVESTIGATED SOLUTIONS IN DIFFERENT EUROPEAN LOCATIONS.....	100

FIGURE 5.8: COP OF SOME OF THE INVESTIGATED SOLUTIONS AND NUMBER OF HOURS PER YEAR AT DIFFERENT OUTDOOR TEMPERATURES IN ROME.....	101
FIGURE 5.9: COP OF SOME OF THE INVESTIGATED SOLUTIONS AND NUMBER OF HOURS PER YEAR AT DIFFERENT OUTDOOR TEMPERATURES IN LISBON	101
FIGURE 5.10: COP OF SOME OF THE INVESTIGATED SOLUTIONS AND NUMBER OF HOURS PER YEAR AT DIFFERENT OUTDOOR TEMPERATURES IN VALENCIA.....	102
FIGURE 5.11: EVOLUTION OF THE ENERGY SAVINGS ASSOCIATED WITH THE CURRENT STATE-OF-THE-ART TECHNOLOGIES FOR COMMERCIAL R744 REFRIGERATION SYSTEMS OPERATING IN WARM REGIONS	103
FIGURE 5.12: ENERGY SAVINGS ACHIEVABLE BY THE COMMERCIAL R744 REFRIGERATION SYSTEMS EQUIPPED WITH MULTI-EJECTOR RACK AND OPERATING IN WARM REGIONS OVER THE “OLD” (CONVENTIONAL BOOSTER CONFIGURATION) AND THE “CURRENT” BENCHMARK (BOOSTER CONFIGURATION WITH PARALLEL COMPRESSION).....	103
FIGURE 5.13: EFFECT OF MT ON THE ANNUAL ENERGY CONSUMPTION OF OV AND OV+PC OVER DXS IN DIFFERENT LOCATIONS	104
FIGURE 5.14: (A) SCHEMATIC OF A R744 BOOSTER REFRIGERATION SYSTEM WITH PARALLEL COMPRESSION AND DE-SUPERHEATER; (B) SCHEMATIC OF A R744 BOOSTER REFRIGERATION SYSTEM WITH PARALLEL COMPRESSION, MT OVERFED EVAPORATORS AND DE-SUPERHEATER	105
FIGURE 5.15: ENERGY SAVING ON THE PART OF PC_VAR, OV+PC (MT = -4 °C) AND OV+PC (MT = -6 °C) OVER DXS IN DIFFERENT LOCATIONS.....	106
FIGURE 5.16: TOTAL POWER INPUT SPLIT INTO THE COMPRESSOR FRACTIONS FOR PC_VAR, EJ_OV AND EJ_OV_AC	108
FIGURE 5.17: VALUES OF PRESSURE LIFT REACHED BY THE INVESTIGATED MULTI-EJECTOR BASED SOLUTIONS	109
FIGURE 5.18: RESULTS OF THE CONVENTIONAL EXERGY ANALYSIS FOR CB (T ₀ = 40 °C)	114
FIGURE 5.19: BREAKDOWN OF THE AVOIDABLE EXERGY DESTRUCTION RATES OF CB (T ₀ = 40 °C)	115
FIGURE 5.20: CONTRIBUTIONS OF EACH COMPONENT BELONGING TO CB TO $\dot{E}_{D,tot}^{AV}$ (T ₀ = 40 °C)	115

FIGURE 5.21: RESULTS OF THE ADVANCED EXERGY ANALYSIS FOR CB ($T_0 = 40\text{ }^\circ\text{C}$).....	116
FIGURE 5.22: INFLUENCE OF DESIGN OUTDOOR TEMPERATURE ON AVOIDABLE EXERGY DESTRUCTION RELATED TO MAIN COMPONENTS BELONGING TO CB.....	119
FIGURE 5.23: INFLUENCE OF DESIGN OUTDOOR TEMPERATURE ON ENDOGENOUS AND EXOGENOUS AVOIDABLE EXERGY DESTRUCTION RELATED TO MAIN COMPONENTS BELONGING TO CB	119
FIGURE 5.24: COMPARISON OF THE EXERGY DESTRUCTION OF THE ENHANCED (EJ_OV) AND REFERENCE (CB) SYSTEMS ($T_0 = 40\text{ }^\circ\text{C}$)	122
FIGURE 5.25: RESULTS OF THE ADVANCED EXERGY ANALYSIS FOR EJ_OV ($T_0 = 40\text{ }^\circ\text{C}$)	123
FIGURE 5.26: SPLITTING OF TEWI RELATED TO DXS INTO ITS DIRECT AND INDIRECT CONTRIBUTIONS	124
FIGURE 5.27: REDUCTION IN TEWI OVER CS ON THE PART OF SOME OF THE INVESTIGATED SOLUTIONS IN VALENCIA AND IN ATHENS.....	126
FIGURE 5.28: SPLITTING OF TEWI RELATED TO DXS+AC INTO ITS DIRECT AND INDIRECT CONTRIBUTIONS FOR CASE I (AT THE TOP) AND CASE II (AT THE BOTTOM).....	127

LIST OF ABBREVIATIONS AND ACRONYMS

Symbols, abbreviations and subscripts/superscripts

0	Dead state
AC	Air conditioning
AIRAH	Australian Institute of Refrigeration, Air conditioning and Heating
appr	Approach
ASHRAE	American Society of Heating, Refrigerating, and Air-Conditioning Engineers
AUX	Auxiliary (or parallel) compressor(s)
AV	Avoidable
BRA	British Refrigeration Association
CB	Conventional R744 booster refrigeration system
CC	Cooling capacity
compr	Compressor(s)
COP	Coefficient of Performance [-]
CS	R134a/R744 cascade refrigeration system
CV	Control volume
D	Destruction
DES	De-superheater
DHW	Domestic Hot Water
diff	Diffuser
DMS	Dedicated Mechanical Subcooling
DXS	R404A multiplex direct expansion refrigeration system

e	Exergy per unit of mass [$\text{kJ}\cdot\text{kg}^{-1}$]
\dot{E}	Exergy rate [kW]
E	Annual energy consumption [$\text{kWh}\cdot\text{y}^{-1}$]
EES	Engineering Equation Solver
EJ	R744 booster refrigeration system using multi-ejector rack, parallel compression and medium temperature overfed evaporator
EJ_OV	R744 booster refrigeration system using multi-ejector rack, parallel compression and both low and medium temperature overfed evaporators
EJ_OV_AC	R744 booster refrigeration system using multi-ejector rack, parallel compression and both low and medium temperature overfed evaporators and integrated with the air conditioning system
EN	Endogenous
evap	Evaporators (Display cabinets/Cold rooms)
EX	Exogenous
exp	Expansion valve
ext	External
GC	Air-cooled gas cooler/condenser
glob	Global
GWP	Global Warming Potential [$\text{kgCO}_{2,\text{equ}} \cdot \text{kg}_{\text{refrigerant}}^{-1}$]
h	Enthalpy per unit of mass [$\text{kJ}\cdot\text{kg}^{-1}$]
h_{fg}	Latent heat of phase change [$\text{kJ}\cdot\text{kg}^{-1}$]
HFC	Hydrofluorocarbon

HFO	Hydrofluoroolefin
HOC	Heat of Combustion [$\text{MJ}\cdot\text{kg}^{-1}$]
HP	High Pressure
HS	High Stage
HTC	High temperature circuit
HVAC	Heating, Ventilation and Air Conditioning
IB	Improved R744 booster refrigeration system
IEA	International Energy Agency
IHX	Internal heat exchanger
in	inlet
IP	Intermediate Pressure
isen	Isentropic
j	j-th stream
k	k-th component
L	Loss
LCCA	Life-Cycle Cost Analysis
LEJ	Liquid ejectors
LF	Load factor [-]
LFL	Lower Flammability Limit [% volume in air]
LP	Low pressure
LS	Low Stage
LT	Low Temperature
LTC	Low temperature circuit

\dot{m}	Mass flow rate [kg·s ⁻¹]
m	Refrigerant charge [kg]
MEJ	Multi-ejector rack
mn	Motive nozzle
MP	Medium Pressure
MS+PC	R744 booster refrigeration system with R290 dedicated mechanical subcooling and parallel compression
MT	Medium Temperature
MTC	Medium Temperature Circuit
MX	Mexogenous
n	System operating lifetime [year]
ODP	Ozone Depletion Potential
OEL	Occupational Exposure Limit [PPMv]
out	Outlet
OV	R744 booster refrigeration system using medium temperature overfed evaporators
OV+PC	R744 booster refrigeration using parallel compression and medium temperature overfed evaporators
P	Pressure [bar]
PAG	Polyalkyl glycol
PAO	Polyalfaolefin
PC	R744 booster refrigeration system using parallel compression (slightly variable intermediate pressure)
PC_VAR	R744 booster refrigeration system using parallel compression (variable intermediate pressure)

PEC	Purchased Equipment Cost [€]
POE	Polyol ester
pp	Pinch Point
\dot{Q}	Heat transfer rate [kW]
r	r-th component
RC	Liquid receiver
rec	Recoverable
s	Entropy per unit of mass [$\text{kJ}\cdot\text{kg}^{-1}\cdot\text{K}^{-1}$]
SEER	Seasonal Energy Efficiency Ratio [-]
sn	Suction nozzle
t	Temperature [$^{\circ}\text{C}$]
TEWI	Total Equivalent Warming Impact [$\text{ton}_{\text{CO}_2\text{equ}}$]
tot	Total
UN	Unavoidable
v	Saturated vapour
VB	Vapour by-pass valve
VEJ	Vapour ejectors
\dot{W}	Power input [kW]

Greek symbols

α	Recycling factor [-]
β	Indirect emission factor [$\text{kg}_{\text{CO}_2}\cdot\text{kWh}^{-1}$]
γ	Annual leakage rate [$\text{kg}\cdot\text{year}^{-1}$]
Δ	Difference

η	Efficiency [-]
ν	Volume per unit of mass [$\text{m}^3 \cdot \text{kg}^{-1}$]
ω	Entrainment ratio [-]

LIST OF APPENDICES

APPENDIX A.1 – CORRELATIONS FOR MULTI-EJECTOR RACK	157
APPENDIX A.2 – GLOBAL EFFICIENCIES OF COMPRESSORS	159

1 INTRODUCTION

Due to both their high energy consumption and the wide use of high-GWP refrigerants, supermarkets are accountable for significant direct and indirect contributions to climate change. The coming into force of the EU F-Gas Regulation 517/2014 (European Commission, 2014) has been significantly promoting the use of natural working fluids in European commercial refrigeration systems. As schematized in Fig. 1.1, this legislative procedure aims at gradually cutting down on hydrofluorocarbons (HFCs). This will lead to a decrease in their supply to the European market by 79% from 2015 to 2030 compared to 2009-2012's average levels.

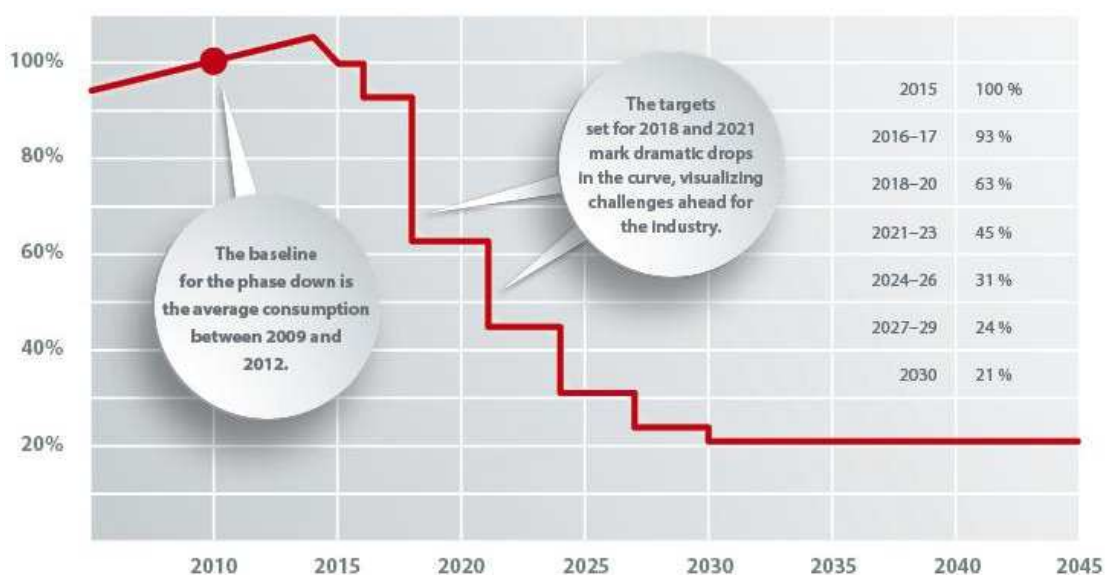


Fig. 1.1 - HFC phase-out schedule (Danfoss, 2016a).

Also, the marked HFC phase-down which will particularly occur in the next 2 years (by 37% in 2018) is expected to cause a great rise in their price, as well as a dramatic reduction in their availability. According to Shecco (2016), a growth in the price of R404A by 15% and in that of R407A, R410A, R407C and R134a by 10% were estimated in 2016. In addition, since January 2020 the EU F-Gas Regulation 517/2014 will also prohibit the maintenance of most of the existing refrigeration equipment using working fluids with a $GWP \geq 2500 \text{ kg}_{\text{CO}_2, \text{equ}} \cdot \text{kg}_{\text{refrigerant}}^{-1}$ (e.g. R404A). An exception will be made until January 2030 to the recycled HFCs (European Commission, 2014).

As showed in Fig. 1.2, most of the typically employed working fluids in refrigeration and air conditioning units (i.e. R134a, R404A and R410A) will be withdrawn soon.

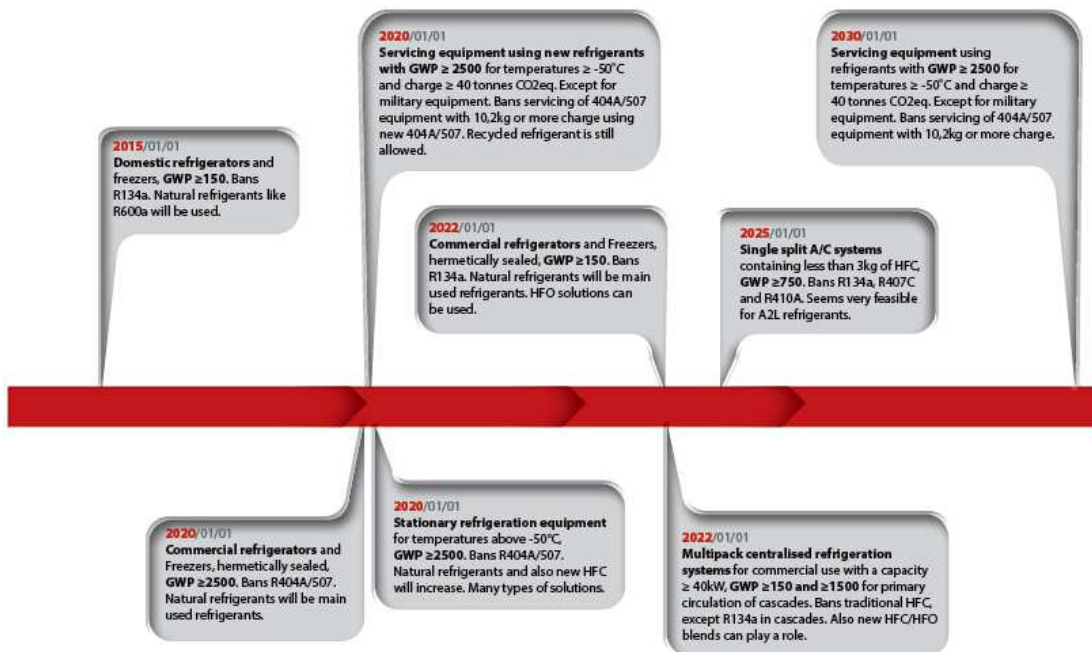


Fig. 1.2 - Refrigeration equipment affected by EU F-Gas Regulation 517/2014, commonly employed refrigerants and possible replacements (Danfoss, 2016a).

The successful achievement of a significant reduction in the environmentally harmful emissions associated with the refrigeration sector will involve two aspects:

- the adoption of low-GWP refrigerants, possibly natural working fluids, so as to (almost) delete their direct environmental impacts. In fact, the adoption of the EU F-Gas Regulation 517/2014 will imply that, in order to attain the expected HFC cut (i.e. by 79% by 2030), the average GWP of refrigerants will have to be brought from 2000 (evaluated in 2016) down to $400 \text{ kg}_{\text{CO}_2, \text{equ}} \cdot \text{kg}_{\text{refrigerant}}^{-1}$ by 2030 through the entire refrigeration sector (Shecco, 2016);

- the usage of solutions which will perform much better than the currently used ones in order to substantially decrease their indirect greenhouse gas emissions into the atmosphere.

The first effects of the coming into force of the EU F-Gas Regulation 517/2014 in the refrigeration sector were summed up by the European Environment Agency (2016):

- the fluorinated gas imports to the EU reduced by approximately 40% in relation to those estimated in 2014 (both by weight and as CO_{2,equ});
- the production of fluorinated gases in the EU decreased by 5% (as CO_{2,equ}) in 2015 in comparison with 2014's levels;
- the supply of F-gases in the EU has gone down by about 24% (both by weight and as CO_{2,equ}) since 2014;
- the EU exports of f-gases have fallen by 2% (by weight) or 1% (CO_{2,equ}) as of 2014.

With respect to R404A (GWP = 3922 kg_{CO_{2,equ}} · kg_{refrigerant}⁻¹), such a refrigerant will be banned in any refrigeration application. Bearing in mind that it is the most currently employed working fluid in European food retail industry, a suitable long-term replacement needs to be identified in this sector. According to the EU F-Gas Regulation 517/2014 (European Commission, 2014), the usage of R134a (GWP = 1430 kg_{CO_{2,equ}} · kg_{refrigerant}⁻¹) as a primary working fluid in cascade supermarket refrigeration systems with a cooling capacity ≥ 40 kW will be allowed in the near future (Fig. 1.2). On the other hand, it is worth remarking that R134a cannot be considered an appropriate investment in the long run for such applications owing to its enormous direct contributions to climate change, as well as to its ever-growing cost. As regards chillers and AC units, R410A (GWP = 2088 kg_{CO_{2,equ}} · kg_{refrigerant}⁻¹) is the refrigerant typically employed in these solutions. This working fluid is also used in supermarkets in order to satisfy the AC and the heating demands. Nowadays its possible climate-friendly alternatives are still a matter of debate.

Carbon dioxide (or R744) is supposed to successfully replace synthetic refrigerants in food retail industry. This “old” refrigerant was widely used at the end of the 19th century in applications in which safety was a crucial requirement (e.g. ships, dairies, meat industries), as it is non-flammable and non-toxic. In the late 1920s, CO₂ was substituted by synthetic working fluids mainly on account of its high operating pressures, very poor

performance at high outdoor temperatures and the failure in advances in CO₂ compressors on the part of manufacturers. In 1990s a renewed interest in such a refrigerant took hold. This was attributable to both prof. Lorentzen's studies (Lorentzen and Pettersen, 1993; Lorentzen, 1994, 1995) and the concurrent phase-out of ozone depleting working fluids due to the entry into force of the Montreal Protocol. At the beginning, researchers' attention mainly focused on mobile air conditioning (Lorentzen and Pettersen, 1993; Lorentzen, 1994) and heat pumping (Lorentzen, 1994, 1995; Nekså et al., 1998) units. However, many scientists greeted most of the first applications with scepticism. In spite of this, a promising diffusion of R744 in heat pump water heaters, as well as a gradual move from indirect to transcritical booster refrigeration solutions in food retails were experienced at a later time. Fig. 1.3 highlights its discovery, period of usage, abandonment and rediscovery in a timeline.

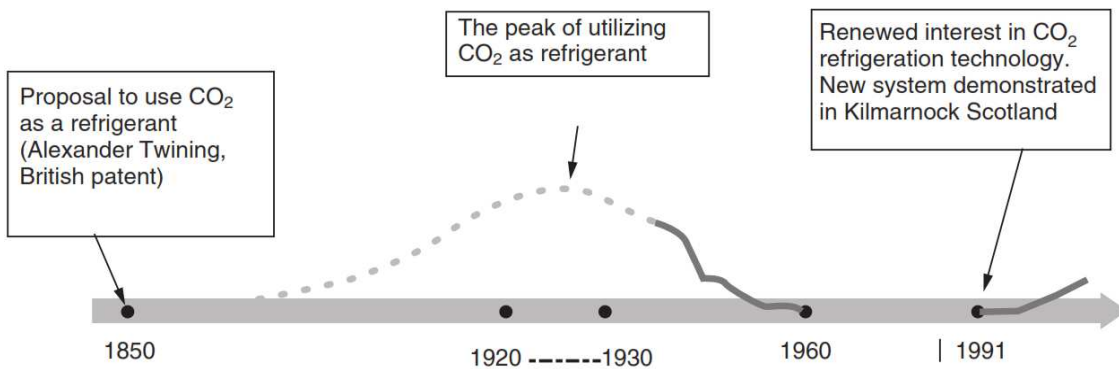


Fig. 1.3 - The history of the carbon dioxide as a refrigerant (Campbell et al., 2007).

The usage of carbon dioxide as a refrigerant for supermarket applications is no longer questionable nowadays. Thanks to its negligible GWP ($\text{GWP} = 1 \text{ kg}_{\text{CO}_2, \text{equ}} \cdot \text{kg}_{\text{refrigerant}}^{-1}$) and the safety level associated with its use (i.e. non-flammability and non-toxicity), R744 is not prone to be phased down. Also, R744 is inexpensive ($< 3 \text{ €} \cdot \text{kg}^{-1}$ with purity $> 99.8\%$) and, in comparison with HFCs, shows higher latent heat, specific heat, density and thermal conductivity and lower viscosity (Ge and Tassou, 2011a). In addition, as far as the commercial refrigeration sector is concerned, both R404A and R410A can be suitably replaced by adopting the recent concept of “all-in-one” (or “fully integrated”) CO₂ refrigeration systems (Hafner et al., 2016; Hafner and Banasiak, 2016; Hafner et al., 2015; Karampour and Sawalha, 2015, 2016a, 2016b). These solutions are tailor-made systems which successfully satisfy the whole AC, refrigeration and domestic hot water (DHW) reclaims, besides meeting most of or even the entire heating need of the selected supermarket. Integrated solutions are also supposed to make pure CO₂ units

more economically competitive with separated HFC systems, as they feature a copious drop in total investment, running and service costs (Hafner et al., 2015). An additional move towards the R744 usage can be associated with both taxes on the HFC purchase (e.g. the tax on R134a is 55.3 €·kg⁻¹ in Norway and 26 €·kg⁻¹ in Spain) and an ever-increasing sensitivity to eco-friendly solutions (e.g. in Austria, Belgium, Germany, Switzerland and the United Kingdom) on the part of many countries. However, as mentioned above, the basic “CO₂ only” configuration is markedly penalized as the cooling medium (e.g. outdoor air, water for space heating and domestic use) temperature increases. This is due to the low critical temperature of the CO₂ (about 31 °C), which implies that the heat rejection process can commonly take place in transcritical conditions. As a consequence, a substantially marked deterioration in the overall performance of this system and a better performance on the part of high GWP-based units is experienced in such running modes. This considerably low energy efficiency with rise in heat sink temperature and some enduring non-technological barriers still prevent these solutions from spreading in warm climates.

1.1 Aim of the study

Since the revival of CO₂ as a refrigerant, many researchers have focused on the enhancement of both the performance and the cost-effectiveness of the commercial CO₂ refrigerating plants operating in cold regions. This has been due to the fact that a basic CO₂ booster refrigeration system can outperform a HFC-based solution only in these areas, as such a configuration is remarkably sensitive to the high outdoor temperatures. As a result, pure CO₂ refrigeration systems have taken root in Northern and Central Europe, whereas they have been replaced by either cascade arrangements or multiplex R404A direct expansion configurations in warm climates. However, the entry into force of the EU F-Gas Regulation 517/2014 will lead to the phase-out of high GWP-refrigerants. These will be replaced by R744 in most of supermarket applications all over Europe, even in the Mediterranean area. As of its commencement, the aforementioned legislative act has also triggered a massive innovation in transcritical R744 technologies for food retail industry. Despite this, nowadays few studies on commercial “CO₂ only” refrigerating units running in high ambient temperature countries are still available.

This study is intended to take steps towards this scientific gap by theoretically assessing the energy and environmental benefits associated with the most advanced technologies for R744 supermarket refrigeration systems operating in Southern Europe. In addition to

this, the “all-in-one” concept has also been (partly) applied. This is an additional noteworthy element of this work, as “fully integrated” R744 configurations will play a pivotal role in the spread of these solutions into warm regions. Furthermore, the advanced exergy analysis of a conventional R744 booster system has also been implemented, as well as some improvement strategies have been indicated. Finally, some future research work has been suggested in order to additionally promote the usage of R744 in retail stores in high ambient temperature countries.

To conclude, this research work will aid to boost the confidence in R744 supermarket refrigerating plants in Southern Europe, foster the adoption of such technologies and finally open the warm region market to R744.

1.2 Methodology

The study has started by assessing the main characteristics of CO₂ as a refrigerant, as well as the different design options for food retail industry. At a later time, the most promising technologies for CO₂ supermarket refrigerating units operating in warm weathers have been identified.

Next, the theoretical energy and environmental performance of the state-of-the-art pure R744 technologies, such as the dedicated mechanical subcooling, the parallel compression, the overfed evaporators and the multi-ejector module, have been investigated by developing some thorough computer simulation models. All the analyses have been based on the common running modes of supermarkets located in Southern Europe. As baselines, a R404A multiplex direct expansion system, a R744/R134a cascade refrigeration arrangement and two conventional R744 booster units have been selected. The results of the energy evaluation have been compared with the ones available in the open literature. In addition, the energy conservations related to the integration of a “CO₂ only” refrigerating plant with the AC unit over separate HFC-based systems, which is a further relevant aspect of the present work, have also been investigated. In order to do this properly, various sizes of both the retail store and the AC unit have been taken into account. As far as the carbon footprint of the investigated refrigeration systems, a Total Equivalent Warming Impact (TEWI)-based assessment has also been implemented. Furthermore, the real enhancement potential and some improvement strategies have been evaluated for a conventional R744 booster solution by implementing a detailed advanced exergy analysis. Such a thermodynamic evaluation represents the most powerful tool to design any energy system. In fact, it can recognise the location, the magnitude and the

sources of inefficiencies, as well as identify both the potential improvements achievable by an individual component and the influence of a component on the others.

Based on the outcomes obtained, it can be claimed that nowadays R744 supermarket refrigeration systems can be adopted with extraordinary energy savings over the currently employed solutions in any climate context. This important accomplishment is attained by means of the application of the multi-ejector concept. In fact, this allows achieving significant reductions in energy consumption even in case of integration of a R744 refrigerating plant with a large AC unit in a superstore located in a high ambient temperature country. As a consequence, these “fully integrated” CO₂ solutions will become more and more affordable and be bound to completely replace any supermarket refrigerating arrangement using both HFC and hydrofluoroolefin (also indicated as HFO or low-GWP or short atmospheric lifetime HFC) all over the world. At last, some future research work has also been suggested.

1.3 Contribution to the knowledge

The contribution of this study to the knowledge can be summarized as follows:

- filling the existing gap in terms of estimation of the energy and environmental benefits related to the state-of-the-art solutions for R744 supermarket refrigeration units operating in Southern Europe in comparison with the currently employed systems;
- exhaustively investigating the energy advantages associated with the multi-ejector concept, which is currently the most promising technological expedient to promote the usage of CO₂ in warm/hot climates;
- bridging the current gap in terms of estimation of the energy and environmental benefits associated with pure CO₂ supermarket refrigeration systems operating in Southern Europe and integrated with the AC unit compared to HFC-based solutions;
- evaluating and recognising the real potential improvements attainable on the part of a conventional R744 booster technology by means of the application of the advanced exergy analysis.

1.4 Publications

This study is based on several previously published articles, which are listed below.

1.4.1 Papers for international conferences

- [1] **Gullo, P.**, Cortella, G., Minetto, S., Polzot, A. Overfed evaporators and parallel compression in commercial R744 booster refrigeration systems – An Assessment of energy benefits. GL2016: Proceedings of the 12th IIR Gustav Lorentzen Natural Working Fluids Conference, 21-24 August 2016; Edinburgh, UK. ID: 1039.
- [2] **Gullo, P.**, Cortella, G., Minetto, S. Potential enhancement investigation of commercial R744 refrigeration systems based on avoidable and unavoidable exergy destruction concepts. GL2016: Proceedings of the 12th IIR Gustav Lorentzen Natural Working Fluids Conference, 21-24 August 2016; Edinburgh, UK. ID: 1041.
- [3] Polzot, A., **Gullo, P.**, D'Agaro, P., Cortella, G. Performance evaluation of a R744 booster system for supermarket refrigeration, heating and DHW. GL2016: Proceedings of the 12th IIR Gustav Lorentzen Natural Working Fluids Conference, 21-24 August 2016; Edinburgh, UK. ID: 1022.
- [4] **Gullo, P.**, Cortella, G. Comparative Exergoeconomic Analysis of Various Transcritical R744 Commercial Refrigeration Systems. ECOS2016: Proceedings of the 29th International Conference on Efficiency, Cost, Optimization, Simulation and Environmental Impact of Energy Systems, 19-23 June 2016; Portorož, Slovenia. ID: 570.
- [5] **Gullo, P.**, Cortella, G. Thermodynamic Performance Evaluation of R744 Supermarket Refrigeration Systems by employing Advanced Exergy Analysis. ECOS2016: Proceedings of the 29th International Conference on Efficiency, Cost, Optimization, Simulation and Environmental Impact of Energy Systems, 19-23 June 2016; Portorož, Slovenia. ID: 399.
- [6] **Gullo, P.**, Cortella, G., Polzot, A. Energy and environmental comparison of commercial R744 refrigeration systems operating in warm climates. ICC2016: Proceedings of the 4th IIR International Conference on Sustainability and the Cold Chain, 7-9 April 2016; Auckland, New Zealand.
- [7] Polzot, A., D'Agaro, P., Cortella, G., **Gullo, P.** Supermarket refrigeration and air conditioning systems integration via a water storage. ICC2016: Proceedings of the 4th IIR International Conference on Sustainability and the Cold Chain, 7-9 April 2016; Auckland, New Zealand.
- [8] Polzot, A., D'Agaro, P., **Gullo, P.**, Cortella, G. Water storage to improve the efficiency of CO₂ commercial refrigeration systems. ICR2015: Proceedings of the

24th IIR International Congress of Refrigeration, 16-22 August 2015; Yokohama, Japan. ID: 339.

- [9] **Gullo, P.**, Elmegaard, B., Cortella, G. Energetic, Exergetic and Exergoeconomic Analysis of CO₂ Refrigeration Systems Operating in Hot Climates. ECOS2015: Proceedings of the 28th International Conference on Efficiency, Cost, Optimization, Simulation and Environmental Impact of Energy Systems, 29 June- 3 July 2015; Pau, France. ID: 52577.

1.4.2 Papers for national journals

- [1] **Gullo, P.**, Polzot, A. Valutazione delle prestazioni di macchine frigorifere a CO₂ per applicazioni commerciali in climi caldi. *ZeroSottoZero* 2017;2:54-61. ISSN: 1122-0376.
- [2] Polzot, A., **Gullo, P.** Analisi delle prestazioni di un sistema integrato a CO₂ per la refrigerazione, il riscaldamento e l'ACS nei supermercati. *ZeroSottoZero* 2017 (**Accepted Manuscript**). ISSN: 1122-0376.

1.4.3 Papers for international journals

- [1] Purohit, N., Khangarot, B.S., **Gullo, P.**, Purohit, K., Dasgupta, M.S. Assessment of alumina nanofluid as a coolant in double pipe gas cooler for trans-critical CO₂ refrigeration cycle. RAAR2016: Proceedings of the International Conference on Recent Advancement in Air Conditioning and Refrigeration, 10-12 November 2016; Bhubaneswar, India. pp. 253-263. (**Being printed in Energy Procedia**)
- [2] Purohit, N., **Gullo, P.**, Dasgupta, M.S. Comparative assessment of low-GWP based refrigerating plants operating in hot climates. RAAR2016: Proceedings of the International Conference on Recent Advancement in Air Conditioning and Refrigeration, 10-12 November 2016; Bhubaneswar, India. pp. 155-165. (**Being printed in Energy Procedia**)
- [3] **Gullo, P.**, Hafner, A., Cortella, G. Multi-ejector R744 booster refrigerating plant and air conditioning system integration – A theoretical evaluation of energy benefits for supermarket applications. *International Journal of Refrigeration* 2017;75:164-176. DOI: [10.1016/j.ijrefrig.2016.12.009](https://doi.org/10.1016/j.ijrefrig.2016.12.009)
- [4] **Gullo, P.**, Cortella, G. Theoretical evaluation of supermarket refrigeration systems using R1234ze(E) as an alternative to high-global warming potential refrigerants. *Science and Technology for the Built Environment* 2016;22(8):1145-1155. DOI: [10.1080/23744731.2016.1223996](https://doi.org/10.1080/23744731.2016.1223996)

- [5] Polzot, A., D'Agaro, P., **Gullo, P.**, Cortella, G. Modelling commercial refrigeration systems coupled with water storage to improve energy efficiency and perform heat recovery. *International Journal of Refrigeration* 2016;69:313-323. DOI: [10.1016/j.ijrefrig.2016.06.012](https://doi.org/10.1016/j.ijrefrig.2016.06.012)
- [6] **Gullo, P.**, Elmegaard, B., Cortella, G. Advanced exergy analysis of a R744 booster refrigeration system with parallel compression. *Energy* 2016;107:562-571. DOI: [10.1016/j.energy.2016.04.043](https://doi.org/10.1016/j.energy.2016.04.043)
- [7] **Gullo, P.**, Elmegaard, B., Cortella, G. Energy and environmental performance assessment of R744 booster supermarket refrigeration systems operating in warm climates. *International Journal of Refrigeration* 2016;64:61-79. DOI: [10.1016/j.ijrefrig.2015.12.016](https://doi.org/10.1016/j.ijrefrig.2015.12.016)

1.5 Disposition of the thesis

This study has been organized as follows:

- **Chapter 2: CO₂ as a refrigerant**
In this section of the present work the properties and the peculiarities of R744 are pointed out.
- **Chapter 3: Supermarket refrigeration systems**
In Chapter 3, the main characteristics of commercial refrigeration units and the use of CO₂ in these applications are disclosed, as well as a detailed literature review is also carried out.
- **Chapter 4: Methods and Materials**
In this chapter the considered case studies, the implemented simulation models and the assumptions made are exhaustively discussed. In addition, the most important concepts related to the conventional and the advanced exergy analyses, as well as the ones associated with the environmental assessment are described.
- **Chapter 5: Results and Discussion**
The results obtained are showed and commented in this section.
- **Chapter 6: Conclusions and Future Work**
In Chapter 6 the main conclusions are summarized and some directions for future work are recognized.

2 CO₂ AS A REFRIGERANT

Carbon dioxide is a natural compound constituting approximately 0.04% (i.e. 400 ppm) of Earth's atmosphere. The commercial production of CO₂ as a refrigerant (R744) is mainly based on the combustion of hydrocarbons and, secondary, on the recovery from industrial applications (Pearson, 2014). With respect to its environmental properties, CO₂ is a refrigerant with a negligible GWP and zero Ozone Depletion Potential (ODP). Also, being non-flammable and non-toxic, R744 will never have any regulatory liability.

In the last few year transcritical R744 refrigeration systems have been gaining a considerable interested in supermarket applications. Therefore, it is expected that these solutions will spread like wildfire worldwide.

In this chapter the main characteristics of CO₂ as a refrigerant are summarized.

2.1 Properties of R744

In Fig. 2.1, two distinctive state points are marked: the critical point and the triple point, which respectively represents the lower and upper limit for the occurrence of any evaporation and condensation process. At the former, the properties of the liquid and gas phases merge into only one called homogenous supercritical fluid. In addition, beyond this point (area delimited by dashes in Fig. 2.1), gas and liquid phases cannot be distinctly distinguished and no phase changes take place. At the triple point, solid, liquid and vapour states coexists in equilibrium and liquid carbon dioxide cannot exist at pressures and temperatures below 5.2 bar and -56.6 °C, respectively. A peculiarity of R744 is that, unlike most of the other refrigerants, its critical and triple point commonly belong to its operating condition range.

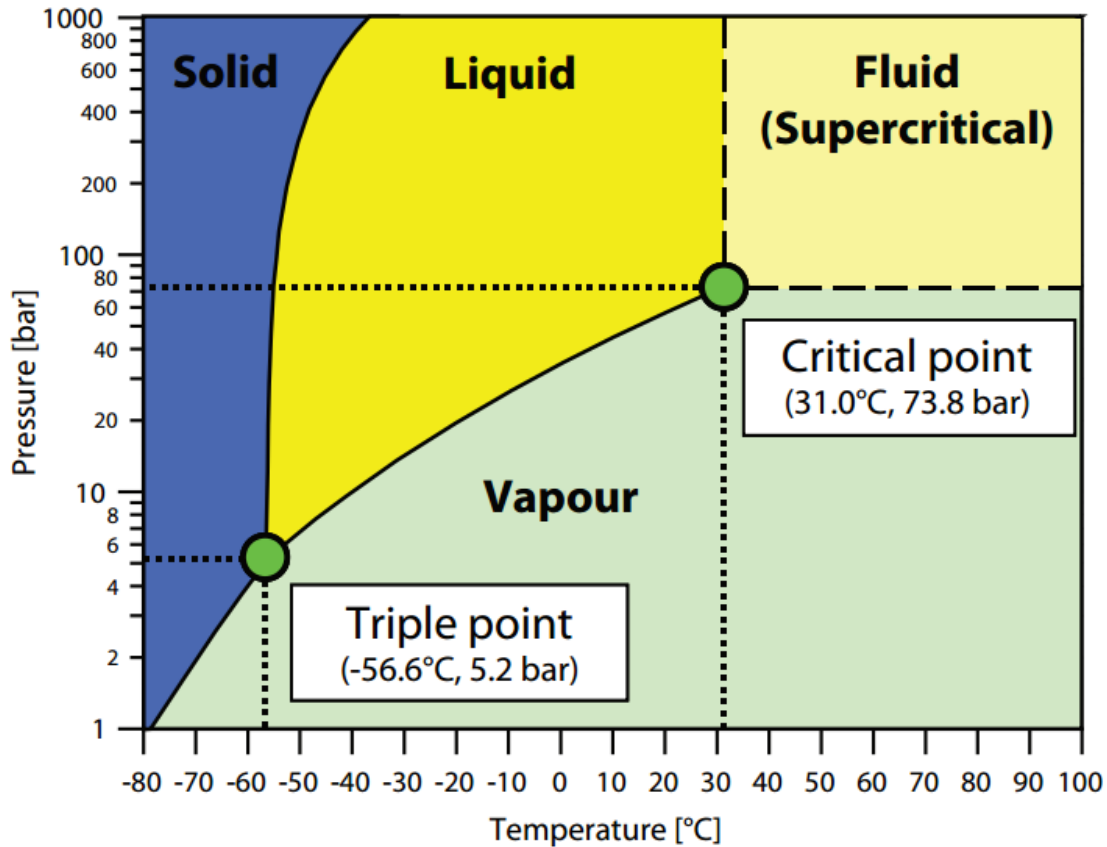


Fig. 2.1 - Phase diagram of CO₂ (Danfoss, 2008).

Fig. 2.1 and Table 2.1 highlight that a very low critical temperature (about 31 °C) and a very high critical pressure (73.8 bar) can be associated with carbon dioxide. For instance, the critical temperature of R404A is 72 °C, which implies that the condensation process can take place at temperatures up to this value. The heat rejection into the atmosphere can thus occur for most of the conventional refrigeration applications. On the other hand, as regards pure R744 units, the condensation process can be held only at temperatures up to about 31 °C. This entails that the transcritical operating conditions commonly take place in such refrigerating plants, especially in warm regions. In Fig. 2.2, the thermodynamic cycle of a refrigeration system using a conventional refrigerant is compared with that of a transcritical CO₂ refrigerating machine. It is possible to notice that the former is characterized by a phase change involving two processes (i.e. the de-superheating and the veritable condensation of the refrigerant), whereas the gas cooling is based on only one process in which the refrigerant is cooled down by thermally interacting with a cooling medium (e.g. outdoor air, water for space heating and domestic use) at (ideally) a constant pressure.

Table 2.1 - Physical, environmental and safety properties of the selected refrigerants.

	<i>R290</i>	<i>R744</i>	<i>R134a</i>	<i>R404A</i>
Chemical formula or composition [% wt]	CH ₃ CH ₂ CH ₂	CO ₂	CH ₂ FCF ₃	44% R125 52% R143a 4% R134a
Molecular weight, [g·mol⁻¹]	44.1	44.0	102.0	97.6
Normal boiling point, [°C]	-42.1	-78.4 (sublimation)	-26.1	-46.2 (bubble point)
Critical temperature, [°C]	96.7	31.0	101.1	72.0
Critical pressure, [bar]	42.5	73.8	40.7	37.3
h_{fg} at -30 °C, [kJ·kg⁻¹]	412.4	303.5	219.5	189.5
h_{fg} at 40 °C, [kJ·kg⁻¹]	307.1	-	163.0	120.3
v_v at -30 °C, [m³·kg⁻¹]	0.259	0.027	0.226	0.095
GWP_{100 years}	3*	1*	1430*	3922*
Safety group	A3	A1	A1	A1
OEL, [PPMv]	1000	5000	1000	1000
LFL, [% vol.]	2.1	0.0	None	None
HOC, [MJ·kg⁻¹]	50.4	n.d.	4.2	-6.6

Thermo-physical properties derived from Lemmon et al., 2013; Safety properties derived from ASHRAE, 2013; * derived from AIRAH, 2012.

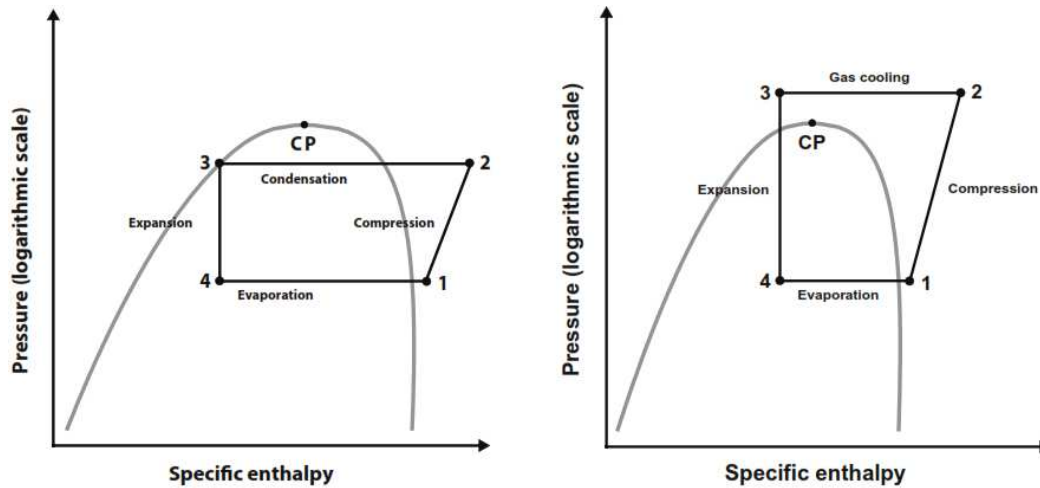


Fig. 2.2 - Comparison of a subcritical (R134a) and a transcritical (R744) thermodynamic cycle in $\log(p)$ - h diagram (Danfoss, 2008).

As mentioned above, the occurrence of the transcritical working operations results in a considerably marked deterioration in the energy efficiency of basic pure R744 systems and, consequently, in better performance on the part of high GWP-based solutions. The higher the hot sink temperature, the more emphasized these outcomes are. This can be showed by employing the example made by Cavallini and Zilio (2007) (Table 2.2.).

Table 2.2 – Performance comparison of vapour compression refrigeration systems using R22 and R744 (Cavallini and Zilio, 2007).

<i>Description</i>	<i>R22</i>	<i>R744</i>
Evaporating temperature [°C]	-10.00	-10.00
Isentropic efficiency [-]	0.80	0.80
Condensing temperature (R22) [°C]	43.00	-
Gas cooler outlet temperature (R744) [°C]	-	31.00
Optimal gas cooler pressure (R744) [bar]	-	78.00
Vapour superheat at compressor inlet [°C]	0.00	0.00
Coefficient of Performance (COP) [-]	3.04	2.52

The evaluation was based on:

- the selection of the outdoor temperature of 28 °C;

- values of the approach temperature (i.e. ΔT_{appr} meaning difference between the temperature of the outgoing hot fluid and the one of the ingoing cold fluid) respectively equal to 5 °C for the R22 condenser and 3 °C for the R744 gas cooler;
- the pressure drop was neglected and all the components were supposed to be well-insulated;
- no degree of subcooling was selected.

The results in Table 2.2 suggest that, despite the low value of approach temperature of the gas cooler, the CO₂ refrigeration system consumes about 20% more energy than the solution using the synthetic refrigerant. As will be exhaustively discussed later, this is due to the enormous irreversibilities taking place in the expansion valve of conventional pure CO₂ units.

On the other hand, unlike HFCs, the use of R744 (in transcritical running modes) is particularly suitable for the production of hot water (e.g. for DHW, space heating, snow smelting and evaporator coils) in commercial refrigeration systems (Kaiser and Fröschle, 2010; Karampour and Sawalha, 2015, 2016a, 2016b; Ge and Tassou, 2014; Hafner et al., 2012, 2014c, 2015, 2016; Polzot et al., 2016c; Reinholdt and Madsen, 2010; Sawalha, 2013; Schönenberger, 2016; Tambovtsev et al., 2011). This is due to the fact that the gas cooling is a distinctive process occurring by sensible cooling, which means that R744 can more appropriately fit the water temperature profile than conventional refrigerants (Fig. 2.3). Therefore, a significant drop in the entropy generation and exergy destruction rate is experienced in R744 gas coolers. A suitable design of the high pressure (HP) heat exchanger permits reaching values of the approach temperature equal to 1-2 K. The implementation of the heat recovery in R744 refrigeration systems is also promoted by the high discharge temperatures obtained. However, an appropriate trade-off between the useful effect and the increase in the required power input needs to be found so as to make the transcritical CO₂ systems (energetically and economically) competitive with HFC-based solutions (Sawalha, 2013). In fact, the higher the gas cooler pressure, the larger the amount of heat which can be provided. On the other hand, this also leads to a growth in the energy consumption and a simultaneous drop in the refrigerating effect. Consequently, a suitable control strategy to maximize the total energy efficiency of the system has to be implemented (Ge and Tassou, 2014; Sawalha, 2013; Tambovtsev et al., 2011).

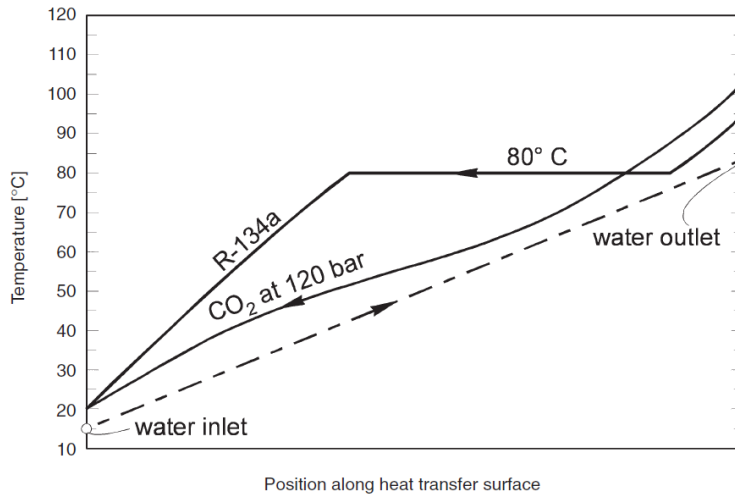


Fig. 2.3 - Temperature profile in a R134a (subcritical) condenser and that in a CO₂ (transcritical) gas cooler (Cavallini and Zilio, 2007).

As shown in Fig. 2.4, CO₂ features very impressive working pressures compared to the other refrigerants. These substantially affect the design and the efficiency of the components, as well as the heat transfer process.

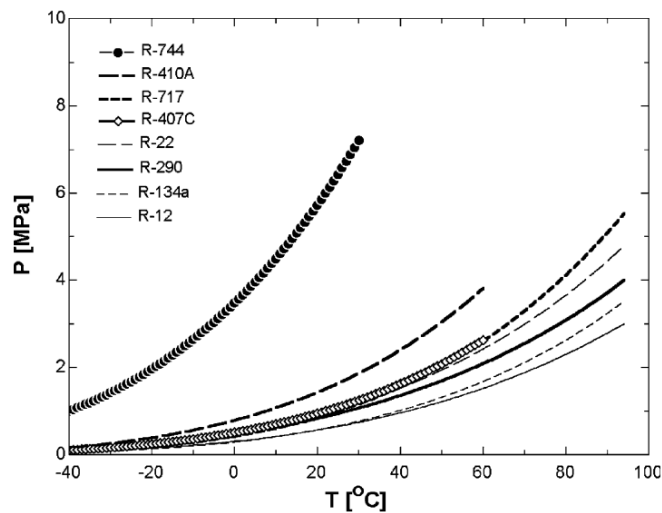


Fig. 2.4 - Vapour pressure for different refrigerants (Kim et al., 2004).

The CO₂ operating pressures are usually 5-10 times as high as those of the conventional working fluids, which entail both the need for some safety measures and some advantages, such as low pressure ratios and vapour pressure drops (Fig. 2.5) and high vapour densities.

Kim et al. (2004) claimed that, at 0 °C and for 1 kPa pressure decrease, CO₂ undergoes a reduction in temperature by 0.01 K, whereas R134a experiences a drop by 0.10 K. As this fall is generally 4-10 times as low as for the synthetic refrigerants, a favourable two-phase distribution within CO₂ heat exchangers occurs.

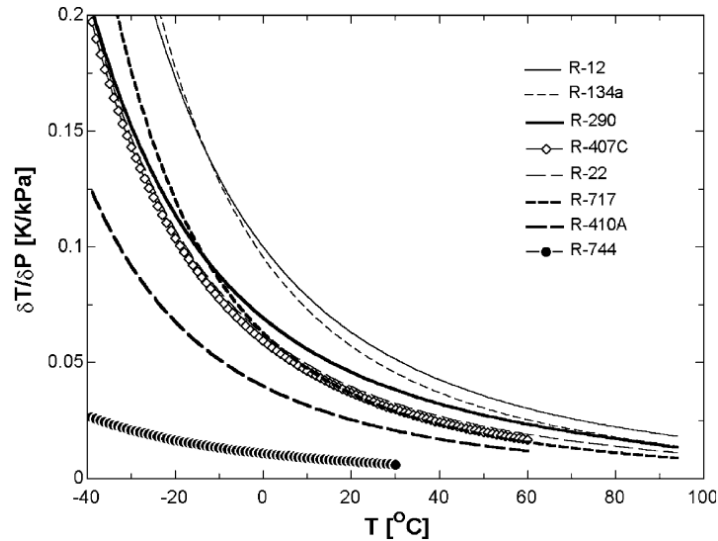


Fig. 2.5 - Slope of saturation curve for different refrigerants (Kim et al., 2004).

As mentioned above, R744 is also characterized by a very high density which, at the same temperature, is respectively 6.7 and 28 times as great as that of R134a and R717 (Pearson, 2014). This suggests that, for a specific volume flow, a larger volumetric cooling capacity (Fig. 2.6) and, consequently, smaller both suction pipes (up to 60-70% in the evaporators in comparison a HFC-based system according to Kim et al., 2004) and compressors (from 5 times over a R404A-based solution to 8 times over a R134a-based solution according to Pearson, 2014) can be obtained in comparison with the other refrigerants.

It is worth remarking that, as volumes of components and pipes for CO₂ applications are small, the stored explosion energy in these systems is comparable to that of conventional units.

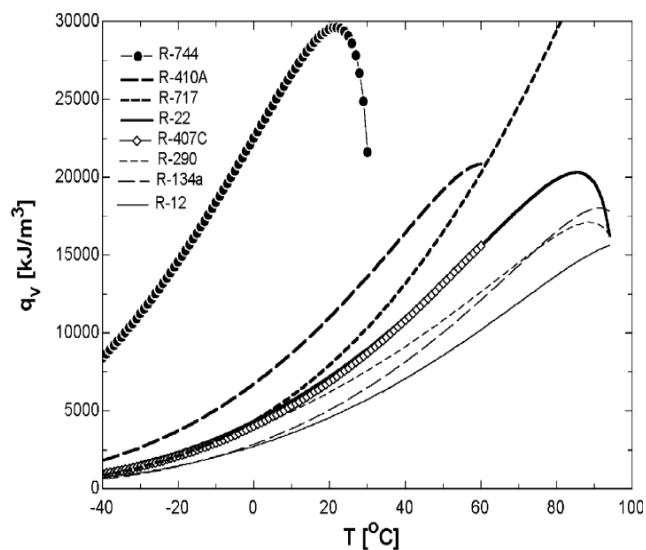


Fig. 2.6 - Volumetric refrigerating capacity for different refrigerants (Kim et al., 2004).

The properties of any supercritical fluid change significantly with temperature in an isobaric process near the critical point and particularly near the pseudocritical points (i.e. points at which the specific heat capacity at constant pressure reaches a peak). Therefore, the Prandtl number for CO₂ in transcritical conditions has a similar behaviour to that of the specific heat capacity at constant pressure depicted in Fig. 2.7. In both cases, a maximum is located at the pseudocritical temperature, which decreases as the pressure increases. In a gas cooler the influence of the temperature on the Prandtl number is strongly depending on the pressure, which causes significant variations in terms of local heat transfer coefficient with respect to these variables. This aspect is fundamental when it comes to properly designing HP heat exchangers for CO₂.

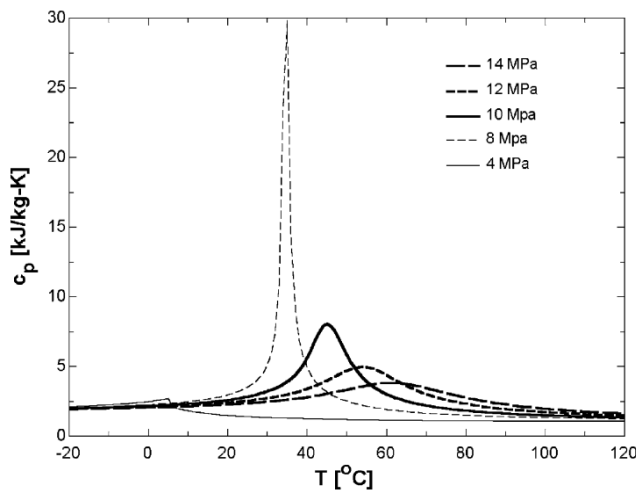


Fig. 2.7 – Specific heat capacity at constant pressure of CO₂ (Kim et al., 2004).

As shown in Fig. 2.8, the maximum specific heating capacity, decreasing as a function of the pressure, occurs at the pseudocritical temperature for a specific pressure.

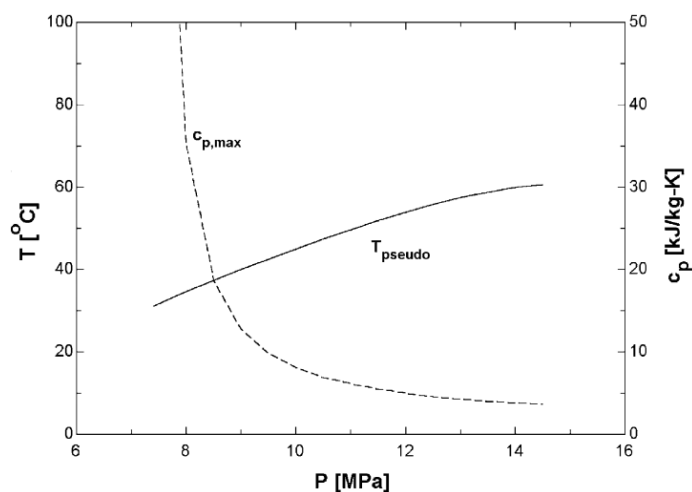


Fig. 2.8 – Pseudocritical temperature and maximum specific heat capacity at constant pressure of CO₂ (Kim et al., 2004).

Carbon dioxide also features a low surface tension, which leads CO₂ boiling heat transfer coefficients to be (typically) twice as high as those of conventional refrigerants (Pearson, 2014), and to a high thermal conductivity, which fosters favourable heat transfer coefficients in both single- and two-phase flows. According to the results by Choi et al.'s (2007) (Fig. 2.9), the mean boiling heat transfer coefficient ratio in horizontal mini-channels is about 1.0:0.8:2.0 for R22:R134a:R744.

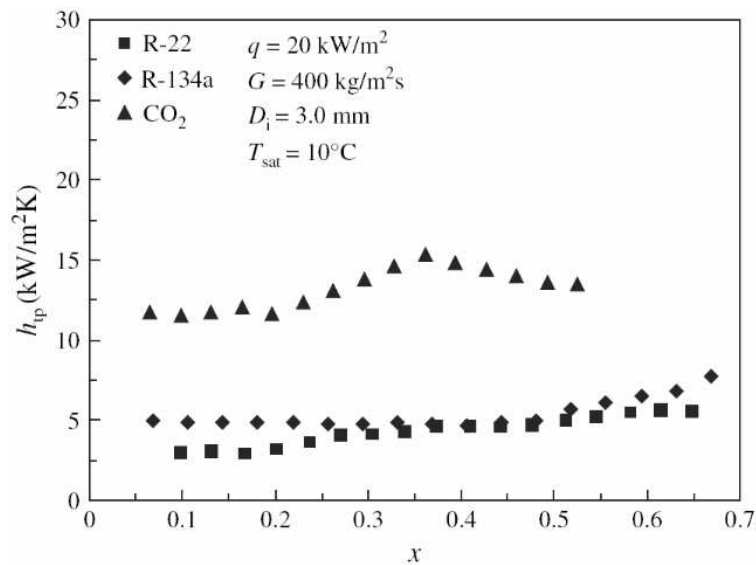


Fig. 2.9 - Comparison of the heat transfer coefficients for R22, R134a and R744 (Choi et al., 2007).

At 0 °C, CO₂ in liquid and vapour states has 20% and 60% higher thermal conductivities than R134a at the corresponding states, respectively. At the same temperature, the viscosity values in vapour state associated with R744 are similar to those related to R134a, whereas the ones in liquid state are 40% as low as those of the latter.

On the other hand, in saturation conditions water and carbon dioxide form a solution which can cause corrosive issues and sludge formation. Also, R744 is not soluble with polyalphaolefin (PAO), whereas it is with polyol ester (POE) and polyalkyl glycol (PAG). Although CO₂ can be used along with many fluids and metals typically employed in refrigeration systems, it can easily penetrate through elastomers. In addition, CO₂ is heavier than the air and therefore it tends to gather to the bottom. At concentrations in terms of volume above 3%, 5% and 10%, CO₂ causes hyperventilation, narcosis and coma, respectively.

2.2 Effect of heat rejection pressure on performance of R744 refrigeration systems in transcritical running modes

The effect of a change by ± 5 bar in the heat rejection pressure in transcritical operating conditions is assessed in Fig. 2.10 at a constant gas cooler outlet temperature (thermodynamic state pointed out as 3). An increase in p_3 by 5 bar (cycle $1_H-2_H-3_H-4_H$) causes an increment respectively by 6% in the cooling capacity and by 10% in the power input, leading to a drop in the COP by 4% in relation to the reference cycle (1-2-3-4). By decreasing p_3 by 5 bar (cycle $1_L-2_L-3_L-4_L$), a reduction respectively by 38% and 10% in the cooling capacity and in the power input are computed, implying a decrement in COP by about 31% in comparison with the nominal conditions (cycle: 1-2-3-4). This simple example shows that in transcritical operating regimes, for a given gas cooler outlet temperature, an optimal discharge pressure which maximizes the COP can be identified (Cavallini and Zilio, 2007; Cecchinato et al., 2009; Kim et al., 2004; Lorentzen, 1994; Sawalha, 2008a).

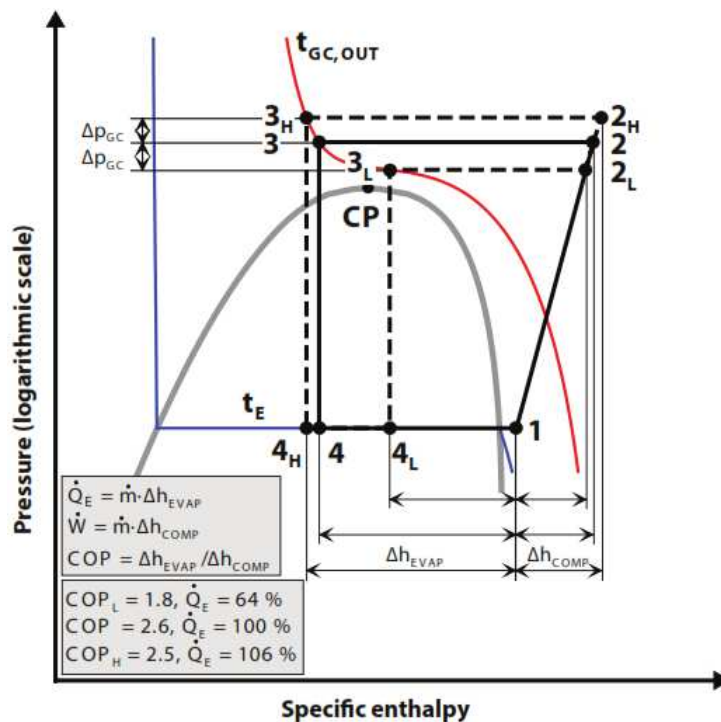


Fig. 2.10 - Effect of the gas cooler pressure on the overall system performance in transcritical running modes (Danfoss, 2008).

The aforementioned result is clearly represented in Fig. 2.11 in which the optimal heat discharge pressure is depicted with the aid of a light green curve as a function of the gas cooler exit temperature. Thus, it can be claimed that the heat rejection pressure in transcritical running modes is induced by the R744 charge, i.e. it is independent from the

saturation pressure. Many correlations aimed at assessing the optimal high pressure have been widely employed in simulation models of CO₂ refrigerating systems for different applications (Brown et al., 2002; Chen and Gu, 2005; Ge and Tassou, 2011a; Kauf, 1998; Liao et al., 2000; Sawalha, 2008a). With respect to supermarket applications, the sensitivity analysis implemented by Ge and Tassou (2011a) showed that the value of the optimal gas cooler pressure is significantly influenced by the isentropic efficiency of the high stage (HS) compressor rack, the external temperature and the effectiveness of the internal heat exchanger located downstream of the gas cooler. Cabello et al. (2008) compared the experimental data of the optimal discharge pressure related to a single-stage R744 refrigerating unit with the outcomes obtained by using four correlations available from the open literature. The authors stated that large drops in the COP can be associated with small errors in pressure. Yang et al. (2015) proposed a new method to remarkably reduce the deviations from the COP_{max}. Some researchers suggested some real-time control strategies of the optimum high pressure (Peñarrocha et al., 2014; Zhang and Zhang, 2011). According to Cecchinato et al. (2010a), this approach could provide a more efficient and robust solution. This study also suggested that the application of the correlations from the literature does not penalize the results considerably when it comes to commercial applications.

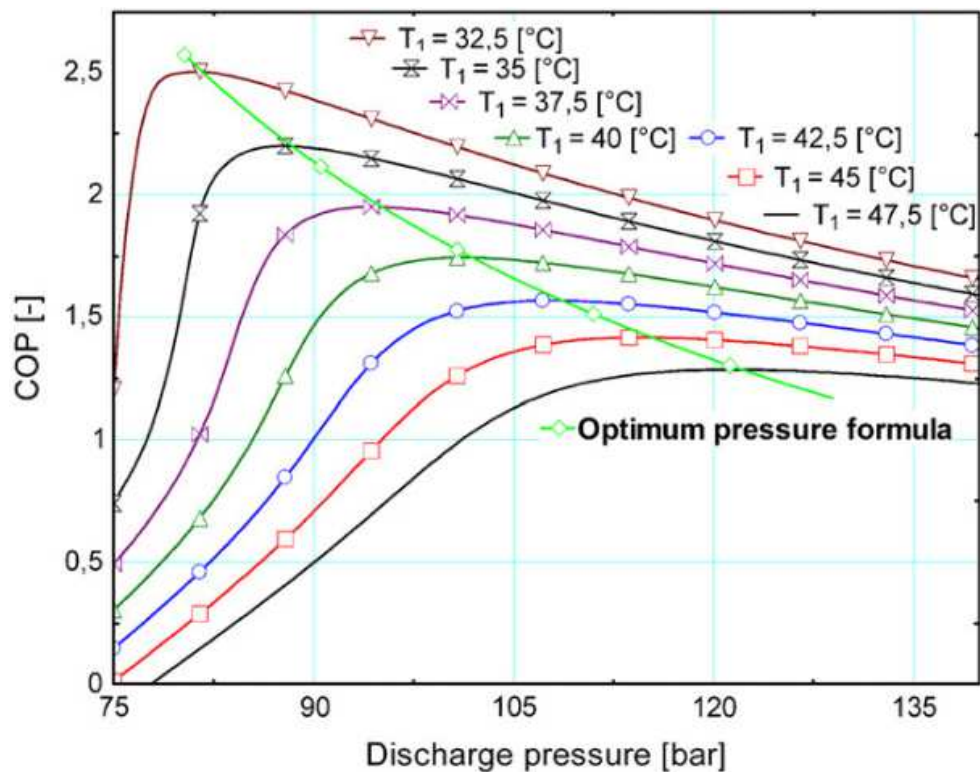


Fig. 2.11 - Optimal heat rejection pressure at different gas cooler exit temperatures (t₁) (Sawalha, 2008a).

Fig. 2.12 displays that the maximum cooling capacity occurs at an optimal heat rejection pressure which is higher than that at which the maximum COP can be identified. It can also be noticed that an increase in the gas cooler pressure from the optimum conditions would lead to a fall in the COP and to a negligible increase in the cooling capacity.

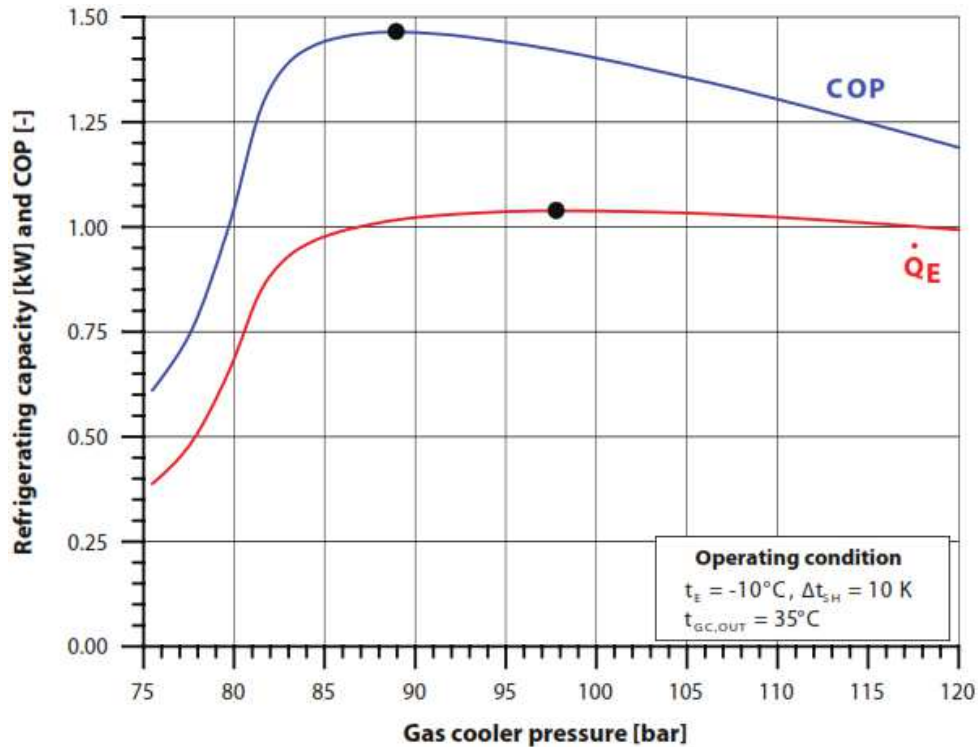


Fig. 2.12 - Effect of the heat rejection pressure on the cooling capacity and the COP (Danfoss, 2008).

As regards the transition operating region, Cecchinato et al. (2007) proposed a control strategy to gradually move from the subcritical to the transcritical running modes. According to the authors, in these operating conditions the heat rejection pressure is assumed to linearly vary with respect to the outdoor temperature within an operating range delimited by an upper and lower limit. These constraints are represented by a couple of values of high pressure and gas cooler/condenser outlet temperature. In addition, the degree of subcooling and the temperature approach can also be varied (Gullo et al., 2016a). Different approaches were suggested by other researchers. Two different external temperatures of transition (i.e. 16 °C and 21 °C) of a CO₂ supermarket system for a medium temperature (MT) application located in the UK were studied by Ge and Tassou (2009). The results obtained revealed that an energy saving by approximately 18% could be attained by employing a transition temperature of 21 °C over that equal to 16 °C. Sharma et al. (2014) adopted a fixed value of high pressure within a certain range of external temperatures.

2.3 Reference thermodynamic cycle for transcritical R744 refrigeration systems

For any subcritical CO₂ refrigeration system, the reversed Carnot cycle represents the theoretical reference cycle. As account of the peculiar heat rejection process occurring in the transcritical CO₂ cycle, the modified Lorentz cycle was proposed as a term of comparison to properly asses the performance of such a thermodynamic cycle. Fig. 2.13 represents Lorentz cycle in a T-s diagram, in which T_m [K] is the average temperature of the cooling medium and T_0 [K] is the heat source temperature. The involved thermodynamic processes are:

- 4s – 1 heat absorption at constant temperature and pressure;
- 1 – 2s isentropic compression;
- 2s – 3 heat rejection at constant pressure;
- 3 – 4s isentropic expansion.

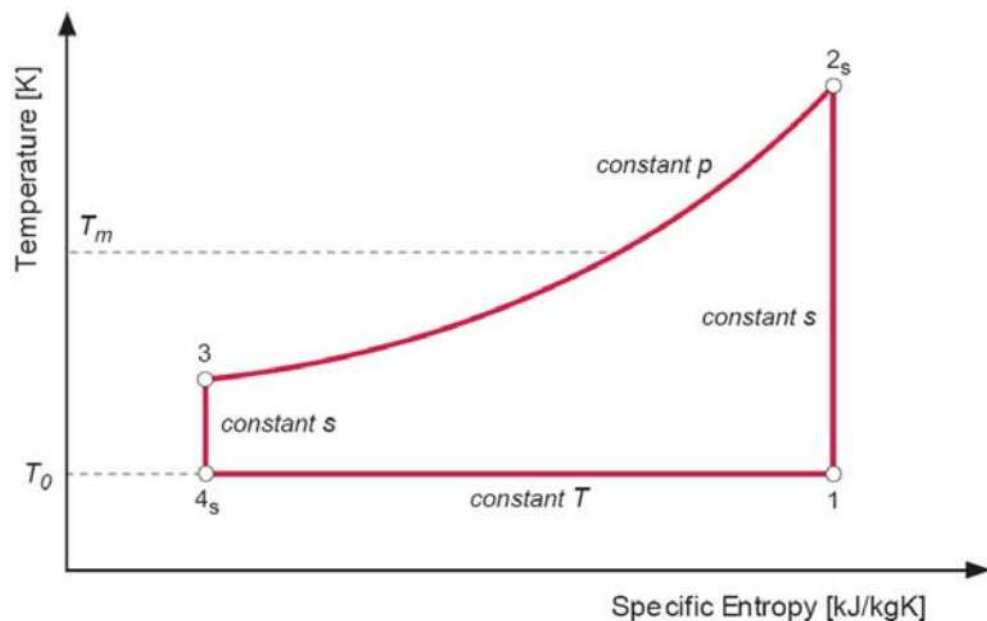


Fig. 2.13 - Modified Lorentz cycle in a T-s diagram (Reulens, 2009).

The coefficient of performance for the modified Lorentz cycle (COP_{LZ}) can be calculated as:

$$COP_{LZ} = \frac{T_0}{T_m - T_0} \quad (2.1)$$

The Lorentz efficiency (η_{LZ}) is defined as the ratio of COP associated with the real transcritical CO₂ cycle (COP_{real}) to COP_{LZ} :

$$\eta_{LZ} = \frac{COP_{real}}{COP_{LZ}} \quad (2.2)$$

As sketched in Fig. 2.14, the real cycle is significantly different from the modified Lorentz cycle. The following thermodynamic processes can be identified:

- 4 – 1' non-isobaric and non-isothermal heat absorption;
- 1' – 1 non-isobaric superheating in the suction line;
- 1 – 2 irreversible polytropic non-adiabatic compression to supercritical pressure;
- 2 – 3 non-isobaric and non-isothermal heat rejection;
- 3 – 4 non-isenthalpic expansion.

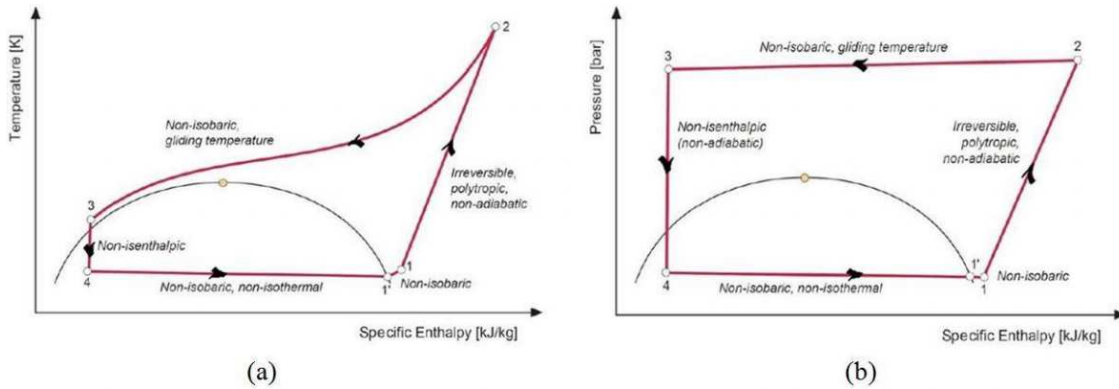


Fig. 2.14 - Real transcritical CO₂ cycle in T-h and p-h diagrams (Reulens, 2009).

3 SUPERMARKET REFRIGERATION SYSTEMS

Supermarkets are energy-consuming applications accountable for 3-4% of the annual electricity consumption in industrialized countries (Reinholdt and Madsen, 2010; Tassou et al., 2011). In relation to other commercial activities, supermarkets feature very high specific energy consumption (roughly $300\div600 \text{ kWh}\cdot\text{m}^{-2}$). As a term of comparison, office buildings consume about $150\div200 \text{ kWh}\cdot\text{m}^{-2}$ (Hafner et al., 2012). About 35-50% of the electricity is required to run the refrigerating equipment (Lundqvist, 2000).

Such an enormous need for energy leads these applications to be responsible for great indirect contributions to climate change. On the other hand, this typology of commercial buildings has become one of the most vital service facilities of modern society. In fact, the total area of supermarkets in both developed and developing countries has been greatly increasing due to many factors, such as the rapid urbanization and the significant openness to foreign investments recently occurred. This is shown in Fig. 3.1, in which the increase in both the number of food retails and total area of the stores from 2000 to 2011 is displayed. According to EY et al. (2014), the average value of supermarket share over the total food market was equal to 44% in 2000 and to 62% in 2011. Furthermore, the frozen food global market is estimated to grow in sale value by 30% comparing predicted 2020's sales with 2014's values (Persistence market research, 2014).

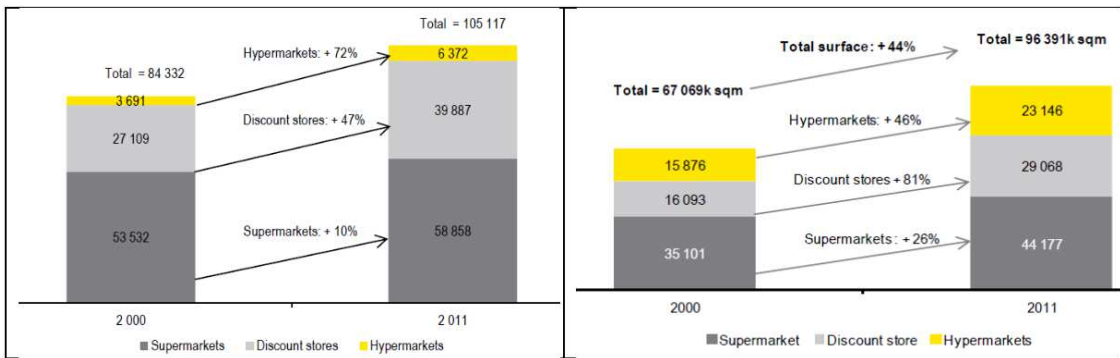


Fig. 3.1 - Growth in both number (left) and total area (right in thousands m²) of retail stores in Europe from 2000 to 2011 (EY et al., 2014).

Refrigerating plants for food preservation operate at two different levels of temperature: medium temperature (MT) and the low temperature (LT). The former ranges from -15 °C to 5 °C in order to maintain the fresh food (e.g. dairy and meat products) at 1 °C to 14 °C, whereas the latter is between -40 °C and -30 °C so as to keep the frozen products at -18 °C to -12 °C.

Depending on the size of the supermarket and on the quantity and type of food, three different refrigeration solutions can be adopted:

- stand-alone (i.e. self-contained or plug-in) units, having a cooling capacity up to 2 kW. For such applications, the refrigerating system is integrated with the display cabinet and the condenser heat is rejected into the supermarket;
- condensing units, featuring a cooling capacity up to about 25 kW, which are used for satisfying the refrigeration reclaim of a small number of display cabinets;
- centralised (or multiplex) systems, involving a cooling capacity up to about 1000 kW. The term multiplex refers to the presence of several compressors operating approximately at the same suction pressure and employing long discharge and suction lines.

Centralised refrigeration systems are categorised as direct applications (i.e. transcritical R744 systems, direct expansion units, cascade configurations) and indirect arrangements (Gullo and Cortella, 2016b; Llopis et al., 2015a; Purohit et al., 2016; Sánchez et al., 2017). The difference is due to the fact that, unlike direct technologies, in the latter a heat transfer fluid (e.g. CO₂) is cooled down by a central refrigerating system and circulated between the display cabinets and the evaporator located in the machinery room.

The present work is based on large commercial refrigeration applications and, therefore, only multiplex solutions were taken into account. However, indirect configurations were not studied, since:

- these solutions rely on low-GWP working fluids which present many drawbacks, such as safety issues (e.g. R717, R290, R1234ze(E), R152a), high cost (e.g. R1234ze(E)), various environmental problems (e.g. R1234ze(E)), poor knowledge of its performance in commercial refrigeration sector (e.g. R1234ze(E), R152a), etc.;
- “CO₂ only” systems are perceived to be permanent alternatives to HFC supermarket technologies worldwide (Shecco, 2016);
- regulations in force still allow opting for R134a in cascade arrangements in large food retails (European Commission, 2014). In spite of its noteworthy environmental impact, R134a is a well-known and safe refrigerant and thus commonly used across all refrigeration sector.

Nevertheless, in Chapter 5 the results of this investigation will be compared with those available in the open literature involving ultra low GWP-based indirect configurations.

In this chapter, the features of commercial refrigeration systems and the use of R744 in these applications are discussed, as well as a detailed literature review is also provided.

3.1 Current trend for supermarket applications

Most of the currently employed working fluids in the refrigeration sector are extremely harmful to the environment (i.e. HFCs). Despite its high GWP, R404A is still widely employed in European food retail applications. These feature high leaks of refrigerant into the atmosphere and, consequently, great direct greenhouse gas emissions. The average annual leakage rate, in fact, is estimated to be equal to 15-20% of the total charge (Hafner et al., 2014a). As for AC units and chillers, R410A is the most common refrigerant. In order to substantially cut greenhouse gas emissions related to the refrigeration sector, EU F-Gas Regulation 517/2014 (European Commission, 2014) was issued. As previously exhaustively explained, its entry into force will force the replacement of the previously mentioned working fluids with low-GWP refrigerants. Thanks to its favourable environmental, safety (i.e. non-toxic, non-flammable) and thermo-physical properties (Ge and Tassou, 2011a), R744 is one of the most promising long-term working fluids in supermarket applications. A further push towards its usage

in food retail industry is provided by “all-in-one” CO₂ configurations. These solutions, in fact, allow completely overcoming the need to find appropriate alternatives to the currently used refrigerants. Besides satisfying the cooling demands, an “all-in-one” CO₂ system also meets most of or even the whole heating need as well as the entire AC and DHW reclaims of a supermarket (Hafner et al., 2016; Hafner and Banasiak, 2016; Hafner et al., 2015; Karampour and Sawalha, 2015, 2016a, 2016b). Integrated solutions are also likely to become more affordable than separated HFC configurations (Hafner et al., 2015). For these reasons, transcritical R744 refrigeration systems have become the mainstream HFC-free technology for food retails in the last few years. As shown in Fig. 3.2, the number of the European supermarkets using “CO₂ only” refrigerating plants increased by about 117% from the end of 2011 to October 2013 (Shecco, 2014). On the other hand, the use of pure R744 solutions is still confined in Northern and Central Europe where these solutions can be more energetically beneficial than the conventional solutions (Sawalha, 2008b). In 2013 only 21 installations (Fig. 3.2), in fact, could be counted in Mediterranean countries (i.e. Spain, Italy) where further efforts need to be addressed to enhance the energy efficiency of transcritical CO₂ configurations substantially. This is also due to non-technological barriers, such as shortage of awareness and knowledge (e.g. trained installers, service technicians) and social and political factors.

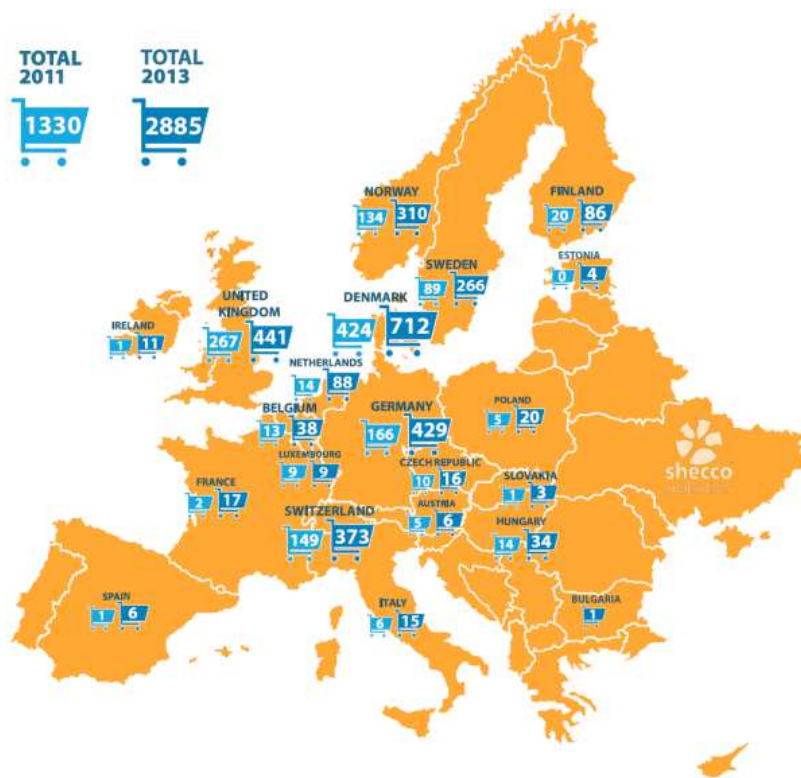


Fig. 3.2 - Market trend from 2011 to 2013 of R744 booster refrigeration systems in European supermarket applications (Shecco, 2014).

The consequences of the entry into force of the EU F-Gas Regulation 517/2014 for European food retail industry can be assessed in Fig. 3.3. It is possible to notice that the number of “CO₂ only” refrigerating plants in the EU, Norway and Switzerland is about 3 times as great as that in 2013. This entails that approximately 8% of the European supermarkets are based on pure CO₂ technologies. In addition, it is important to highlight that there are about 11000 stores employing transcritical R744 systems worldwide and approximately 8730 of them are located in Europe (Shecco, 2016). This means that the UE is the current leader when it comes to transcritical R744 technologies. Also, the number of pure CO₂ installations in Mediterranean Europe increased by roughly 8 times from 2013 to 2016. Many other supermarkets using such systems are expected to be open all across Europe in the near future (Shecco, 2016).

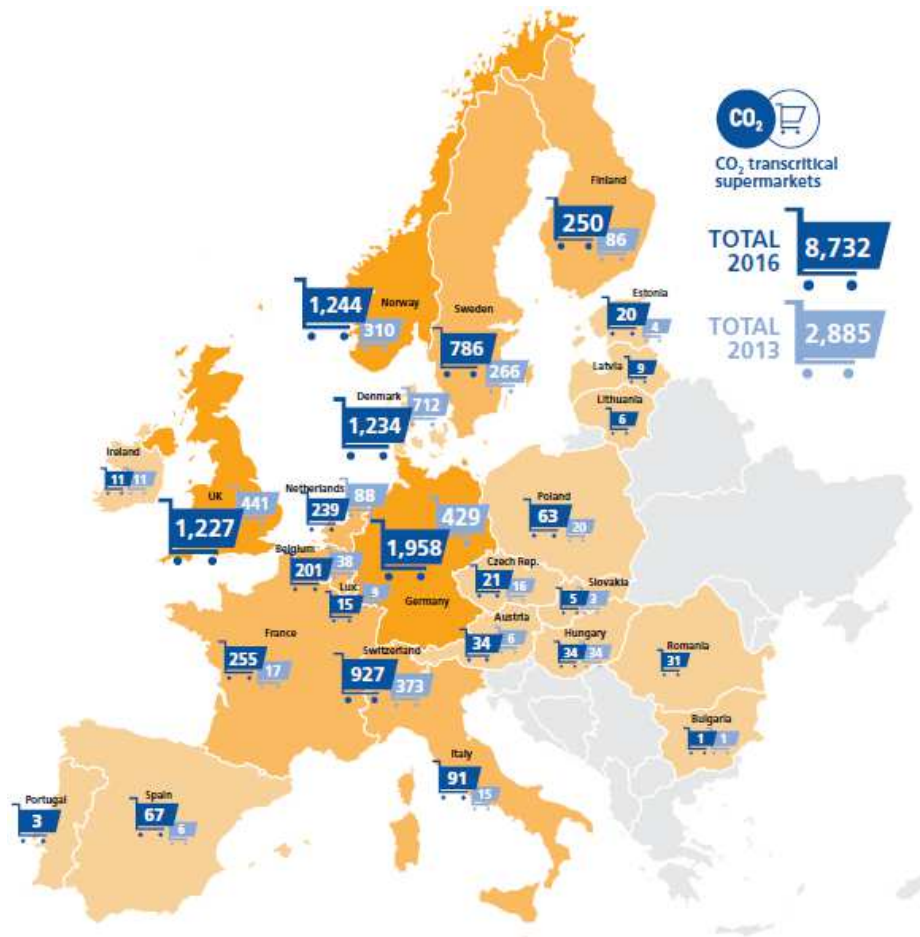


Fig. 3.3 – Growth in European supermarkets employing transcritical R744 refrigeration systems from 2013 to 2016 (Shecco, 2016).

Although the recent great increase in the number of CO₂ supermarket refrigeration systems in Southern Europe, these units are still mainly used in cold regions. This lower market penetration is due to the higher sensitivity of the CO₂ refrigeration solutions to the

cooling medium temperatures than the configurations using other working fluids and, as previously mentioned, to some non-technological barriers. From the energy point of view, a CO₂ refrigeration system working in subcritical conditions performs comparably to or even better than the one using a conventional refrigerant (Gullo et al., 2016a). On the other hand, the high discharge pressure and the large reduction in the refrigerating effect, which are reached as soon as transcritical operations occur, lead to substantially poor performance of the R744 refrigeration systems as the heat sink temperature increases. This result is clearly highlighted in Fig. 3.4 in which it is shown that a HFC-based refrigerating plant has lower energy efficiencies than a transcritical CO₂ refrigeration system up to roughly 15 °C. At higher outdoor temperatures, the latter perform much worse than the currently employed solutions.

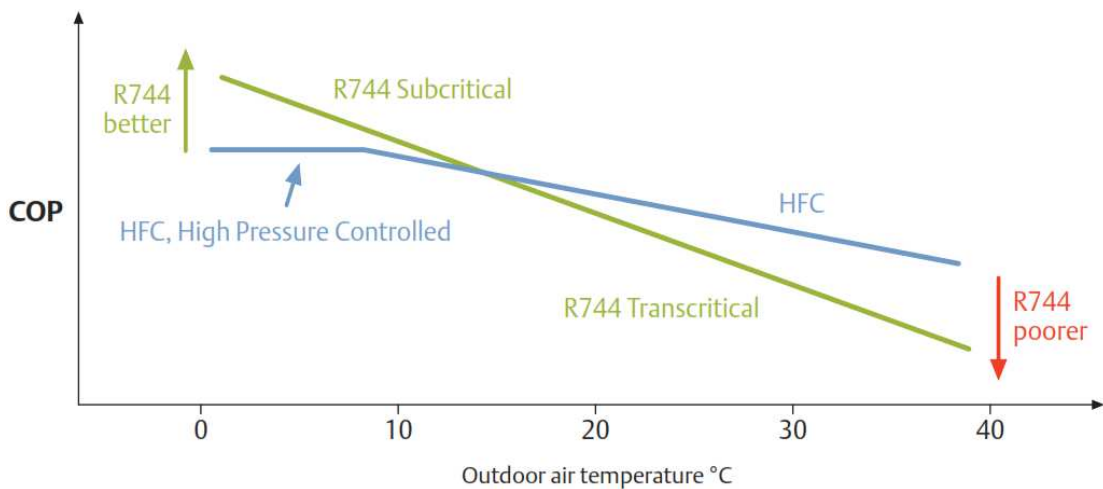


Fig. 3.4 – Effect of the external temperature on COP of both a transcritical CO₂ refrigeration system and a HFC-based refrigerating plant (EMERSON Climate Technologies, 2010).

Therefore, the re-positioning of the so-called “CO₂ efficiency equator” (blue line in Fig. 3.5) has become the most important key research area with respect to the commercial pure R744 refrigeration systems. Above this efficiency limit, “CO₂ only” supermarket refrigeration units result energetically competitive over the traditional HFC systems, i.e. in the locations characterized by a yearly average outdoor temperature below about 15 °C (Matthiesen et al., 2010). The opposite result is obviously obtained below the “CO₂ efficiency equator”.

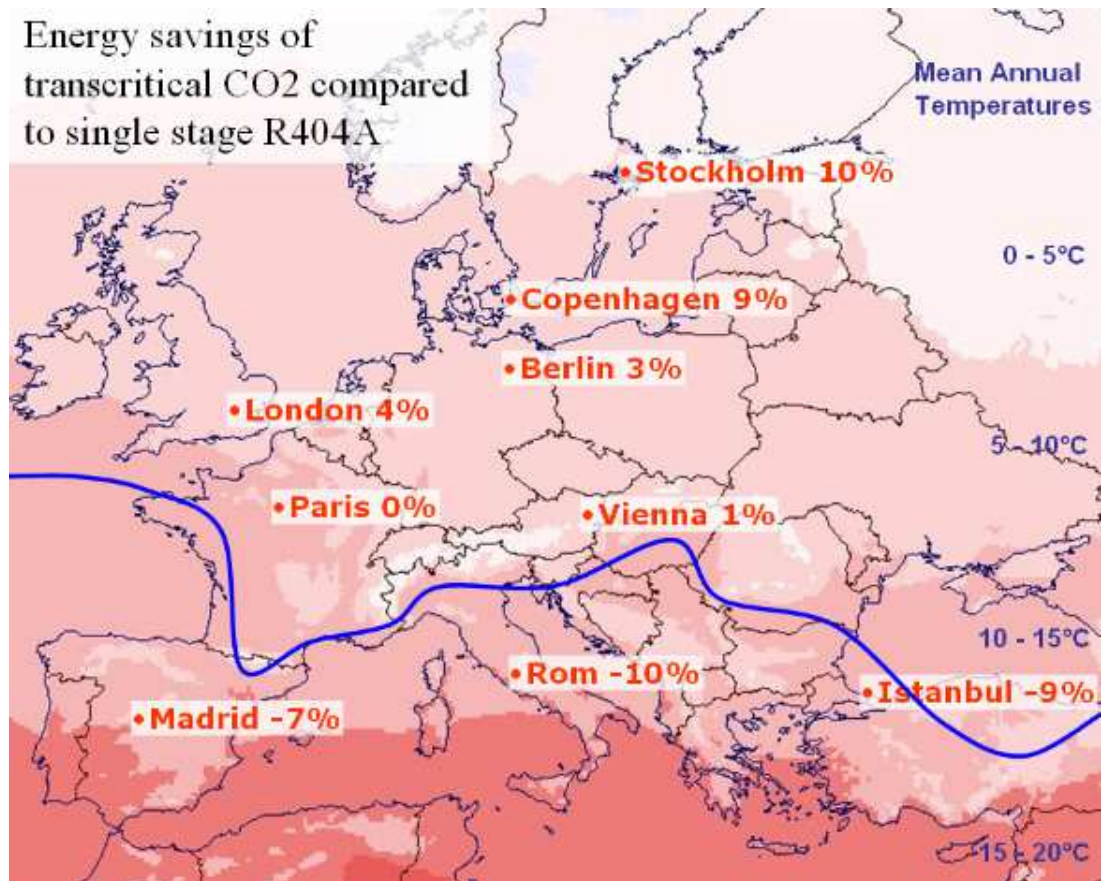


Fig. 3.5 - Energy saving of a single-stage R744 refrigeration system over a R404A direct expansion solution in different locations (Matthiesen et al., 2010).

A strong argument in favour of pure R744 solutions is that they exhibit the greatest enhancement potentials in terms of energy conservation, integration with the HVAC unit and cost-effectiveness (Hafner et al., 2014a). The heat recovery implementation allows effectively producing hot and warm water at various levels of temperature and for different purposes, such as DHW production (70-50 °C), space heating (50-40 °C), fresh air pre-heating or snow melting (40-30 °C). Reinholdt and Madsen (2010) and Tambovtsev et al. (2011) suggested that satisfying payback times can be achieved by transcritical R744 refrigeration systems putting some heat recovery into effect. In fact, significant prospects for both a noteworthy cost reduction and a significant drop in the electricity consumption can be attained by integrating the refrigerating plant with the heating unit. These results can be achieved by any pure CO₂ supermarket refrigeration solution independently from the location, as well as from the store and heating system size. Also, it is worth remarking that the heating and the air conditioning units are responsible for about 20% of the total consumption in a supermarket (Cecchinato et al., 2010b; Hafner et al., 2014a). Bearing in mind this, the additional coupling with the AC

unit would lead to further economic benefits in warm climates provided that a highly efficient technological expedient is employed. This is due to the fact that it is necessary to energetically offset the heavy AC reclaims required for long periods over the year in such climate contexts. This result was theoretically proved by Karampour and Sawalha (2015) who showed that an “all-in-one” CO₂ booster configuration with parallel compressor and integrated with the AC unit is energetically justifiable at outdoor temperatures below 20-25 °C (i.e. cold climates). On the other hand, the authors also pointed out that great results can be achieved in heating modes. At a later time, these outcomes were experimentally confirmed with the aid of some field data gathered in a small-medium size supermarket located in the middle of Sweden (Karampour and Sawalha, 2016a, 2016b). Besides being able to provide the whole AC demand, in fact, this refrigerating plant also features enhancements in COP_{AC} and in COP_{tot} respectively by 25% and by 8% over the solution without parallel compression at outdoor temperatures up to 24 °C. Furthermore, the authors also estimated performance similar to or better than conventional heat pumping systems in heating modes. Cecchinato et al. (2012) showed that, depending on the boundary conditions, the integrated CO₂ refrigerating plants can accomplish similar total energy consumption to that of separated HFC-based configurations.

3.2 Transcritical R744 configurations

Many layouts as early “CO₂ only” refrigeration systems for supermarket applications have been suggested (Cecchinato et al., 2009, 2012; Kaiser and Fröschle, 2010; Sawalha, S., 2008b, 2013; Giroto et al., 2004; Tassou et al., 2011; Matthiesen et al., 2010). Giroto et al. (2004) estimated that a R744 refrigerating plant consumes 10% more energy than a R404A multiplex system in the North of Italy. The authors also proposed some possible enhancements, such as decreasing the approach temperature of the gas cooler, using two-stage compression for the MT system and drawing the vapour from the liquid receiver. The centralized R744 systems theoretically studied by Sawalha (2008b) bring the annual energy consumption from 4% down to 12% in Stockholm (Sweden) in comparison with a R404A direct expansion configuration. The author also demonstrated that these units are not appropriate substitutes for HFC solutions in warm climate contexts. The extensive evaluation by Cecchinato et al. (2009) on various transcritical CO₂ refrigeration units pointed out that the configurations based on two-stage throttling and two-stage compression are promising systems in extreme operating conditions. All-CO₂ cascade

refrigeration systems took hold owing to an easily predictable shift from subcritical CO₂ units (i.e. cascade/indirect arrangements) to transcritical CO₂ systems so as to replace the environmentally harmful refrigerants used in the former. In addition, these permitted also uptaking the limitations related to conventional cascade solutions, like service and installation complexity (Tassou et al., 2011), as well as they make the oil return management easier (Matthiesen et al., 2010; Tassou et al., 2011). However, due to many factors, such as poor performance, extra costs, complicated control strategy, etc., the booster-based architectures have become the most popular “CO₂ only” systems in commercial refrigeration sector. Also, the EU F-Gas Regulation 517/2014 has been a substantial driving force for the enormous technological development experienced by commercial CO₂ booster technologies. This, besides discouraging the usage of HFCs, has led such solutions to have similar to or slightly higher (5-10%) total installation costs than HFC-based units.

3.2.1 Conventional transcritical booster system

A more economic and energy advantageous configuration compared to the early proposed “CO₂ only” units is the so called transcritical CO₂ booster refrigeration system (Fig. 3.6).

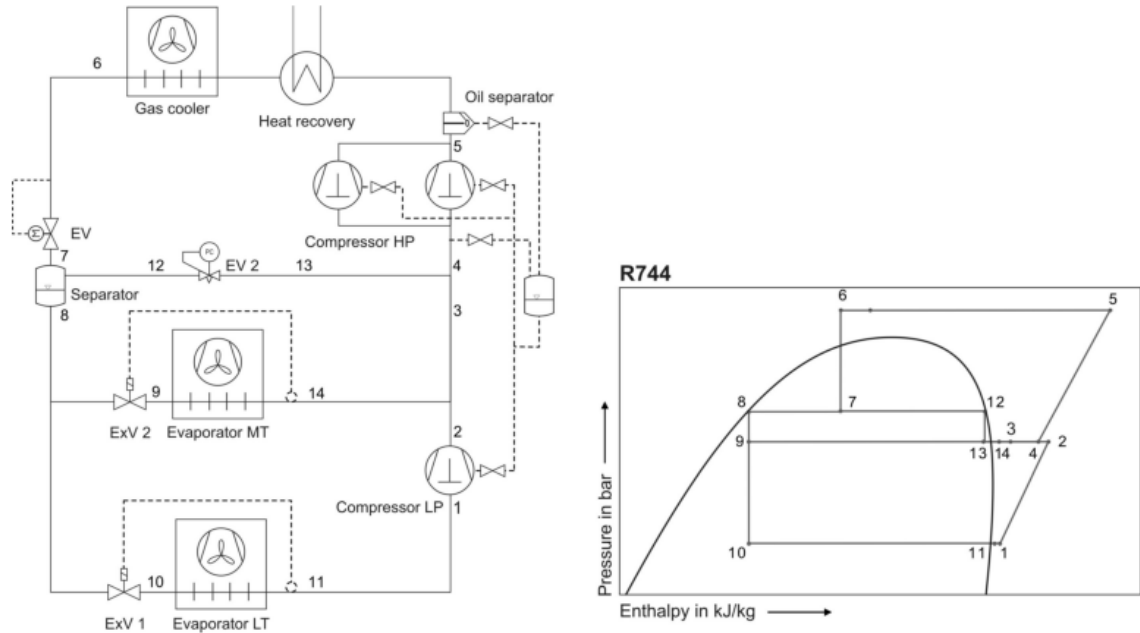


Fig. 3.6 - Conventional R744 booster refrigeration system implementing heat recovery and corresponding p-h diagram (Kaiser and Fröschle, 2010).

Similarly to the all-CO₂ cascade arrangement, this technology also involves R744 as the only refrigerant. The term “booster” refers to the low stage (LS) compressors behaving as boosters in order to raise the refrigerant pressure. Such a solution features four pressure

levels, i.e. high pressure at the gas cooler/condenser, the intermediate pressure (IP) at the separator, the medium pressure (MP) at the MT display cabinets and the low pressure (LP) at LT evaporators. The HP heat exchanger acts as a condenser at low outdoor temperatures, otherwise it operates as a gas cooler in transcritical conditions. In the latter case, the ingoing CO₂ undergoes a reduction in temperature without involving no phase change. The outgoing fluid from the gas cooler/condenser is throttled and split into its vapour and liquid components within the separator. The vapour (i.e. flash gas) is then isenthalpically expanded from IP to MP by means of the flash gas by-pass valve. This refrigerant fraction is compressed by the HS compressor rack along with the mass flow rates exiting both the LS compressors and the MT display cabinets to HP. As the flash gas by-pass valve controls the liquid receiver pressure (and thus the correct feeding of the evaporators), this component plays a crucial role in the performance of such a solution. Also, Sawalha et al. (2015) showed that increases in COP_{tot} up to 16% can be achieved by removing the flash gas from the liquid receiver. The booster refrigeration cycle has been extensively investigated in the last few years (Ge and Tassou, 2011a, 2011b; Sharma et al., 2015; Shilliday, 2012). Nowadays this layout is widely employed in Northern Europe and represents the first generation of transcritical CO₂ refrigeration systems. The first prototype was developed in the framework of the EU Project “Life” at Danish Technological Institute in June 2006 and installed in a Danish supermarket in March 2007. An energy saving and a reduction in the environmental impact respectively equal to about 4% and to about 52% were estimated over a parallel R404A system (European Commission, 2008). The system has been operating since then with no relevant problems, leading to a wide spread of this technology in the other countries. By 2009, in fact, 200 installations in Northern Europe could be counted (Matthiesen et al., 2010). Ge and Tassou (2011b) demonstrated that a R744 booster system has similar energy consumption than a R404A direct expansion unit in a retail store located in Glasgow (UK). Sharma et al. (2015) experimentally studied the performance of a laboratory-scale R744 booster solution so as to evaluate the possible energy benefits for American food retails. The filed measurements collected by Sawalha et al. (2015) in five Swedish supermarkets revealed that COP_{S_{tot}} of “new” pure CO₂ systems (i.e. booster layouts) were 35-40% greater than those of the “old” ones (i.e. separated units). At a later time, Sawalha et al. (2017) also disclosed that these “new” transcritical R744 solutions can outperform HFC systems at external temperatures below 24 °C. In addition, such technologies were found to reduce

the energy consumption by 20% compared to HFC systems in an average size food retail in Stockholm (Sweden).

It is important to notice that due to the high values of temperature lift, the largest irreversibilities occurring in a transcritical CO₂ unit can be associated with the expansion valve (Fazelpour and Morosuk, 2014). This issue can be partially overcome by adopting some technological expedients, like a subcooler (or an internal heat exchanger), a liquid receiver at intermediate pressure, an ejector or an expander. For this reason, more recently many researchers have focused their attention on more promising solutions mainly derived from the basic booster configuration and employing different technologies, such as the dedicated mechanical subcooling, the parallel compression, the overfed evaporators and the multi-ejector concept (Hafner et al., 2014b). In fact, as mentioned above, the use of CO₂ supermarket refrigeration systems in warm climates requires specific technical solutions to make them competitive with conventional HFC-based plants.

3.2.2 Transcritical booster system with dedicated mechanical subcooling

The configuration with dedicated mechanical subcooling represents an interesting solution in order to drop the energy consumption of R744 refrigeration systems which are run in warm climates (Beshr et al., 2016; Hafner and Hemmingsen, 2015; Hafner et al., 2014d, 2014b; Gullo et al., 2016b, 2016a; Llopis et al., 2016b; Llopis et al., 2015b; Eikevik et al., 2016; Mazzola et al., 2016). Such a solution, which is schematised in Fig. 3.7, includes an additional vapour-compression refrigeration unit (i.e. a self-contained unit). This cools down the CO₂ leaving the gas cooler/condenser by promoting the vaporization of the working fluid flowing through the subcooler, which is typically a plate heat exchanger. As a consequence, a decrease in the refrigerant quality entering the liquid receiver and thus an enhancement in the overall performance are achieved. Furthermore, the optimal gas cooler pressure is also reduced (Gullo et al., 2016a; Llopis et al., 2015b) in comparison with the conventional configuration, allowing a further reduction in the total energy consumption.

Fig. 3.8 compares a conventional booster system (dashed line) with a booster solution with dedicated mechanical subcooling (solid line) in a $\log(p)$ - h diagram. The difference is represented by the thermodynamic transformation indicated as 2–3, which describes the subcooling process before CO₂ enters the HP expansion valve (3–4). On the contrary, the refrigerant exiting the gas cooler/condenser is directly throttled (2–4') in a conventional booster solution.

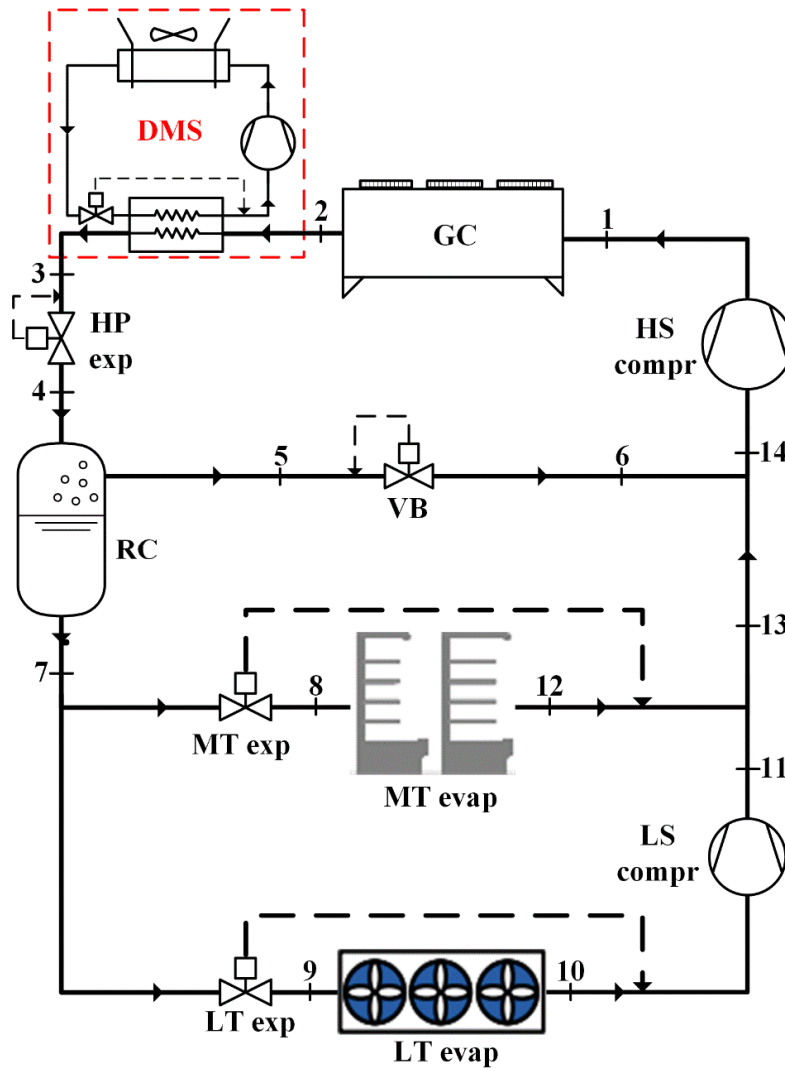


Fig. 3.7 - Schematic of a R744 booster refrigeration system with dedicated mechanical subcooling.

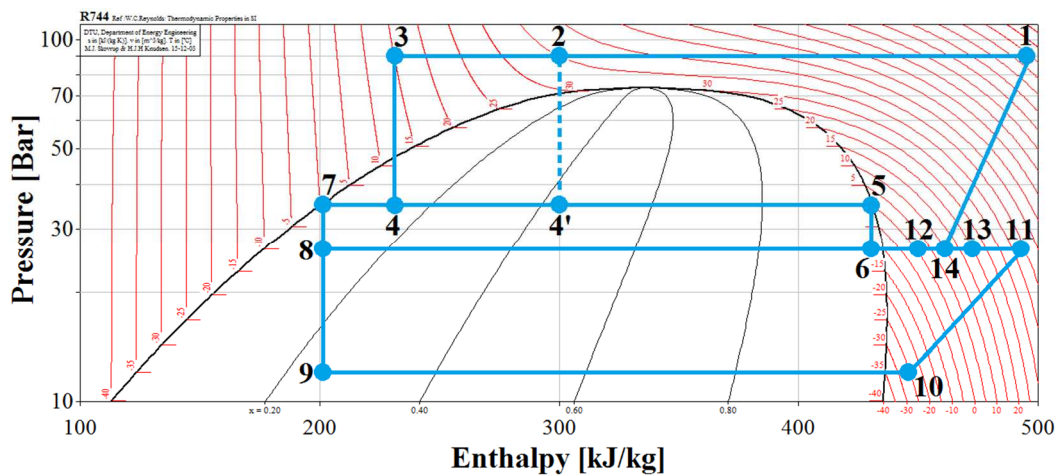


Fig. 3.8 - $\log(p)$ - h diagram of R744 booster refrigeration systems with and without dedicated mechanical subcooling.

Thornton et al. (1994) proved the existence of an optimal subcooling temperature. This is mainly influenced by the temperature at which the heat of condensation is rejected into the external heat sink and the one of the heat source from which vaporization heat is extracted. The experimental investigation by Qureshi and Zubair (2013) showed that a subcooling loop can improve both the cooling capacity and the exergy efficiency of a basic system. Llopis et al. (2015b) evaluated the potential enhancements which could be fulfilled by utilizing a subcooling cycle on the part of both a conventional CO₂ system and a CO₂ cycle with double-stage compression and intercooling. At the outdoor temperature of 30 °C and with a degree of subcooling of 5 °C, the COP of the former and that of the latter respectively increase by 13.7% at the evaporating temperature of -5 °C and by 13.1% at -30 °C. The authors also suggested that the achievable improvements were independent from the working fluid of the subcooling loop. Llopis et al. (2016b) demonstrated experimentally that enhancements in COP ranging from 6.9% to 30.3% at the evaporating temperature of -10 °C can be attained by adopting such a technology. The laboratory tests performed by Beshr et al. (2016) at steady state conditions were employed to build an experimentally validated simulation model of a CO₂ booster refrigeration system with R134a dedicated mechanical subcooling. According to Hafner and Hemmingsen (2015), a R290 dedicated mechanical subcooling loop reduces the annual electricity consumption down to 23% in comparison with a R404A direct expansion system, depending on the selected location. The field measurements gathered by Mazzola et al. (2016) suggested that energy savings by approximately 25% can be achieved over a conventional CO₂ booster system. The estimation was made by considering outdoor temperatures ranging from 40 °C to 48 °C. In addition, the authors evaluated a drop in the heat rejection pressure by about 10 bar at 40 °C. Eikevik et al. (2016) suggested the use of a R290 subcooling loop in which the R290 is employed as the cooling medium for the CO₂ gas cooler. This allows the CO₂ refrigeration system to perform in subcritical conditions in any running mode. In addition, the authors also assessed increase in COP:

- up to 15% by rising the velocity of the air flowing through the CO₂ condenser;
- from 8.84% at 18.7 °C to 6.91% at 40 °C by opting for a new design of the CO₂-R290 condenser.

It is important to highlight that the usage of the subcooler leads to a significant growth in the investment cost and noteworthy problems in terms of reliability.

3.2.3 Transcritical booster system with parallel compression

In a conventional CO₂ booster configuration, the flash gas undergoes a throttling process to reduce its pressure to MP and, at a later time, it is drawn by the HS compressors and compressed to HP. The performance of pure R744 refrigeration systems are thus noticeably deteriorated in extreme operating conditions, as the amount of flash gas generated in the liquid receiver (RC) increases significantly with rise in outdoor temperature. Fig. 3.9 shows this phenomenon, highlighting as in transcritical operations the mass flow rate of the flash gas is on average equal to 45% of the total mass flow rate. It is also pointed out that both the total and the vapour mass flow rate increase suddenly at temperatures over 38 °C. This is due to the high gas cooler outlet temperature and thus to the high quality of the refrigerant going into RC. The amount of vapour becomes equal to 50% of the refrigerant total mass flow rate at the external temperature of 40 °C. This drawback can be partly overcome by employing one or more auxiliary (or parallel) compressor(s) (AUX) to compress a part of or the total amount of the flash gas from IP to HP (Fig. 3.10). As a result, a relevant energy saving can be attained in comparison with a conventional booster system. Alternatively, the auxiliary compressor(s) can be linked to the suction line of the HS compressors by using a 3-way valve. This permits benefiting from having a further frequency controlled compressor at relatively high cooling needs and moderate external temperatures (Javerschek et al., 2016).

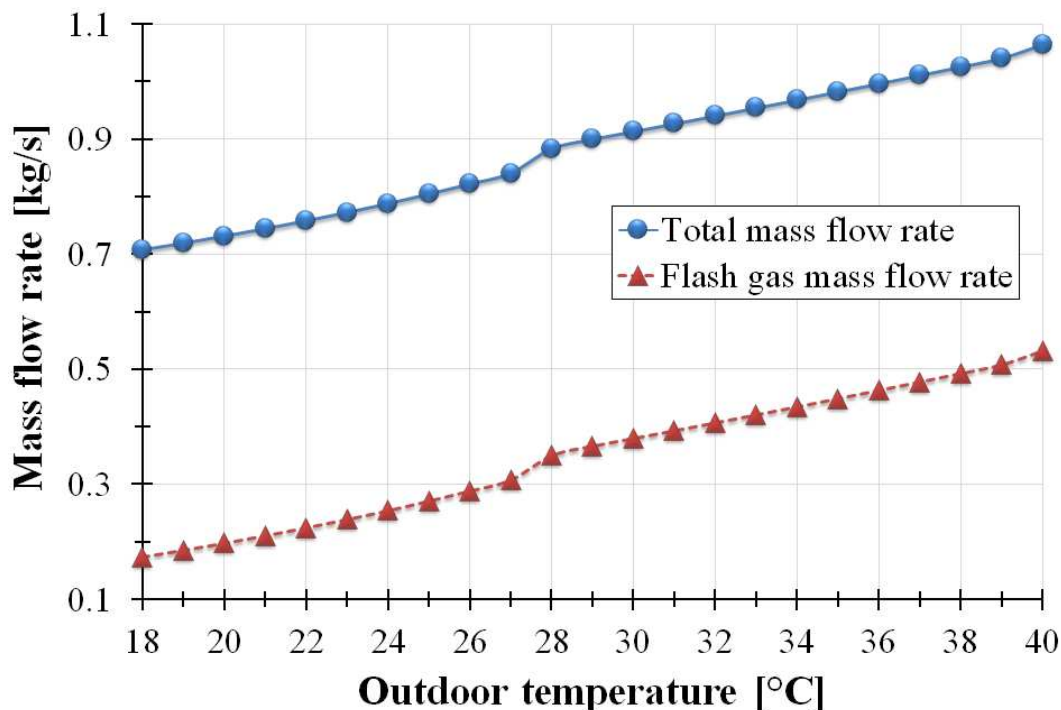


Fig. 3.9 - Total mass flow rate and flash gas mass flow rate of a transcritical R744 booster refrigeration system ($t_{MT} = -10$ °C, $t_{LT} = -35$ °C).

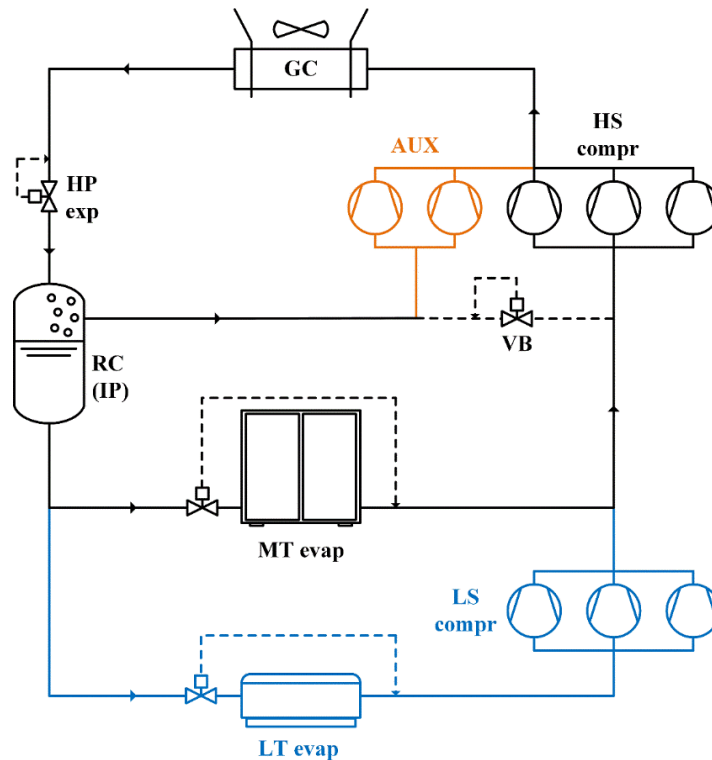


Fig. 3.10 - Schematic of a R744 booster refrigeration system with parallel compression.

Since 2009 this configuration has supplanted the conventional booster unit as the benchmark for commercial pure CO₂ solutions. The adoption of the parallel compression represents the first step towards the use of R744 in warm regions. In particular, this configuration (including the recovery of some heat for DHW production and space heating) represents the second generation of CO₂ refrigeration systems in food retail industry. The $\log(p)$ - h diagram of the CO₂ solution with parallel compressor is shown in Fig. 3.11.

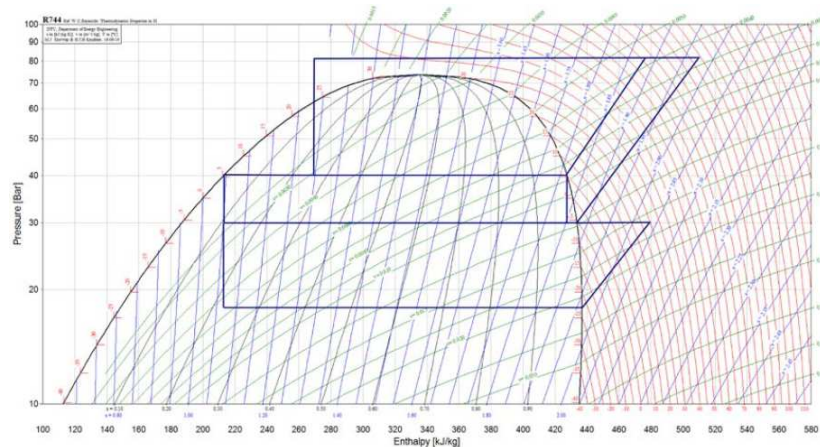


Fig. 3.11 - $\log(p)$ - h diagram of a R744 booster refrigeration system with parallel compression.

The importance of the intermediate pressure as an optimization parameter of the performance of such a configuration was highlighted by Bell (2004) and by Minetto et al. (2005). Its optimum value is more influenced by the evaporator temperature rather than the heat rejection pressure, as demonstrated by Sarkar and Agrawal (2010). Despite this, the current tendency is to keep it fixed (or slightly variable) in order to avoid high pressure values inside the supermarket and make the expansion process more stable (Minetto et al., 2015). According to Sarkar and Agrawal (2010), the parallel compression is a more effective solution to improve the efficiency of a single-stage CO₂ cycle than both the configuration with two-stage compression and flash gas by-pass and the one with parallel compression and subcooler. Chiarello et al. (2010) performed an experimental campaign and implemented a theoretical model in order to prove the obtainable enhancements. The experimental apparatus, although it showed interesting results, was mainly run in subcritical conditions. A test rig was built by Minetto et al. (2005) to prove the feasibility of this solution and the possibility to overcome the technological issues associated with it, such as the lubricant oil return. The authors also showed theoretically that a CO₂ system with parallel compression can accomplish good results in terms of both cooling capacities and COPs over a conventional unit. Different control strategies and their influence on the annual energy efficiency for parallel compression-based CO₂ solutions were experimentally and analytically investigated by Javerschek et al. (2016). The results revealed that for a fully integrated solution the optimization of their intermediate pressure in warm cities (i.e. Athens) leads to an increase in Seasonal Energy Efficiency Ratio (SEER) by 4.2% over the same solution with an intermediate pressure fixed to 40 bar. On the other hand, these benefits are negligible in locations characterized by more moderate climatic conditions (i.e. Edinburgh). Da Ros (2005) compared a conventional single-stage R744 cycle operating at the evaporating temperature of -10 °C with a solution with parallel compression and a system with double-stage compressor. The author took into account both a constant and a freely variable pressure difference between the gas cooler and the liquid receiver. In all the evaluated cases, the system with the two-stage compressor performs better than the other ones. A theoretical model was implemented by Chesi et al. (2014) to find out the best operating conditions as well as the effect of the liquid separator efficiency, the intermediate pressure and the compressors volumetric flow ratio on the performance of the overall system. The authors asserted that the largest enhancements in cooling capacity arise at gas cooler pressures different from those at which maximum COPs occur. An experimental investigation was also implemented by

considering different high pressures, gas cooler outlet temperatures and evaporating temperatures. Both the analyses confirmed that the use of an auxiliary compressor can significantly improve the performance of a conventional CO₂ refrigeration system. Pressure drop in the suction line, unintentional superheating and a faulty separation between vapour and liquid within the receiver can worsen the performance of the real cycle strongly. The operating conditions which guarantee an increase in the efficiency of a single-stage CO₂ unit using parallel compression by at least 10% over a single-stage CO₂ unit with flash-gas injection were studied by Fritschi et al. (2016). This investigation was based on the development of a numerical model which was validated against some experimental data. Sharma et al. (2014) demonstrated that such a configuration is energetically justifiable over a R404A direct expansion solutions at annual average temperatures up to approximately 14 °C. Gullo et al. (2015) implemented a comparative thermodynamic analysis between a basic transcritical CO₂ refrigerating plant and the one including an auxiliary compressor. The evaluation was implemented at cooling medium temperatures ranging from 30 °C to 50 °C. In comparison with the conventional unit, the advanced system exhibited on average a reduction in the power input by 18.7% and a decrease in the irreversibilities taking place in the throttling valve by 50%, respectively. An average increase in the total purchased equipment cost (PEC) by 23.4% and an average decrement by 6.7% of the final cost of the product were also observed. The study by Polzot et al. (2016c) revealed that the adoption of a parallel compressor is necessary in order to make a R744 booster configuration coupled with the heating system energetically competitive. On the other hand, the usage of an additional air-cooled evaporator as a heat source allows the system to satisfy the whole heating demand for the selected supermarket. The assessment was implemented in two different Italian climatic conditions. According to Polzot et al. (2016b), the integration of a R744 refrigeration system using parallel compression with a fire prevention tank permits attaining similar annual energy consumption to that of a R134a/CO₂ cascade system in Northern Italy. However, energy savings up to 5% over a separated solution can be achieved by thermally coupling a heat pump unit with the previously mentioned solution (Polzot et al., 2016a).

3.2.4 Transcritical booster system with overfed evaporators

The overfeeding of the MT display cabinets can be successfully achieved by adopting some liquid ejectors (LEJ), as shown in Fig. 3.12. The aim of LEJ is to pump some liquid collected in the receiver at MP back to that at IP.

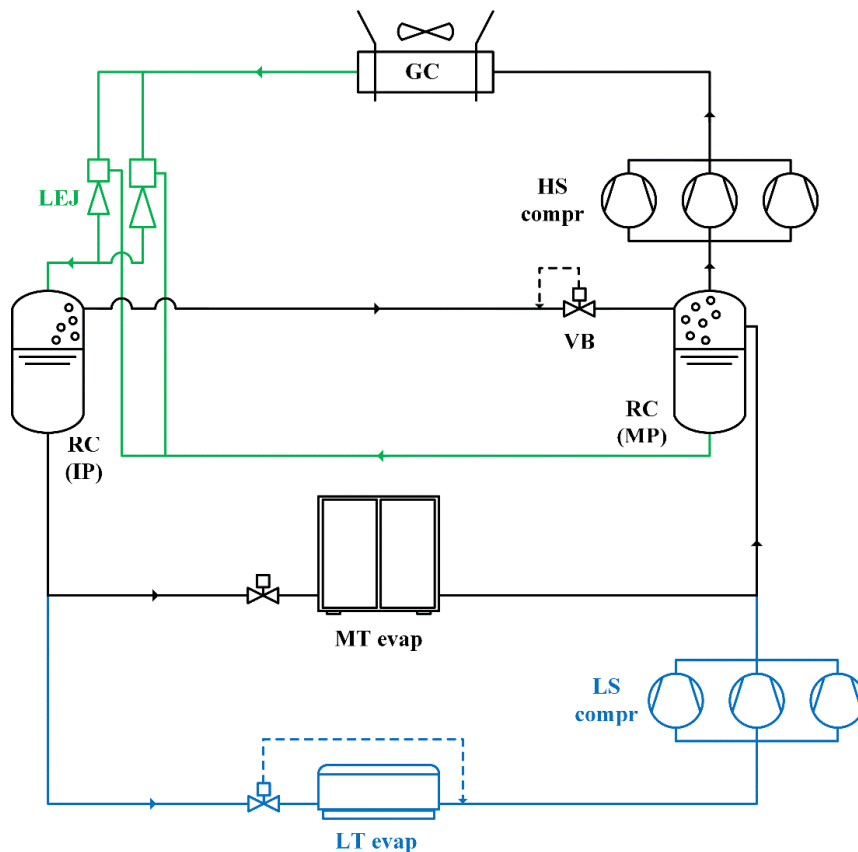


Fig. 3.12 - Schematic of a R744 booster refrigeration system with MT overfed evaporators based on the adoption of liquid ejectors.

The same purpose can be achieved by replacing LEJ with a pump and a HP expansion valve, as shown in Fig. 3.13 (Giroto, 2012). It is important, in fact, to highlight that in both cases the main energy benefit can be attributed to the MT increment. In addition to this, the pump power input in a system similar to that represented in Figure 3.13 can be neglected (Giroto, 2012; Minetto et al., 2014a).

The advantages of overfeeding an evaporator can be explained with the aid of Fig. 3.14. Being the air inlet temperature imposed, the adoption of a certain degree of superheating in dry-expansion evaporators implies that the saturation temperature at these heat exchangers has to be pushed down (Fig. 3.14a). Thus the possible disappearance of the superheating would permit raising their working temperature (3.14b). In fact, the large amount of liquid collected in the IP liquid receiver by employing LEJ (Fig. 3.12) or a pump (Fig. 3.13) permits the refrigerant to enter the MT evaporators with a very low value of quality. On account of this, in comparison with a dry-expansion evaporator, the refrigerant leaving an overfed evaporator is in two-phase conditions with a high vapour content (Minetto et al., 2014a).

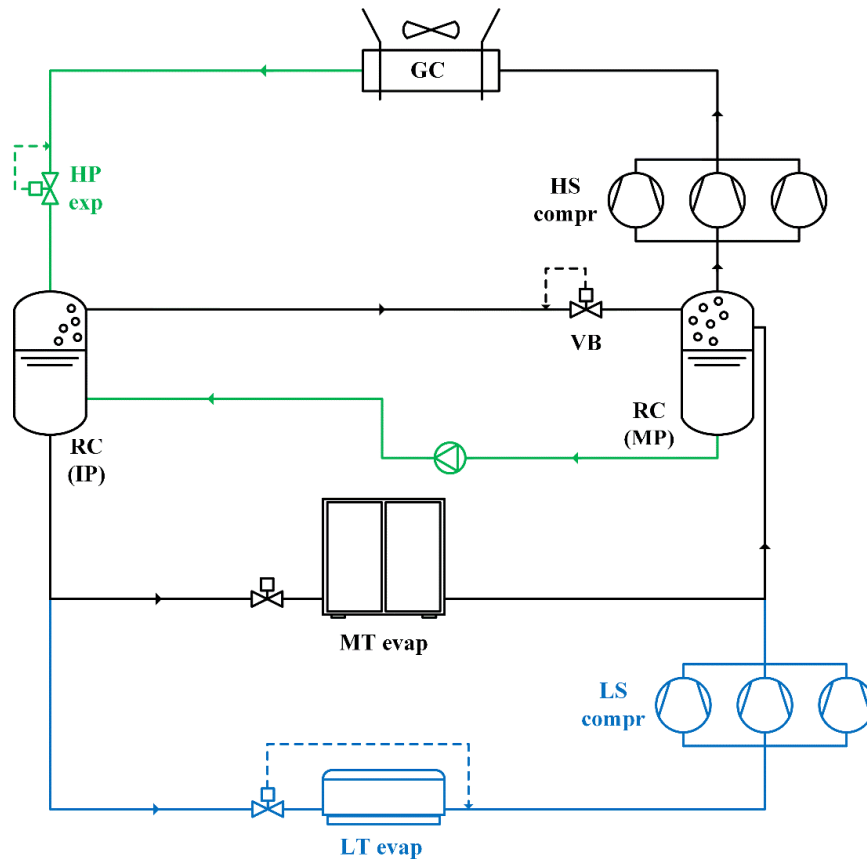


Fig. 3.13 - Schematic of a R744 booster refrigeration system with MT overfed evaporators based on the adoption of a pump.

Thanks to the absence of the superheating, the refrigerant-side heat transfer does not drop as typically happens in the superheated region. Therefore, the entire heat transfer area is optimally used being completely at the evaporation temperature. In fact, although the superheating process involves a small portion of the heat transfer process occurring in a dry-expansion evaporator, it penalizes the global heat transfer performance substantially. This is due to the fact that the overall heat transfer coefficient associated with a one-phase process is much lower than that related to a phase transition process. It is worth mentioning that, in comparison with a conventional evaporator, the heat transfer area of an overfed evaporator does not need to be enlarged. In fact, the substantial enhancement in its overall heat transfer coefficient counterbalances the growth in its heat transfer area due to the decrease in the heat exchanger temperature difference. The energy advantages associated with overfed evaporators by means of LEJ were experimentally evaluated by Minetto et al. (2014a). The authors pointed out that the compressor power input can be reduced approximately by 13% in relation to a conventional solution. The assessment was fulfilled at the air temperature of about 0 °C and at the outdoor temperature of about 16 °C.

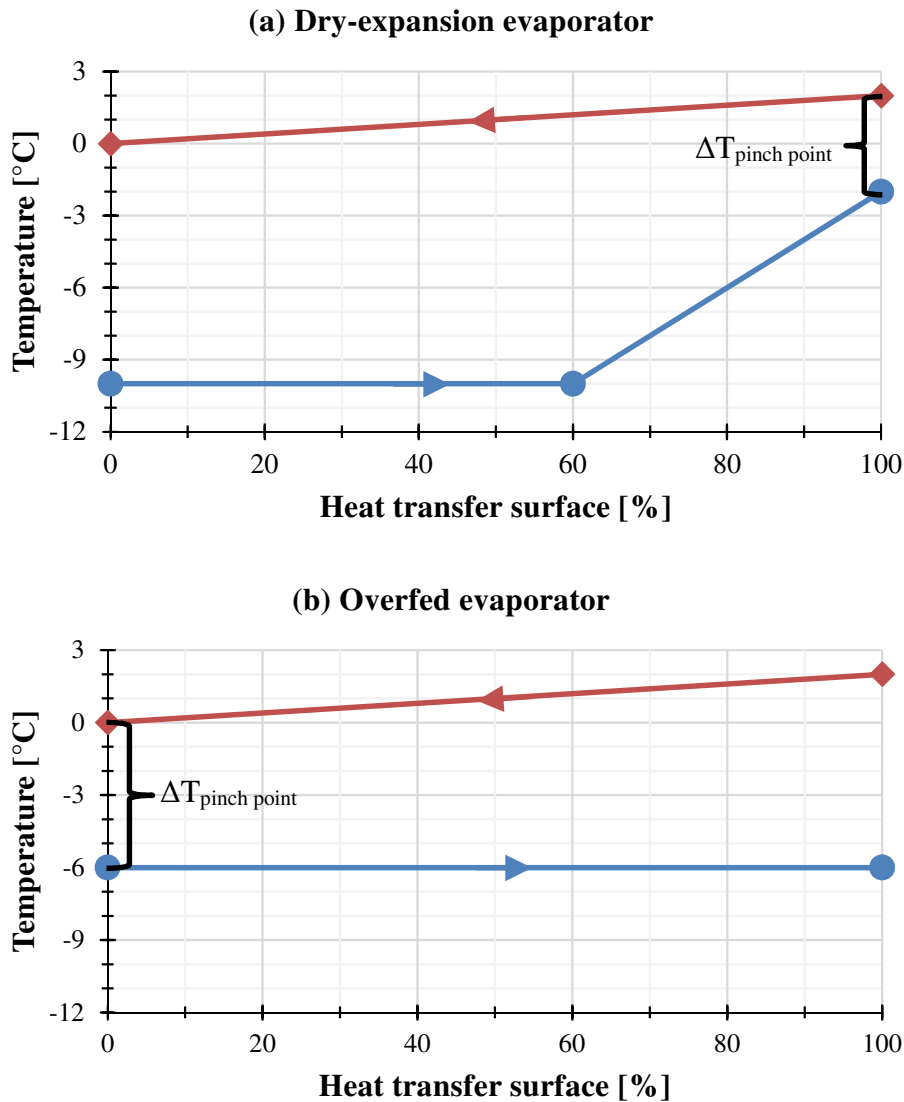


Fig. 3.14 - Typical operating conditions for a dry-expansion evaporator (a) and for an overfed evaporator (b).

As a final remark as regards real applications, it is worth remarking that, unlike ejectors, pumps are very expensive components, whose reliability is also strongly questionable in supermarket refrigeration systems. The only reason why the solution in Fig. 3.13 was investigated in the present study rather than that in Fig. 3.12 is for its much greater ease to simulate it with an insignificant difference in terms of performance.

3.2.5 Combined transcritical booster systems

The technology involving a mechanical subcooler loop can be combined with that of the parallel compression in order to obtain the benefits associated with both solutions (Fig. 3.15).

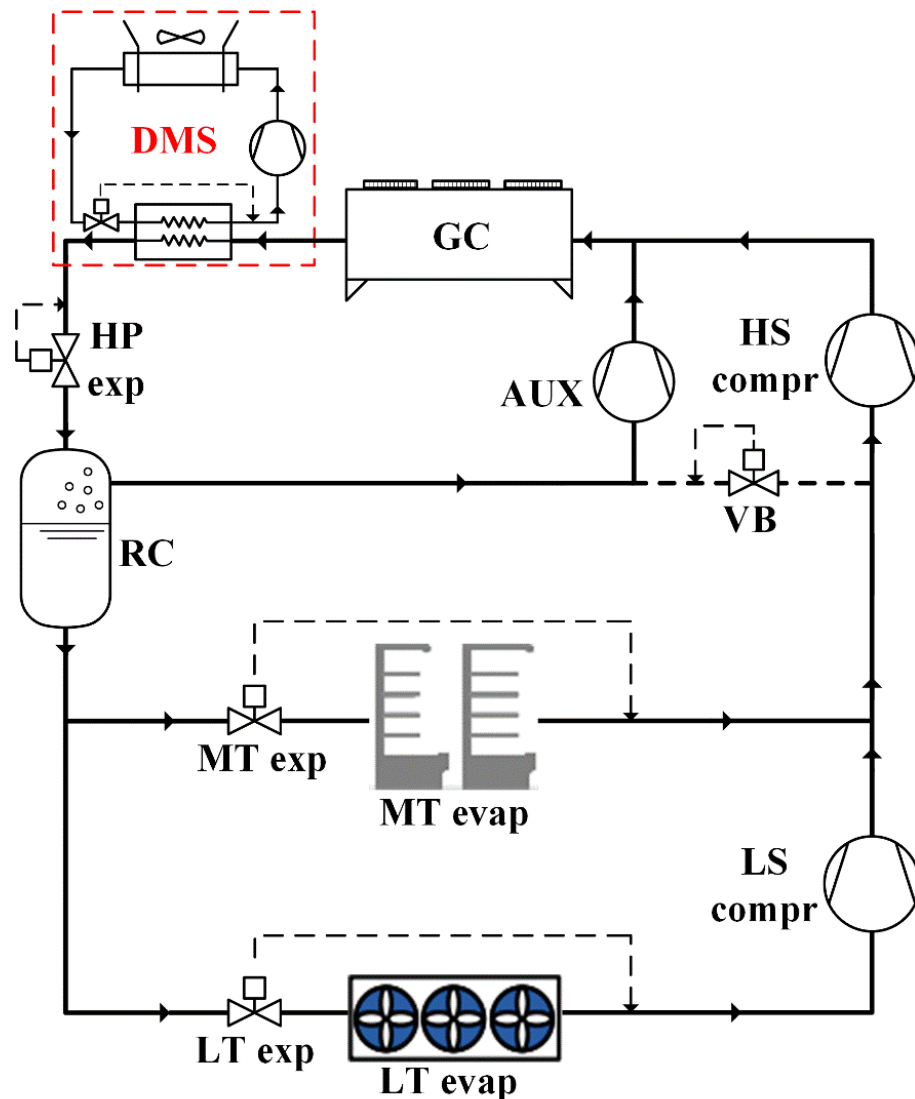


Fig. 3.15 - Schematic of a R744 booster refrigeration system with dedicated mechanical subcooling and parallel compression.

A similar system including DHW production was installed in a hypermarket located in Alzira (Spain) in 2013 (Frigo-Consulting LTD, 2014). It was claimed that energy savings up to 10% could be achieved in comparison with a HFC-based solution. Also, the gas cooler exit temperature was maintained below 26 °C all year round.

The usage of an auxiliary compressor can also be applied to a CO₂ refrigerating plant with MT overfed display cabinets, as shown in Fig. 3.16.

The thermodynamic cycle of a R744 refrigeration system with parallel compression (dotted lines) is compared with that of a R744 refrigeration system with parallel compression and MT overfed evaporators (solid lines) in a $\log(p)$ - h diagram in Fig. 3.17. For the latter, it is possible to notice the increase in the suction pressure of both the HS compressors and the auxiliary compressor.

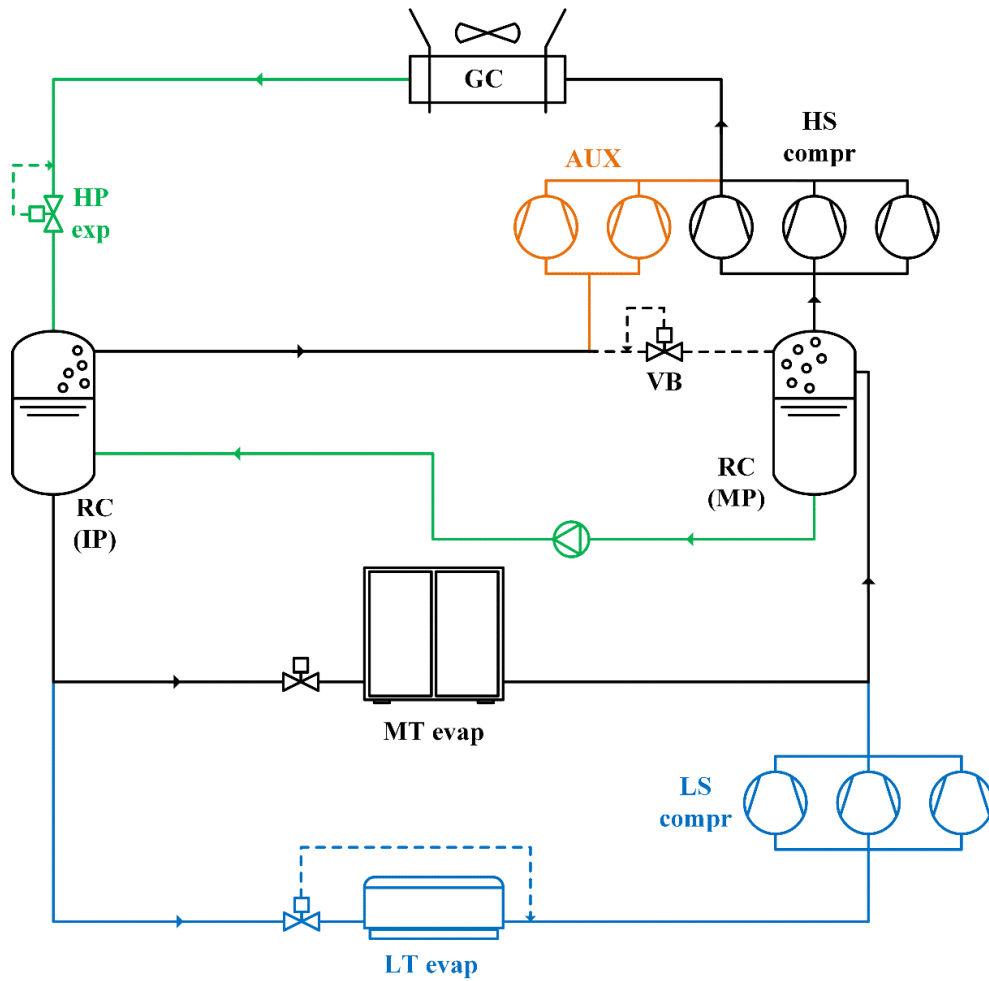


Fig. 3.16 - Schematic of a R744 booster refrigeration system with MT overfed evaporators and parallel compression.

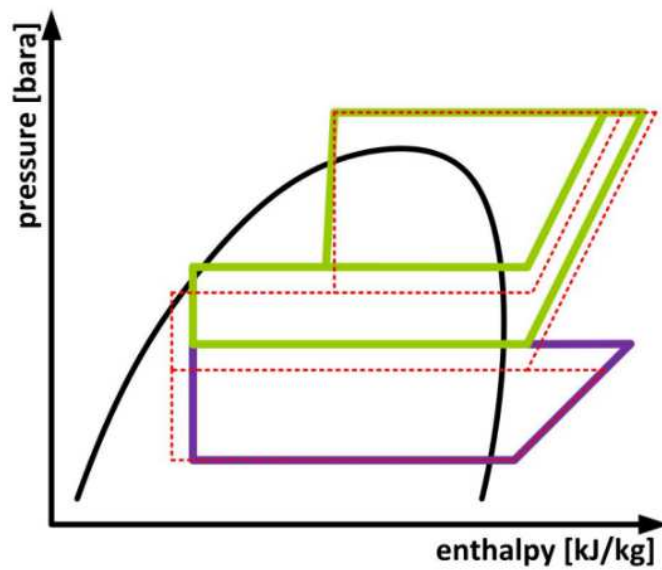


Fig. 3.17 – Effect of the overfeeding of the MT evaporators on a R744 booster refrigeration system with parallel compression in the $\log(p)$ - h diagram (Wiedenmann, 2015).

3.2.6 Transcritical booster systems with multi-ejector rack

Different expedients and layouts have been proposed to enhance the energy efficiency of the CO₂ refrigerating plants at high operating temperatures. The most promising technology seems to be the one based on the adoption of some ejectors instead of the conventional expansion valves, which feature the highest exergy destruction rates in transcritical operations (Fazelpour and Morosuk, 2014). Any throttling valve, in fact, operates (roughly) in isenthalpic conditions, implying that the energy kinetic due to the pressure decrease is converted into friction and, consequently, into a drop in the useful effect as well. The higher the difference between the heat rejection and the heat absorption pressure, the more noticeable the aforementioned penalization is. This drawback is particularly marked in R744 refrigerating machines, as they commonly experience transcritical running modes (Fig. 3.18). On the other hand, this also implies that “CO₂ only” solutions are capable of achieving much greater enhancements in COP than HFC-based systems by employing a work recovery device.

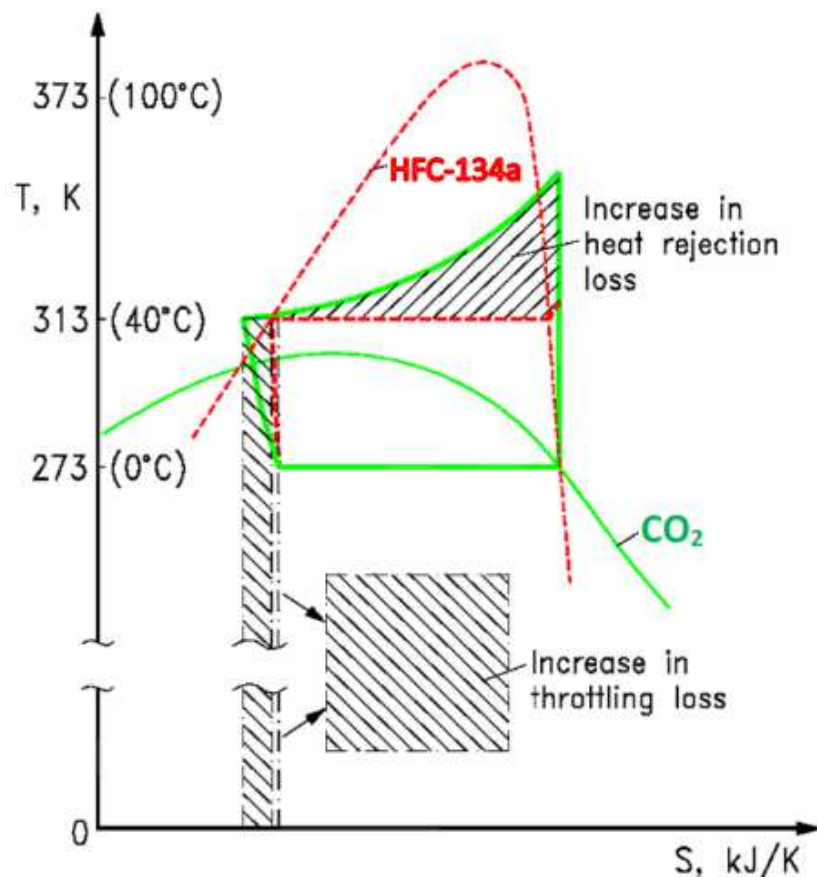


Fig. 3.18 - T-s diagram for R134a and R744 (Nekså et al., 2016).

In order to quantify how larger the irreversibilities associated with the expansion valve of a single-stage CO₂ machine in comparison with those of a conventional system, the same

example as the one reported in Table 3.1 was considered again. Cavallini and Zilio (2007) selected a constant temperature for the cold source equal to $-5\text{ }^{\circ}\text{C}$ and an increase in the temperature of the air flowing through the R22 condenser by 10 K. Table 2.2 shows that the expansion valve of the transcritical cycle is by far the component involving the highest contribution to the total irreversibilities (i.e. efficiency defect) between the two selected systems.

Table 3.1 – Contributions of each component to total irreversibilities (i.e. efficiency defect) occurring in a vapour compression refrigeration system using R22 and R744 (Cavallini and Zilio, 2007).

Parameter	R22	R744
Compressor efficiency defect [-]	0.173	0.171
Gas cooler efficiency defect [-]	-	0.170
Condenser efficiency defect [-]	0.224	-
Expansion valve efficiency defect [-]	0.161	0.294
Evaporator efficiency defect [-]	0.068	0.055

This thermodynamic penalization takes place in commercial refrigeration for two reasons:

- high outdoor temperatures;
- need to satisfy the heating reclaim in supermarkets, which commonly forces the system to work in transcritical operating conditions, although the low external temperature would permit it to operate in subcritical running modes. This occurs in an attempt to increase the amount of recoverable heat from the gas cooler.

In order to recover some of such an energy content associated with the expansion process, either an expander or an ejector can be employed. Since the former is expensive (comparable cost and complexity to compressors) and easily damageable due to the presence of a large amount of liquid, the researchers' attention has been considerably focusing on the ejectors thanks to its cheapness, absence of moving parts and ability to handle two-phase flows with no damage. In addition, Ozaki et al. (2004) demonstrated that a CO₂ refrigeration unit using a two-phase ejector can attain an enhancement in its performance similar to that showed by a CO₂ solution with expander. As for commercial refrigeration sector, Neksa et al. (2010) claimed that even the solution with parallel

compression is more energy competitive than that equipped with an expander at outdoor temperature up to 40 °C.

Fig. 3.19 refers to the working principle of an ejector as a substitute for a conventional expansion device with the purpose of reducing its irreversibilities. An ejector consists of the motive nozzle, the suction nozzle, a mixing section and a diffuser. The refrigerant exiting the gas cooler/condenser, defined as the primary fluid, is expanded and accelerated through the motive (or primary) nozzle. Due to the pressure difference between the expanded stream and the refrigerant in the MP liquid receiver (secondary fluid), part of the secondary fluid is entrained into the suction (or secondary) nozzle. Both streams are then blended in the mixing section and a part of the remaining kinetic energy of the refrigerant is converted into a pressure increase through the diffuser.

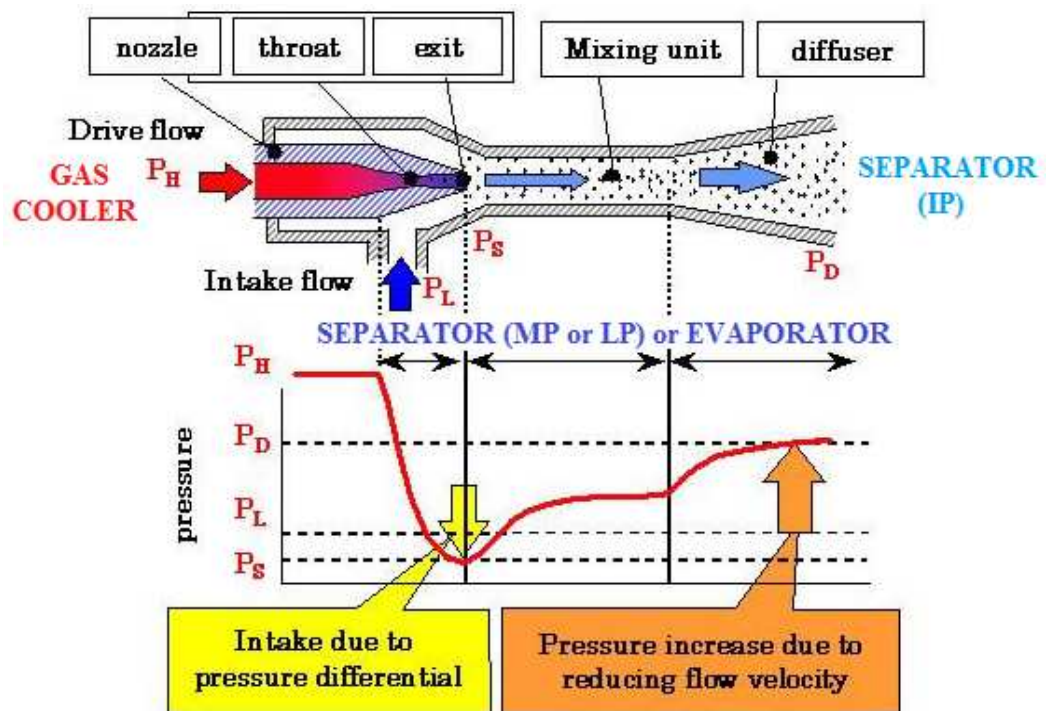


Fig. 3.19 - Working principle of an ejector.

The performance of an ejector for expansion work recovery can be described by three parameters, such as the mass entrainment ratio (ω), the pressure lift (P_{lift}) and its efficiency (η_{ejector}).

The mass entrainment ratio, which is equal to the ratio of the suction mass flow rate to the motive mass flow rate (Eq. 3.1), defines the capability of an ejector to intake (or pump) some refrigerant:

$$\omega = \frac{\dot{m}_{sn}}{\dot{m}_{mn}} \quad (3.1)$$

The pressure lift, which can be computed through Eq. 3.2, represents the ratio of the ejector outlet pressure to the ejector suction pressure. It quantifies how much the entrained fluid can be lifted.

$$P_{lift} = \frac{P_{diff,out}}{P_{sn,in}} \quad (3.2)$$

Both mass entrainment ratio and pressure lift should be typically as high as possible since:

- the higher the value of the pressure lift, the lower the pressure ratio of the compressor is;
- the higher the mass entrainment ratio, the lower the mass flow rate of the compressor is.

Although the ejector efficiency increases with rise in pressure lift and/or mass entrainment ratio (see Eq. 3.4), too high values of the mass entrainment ratio imply significant reductions in the primary mass flow rate. As a consequence, the primary flow is too weak to entrain the suction flow into the ejector. This means that these two parameters have to be assessed simultaneously as the ejector tend to strike a balance between them. This device, in fact, is capable of pre-compressing either a large amount of the secondary refrigerant through a small pressure difference or a small amount of the secondary refrigerant through a large pressure difference. The effects of both can be taken into account by using the efficiency of the overall ejector ($\eta_{ejector}$) proposed by Elbel and Hrnjak (2008). The ejector efficiency, as shown in Eq. 3.3, is equal to the ratio of the actual amount of the work recovered by means of the ejector to the maximum amount of the work which could be theoretically recovered.

$$\eta_{ejector} = \frac{\dot{W}_{rec}}{\dot{W}_{rec,max}} \quad (3.3)$$

According to Elbel and Hrnjak (2008), the numerator in Eq. 3.3 can be computed as the required power to isentropically compress the suction mass flow rate from the suction inlet to the diffuser outlet pressure (C-D in Fig. 3.20). In fact, the suction flow expands from the evaporating to the mixing pressure, while the primary flow expands from the high to the mixing pressure. At a later time, both flows reach the diffuser exit pressure after undergoing a compression process. The net useful effect is thus represented by a pre-compression of part of the refrigerant (i.e. the secondary flow) from the evaporating to the diffuser pressure by taking advantage of the expansion of the primary flow from the gas cooler/condenser to the diffuser outlet pressure. On the other hand, the denominator in Eq. 3.3 can be defined as the power which can be recovered by an

isentropic expansion of the motive mass flow rate from the motive inlet to the diffuser outlet pressure (A-B in Fig. 3.20). The efficiency of an ejector can thus be computed as follows:

$$\eta_{ejector} = \frac{\dot{W}_{rec}}{\dot{W}_{rec,max}} = \frac{\dot{m}_{sn}}{\dot{m}_{mn}} \cdot \frac{h(P_{diff,out},s_{sn,in}) - h_{sn,in}}{h_{mn,in} - h(P_{diff,out},s_{mn,in})} = \omega \cdot \frac{(h_C - h_D)}{(h_A - h_B)} \quad (3.4)$$

It is important to highlight that, when it comes to quantifying the efficiency of the ejector components (Kornhauser, 1990) by employing some experimental data, it is needed to quantify the mixing pressure. However, in the hypothetical case that this value is known, it generally occurs that highly inaccurate values of the refrigerant specific enthalpy are computed owing to possible thermal non-equilibrium phenomena. On the other hand, its knowledge is not required by using Eq. 3.4, as the ejector can be treated as a black box characterized by various expansion and compression processes. In addition, $\eta_{ejector}$ can be calculated by means of some parameters which are easily measurable with a substantial correctness. However, it is also obvious that the ejector performance cannot be estimated with the aid of only one parameter.

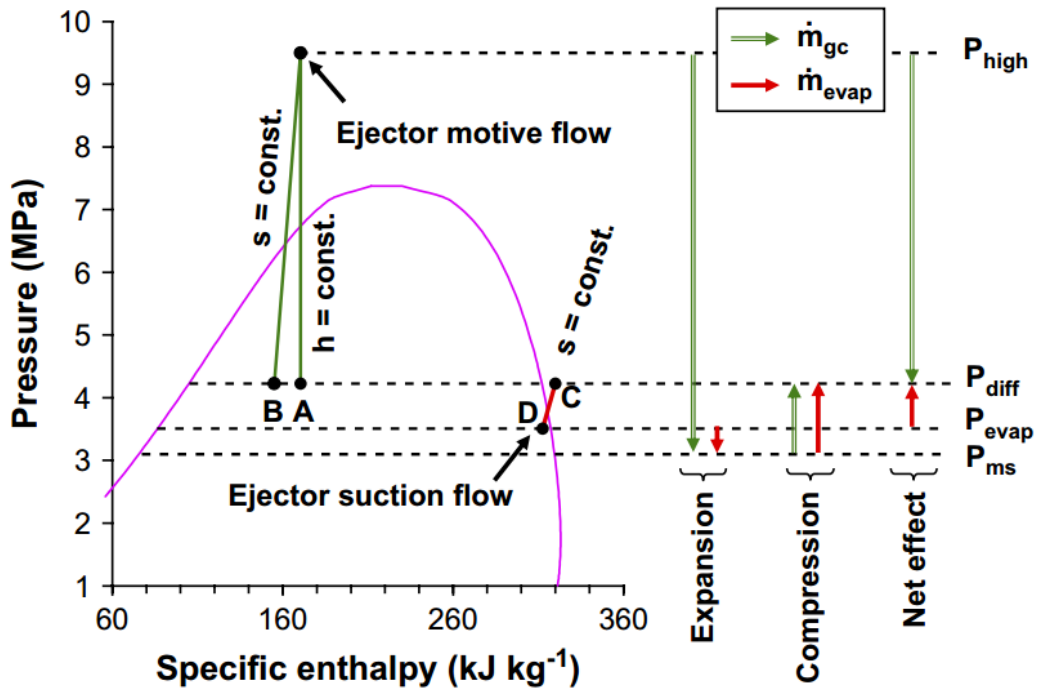


Fig. 3.20 - Expansion and compression of driving and driven flows in a R744 ejector for expansion work recovery (Elbel and Hrnjak, 2008).

As shown in Fig. 3.21, two main energy advantages can be associated with the adoption of a two-phase ejector: (i) increase in the refrigerating effect since the working fluid goes into the evaporator at almost saturated conditions; (ii) reduction in the compressor power

input as the refrigerant is compressed from an intermediate pressure to the high one. Consequently, besides being affordable and reliable, this technology represents, especially in warm/hot weathers, the solution with the highest potential in energy saving for food retail applications (Hafner and Hemmingsen, 2015; Hafner et al., 2016, 2014d, 2014c, 2014b, 2014a, 2012; Minetto et al., 2015, 2014b; Schönerberger, 2016). Bilir and Ersoy (2009) claimed that ejectors for work recovery are particularly promising for refrigerating plants running in tropical countries and desert area.

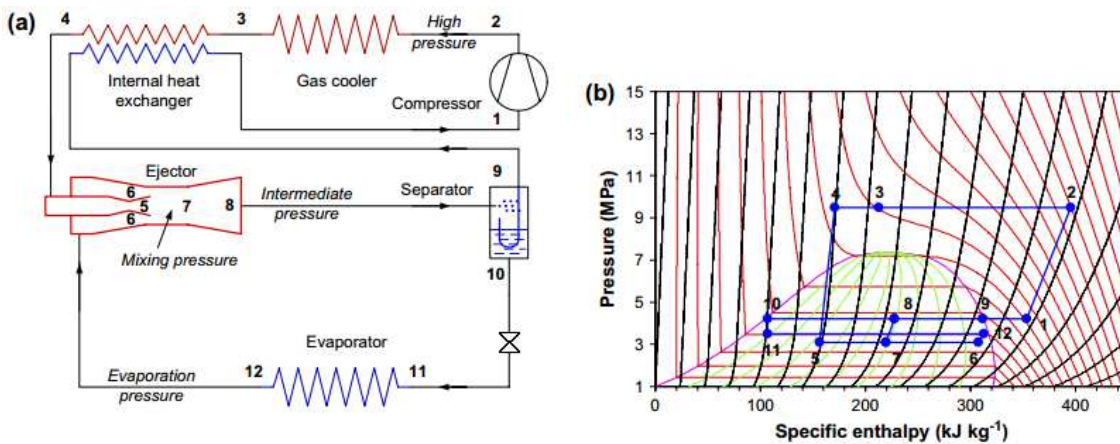


Fig. 3.21 - Schematic (a) and corresponding P-h diagram (b) of a transcritical R744 refrigeration system using an ejector to recover some expansion work (Elbel and Hrnjak, 2008).

Gullo and Cortella (2016) proved that a one-stage CO₂ system using an ejector for expansion work recovery is a more cost-effective solution than that with parallel compression. Experimental results have showed enhancements in COP by R744-based solutions using two-phase ejectors ranging from 7% (Elbel and Hrnjak, 2008) to 26% (Nakagawa et al., 2011). The current research regarding this solution is concentrated on the adjustable needle-based ejector and on the multi-ejector concept. Smolka et al. (2016) demonstrated that the former presents highly depreciated efficiencies in off-design running modes.

A multi-ejector rack (MEJ), whose concept was introduced by Hafner et al. (2014a, 2012), includes some vapour ejectors (typically from 4 to 6) and some liquid ejectors (usually 2), which are all fixed geometry devices of different sizes and connected in parallel among them. The former (VEJ) deal with the refrigerant coming out of the high pressure heat exchanger to guarantee the occurrence of the optimal high-side working conditions in any operating mode. This implies that a part of the vapour in the MP receiver is entrained into VEJ and the total amount of the refrigerant enters the IP receiver. The parallel

compressor(s) then compress(es) a significant mass flow rate of R744 from IP (higher than MP) to the HP. The reduction in the mass flow rate of the refrigerant drawn by the HS compressors entails a substantial energy saving in comparison with conventional booster solutions. At least one of the ejectors designated for vapour removal operates permanently and the required capacity is constantly matched by changing their combination. As for the liquid ejectors (LEJ), their purpose is to pump some liquid back to the IP receiver to foster the overfeeding of the MT evaporators.

According to Minetto et al. (2014b), the resulting growth of the annually working time of the auxiliary compressors allows increasing the energy benefits associated with their use and reducing the maintenance problems.

The multi-ejector block and its main components are showed in Fig. 3.22. Up to 6 ejectors (2), activated by a conventional coil (3), are hosted within the multi-ejector block (1). The gas cooler/condenser is connected to port 4, whereas the suction of the refrigerants occurs through port 5. Port 6 is used for discharging the total amount of refrigerant, while the sensors (7) for each port measure the pressure.

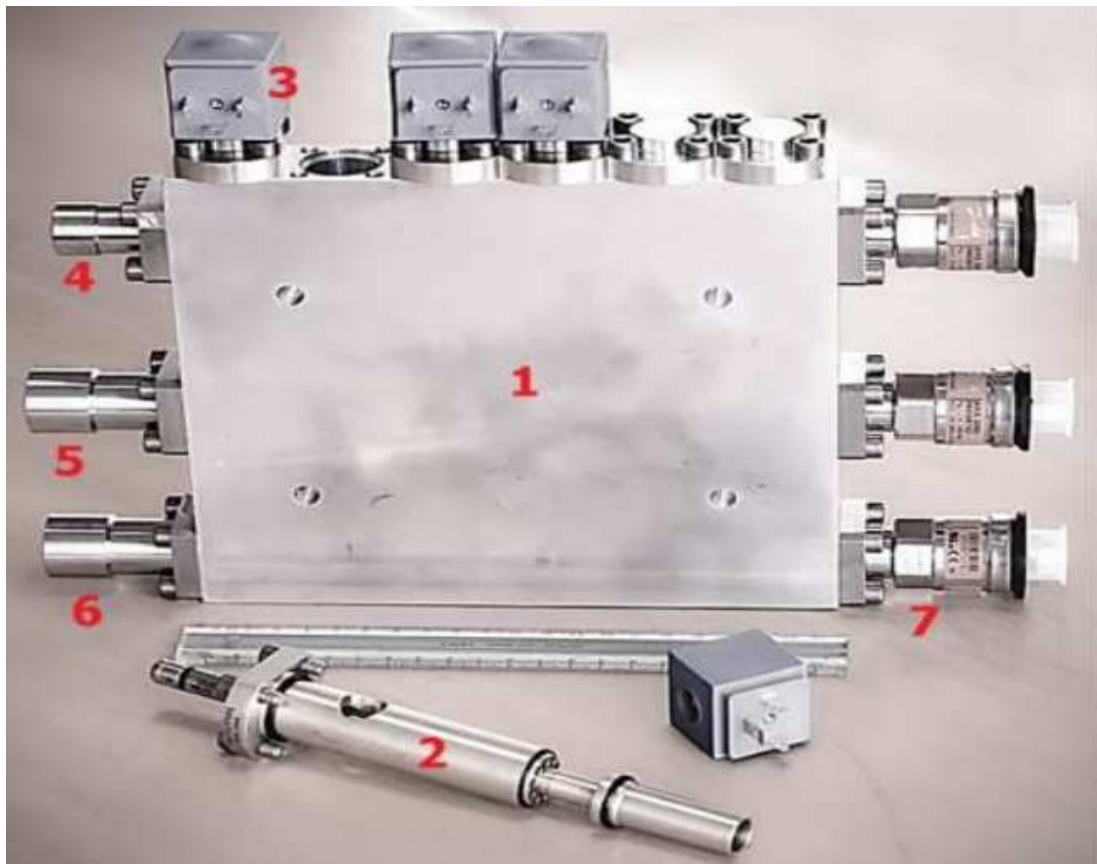


Fig. 3.22 - Multi-ejector block and its main components (Hafner and Banasiak, 2016).

Banasiak et al. (2015) claimed that a multi-ejector rack is capable of controlling the gas cooler pressure and, concurrently, recovering some expansion work more successfully than an individual fixed geometry ejector. The authors also fulfilled the design, the manufacturing and the performance mapping of a multi-ejector arrangement operating in a commercial CO₂ refrigeration system. The adoption of the multi-ejector concept on the part of a configuration with parallel compression reduces the energy consumption by 12% in wintertime, as estimated by Hafner et al. (2014c). The evaluation took into account a supermarket operating in Fribourg (Switzerland). Such a technology allows achieving an increase in the efficiency of the system up to 30% over a conventional booster solution, especially during high outdoor temperature periods (Hafner et al., 2014a). According to Hafner et al. (2012), the use of a multi-ejector rack is more energetically beneficial in Southern Europe. In such a region, a decrease in the electricity consumption by about 11% can be attained over a configuration without ejectors. Efficiencies of the individual ejector working in a multi-pack of 30% were experimentally measured by Banasiak et al. (2014). The use of the multi-ejector concept in a supermarket operating in Bari (Italy) leads to an energy saving by 22.5% over a conventional single-stage CO₂ refrigerating plant (Minetto et al., 2014b). The experimental data collected by Haida et al. (2016) showed that a multi-ejector R744 refrigeration unit accomplishes improvements in the COP by 7% over a R744 system with parallel compression. In comparison with the latter, the authors also estimated an increase in the exergy efficiency by 13.7%. Hafner et al. (2016) gathered some field measurements from a refrigerating plant located in Spiazzo (North of Italy). The experimental data were collected from the 1st of May 2015 to the 30th of October 2015 at external temperatures ranging from 22 °C to 35 °C. Reductions in the energy consumption from 15% to 30% were assessed over the configuration with parallel compressor. The results were found to be strongly depending on both the AC demand and the outdoor temperature. In addition, the refrigeration system was capable of satisfying the total AC need of the supermarket. Schönenberger (2016) assessed energy savings by using the multi-ejector concept ranging from 15% to 25% over a R744 refrigerating plant with parallel compression in two Swiss stores. The author highlighted that the outcomes substantially depended on the heat demand, the application and the climatic conditions. The data from the field gathered in various retail stores by Fredslund et al. (2016) suggested that the efficiency of the vapour ejectors reached in real applications is about the same as the one measured in the laboratory (and above 0.25). In addition, reductions in the energy consumption ranging from 10% to 15% at the outdoor

temperature of around 30 °C and equal to roughly 4% at about 27 °C were estimated for a solution with and without coupling with the AC unit, respectively. The latter outcome was due to the occurrence of some oil return issues.

Fig. 3.23 sketches a booster system with a multi-ejector pack, parallel compression and MT overfed evaporators. The thermodynamic cycle represented in Fig. 3.17 also refers to the layout sketched in Fig. 3.23.

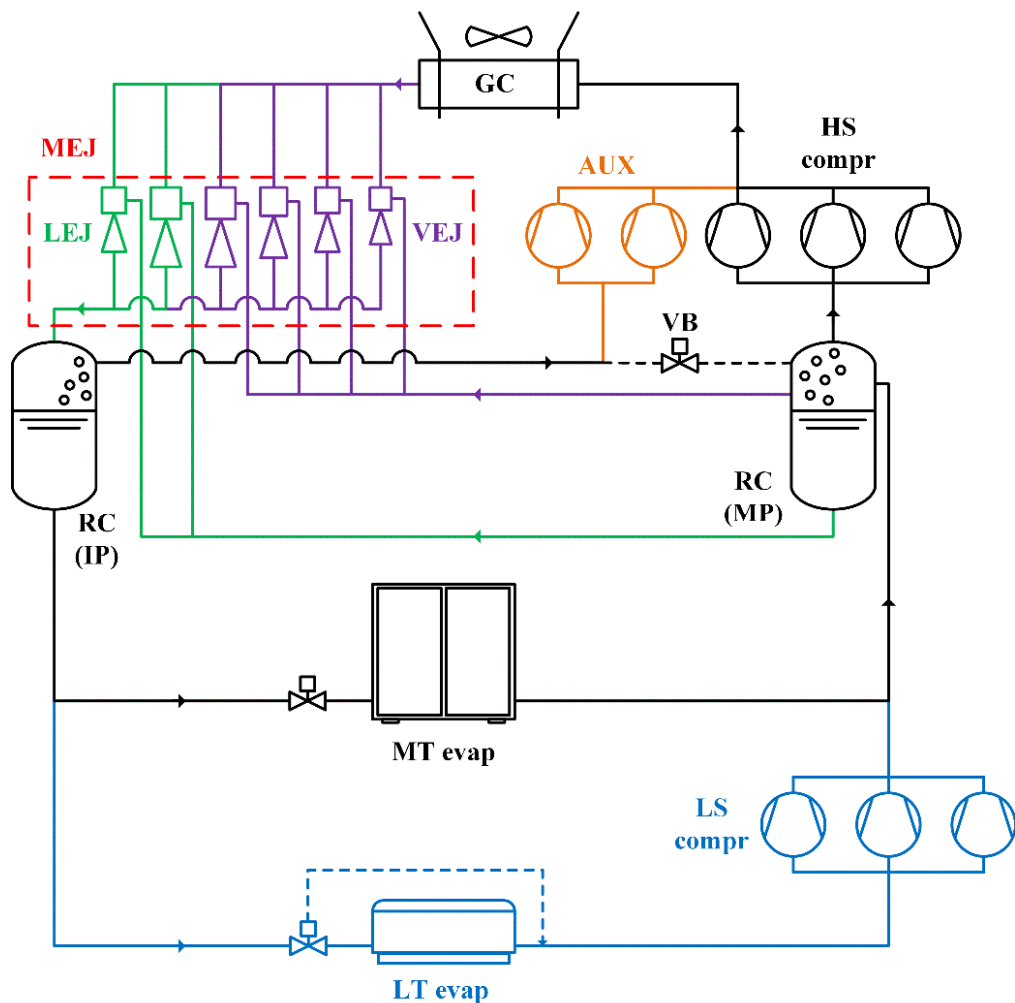


Fig. 3.23 - Schematic of a R744 booster refrigeration system with parallel compression, MT overfed evaporators and multi-ejector rack.

The adoption of an internal heat exchanger (IHX) located downstream of the IP receiver and upstream of the LS compressors permits also overfeeding the LT display cabinets (Minetto et al., 2015; Schönerberger, 2016), as schematized in Fig. 3.24 (EJ_OV). However, the use of a LT accumulator is necessary to trap the possible liquid leaving the LT evaporators (Schönerberger, 2016). According to Hafner and Banasiak (2016), the increase in the evaporating temperatures permits reducing the frost formation and the number of defrost cycles.

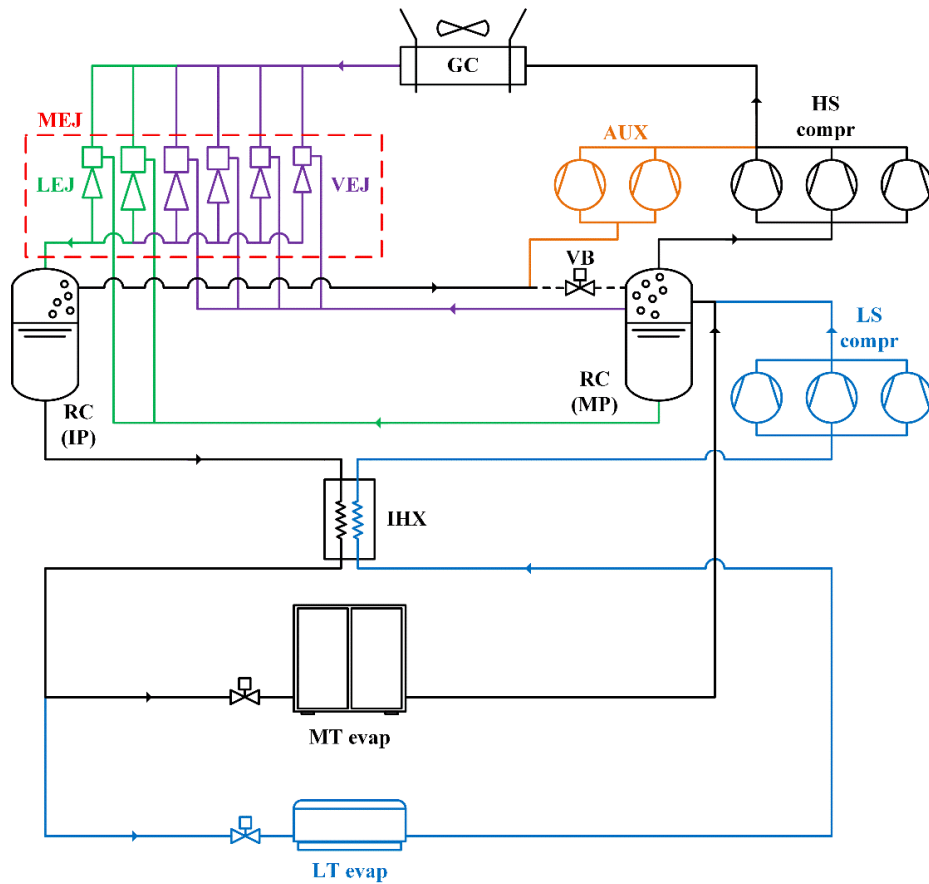


Fig. 3.24 - Schematic of a R744 booster refrigeration system with parallel compression, LT and MT overfed evaporators and multi-ejector rack.

In Fig. 3.25 the effect of the increase in LT on the solution equipped with a multi-ejector pack is shown in the $\log(p)$ - h diagram.

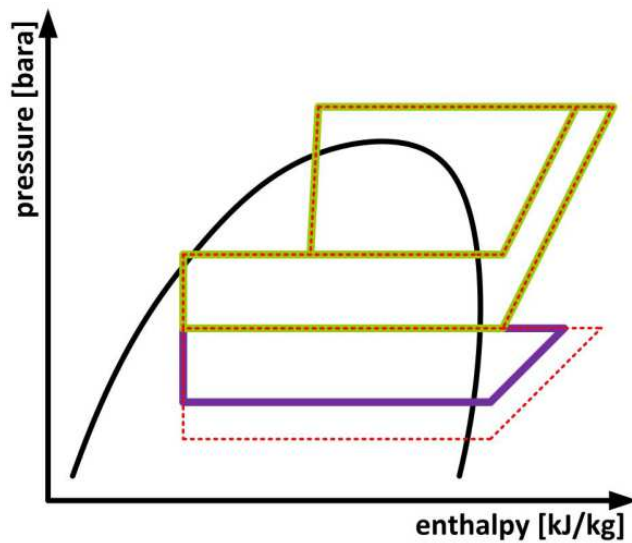


Fig. 3.25 – Effect of the overfeeding of the LT evaporators on a R744 booster refrigeration system equipped with multi-ejector rack in the $\log(p)$ - h diagram (Wiedenmann, 2015).

Fig. 3.26 shows a pure CO₂ booster refrigerating unit using a multi-ejector block installed in a Swiss supermarket (Hafner et al., 2014c).



Fig. 3.26 – Left-hand side: 2 parallel compressors, 4 HS and 4 LS compressors; Right-hand side: 1 liquid ejector at the bottom, 2 vapour ejectors at the top (Hafner et al., 2014c).

Also, it is worth remarking that the solution equipped with the multi-ejector rack guarantees a significant level of safety. In fact, in case of failure of the auxiliary compressors, the flash gas can be removed from the IP liquid receiver by employing VB. In addition, in the event of the possible malfunction of LEJ or a reduced amount of liquid, the evaporators can be switched to the superheated mode in any operating conditions. Furthermore, the system is also equipped with conventional expansion valves downstream of the gas cooler/condenser in order to, if it is necessary, substitute (or simply work in parallel with) VEJ. Moreover, the auxiliary compressors can always take over the HS compressors. Finally, the presence of the separator at MT and that of both a low pressure receiver downstream of the LT evaporators and the internal heat exchanger prevent the corresponding compressors from drawing any liquid.

In 2015, a hypermarket using this technology was open in Timisoara (Romania). The usage of a multi-ejector arrangement combined with the heat recovery implementation and the DHW production are supposed to lead to a reduction in the energy consumption up to 13% in relation to a solution with parallel compression (Frigo-Consulting LTD, 2015). Italy's largest hypermarket (10000 m²) started recently operating in Milan employing an "all-in-one" CO₂ configuration with multi-ejector arrangement (Danfoss, 2016b). Thanks to this technology as well as an integrated control of HVAC, light and refrigeration, the energy savings are expected to be around 50%.

3.2.7 Fundamental aspects for diffusion of transcritical booster systems in warm regions

Table 3.2 lists the bright sides and drawbacks associated with the state-of-the-art HFC-free technologies previously mentioned solutions.

As a main remark of Chapter 3, it is important to highlight that the penetration of the transcritical CO₂ refrigerating plants in warm regions is strongly depending on two factors:

- the adoption of the “all-in-one” concept;
- the diffusion of a suitable technology capable of reducing their total energy consumption significantly.

As a result, “CO₂ only” solutions will become much more affordable than conventional separated HFC systems. The conclusion stated above is obviously based on the omission of the current in force technological barriers, which are beyond the scope of this study.

Table 3.2 – Advantages and disadvantages of transcritical CO₂ booster configurations (Hafner, 2016; Wiedenmann, 2015).

<i>Configuration</i>	<i>Advantages</i>	<i>Disadvantages</i>
<i>Dedicated mechanical subcooling</i>	<ul style="list-style-type: none"> • Efficiency at (quite) high outdoor temperatures 	<ul style="list-style-type: none"> ▪ Additional costs for subcooling loop ▪ Challenges with reliability due to complicated control system ▪ Promising technology mainly for small systems
<i>Parallel compression</i>	<ul style="list-style-type: none"> • Relief for HS compressors • Reduction in swept volumes of compressors • Efficiency in mild climates • Integration with heating system 	<ul style="list-style-type: none"> ▪ More economically convenient for large cooling capacities (> 100 kW) ▪ Not energetically competitive combined with AC unit in warm regions ▪ Higher investment cost than conventional booster
<i>Multi-ejector rack</i>	<ul style="list-style-type: none"> • Overfed evaporators all over the year • Pressure lift can be suitably optimized according to AC demand • Relief for HS compressors • Higher utilization of auxiliary compressors • Efficiency at very high outdoor temperatures • Possibility of combination with HVAC unit in any climatic conditions • Reduction in peak energy demand up to 30% 	<ul style="list-style-type: none"> ▪ Requires a liquid receiver at low pressure ▪ Need for some further investigations

3.3 High GWP-based configurations

3.3.1 Cascade system

As shown in Fig. 3.27, a cascade system consists of two circuits (i.e. LTC and HTC), which interact with each other by using the so-called cascade condenser. The vaporization of the refrigerant in the high temperature circuit (HTC) takes place as a consequence of the heat rejection from the low temperature circuit (LTC). The cascade condenser, in fact, operates as a condenser for LTC and as an evaporator for HTC under an appropriate temperature difference between the two selected working fluids. In the case of commercial refrigeration plants, HTC has some additional evaporators which are used for cooling down chilled food display cabinets and cold rooms.

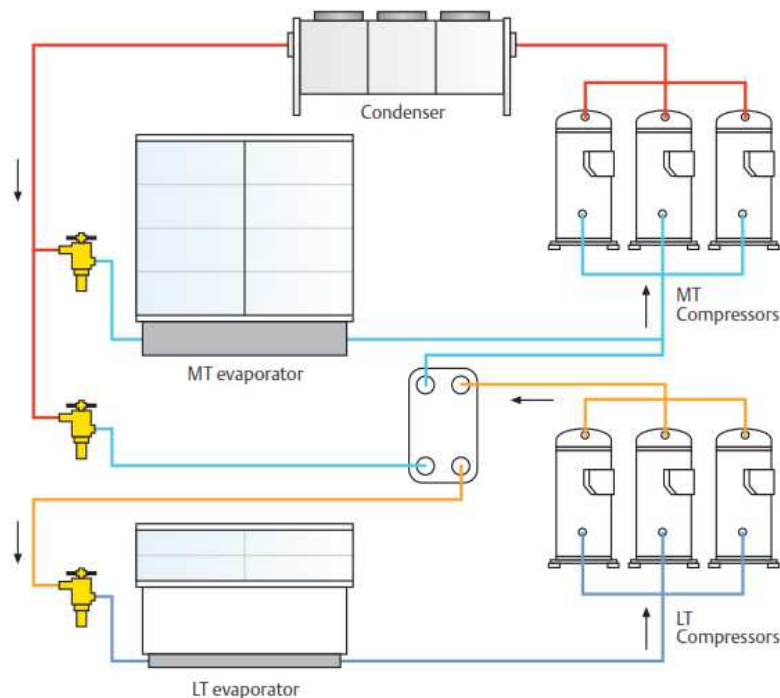


Fig. 3.27 - Schematic of a cascade refrigeration system for supermarket applications (EMERSON Climate Technologies, 2010).

R744 is being widely utilized as the secondary working fluid of indirect/cascade systems in which it can perform at the most favourable conditions, namely distant from the critical temperature and at acceptable operating pressures. In such configurations, R744 is employed in LTC and thus it operates in subcritical conditions in any running mode. In this case its use allows decreasing pump power input and pipe size, as well as it features good heat transfer properties (Ge and Tassou, 2011a). As an example, Bansal (2012) estimated a drop in the inner diameters by 60-70%. According to Tassou et al. (2011), a low refrigerant charge can also be associated with these configurations. On the other hand,

the adoption of two different circuits implies different components and different lubricant oils. Consequently, cascade systems are characterized by a great complexity in terms of both installation and maintenance (Tassou et al., 2011). The refrigerant flowing in HTC can be chosen among different fluids, both natural (R717, R290, R1270) and synthetic ones (R134a, R404A). Due to the flammability and/or the toxicity of the former and to the high GWP of the R400 series and in accordance with the regulation currently in force (European Commission, 2014), R134a is a good candidate to be used in upper cascade systems with cooling capacity over 40 kW. As its Normal Boiling Point is equal to about $-26\text{ }^{\circ}\text{C}$, the usage of this working fluid is restricted to MT applications.

The thermodynamic cycle of a R134a/R744 cascade refrigeration system is depicted in a T-s diagram in Fig. 3.28.

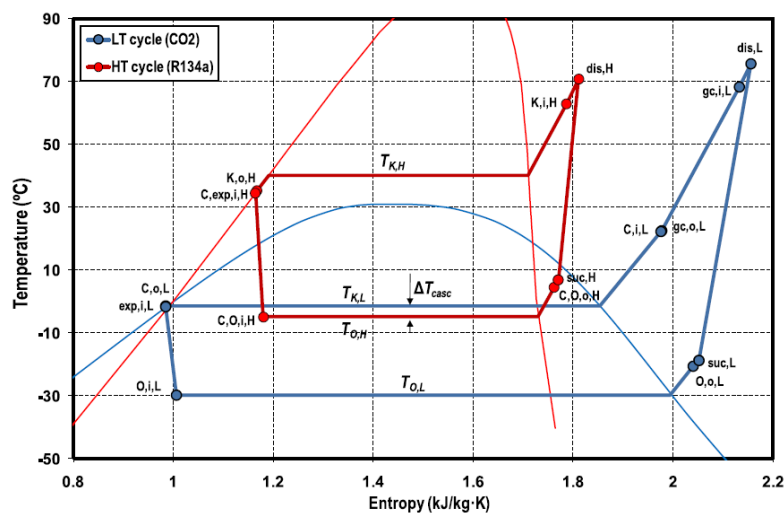


Fig. 3.28 – T-s diagram of a R134a/R744 cascade refrigeration system (Sanz-Kock et al., 2014).

Despite the cascade condenser cost, the additional heat transfer level and the involved high complexity, many studies on cascade solutions using CO_2 in LTC have been implemented (Getu and Bansal, 2008; Messineo, 2012; Aminyavari et al., 2014; Dopazo et al., 2009; Lee et al., 2006; Rezayan and Behbahaninia, 2011; Yilmaz et al., 2015; Llopis et al., 2015a, 2016a; Sanz-Kock et al., 2014; Souza et al., 2015; Cabello et al., 2017; Sánchez et al., 2017). This is due to the fact that, compared to R404A direct expansion systems, these configurations permit successfully reducing the supermarket carbon footprint by both using less environmentally harmful refrigerants (i.e. R134a) and dropping the working fluid charge. According to Llopis et al. (2015a), these arrangements are suitable alternatives to high GWP-based plants in LT applications. The authors also justify the use of “ CO_2 only” systems only in cold climates. Sanz-Kock et al. (2014)

gathered experimental measurements regarding a R134a/CO₂ cascade refrigeration system varying the evaporating temperature from -40 °C to -30 °C and the condensing temperature from 30 °C to 50 °C, respectively. The experimental setup exhibited cooling capacities from 4.5 to 7.5 kW. Several parameters were taken into account, such as performance of the compressors, temperature difference in the cascade condenser, cooling capacity and COP. At the constant LS evaporating temperature of -30 °C, an average decrement in COP by 18% is obtained for each increase in the condensing temperature of HTC by 10 °C. On the other hand, keeping HS condensing temperature at 40 °C, the COP is brought down on average by 12% for each decrease in the LS evaporating temperature by 5 °C. Furthermore, the authors found out that the LS condensing temperature does not influence COP significantly. Cooling capacity was observed to be more depending on the LS evaporating temperature rather than on the HS condensing temperature. The experimental results by Souza et al. (2015) confirmed that COP of such a solution goes up with decrease in the CO₂ compressor operating frequency. The replacement of R134a with R152a in such a technology does not affect the energy performance significantly, as experimentally proved by Cabello et al. (2017). The experimental laboratory tests conducted by Llopis et al. (2016a) revealed that the adoption of an internal heat exchanger in a HFC134a/R744 cascade plant brings the cooling capacity from 1.1% down to 2.4%, whereas the COP goes up to 3.7%. The assessment was implemented at evaporating and condensing temperatures respectively ranging from -40 °C to -30 °C and from 30 °C to 50 °C. The 24 hour tests carried out at stable operating conditions by Sánchez et al. (2017) pointed out that increases in energy consumption up to 14% can be assessed by substituting a R134a/CO₂ cascade system with a R134a/CO₂ indirect arrangement. The results obtained depend on both the condensing temperature and the secondary fluid selected.

Fig. 3.29, which shows the total production and release of R134a in the form of CO₂ equivalent of greenhouse gases, highlights that more than half of all R134a ever produced is still in the atmosphere. This implies that such a refrigerant is not a sustainable working fluid for the whole world. Consequently, although interesting energy savings can be accomplished by R134a/CO₂ cascade refrigeration systems, its usage should be strongly discouraged, especially in supermarket applications which have high annual leakages. In addition, it is worth remarking that many Countries have promotes tax on HFC purchase in an attempt to promote climate-friendly technologies and that R134a price raised by 10% in 2016 (Shecco, 2016).

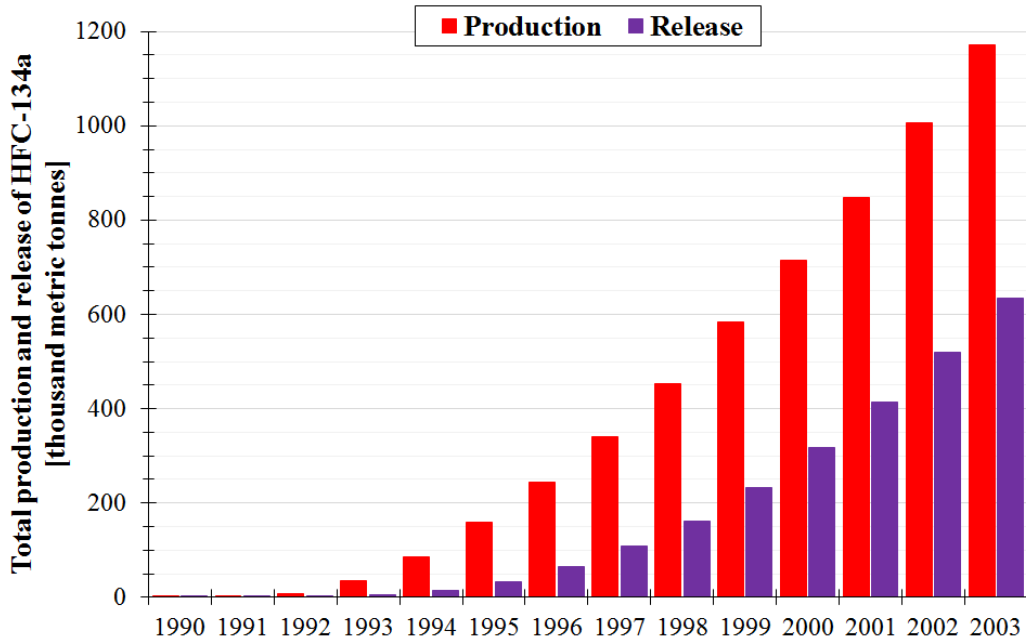


Fig. 3.29 - Total production and atmospheric release of HFC-134a (Alternative Fluorocarbons Environmental Acceptability Study, 2006).

The results showed in both Fig. 3.30(a) and Fig. 3.30(b) further aim at persuading to use any synthetic refrigerants. Fig. 3.30(a) displays that European supermarkets were accountable for about one third of HFC consumption in 2010 in Europe. Also, the largest HFC market request in 2015 was owing to the commercial refrigeration sector, as highlighted in Fig. 3.30(b). In addition, it is worth remarking that nowadays R134a features an atmospheric lifetime of about 14-16 years, as well as that its GWP over 20 years is $3830 \text{ kg}_{\text{CO}_2,\text{equ}} \cdot \text{kg}_{\text{refrigerant}}^{-1}$, which is almost three times as high as the value which is usually indicated ($\text{GWP}_{100 \text{ years}}$). Carr-Shand et al. (2009) pointed out that from 18% up to 30% of the contribution to climate change on the part of supermarkets is depending on the selected refrigerant.

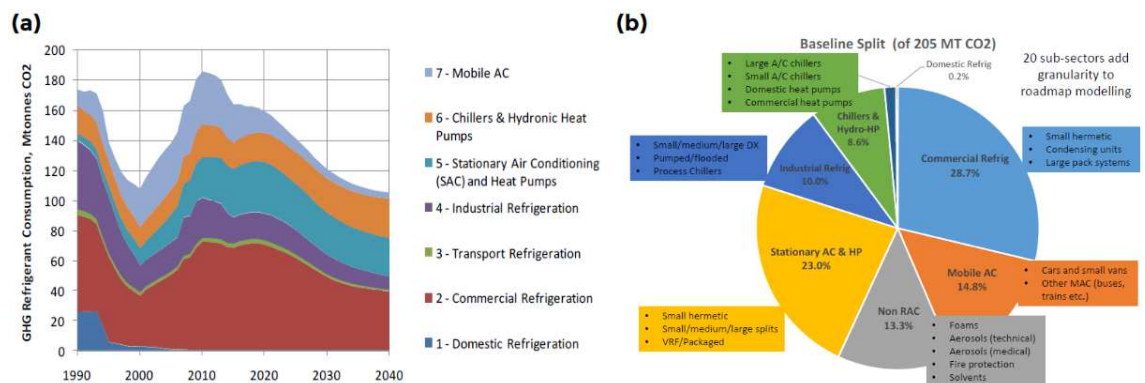


Fig. 3.30 - (a) HFC consumption in Europe (SKM Enviros, 2012); (b) Market sectors needing HFCs (EPEE, 2015).

3.3.2 R404A multiplex direct expansion system

The multiplex direct expansion configurations (Fig. 3.31) still represent Europe's most widely employed solutions thanks to their significant reliability, cheapness and ease of capacity control. Two centralised units separately serve the LT and MT loads involving 3-8 semi-hermetic reciprocating compressor located in the machinery room connected to a condenser being on the roof and to the evaporators in the display cabinets. The refrigerant is directly circulated through the sale areas by means of long pipes. The marked length of the latter represents the main drawback of these solutions as it causes enormous leakages of working fluid and thus a large charge of the refrigerant (Tassou et al., 2011). According to EMERSON Climate Technologies (2010), the refrigerant charge for a centralised R404A system is equal to $4 \text{ kg}_{\text{refrigerant}} \cdot \text{kW}_{\text{load}}^{-1}$ for the one serving the LT load and $2 \text{ kg}_{\text{refrigerant}} \cdot \text{kW}_{\text{load}}^{-1}$ for that serving the MT load, respectively.

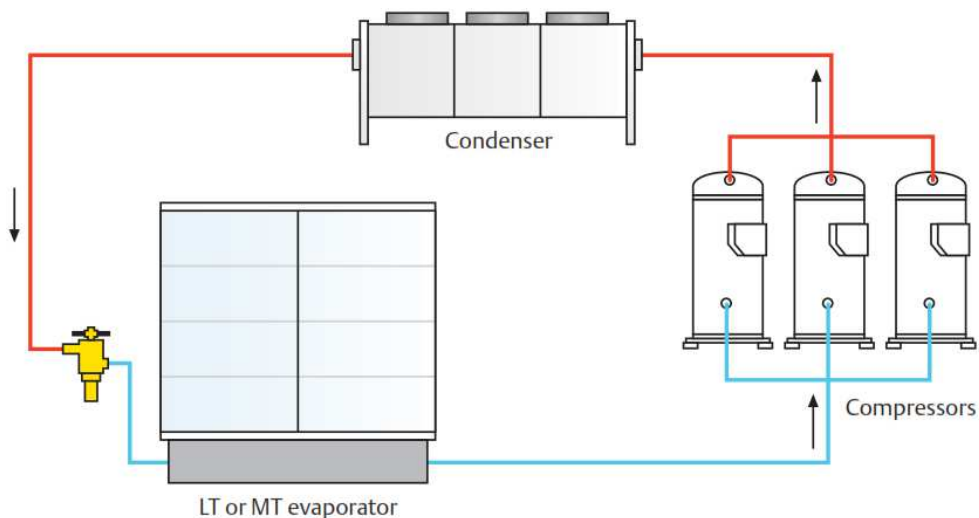


Fig. 3.31 – Schematic of a multiplex direct expansion system (EMERSON Climate Technologies, 2010).

4 METHODS AND MATERIALS

In this chapter the investigated case studies and the implemented simulation models are exhaustively explained. Furthermore, the selected operating conditions and model of the chosen air conditioning units are thorough described. Finally, the most important concepts associated with the conventional and advanced exergy analyses, as well as with that of the environmental assessment are illustrated.

4.1 Case studies

4.1.1 Operating conditions of conventional booster solutions

The effect of the reduction in both the gas cooler/condenser approach temperature and the minimum condensing one on the consumption of a booster configuration was evaluated. In order to do this, a “conventional” booster solution, indicated as CB, and an “improved” booster, pointed out as IB, were included in this investigation.

As regards CB, a minimum temperature and an approach temperature of the condenser both equal to 10 °C were chosen. As soon as the transcritical running modes occurred, an approach temperature of the gas cooler of 5 K was adopted.

With respect to IB, a minimum temperature and an approach temperature of the condenser respectively equal to 9 °C and 3 K were selected. In addition, in transcritical operations the approach temperature was brought down to 2 K.

Furthermore, a degree of subcooling of 2 K was selected in subcritical conditions in both refrigerating plants. The intermediate pressure was kept equal to 35 bar for both CB and IB, since its influence on the performance is almost negligible (Ge and Tassou, 2011a).

4.1.2 Operating conditions of solution with dedicated mechanical subcooling

Gullo et al. (2016a) showed that, in order to achieve a satisfying energy saving, it is necessary to adopt a parallel compressor on the part of the configuration with subcooling loop operating in warm climates. Due to this, only such a combined system was investigated in this study.

The same boundary conditions as the ones associated with IB were applied to this solution, which was pointed out as MS+PC. Furthermore, the outlet temperature of the gas cooler/condenser was kept equal to 15 °C. The reason for this assumption lies in the fact that additional reductions in this variable do not imply any noteworthy energy benefit, as demonstrated by Gullo et al. (2016a). Also, R290 was selected as the refrigerant for the subcooling loop, since the usage of R1279 offers slightly poorer performance (Gullo et al., 2016a). Gullo et al. (2016a) proved that this was mainly due to the technological constraints (i.e. lower maximum evaporating temperature of the subcooler using R1270 than that employing R290) of the R1270 compressor.

These further assumptions were made:

- i. approach temperature of the condenser of the mechanical subcooling loop added up to 8 K;
- ii. it was assumed that the R290 compressor operated at as high evaporating temperature as possible in accordance with its operating envelope;
- iii. the subcooling loop and the auxiliary compressor were supposed to be switched off in subcritical running modes. The latter was supposed to be replaced with VB in these operating conditions.

As mentioned above, the intermediate pressure becomes a key parameter for the optimization procedure in case of the use of an auxiliary compressor (Bell, 2004; Minetto et al., 2005). The results obtained by Gullo et al. (2016a) indicated that, in the case of systems similar to MS+PC, the influence of the intermediate pressure is almost negligible. Consequently, if a fixed subcooler outlet temperature is assumed, the performance of such a configuration is mainly affected by the high pressure. The reason for this result lies in the low quality of the refrigerant flowing into the liquid receiver thanks to the presence of the subcooler. For a solution resembling MS+PC, in fact, IP tends to be as low as possible in accordance with the technological constraints of the flash tank (Gullo et al., 2016a). Owing to this, the intermediate pressure of MS+PC was chosen and kept equal to 35 bar.

4.1.3 Operating conditions of solutions equipped with parallel compression

As previously mentioned, Bell (2004) and Minetto et al. (2005) showed that the intermediate pressure is an optimization parameter for the configuration with parallel compression. On the other hand, the present propensity is to maintain it fixed (or slightly variable) so as to make the expansion process more stable and avoid high pressures in the sale area (Minetto et al., 2015).

In this paper, two CO₂ refrigerating plants using parallel compression with two different control strategies for IP (i.e. PC and PC_VAR) were studied. The intermediate pressure was ranged from 35 bar to 40 bar for the configuration pointed out as PC and from 35 bar to 55 bar for the solution indicated as PC_VAR. The first upper limit was used for simulating the working operations of the currently state-of-the-art solutions, whereas the second one represents a technological constraint for the selected auxiliary compressors. In all the evaluated cases, the parallel compressors were supposed to be switched off in subcritical operating conditions. This was due to the fact that the amount of flash gas was assumed to be lower than the minimum suction volume rate of the smallest parallel compressor. In these running modes, the excess vapour was removed by throttling it to MP via VB. In addition, the same operating conditions as those of IB were used for both PC and PC_VAR.

4.1.4 Operating conditions of solutions equipped with overfed evaporators

Two configurations employing overfed evaporators were assessed in this investigation, i.e. with (OV+PC) and without (OV) auxiliary compressors. In both cases, a minimum condensing temperature of 12.5 °C was selected, whereas IP was taken as 5 bar higher than MP (Giroto, 2012). Also, the evaporator outlet quality and the pump efficiency were selected equal to 0.9 and to 0.5 (Minetto et al., 2014a), respectively. With respect to the approach temperature of the HP heat exchanger, it was assumed equal as 3 K in subcritical running modes and as 2 K in transcritical operating conditions.

4.1.5 Operating conditions of solutions equipped with multi-ejector rack

The investigation of the multi-ejector arrangement was conducted by optimizing the pressure lift (Hafner et al., 2014a). Its minimum and maximum values were taken as 4 bar (Banasiak et al., 2015) in order to guarantee an appropriate feeding of the evaporators and as 15 bar (Hafner et al., 2015), respectively. An upper limit of the efficiency of the multi-ejector rack of 0.4 was chosen. A correlation (see Appendix A.1) derived from the

experimental data collected by Haida et al. (2016) was implemented for the rack operating in transcritical conditions. As for the transition and subcritical running modes, the experimental data gathered by Palacz et al. (2015) were employed to extrapolate a suitable correlation (see Appendix A.1). In all the cases, the entrainment ratio was computed as a function of both the optimal pressure lift and the gas cooler/condenser outlet temperature. In this study, the configuration with multi-ejector pack and MT overfed evaporators was pointed out as EJ. An effectiveness of 0.5 was assumed for the IHX belonging to the solution which also has LT overfed evaporators (EJ_OV). Also, both EJ and EJ_OV have the same boundary conditions as IB. Similarly to the previously presented systems, the auxiliary compressors were replaced with a by-pass valve in subcritical operating conditions. In addition, it is important to remark that LEJ were not included in this investigation. This could be suitably justified by bearing in mind that:

- unlike VEJ, LEJ start operating only if the liquid indicator of the MP receiver exceeds a prefixed threshold;
- the main energy benefit of the liquid ejectors is associated with the rise in the evaporating temperature (Minetto et al., 2014a). This was supposed to be accomplished all over the year (Hafner and Banasiak, 2016);
- the quality of the refrigerant leaving the overfed heat exchangers was supposed equal to 1. The final outcomes were not substantially influenced by making this assumption, as the refrigerant coming out of the overfed evaporators typically has a quality about equal to 0.9 (Minetto et al., 2014a).

In a configuration resembling EJ and EJ_OV, both the vapour ejectors and the parallel compressors play a crucial role. The reliability and the manufacturability of a multi-ejector arrangement have already been proven, as well as its control system has already been successfully implemented (Banasiak et al., 2015; Banasiak et al., 2014; Hafner et al., 2016; Hafner et al., 2014c; Schönerberger, 2016). However, one of the main challenges which still needs to be overcome is represented by demonstrating the necessity to improve the performance of the parallel compressors to the manufacturers. The reason for this can be explained by assessing the field measurements collected by Hafner et al. (2016). These outcomes revealed that the use of the multi-ejector concept leads to:

- significant reductions in the mass flow rate associated with the HS compressors to the detriment of the parallel compressors. This can even take place in the event that AC is not demanded;

- the complete switching off of the HS compressors just as AC is requested. In this case, the vapour is totally compressed to HP by the auxiliary compressors.

These outcomes allow claiming that the required power input of the parallel compressors has a great contribution to the total energy consumption, as they deal with large amounts of refrigerant. As a consequence, substantial benefits could be obtained by enhancing the performance of such components. These would be particularly marked in warm climates and for pure CO₂ solutions integrated with the AC unit. To the best of the author's knowledge, the energy savings related to an increase in the efficiency of the parallel compressors have never been evaluated for multi-ejector CO₂ refrigerating units. This assessment could significantly promote the diffusion of more efficient components and a reduction in the operating costs. Therefore, an additional push towards the usage of the "CO₂ only" refrigerating plants in warm regions could be achieved. For this reason, this evaluation has been carried out for various sizes of the supermarket and considering the integration of the refrigeration plant with AC systems of different capacities as regards the most promising configuration (i.e. EJ_OV). Furthermore, it is worth remarking that few studies about the energy performance of multi-ejector R744 booster supermarket refrigeration systems integrated with the AC unit are currently available in the open literature. In addition, the present tendency regarding supermarket applications is to have "all-in-one" CO₂ refrigeration system (Hafner et al., 2016; Hafner and Banasiak, 2016; Hafner et al., 2015; Karampour and Sawalha, 2015, 2016a, 2016b).

4.1.6 Operating conditions of HFC-based systems

In this study, the cascade configuration and the R404A multiplex direct expansion system were respectively pointed out as CS and DXS. A minimum condensing temperature of 25 °C and an approach temperature of the condenser of 10 K were selected for both these solutions. This implied that:

- at outdoor temperatures less than or equal to 15 °C, the condensing temperature of both CS and DXS was fixed equal to 25 °C;
- at outdoor temperatures above 15 °C, the condensing temperature of both CS and DXS was equal to the sum of the outdoor temperature (t_{ext}) and ΔT_{appr} .

As for the cascade system, the temperature difference of the cascade condenser was assumed equal to 5 K.

4.1.7 Common operating conditions

For the case studies which do not involve the integration with the AC unit, the design cooling capacities were chosen equal to 120 kW and to 25 kW for the MT and the LT loads (Giroto et al., 2004), respectively. This scenario intends to simulate the running modes of a typical food retail application. In order to properly assess the advantages related to the usage of the overfed evaporators, the medium evaporating temperature was increased by 6 K (Wiedenmann, 2015) for OV, OV+PC, EJ and EJ_OV, while an increment by 8 K (Wiedenmann, 2015) was selected for the low evaporating temperature of EJ_OV. On the contrary, MT and LT added up to -10 °C and -35 °C (Giroto et al., 2004) for all the dry-expansion evaporators, whose degree of superheating was selected equal to 5 K. In addition, an increment in the refrigerant temperature by 5 K in all the suction lines was assumed. In all the evaluated cases, the deviation from the design running modes caused by the variations of the boundary conditions was considered by adopting the correlation suggested by Zhang (2006):

$$Load\ fraction = \left(1 - (1 - min) \frac{(30 - t_{ext})}{(30 - 5)}\right) \quad (4.1)$$

in which *min* denotes the minimum fraction of design load (equal to 0.66 for MT and to 0.8 for LT). According to the author, in fact, the cooling capacities increase with rise in outdoor temperature. In particular, the MT refrigeration load is more sensitive to the external temperature than the LT cooling capacity. Unlike LT evaporators, in fact, open display counters at MT are often adopted. The main reason why the outdoor temperature influences the cooling load can be associated with the fact that it is also affects the relative humidity. This implies that the relative humidity of the store varies as a function of the external temperature, as well as the frost formation in the evaporators and, consequently, the refrigerating capacity. According to Zhang (2006), the cooling loads range between a minimum value and the design one. The former is reached at external temperatures less than or equal to 5 °C. The design refrigeration capacities are obtained at outdoor temperatures greater than or equal to 30 °C. The reason for this lies in the presence of the heating system and in that of the AC unit, which maintain the supermarket temperature within certain limits.

The consumption related to all the fans was taken as 3% of the heat capacity rejected through the corresponding heat exchanger (Karampour and Sawalha, 2015). Also, pressure drop was neglected and all the expansion valves were treated as isenthalpic devices, as well as all the components were considered well-insulated.

4.1.8 Integration with the air conditioning unit

The AC unit maintains the ambient temperature of the store at about 23-25 °C. Their size and the employed technology strongly depends on the supermarket size. Movable plug-in units are for small applications, whereas stationary systems are used for large applications. Some of these systems are reversible, i.e. they can be used as heat pumping systems in wintertime. A R410A refrigeration unit was selected to match the cooling demand associated with the AC system and separately perform along with DXS. Except for its evaporating temperature, which was taken as 3 °C (Karampour and Sawalha, 2015), the same assumptions as the ones made for DXS were adopted. EJ_OV was chosen as an “all-in-one” solution (and pointed out as EJ_OV_AC), which presents an additional overfed evaporator at 5 °C to satisfy the cooling reclaim of the AC unit (Fig. 4.1). This solution represents the third generation of pure CO₂ supermarket refrigeration systems.

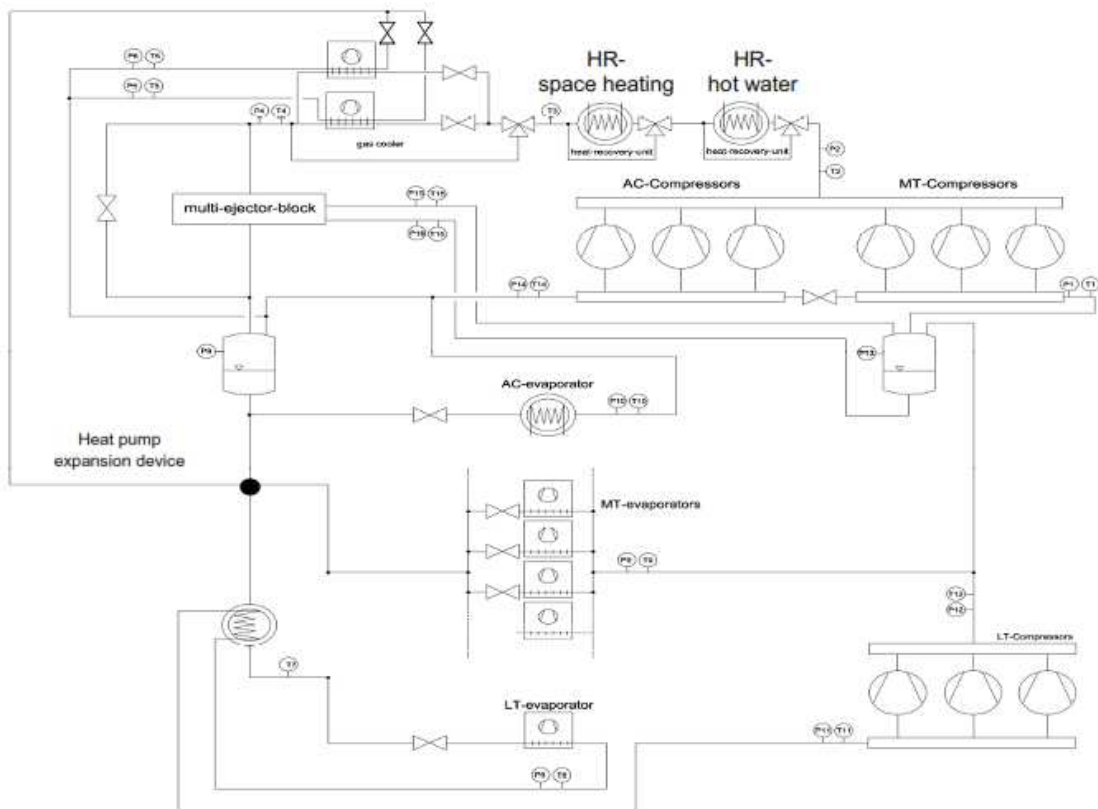


Fig. 4.1 - Schematic of an “all-in-one” R744 booster refrigeration system with parallel compression, LT and MT overfed evaporators and multi-ejector rack (Hafner et al., 2016).

Similarly to the cooling capacities, the AC load for both EJ_OV_AC and the separated HFC-based solution (DXS+AC) was assumed to be linearly depending on the outdoor temperature. In particular, the AC capacity was (linearly) ranged from a minimum value

(equal to 0 kW) to the design one. These limits were respectively supposed to be reached at $t_{ext} = 5\text{ }^{\circ}\text{C}$ and at $t_{ext} \geq 30\text{ }^{\circ}\text{C}$. In addition, it was assumed that the AC demand started weighing on both EJ_OV_AC and DXS+AC at $t_{ext} \geq 24\text{ }^{\circ}\text{C}$. At lower outdoor temperatures, if necessary, free cooling was supposed to occur. Three scenarios based on the assumption of the design load of the AC system equal to 50% (*Scenario I*), 100% (*Scenario II*) and 200% (*Scenario III*) of MT cooling capacity were investigated.

4.2 Simulation models

Models of the cycles were implemented in Engineering Equation Solver (EES) (F-Chart Software, 2015a), which were based on the fundamental thermodynamic equations at steady state.

As mentioned above, in transcritical operating conditions any “CO₂ only” refrigeration system features an optimal gas cooler pressure as a function of the external temperature (Cavallini and Zilio, 2007; Cecchinato et al., 2009; Kim et al., 2004; Lorentzen, 1994; Sawalha, 2008a). In addition, the intermediate pressure for PC and PC_VAR (Bell, 2004; Minetto et al., 2005) and P_{lift} for EJ and EJ_OV (Hafner et al., 2014a) are additional optimization parameters. Table 4.1 sums up the independent variables which were adopted to implement the optimization procedures of the R744 booster refrigeration systems under investigation. The DIRECT algorithm Method was used in case of two or more optimization variables, otherwise the Golden Section search Method was applied (F-Chart Software, 2015b). In all cases, the minimization of the total energy consumption was chosen as the objective function.

Table 4.1 - Independent variables for the optimization procedures of the R744 booster refrigeration systems under investigation.

<i>Configurations</i>	<i>Transition conditions</i>	<i>Transcritical conditions</i>
CB, IB, MS+PC, OV and OV+PC	-	P_{GC}
PC and PC_VAR	IP	IP, P_{GC}
EJ and EJ_OV	P_{lift}	P_{lift} , P_{GC}

As previously explained, a CO₂ booster refrigeration system operates in subcritical conditions if the outdoor temperature is low enough, whereas transcritical operations occurs at high external temperatures. In order to improve its performance, it is necessary

to define a transition zone which occurs at intermediate outdoor temperatures and which depends on the ability of the gas cooler/condenser to reject heat into the surroundings. A procedure similar to the one adopted by Cecchinato et al. (2007) was used for determining the conditions in which transcritical operations took place. As sketched in Fig. 4.2, four operational zones were defined. Zone I referred to the subcritical conditions in which, independently of the external temperature, the condensing temperature was kept equal to its minimum value, in accordance with Table 4.2 and Table 4.3. As a result of this, the energy consumption was constant. The shift from Zone I to Zone II depended on the approach temperature of the gas cooler/condenser and on the outdoor temperature. Since in both Zone I and Zone II a degree of subcooling of 2 K was selected, it occurred at values of external temperatures over 4 °C for IB, MS+PC, PC, PC_VAR, EJ and EJ_OV, whereas it took place over -2 °C for CB. Starting from such conditions, the system entered the subcritical zone in which the condensing temperature was ranged according to the external temperature (Zone II). The R744 condenser outlet temperature could thus be evaluated as follows:

$$t_{out,GC} = t_{ext} + \Delta T_{appr,GC} \quad (4.2)$$

The transition zone (Zone III) was the one in which the system moved gradually from the subcritical conditions to the transcritical ones. Conforming to the chosen condenser approach temperatures (Table 4.2 and Table 4.3), these conditions took place at external temperatures higher than 17 °C for IB, MS+PC, PC, PC_VAR, OV, OV+PC, EJ and EJ_OV and higher than 10 °C for CB. According to Cecchinato et al. (2007), Zone III could be defined by identifying an upper and a lower limit in terms of high pressure and gas cooler/condenser outlet temperature. In accordance with both such boundary conditions and the external temperature, the high pressure heat exchanger varied its working conditions linearly (segment A-B in Fig. 4.2). The condenser outlet temperature and the condensing one at the point A in Fig. 4.2 were set to 20 and 22 °C, respectively. The gas cooler outlet temperature and the upper limit of the high pressure, indicated as the point B in Fig. 4.2, were chosen equal to 29 °C and 75 bar (Table 4.2 and Table 4.3), respectively. In these running modes, the approach temperature of the gas cooler/condenser decreased from 3 K (point A in Fig. 4.2) for IB, MS+PC, PC, PC_VAR, OV, OV+PC, EJ and EJ_OV to 2 K (point B in Fig. 4.2) and from 10 K (point A in Fig. 4.2) to 5 K (point B in Fig. 4.2) for CB. The system operated along the conditions represented by the segment A-B in Fig. 4.2, following for IB, MS+PC, PC, PC_VAR, OV, OV+PC, EJ and EJ_OV the equations below:

$$t_{out,GC} = 0.9 \cdot t_{ext} + 4.7 \quad (4.3)$$

$$p_{GC} = 1.6633 \cdot t_{out,GC} + 26.763 \quad (4.4)$$

and

$$t_{out,GC} = 0.6429 \cdot t_{ext} + 13.571 \quad (4.5)$$

$$p_{GC} = 1.6633 \cdot t_{out,GC} + 26.763 \quad (4.6)$$

for CB.

Furthermore, this control strategy allowed reducing the degree of subcooling of the condenser/gas cooler from 2 K to a null value.

Transcritical conditions (Zone IV) took place at outdoor temperatures over 27 °C for IB, MS+PC, PC, PC_VAR, OV, OV+PC, EJ and EJ_OV and over 24 °C for CB.

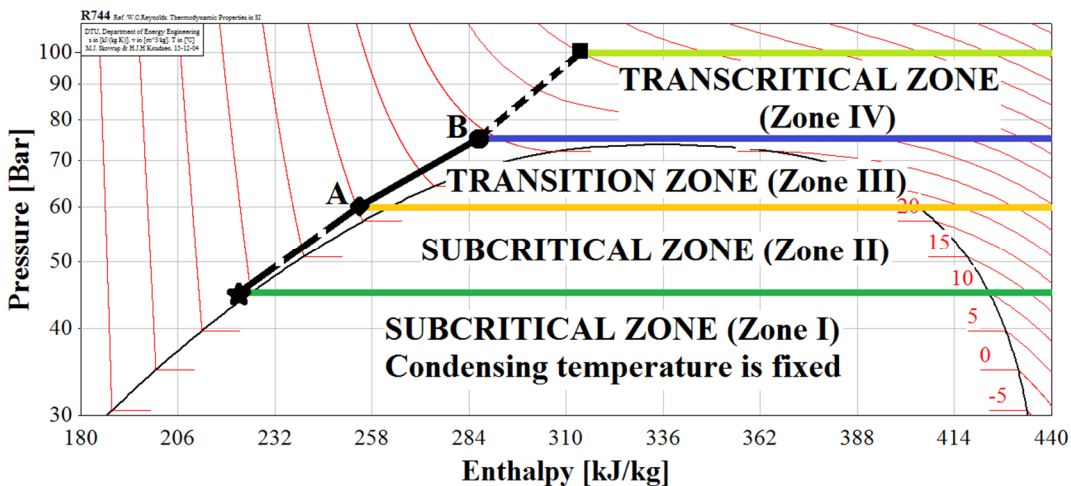


Fig. 4.2 - Definition of the operating zones for the R744 booster refrigeration systems under investigation.

Table 4.2 for CB and Table 4.3 for the other investigated solutions summarize the different selected operating zones. As regards OV and OV+PC, their minimum condensing temperature was equal to 12.5 °C. This implied that:

- Zone I took place at outdoor temperatures less than or equal to 7.5 °C;
- Zone II occurred at external temperatures above 7.5 °C and less than or equal to 17 °C with $t_{out,GC,MAX} = 20$ °C and $t_{GC,MAX} = 22$ °C, respectively;
- Zone III and Zone IV were the same as pointed out in Table 4.3.

Table 4.2 - Operating zones for CB.

<i>Zone</i>	t_{ext} [°C]	$t_{outGC,MAX}$ [°C]	$t_{GC,MAX}$ [°C]	$P_{GC,MAX}$ [bar]
I	$t_{ext} \leq -2$	8	10	45.02
II	$-2 < t_{ext} \leq 10$	20	22	60.03
III	$10 < t_{ext} \leq 24$	29	-	75.00
IV	$24 < t_{ext} \leq 41$	46	-	106.00

Table 4.3 - Operating zones for the other investigated booster solutions.

<i>Zone</i>	t_{ext} [°C]	$t_{outGC,MAX}$ [°C]	$t_{GC,MAX}$ [°C]	$P_{GC,MAX}$ [bar]
I	$t_{ext} \leq 4$	7	9	43.92
II	$4 < t_{ext} \leq 17$	20	22	60.03
III	$17 < t_{ext} \leq 27$	29	-	75.00
IV	$27 < t_{ext} \leq 41$	43	-	106.00

It is important to highlight that a further reduction in the values of $t_{outGC,MAX}$ pointed out in Table 4.2 and Table 4.3 is risky, since the vapour inside the separator downstream of the HP control valve would collapse. This would cause a fatal decrease in the pressure level of the separator, which would imply serious issues in the feeding of the various expansion devices of all the evaporators with liquid CO₂.

A “global efficiency” for the compressors was defined as the ratio of the power input calculated at the isentropic conditions and the power input declared by the manufacturers. The global efficiencies of the compressors were derived from BITZER Software (BITZER, 2015) and Dorin Software (Dorin, 2015) as a function of the pressure ratio. All the chosen compressors were semi-hermetic reciprocating ones and all their suggested technological constraints were respected.

4.3 Thermodynamic analyses

4.3.1 Energy analysis

The comparison in terms of annual energy consumption was based on the climate conditions in five warm cities located in Southern European, i.e. Rome (Italy), Lisbon (Portugal), Valencia (Spain), Athens (Greece) and Seville (Spain). According to Fig. 4.3, the external temperature was less than or equal to 4 °C for about 5.7% of the time over the year in Rome, 0.1% in Lisbon, 1.6% in Valencia, 2% in Athens and 1.3% in Seville. It ranged from 5 °C to 17 °C for about 55.7% of the time in Rome, 57.1% in Lisbon, 48.5% in Valencia, 49.4% in Athens and 48.5% in Seville. The outdoor temperature exceeded 17 °C reaching values up to 27 °C for about 33.6% of the time in Rome, 39.9% in Lisbon, 43.9% in Valencia, 37.7% in Athens and 36.4% in Seville. Also, the outdoor temperature is greater than 27 °C for about 5% of the time over the year in Rome, 2.9% in Lisbon, 5.9% in Valencia, 10.8% in Athens and 13.7% in Seville.

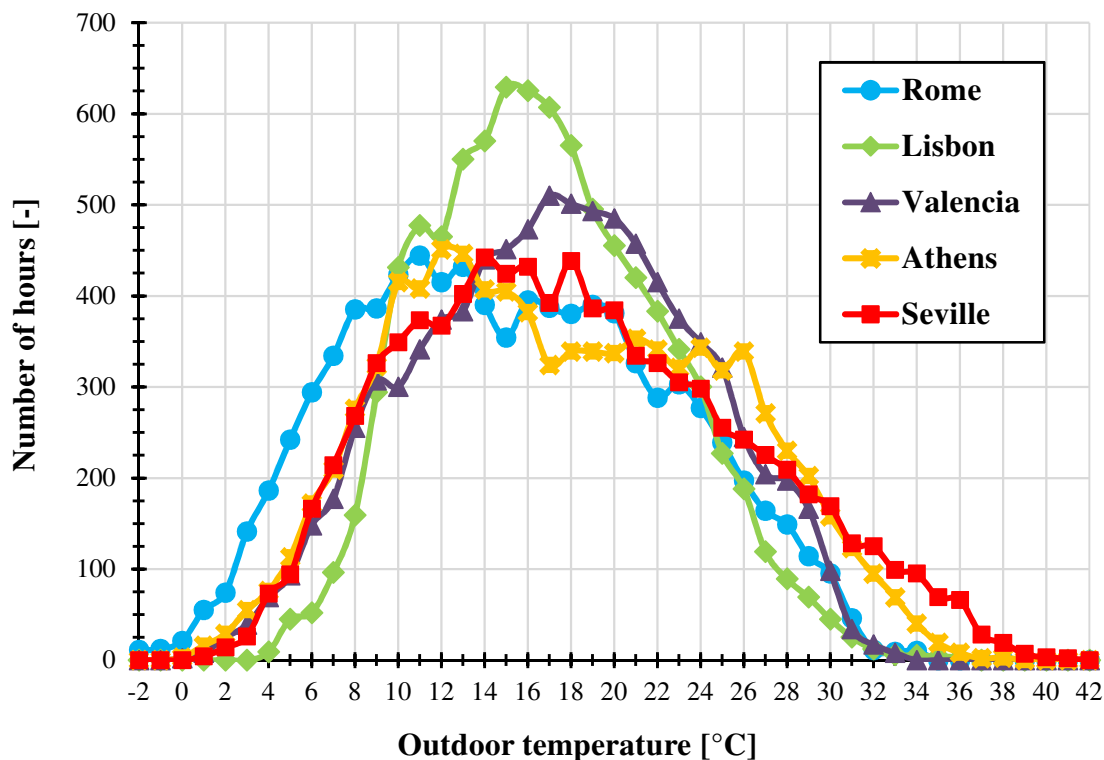


Fig. 4.3 - Number of hours per year at different outdoor temperatures in the selected locations (Remund et al., 2014).

In particular, the energy consumption of the evaluated systems in each of the selected locations was calculated as follows:

- estimation of the number of hours per year at which each of the outdoor temperatures belonging to the range -2 °C to 42 °C occurred (Fig. 4.3);
- computation of the total power input of each of the investigated solutions at each of the outdoor temperatures belonging to the range -2 °C to 42 °C;
- the total power input computed at each of the external temperatures between -2 °C to 42 °C and for each of the selected systems was then multiplied by the number of hours for which the corresponding outdoor temperature took place over the year in the chosen cities;
- finally, the annual energy consumption for each of the evaluated solutions in each of the selected locations was assessed by summing these products.

4.3.2 Exergy analysis

The conventional energy-based methods are widely employed tools thanks to its simplicity of application and intuitive interpretation of the results. On the other hand, the only thermodynamic irreversibilities recognised by them are the transfers of energy into the surroundings. However, the highest thermodynamic inefficiencies are those due to the irreversibilities occurring in the investigated system. The application of the conventional exergy analysis reveals the location, the magnitude and the sources of these inefficiencies. This kind of evaluation is thus much more appropriate than energy-based analyses when it comes to properly design and enhance the performance of any energy system. Nevertheless the conventional exergy analysis assesses neither the mutual interdependencies among the system components nor the potential to enhance a component. For this reason, in addition to the conventional energy assessments, the advanced exergy analysis was also carried out in this study.

Exergy is defined as the maximum useful work which can be obtained when the system under consideration reaches the thermodynamic equilibrium with the surroundings by interacting only with it. In this paper, the exergy analyses were based on the study presented by Morosuk and Tsatsaronis (2009) and on the application of the exergy rate balance at steady state (Moran et al., 2011) to each component.

$$\sum_j \left(1 - \frac{T_0}{T_j}\right) \cdot \dot{Q}_j - \dot{W}_{CV} + \sum_{in} \dot{m}_{in} \cdot e_{in} - \sum_{out} \dot{m}_{out} \cdot e_{out} - \dot{E}_D = 0 \quad (4.7)$$

It is important to notice that T_0 and T_j refer to temperatures measured by using Kelvin temperature scale. In addition, the variations in terms of chemical, kinetic and potential exergy were assumed negligible.

Exergy destruction (\dot{E}_D) is accordingly the source of thermodynamic irreversibilities, which means that the quantification of these allows the determination of the inefficiencies in the system. On the other hand, exergy losses (\dot{E}_L) are owing to the interaction between the surroundings and the system in the form of transfers of matter, heat and work.

The exergy efficiency (η_{exergy}) of a refrigeration machine can be defined as:

$$\eta_{\text{exergy}} = 1 - \frac{\dot{E}_D + \dot{E}_L}{W_{\text{tot}}} \quad (4.8)$$

The dead state temperature and the dead state pressure amounted to the outdoor temperature and to 1.01 bar, respectively. It is worth remarking that the results of the exergy analysis are not influenced substantially by the definition of the dead state (Ommen and Elmegaard, 2012).

The air temperature at the inlet and outlet of the MT evaporator were respectively taken as 2 °C and 0 °C (http://www.enex-ref.com/download/Enjector_promo_eng.pdf). Similarly, the air temperatures at the inlet and outlet of the LT evaporator were selected equal to -23 °C and to -25 °C, respectively. With respect to the air coming out of the gas cooler/condenser, its temperature was chosen 5 K higher than that at the inlet of the HP heat exchanger (Gullo et al., 2016c). The gas cooler/condenser pinch point temperature was assumed to equal the approach one in all the implemented exergy analyses (Gullo et al., 2016c). Also, the values of heat rejection pressure were kept equal to those computed for the conventional exergy analysis in all the evaluations (Gullo et al., 2016c).

4.3.3 Advanced exergy analysis

The advanced exergy evaluation is an appropriate tool to design any energy system since it allows overcoming the limitations of the conventional analyses (Açikkalp et al., 2014; Gungor et al., 2013; Chen et al., 2015). This purpose is accomplished as it reveals the real thermodynamic inefficiencies and the processes that cause them for each component of the investigated system. The advanced exergy evaluation, in fact, can find the location, the magnitude and the sources of inefficiencies, as well as it assesses both the potential enhancements achievable by an individual component and the influence of a component on the other ones. In addition, the sections above highlighted how the interest in transcritical R744 supermarket refrigeration systems has been growing greatly in the last few years. Therefore, the combination of these two topics is particularly promising, as already demonstrated by Gullo et al. (2016c). Morosuk et al. (2012) applied such an evaluation to an ammonia refrigeration machine working according to the Voorhees'

principle. The outcomes highlighted that close attention should be paid to the evaporator. The advanced exergy analysis was applied by Chen et al. (2015) to a R245fa refrigeration system equipped with an ejector as the compressor replacement and with a cooling capacity of 10 kW. The analysis revealed that the large irreversibilities occurring in the ejector are mainly endogenous. Furthermore, the temperature difference in the condenser also plays a pivotal role in the performance of the overall system. This assessment was also implemented by Bai et al. (2016) so as to study a one-stage CO₂ refrigerating unit using a two-phase ejector. The outcomes revealed that the designer's attention should be mainly focused on the compressor, followed by the ejector and then the evaporator. Also, the evaporator affects the irreversibilities associated with both the compressor and the ejector significantly. The authors also estimated reductions by 81.7% by increasing the efficiencies of the ejector components from 0.5 to 0.9. An advanced exergy analysis based on some experimental data was applied by Sarkar and Joshi (2016) to a CO₂ heating pumping unit for simultaneous water cooling and heating. The outcomes suggested that the design should mainly pay attention to the compressor enhancement to improve the whole system performance. Morosuk and Tsatsaronis (2008) implemented the advanced exergy assessment of an absorption refrigerating system and, later, additional evaluations were carried out by Gong and Goni Boulama (2015; 2014). Great enhancements could be achieved on the part of the gas cooler/condenser of a CO₂ booster refrigerating plant with auxiliary compressor operating at optimized intermediate pressure by rising MT, as recommended by Gullo et al. (2016). Mosaffa et al. (2014) employed such a method to study the thermodynamic performance of an air conditioning system made up of a vapour compression refrigerating machine and a heat thermal storage. The evaluation performed by Erbay and Hepbasli (2014) was based on the experimental data gathered from a ground-source heat pump drying system. The outcomes suggested that the designer's efforts should be mainly addressed to the condenser. Gungor et al. (2013) showed that the irreversibilities taking place in a gas engine heat pump are mainly preventable, apart from those of the evaporator, the compressor and the drying cabinet. The enhancement of the turbo air compressor allows bringing down the inefficiencies occurring in a trigeneration system, as demonstrated by Açıkkalp et al. (2014).

4.3.3.1 Endogenous and exogenous exergy destruction

The splitting of the exergy destruction into its endogenous and exogenous components allows determining the sources of inefficiencies. The endogenous exergy destruction within the k -th component ($\dot{E}_{D,k}^{EN}$) is defined as the part of the irreversibilities which occur

when this component is operating in real conditions and all the other ones are operating ideally. The exogenous exergy destruction within the k -th component ($\dot{E}_{D,k}^{EX}$) is owing to the inefficiencies which take place in the remaining components (Morosuk et al., 2012; Morosuk and Tsatsaronis, 2009; Tsatsaronis, 2008).

$$\dot{E}_{D,k} = \dot{E}_{D,k}^{EN} + \dot{E}_{D,k}^{EX} \quad (4.9)$$

In order to calculate the endogenous destruction rate associated with the k -th component, it is necessary to realize the so-called *hybrid I cycle*. In such a thermodynamic cycle, the component being considered operates at real conditions and all the remaining components work at theoretical operation conditions (i.e. $\dot{E}_{D,k} = 0$ if it is possible, otherwise $\dot{E}_{D,k} = \min$). The number of hybrid cycles which has to be implemented is equal to the number of the components of the investigated system. According to the selected components, these running modes can be reached by adopting the most suitable parameter in the second column of Table 4.4. It is thus possible to notice that, all the compressors and all the expansion valves were taken into account as isentropic devices in theoretical conditions. As regards the heat exchangers, their minimum temperature difference was selected equal to 0 K (Morosuk et al., 2012; Morosuk and Tsatsaronis, 2009).

Table 4.4 - Assumptions made to implement the advanced exergy analysis.

Compressors	$\eta_{glob}^{EN} = 1.00$	$\eta_{glob}^{UN} = 0.94$
Expansion valves	$\eta_{isen}^{EN} = 1.00$	-
Multi-ejector rack	-	$\eta_{isen}^{UN} = 0.60$
Heat exchangers	$\Delta T_{pp}^{EN} = 0.00 \text{ K}$	$\Delta T_{pp}^{UN} = 0.50 \text{ K}$

Therefore, for a conventional vapour compression refrigeration machine, four *hybrid I cycles* have to be developed (Fig. 4.4):

- compressor ($\dot{E}_{D,CM}^{EN}$) = cycle 1_T-2_E-3_T-4_T
- condenser ($\dot{E}_{D,CD}^{EN}$) = cycle 1_T-2_E^{*}-3_E-4_E
- throttling valve ($\dot{E}_{D,TV}^{EN}$) = cycle 1_T-2_T-3_T-4_E
- evaporator ($\dot{E}_{D,EV}^{EN}$) = cycle 1_R-2_E-3_T-4_E^{*}

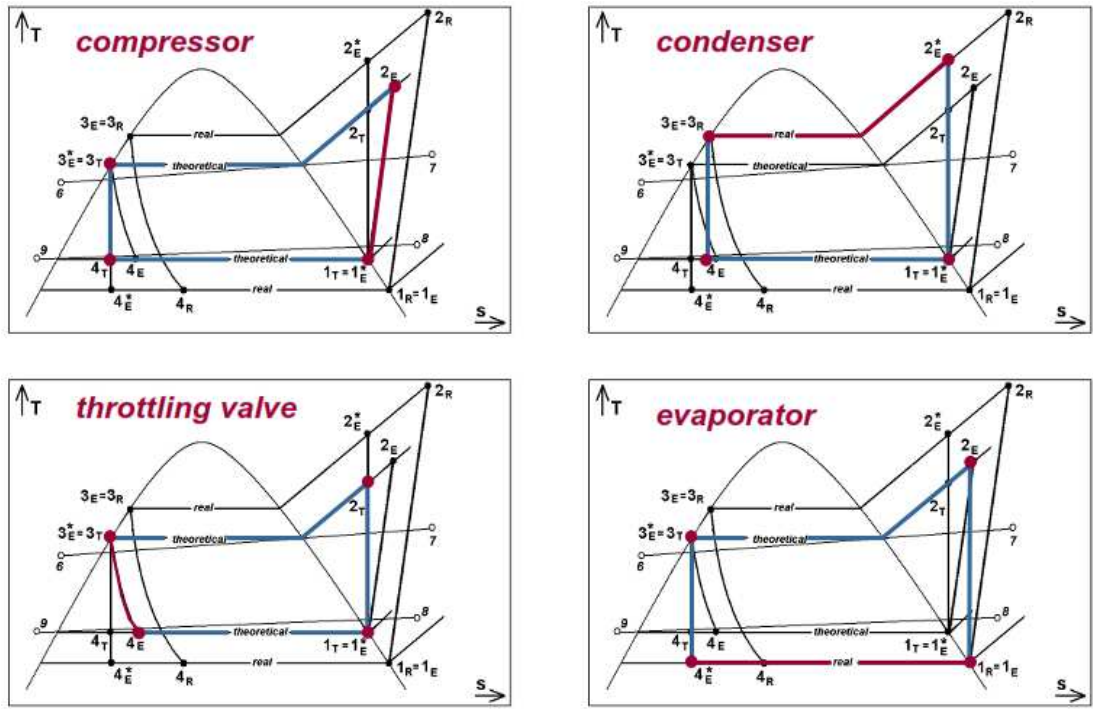


Fig. 4.4 - Thermodynamic cycles in endogenous operation conditions for a conventional vapour compression refrigeration system (Tsatsaronis, 2010).

After calculating $\dot{E}_{D,k}$ through the application of the conventional exergy analysis and $\dot{E}_{D,k}^{EN}$ as mentioned above, $\dot{E}_{D,k}^{EX}$ can be computed through Eq. 4.9.

In the present investigation the superheating occurring in the suction lines was neglected in the advanced exergy analysis.

4.3.3.2 Avoidable and unavoidable exergy destruction

The unavoidable exergy destruction (\dot{E}_D^{UN}) refers to the part of irreversibilities which cannot be avoided even if the best available component is being used due to the technological limitations, such as manufacturing methods, cost and accessibility of materials. Unlike the total exergy destruction, \dot{E}_D^{AV} reveals the real potential improvements that the component which is being evaluated can achieve and, thus, the part of inefficiencies to which the designer should pay attention (Morosuk et al., 2012; Morosuk and Tsatsaronis, 2009; Tsatsaronis and Moungh-Ho, 2002).

$$\dot{E}_{D,k} = \dot{E}_{D,k}^{UN} + \dot{E}_{D,k}^{AV} \quad (4.10)$$

The unavoidable irreversibilities can be computed by implementing a thermodynamic cycle (Fig. 4.5) based on the assumptions listed in the third column of Table 4.4. Such values point out that, even if the best available heat exchangers had selected, the irreversibilities associated with their corresponding temperature difference (ΔT_{pp}^{UN}) would

occur. As for the compressors, though the best accessible compressor had chosen, some inefficiencies (η_{glob}^{UN}) would take place. The chosen values depict the technological constraints of the air-cooled gas coolers, of the evaporators using the air as the secondary fluid, of the multi-ejector module and of the CO₂ semi-hermetic reciprocating compressors for the near future. It is important to mention that although the assumptions made to simulate the unavoidable operating conditions are mainly based on the designer's knowledge/experience, general trends can be recognized.

The thermodynamic cycles of a vapour compression refrigeration unit in both real (1_R-2_R-3_R-4_R) and theoretical (1_{RU,D}-2_{RU,D}-3_{RU,D}-4_{RU,D}) operation conditions are sketched in Fig. 4.5.

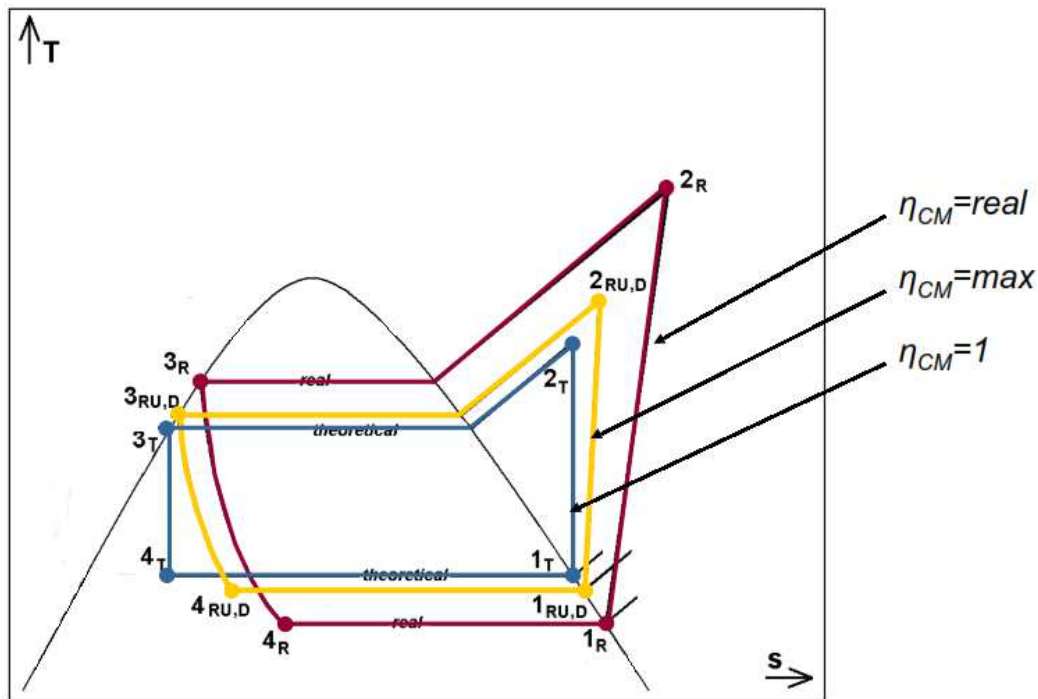


Fig. 4.5 - Real and theoretical thermodynamic cycles for a conventional vapour compression refrigeration system (Tsatsaronis, 2010).

At a later time, $\dot{E}_{D,k}^{AV}$ can be computed by subtracting $\dot{E}_{D,k}^{UN}$ from $\dot{E}_{D,k}$ (Eq. 4.10). In this paper, a procedure similar to the one used by Morosuk and Tsatsaronis (2009) was applied to compute \dot{E}_D^{UN} .

It is important to remark that P_{lift} value for the multi-ejector module was maintained constant in all the analyses. In addition, the effectiveness of IHX was taken as 0.9 at unavoidable operation conditions. Also, the consumption associated with the fans was

selected equal to 0.5% of the heat transfer rate of the corresponding HP heat exchanger for the unavoidable operating conditions.

4.3.3.3 Combining of the two splitting approaches

The previously mentioned components of the exergy destruction can be further split to improve the understanding and the detection of the potential inefficiencies:

$$\dot{E}_{D,k} = \dot{E}_{D,k}^{UN,EN} + \dot{E}_{D,k}^{UN,EX} + \dot{E}_{D,k}^{AV,EN} + \dot{E}_{D,k}^{AV,EX} \quad (4.11)$$

where $\dot{E}_{D,k}^{UN,EN}$ is the unavoidable endogenous exergy destruction, whereas $\dot{E}_{D,k}^{UN,EX}$ refers to the unavoidable exogenous exergy destruction. They cannot be decreased because of the technical limitations associated with the k -th component and with the remaining components, respectively. Improving the efficiency of the k -th component allows reducing the endogenous avoidable part of its exergy destruction ($\dot{E}_{D,k}^{AV,EN}$), whereas the drop in the irreversibilities occurring in the remaining components leads to a decrease in the exogenous avoidable part of its exergy destruction ($\dot{E}_{D,k}^{AV,EX}$) (Morosuk et al., 2012; Morosuk and Tsatsaronis, 2009; Tsatsaronis, 2008).

The values of $\dot{E}_D^{UN,EN}$ were calculated in the same way as Morosuk and Tsatsaronis (2009). In particular, the k -th component was considered operating at unavoidable conditions (through the selection of the appropriate parameter in the third column of Table 4.4), whereas all the remaining components was simulated in theoretical operation conditions (in conformity with subsection 4.3.3.1). The other parts making up the exergy destruction rate of the k -th component can be computed as follows:

$$\dot{E}_{D,k}^{UN,EX} = \dot{E}_{D,k}^{UN} - \dot{E}_{D,k}^{UN,EN} \quad (4.12)$$

$$\dot{E}_{D,k}^{AV,EN} = \dot{E}_{D,k}^{EN} - \dot{E}_{D,k}^{UN,EN} \quad (4.13)$$

$$\dot{E}_{D,k}^{AV,EX} = \dot{E}_{D,k}^{EX} - \dot{E}_{D,k}^{UN,EX} \quad (4.14)$$

The computational procedure of the advanced exergy analysis is summarized with the aid of Fig. 4.6.

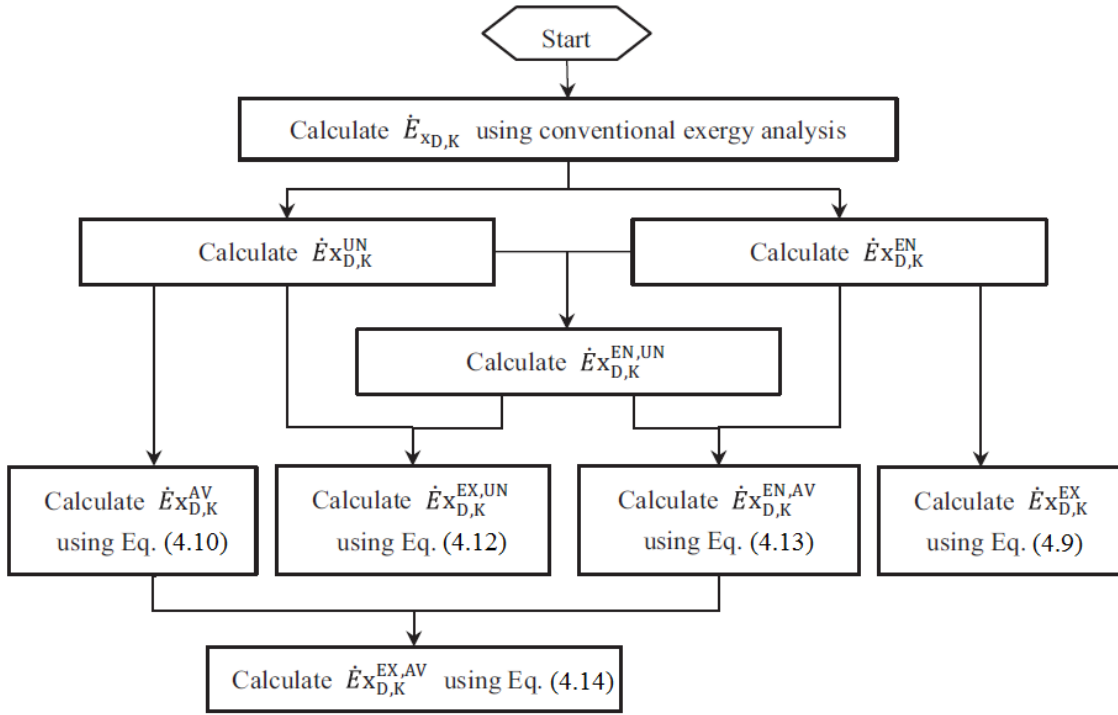


Fig. 4.6 – Flow chart for the advanced exergy analysis.

4.3.3.4 Interaction among the components

The simultaneous interactions among all the components of the evaluated system generate the so-called mexogenous exergy destruction ($\dot{E}_{D,k}^{MX}$), which can be calculated as:

$$\dot{E}_{D,k}^{MX} = \dot{E}_{D,k}^{EX} - \sum_{\substack{r=1 \\ r \neq k}}^n \dot{E}_{D,k}^{EX,r} \quad (4.15)$$

$\sum_{\substack{r=1 \\ r \neq k}}^n \dot{E}_{D,k}^{EX,r}$ represents the exogenous exergy destruction of the k -th component caused by the irreversibilities which take place in the r -th component (Morosuk et al., 2012; Wang et al., 2012). In particular, to compute $\dot{E}_{D,k}^{EX,r}$ another cycle in which both the investigated component (k -th component) and another component (r -th component) operate at real conditions and the remaining $n-2$ components work at ideal running modes (the so-called *hybrid II cycle*) has to be implemented. As a result, the exogenous exergy destruction rate related to k -th component and due to the r -th component ($\dot{E}_{D,k}^{EX,r}$) can be estimated. The difference between $\sum_{\substack{r=1 \\ r \neq k}}^n \dot{E}_{D,k}^{EX,r}$ and $\dot{E}_{D,k}^{EX}$ is defined mexogenous exergy destruction ($\dot{E}_{D,k}^{MX}$), which is ascribable to the simultaneous interconnections among the remaining components.

The splitting of the exergy destruction associated with the k -th component for the advanced exergy analysis is summarized in Fig. 4.7.

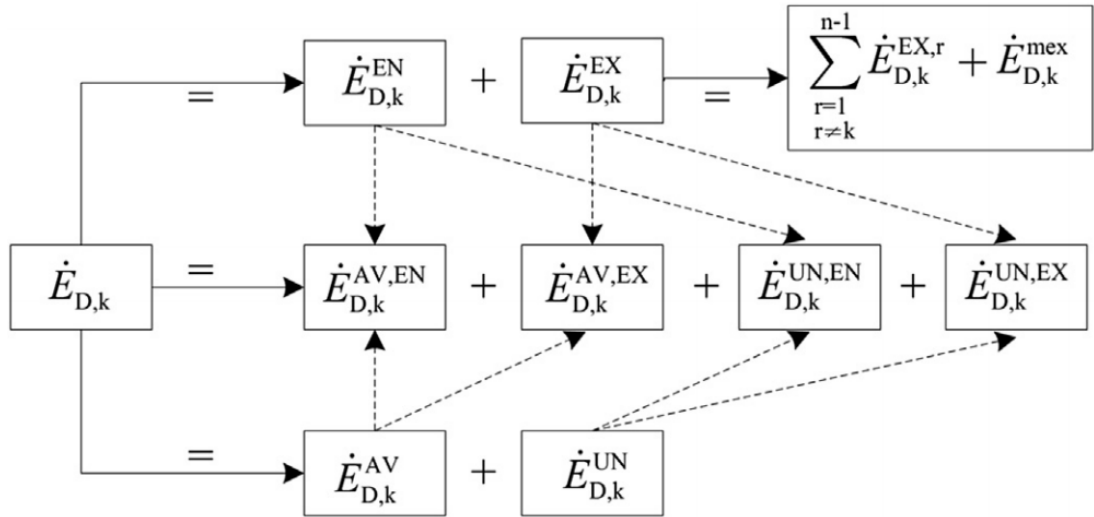


Fig. 4.7 - Sketch of the splitting of the exergy destruction associated with the k -th component for the advanced exergy analysis.

4.4 Environmental analysis

The environmental analysis implemented in this study was based on the evaluation TEWI, which is a parameter assessing both the direct and the indirect contribution to climate change of the investigated system. The former is due to the refrigerant leaks into the atmosphere, whereas the latter is due to the greenhouse gas emissions associated with the process of electricity generation to run the refrigeration plant. It is defined as (BRA, 2006):

$$TEWI = TEWI_{direct} + TEWI_{indirect} \quad (4.16)$$

$$TEWI_{direct} = GWP \cdot \gamma \cdot n + GWP \cdot m \cdot (1 - \alpha) \quad (4.17)$$

$$TEWI_{indirect} = E \cdot \beta \cdot n \quad (4.18)$$

As far as the evaluated solutions were concerned, the below assumptions were made:

- the GWP of R134a and that of R404A were selected equal to $1430 \text{ kg}_{\text{CO}_2,\text{equ}} \cdot \text{kg}_{\text{refrigerant}}^{-1}$ and $3922 \text{ kg}_{\text{CO}_2,\text{equ}} \cdot \text{kg}_{\text{refrigerant}}^{-1}$, respectively (AIRAH, 2012), whereas the direct contribution to climate change on the part of all the natural refrigerants selected in this study was assumed negligible (Gullo et al., 2016a; Gullo et al., 2016b; Llopis, 2015a);

- an annual leakage rate for both DXS and CS of 15% was chosen (EMERSON Climate Technologies, 2010; Shilliday, 2012), whereas it added up to 5% for the mechanical subcooling cycles since it was supposed to be completely confined in the machinery room (Llopis et al., 2015a);
- the operating life of all the selected systems was evaluated equal to 10 years (EMERSON Climate Technologies, 2010; Shilliday, 2012);
- R134a charge in HTC of the cascade refrigeration system was chosen equal to $2 \text{ kg}_{R134a} \cdot \text{kW}_{cc}^{-1}$ (EMERSON Climate Technologies, 2010);
- the charge of R404A in MTC and that in LTC were assumed equal to $2 \text{ kg}_{R404A} \cdot \text{kW}_{cc}^{-1}$ and $4 \text{ kg}_{R404A} \cdot \text{kW}_{cc}^{-1}$ (EMERSON Climate Technologies, 2010), respectively;
- 95% of the refrigerant was assumed to be recycled (EMERSON Climate Technologies, 2010);
- the CO₂ emission due to the electricity generation was chosen equal to $0.241 \text{ kg}_{\text{CO}_2,\text{equ}} \cdot \text{kWh}^{-1}$ (Llopis et al., 2015a) in Valencia and in Seville, to $0.720 \text{ kg}_{\text{CO}_2,\text{equ}} \cdot \text{kWh}^{-1}$ (IEA, 2013) in Athens, to $0.402 \text{ kg}_{\text{CO}_2,\text{equ}} \cdot \text{kWh}^{-1}$ (IEA, 2013) in Rome and to $0.303 \text{ kg}_{\text{CO}_2,\text{equ}} \cdot \text{kWh}^{-1}$ (IEA, 2013) in Lisbon.

As regards the AC unit, the environmental analyses were based on:

- a value of TEWI for R410A equal to $2088 \text{ kg}_{\text{CO}_2,\text{equ}} \cdot \text{kg}_{\text{refrigerant}}^{-1}$ (AIRAH, 2012);
- an annual leakage rate 7% was chosen (AIRAH, 2012);
- an operating life of all the selected systems of 10 years;
- a R410A charge equal to $2 \text{ kg}_{R410A} \cdot \text{kW}_{cc}^{-1}$;
- 95% of the refrigerant was supposed to be recycled.

5 RESULTS AND DISCUSSION

The results obtained are showed and exhaustively commented in this chapter. A comparison with the results available in the open literature is also made.

5.1 Results of thermodynamic analyses

5.1.1 Results of energy analysis

As far as the energy assessment was concerned, the distinctive parameters of the investigated solutions and some sensitivity analyses were carried out. In addition, the energy savings related to the most currently advanced “CO₂ only” solutions were estimated for a typical supermarket application ($\dot{Q}_{MT,design} = 120$ kW, $\dot{Q}_{LT,design} = 25$ kW) in five different warm locations, i.e. Rome (Italy), Lisbon (Portugal), Valencia (Spain), Athens (Greece) and Seville (Spain). Two different HFC-based configurations and two R744 booster refrigerating plants were selected as baselines. The results obtained were found to be consistent with the ones available in the open literature. Furthermore, the energy benefits related to the usage of a de-superheater on the part of some of the selected systems were computed. Finally, the energy consumption of a CO₂ refrigeration system equipped with a multi-ejector module and integrated with the AC unit was compared with that of separated HFC solutions. This assessment took into account three different warm locations, different sizes of both the AC system and the supermarket and the influence of the auxiliary compressor efficiency on the overall performance.

5.1.1.1 Optimal heat rejection pressure for a typical supermarket

In Fig. 5.1 the optimal gas cooler pressures of all the investigated CO₂ solutions for a typical food retail application ($\dot{Q}_{MT,design} = 120$ kW, $\dot{Q}_{LT,design} = 25$ kW) are plotted.

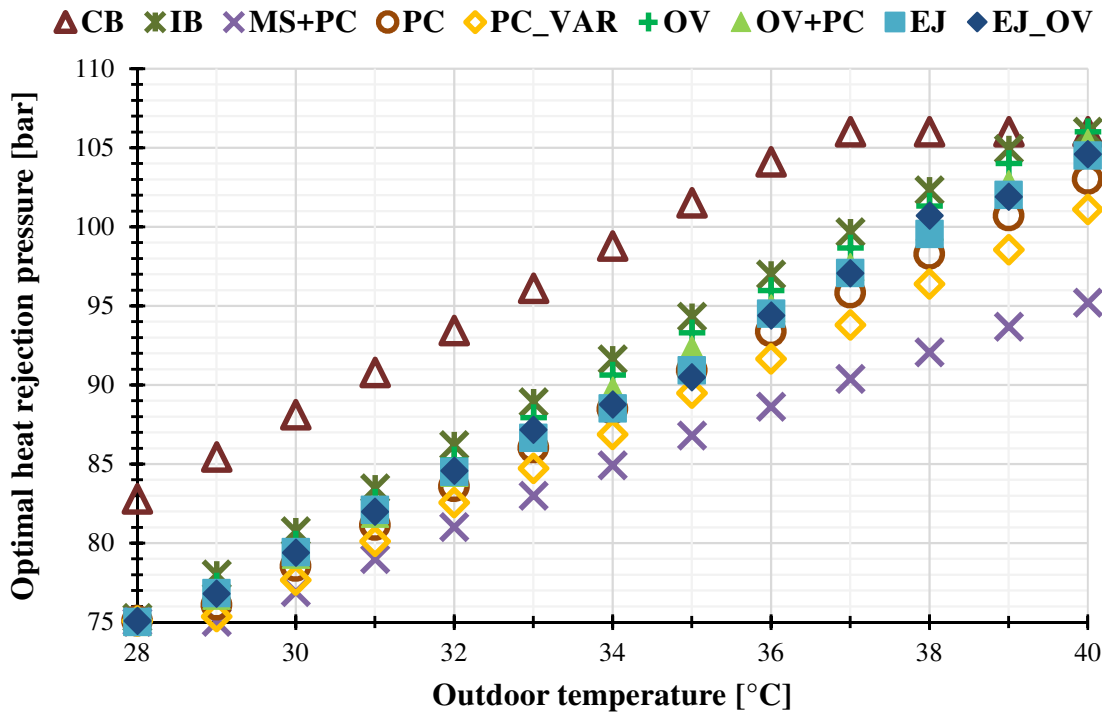


Fig. 5.1 - Optimal heat rejection pressure for all the investigated R744 booster refrigerating solutions as a function of the outdoor temperature.

Due to the high value of the gas cooler approach temperature, CB featured the highest optimal heat rejection pressures. At $t_{ext} = 28$ °C, the discharge pressure of CB was 9.1% higher than that of IB. On the one hand, CB reached the maximum value of HP (i.e. 106 bar, which represents a technological constraint for the selected HS compressors) starting from $t_{ext} = 37$ °C, whereas this value was obtained at $t_{ext} = 40$ °C for IB. At $t_{ext} = 37$ °C, the heat rejection pressure associated with CB was 6% as high as that of IB. The removal of the flash gas from the liquid receiver via auxiliary compressors led to reductions in the optimum heat rejection pressure up to 4% on the part of PC and to 6.1% for PC_VAR over IB. MS+PC dropped the gas cooler pressure, at best, by 10.7% compared to IB. All the other investigated solutions showed similar values of optimum HP to those related to IB. In comparison with IB, in fact, OV and OV+PC had, at best, 1.1% and 2.2% lower gas cooler pressure, respectively. As regards EJ and EJ_OV, the highest reduction was equal to 3.6% and 4.1%, respectively.

It can be concluded that the life expectancy of the CO₂ compressors belonging to MS+PC is longer than those employed in the other investigated solutions.

5.1.1.2 Comparison in terms of COP for a typical supermarket

Fig. 5.2 compares the COPs of all the evaluated solutions for a conventional commercial refrigeration application ($\dot{Q}_{MT,design} = 120$ kW, $\dot{Q}_{LT,design} = 25$ kW). It clearly shows that CB was not a suitable configuration for the investigated locations, consuming from 0.9% ($t_{ext} = 8$ °C) up to 30.8% ($t_{ext} = 40$ °C) more electricity than DXS. In addition, it was also possible to notice that IB, PC, PC_VAR and MS+PC had better performance than DXS at outdoor temperatures up to 14 °C, whereas the baseline outperformed them starting from $t_{ext} = 15$ °C. According to Matthiesen et al. (2010), this value represents the current energy limit for R744 refrigerating plants defined as the “CO₂ equator”. Also, it is important to highlight that PC, PC_VAR and MS+PC performed in the same way as IB at $t_{ext} \leq 17$ °C. IB consumed from 1.6% to 20.5% more electricity than DXS at external temperatures ranging from 15 °C to 40 °C. The occurrence of the transition operating conditions (17 °C $< t_{ext} \leq 27$ °C) put all the auxiliary compressors into operation (highlighted in Fig. 5.2 by a sudden increase in COP at $t_{ext} = 18$ °C) allowing PC and PC_VAR to save up to 2.4% more energy than DXS. At the extreme working modes the performance of the solution with parallel compression was significantly deteriorated on account of the large amount of flash gas generated in the receiver. At outdoor temperatures above 28 °C, the energy consumption associated with PC and PC_VAR was respectively from 4.2% to 10.2% and from 2.8% to 8.3% higher than that of DXS. In comparison with PC, a further reduction in the energy consumption up to 2.1% could be achieved by adopting PC_VAR. The reason for this result could be justified by considering that in transcritical modes:

- the optimal intermediate pressure was much higher than that evaluated in transition conditions (see Fig. 5.4);
- at the same outdoor temperature, the parallel compressor running in PC reached lower values of pressure ratio than that working in PC_VAR. However, the global efficiency of the former was lower than that of the latter.

As regards MS+PC, at outdoor temperatures ranging from 15 °C to 17 °C it featured slightly higher energy consumption (+1% ÷ +2%) than the R404A-based solution. The combination of the mechanical subcooling loop and that of the auxiliary compressor permitted MS+PC to outperform DXS at more extreme operating conditions. The energy

savings associated with DXS ranged from 5.3% (at $t_{\text{ext}} = 18\text{ }^{\circ}\text{C}$) to 13.7% (at $t_{\text{ext}} = 40\text{ }^{\circ}\text{C}$). It is also important to notice that MS+PC was slightly penalised at outdoor temperatures ranging from $18\text{ }^{\circ}\text{C}$ to $22\text{ }^{\circ}\text{C}$ due to the operating envelope of the R290 compressor. The overfeeding of the MT evaporators (OV) led to drop in electricity consumption from 43% (at $t_{\text{ext}} = 7\text{ }^{\circ}\text{C}$) to 0.7% (at $t_{\text{ext}} = 28\text{ }^{\circ}\text{C}$). On the other hand, some deteriorations in terms of COP were obtained due to a higher minimum condensing temperature (i.e. $12.5\text{ }^{\circ}\text{C}$) in comparison with the other investigated transcritical CO_2 systems. In transcritical running modes, this technology was not adequately energy beneficial due to the fact that OV consumed from 1.4% (at $t_{\text{ext}} = 29\text{ }^{\circ}\text{C}$) to 12% (at $t_{\text{ext}} = 40\text{ }^{\circ}\text{C}$) more electricity in comparison with DXS. The adoption of an auxiliary compressor made OV energy make it competitive with DXS at outdoor temperatures up to $32\text{ }^{\circ}\text{C}$, leading to reduction in the electricity consumption from 42.9% at $t_{\text{ext}} = 6\text{ }^{\circ}\text{C}$ to 0.9% at $t_{\text{ext}} = 32\text{ }^{\circ}\text{C}$. On the other hand, the energy consumption related to OV+PC was estimated to be from 0.2% (at $t_{\text{ext}} = 33\text{ }^{\circ}\text{C}$) to 4.1% (at $t_{\text{ext}} = 40\text{ }^{\circ}\text{C}$) higher than that of DXS at higher external temperatures.

Unlike PC, PC_VAR and MS+PC, COPs associate with both OV and OV+PC exceeded those of DXS at text ranging from $15\text{ }^{\circ}\text{C}$ to $17\text{ }^{\circ}\text{C}$. Both the configurations equipped with the multi-ejector arrangement could outperform all the previously mentioned systems over the considered range of temperatures. In particular, at outdoor temperatures from $0\text{ }^{\circ}\text{C}$ to $40\text{ }^{\circ}\text{C}$ EJ and EJ_OV respectively showed an increment in COP ranging from 77.6% to 13% and from 96.3% to 17.7% compared to DXS. In transcritical conditions, COPs related to EJ and EJ_OV were on average 14.3% and 19.1% higher than those of DXS, respectively. In fact, in relation to EJ, the overfeeding of both the evaporators entailed an additional improvement in the performance ranging from 10.5%, computed in subcritical conditions, to 3.3%, calculated in transcritical operations.

Considering IB as the baseline, it was possible to observe that:

- parallel compression-based systems (PC and PC_VAR) had approximately from 6.4% to 11% in transition running modes and from 11.1% to 15.5% in transcritical operation conditions lower consumption;
- MS+PC consumed from 9.4% ($t_{\text{ext}} = 18\text{ }^{\circ}\text{C}$) to 43% ($t_{\text{ext}} = 40\text{ }^{\circ}\text{C}$) less energy than IB;
- the overfeeding of the MT evaporators (OV) allowed bringing the energy consumption from 16.7% down to 10.7%. The additional usage of an auxiliary

compressor (OV+PC) entailed energy saving ranging from 24.8% to 18.9% over IB;

- in transcritical running modes the major energy savings on the part of both EJ and EJ_OV over IB were revealed which, at worst, could reach values of 35.5% and 41.2% and, at best, of 44.5% and 49.9%, respectively. At external temperatures from 18 °C up to 27 °C, decreases in annual electricity consumption from 28.6% to 37.3% on the part of EJ and from 36.9% to 44.4% by EJ_OV were obtained.

Also, PC and PC_VAR were suitable replacements for CS at outdoor temperatures up to 19 °C, whereas the cascade configuration was capable of outperforming them at more extreme operating conditions and dropping the energy consumption up to about 27%. On the other hand, MS+PC had from 45.1% to 0.3% higher energy savings at external temperatures up to 24 °C and from 0.7% to 8.7% greater electricity consumption in comparison with CS at higher external temperatures. The combination of overfed evaporators with the technology of parallel compression (OV+PC) made pure CO₂ configurations energy competitive with CS up to $t_{\text{ext}} = 26$ °C (from -43.6% at $t_{\text{ext}} = 8$ °C to -1.4% at $t_{\text{ext}} = 26$ °C). At external temperatures above the previously mentioned value, OV+PC performed worse than CS (from +0.5% at $t_{\text{ext}} = 27$ °C to +23% at $t_{\text{ext}} = 40$ °C). With respect to EJ, such a solution reduced the electric power consumption from 56.2% (at $t_{\text{ext}} = 4$ °C) to 0.6% (at $t_{\text{ext}} = 32$ °C). At higher external temperatures, increases in energy consumption up to 8.5% were estimated for EJ over CS. The most advanced solution (EJ_OV) had better COPs than the latter up to $t_{\text{ext}} = 35$ °C (from -100.7% at $t_{\text{ext}} = 4$ °C to -0.8% at $t_{\text{ext}} = 35$ °C), whereas the difference in electric energy consumption became negligible at higher external temperatures. These outcomes are due to the need to collect additional experimental data to enhance the ejector performance simulation. In fact, as suggested by Shecco (2016), two-phase ejectors for expansion work recovery operate efficiently at outdoor temperatures up to 44 °C compared to HFC-based systems. Better performance of CS over DXS can be justified by considering that R404a is a working fluid which is usually chosen to decrease the initial investment costs, whereas R134a is typically selected to improve the system performance at high ambient temperature countries.

Finally, it is worth highlighting that EJ_OV had from 24.7% to 33.7% lower electricity consumption than PC_VAR over the selected range of temperatures. Furthermore, such a configuration brought the required power consumption from 38.3% down to 4.7% and

from 37.5% down to 11.7% respectively over MS+PC and OV+PC at external temperatures ranging from 0 °C to 40 °C.

To sum up, it could be claimed that:

- the warmer the weather, the more it was necessary to adopt advanced expedients so as to make transcritical R744 systems energy beneficial in relation to HFC-based configurations;
- the energy efficiency limit of an “improved” CO₂ booster unit compared to a R404A direct expansion system was at t_{ext} around 14 °C (i.e. subcritical running modes);
- the use of either the parallel compression or MT overfed evaporators pushed the aforementioned limit to about 27-28 °C, with the latter presenting better performance than the former. In addition, the two evaluated control strategy for the intermediate pressure for the solutions with the auxiliary compressor did not reveal any noteworthy enhancements in COP;
- by combining these two technologies (i.e. auxiliary compressors with MT overfed display counters) transcritical R744 solutions had higher COPs than a R404A unit at t_{ext} up to about 32 °C. Another bright side related to the usage of MT overfed evaporators was that, unlike parallel compression-based solutions, it permitted outperforming the solutions using HFCs even at outdoor temperatures ranging from 15 °C to 17 °C;
- the configuration coupling the dedicated mechanical subcooling with parallel compression can be suitably substituted with more affordable and reliable systems, such as the one with parallel compressors and MT overfed evaporators in mild/warm regions and the multi-ejector module in warm/hot locations;
- the multi-ejector based configurations presented no energy efficiency limits compared to the currently used technologies, allowing to assert that nowadays “CO₂ only” refrigerating plants could suitably replace R404A units in any climate context.

At last, all the investigated advanced transcritical systems showed similar performance to a R134a/R744 cascade arrangement at t_{ext} up to about 29 °C, whereas at higher outdoor temperatures the latter could be replaced only with either the multi-ejector based solutions or that with subcooling loop.

Although MS+PC offered some modest energy conservations in hot regions, both the total investment cost and the implementation of the control system associated with this solution could penalize it substantially. As shown in Fig. 5.3, the required cooling capacity of the mechanical subcooling loop ranged from 12.4 kW to 78.6 kW. This means that the mechanical subcooler would have run at part load for most of the time, as well as it should be very large. Furthermore, it can be claimed that the adoption of such a solution is likely more suitable for small supermarkets.

As previously claimed, the intermediate pressure is an optimization parameter for the configurations using an auxiliary compressor (Bell, 2004; Minetto et al., 2005). As depicted in Fig. 5.4, PC and PC_VAR presented the same optimal intermediate pressure at outdoor temperatures up to 24 °C, at which IP added up to about 40 bar (maximum intermediate pressure for PC). This was due to the fact that the same auxiliary compressors were selected for PC and PC_VAR. Increases in terms of liquid receiver pressure from 1.5% to 4.8% on the part of PC over PC_VAR were estimated at external temperatures up to 27 °C. Also, it was possible to notice a sharp increase in the optimum intermediate pressure as soon as the transcritical operations took place. This result could be associated with the significant increment in the amount of vapour which had to be drawn at high external temperatures. In these conditions, in fact, the intermediate pressure had to be risen in order to be capable of substantially decreasing the electrical consumption of the additional compressor. The liquid receiver pressure was equal to 45.7 bar at 28 °C and it reached the value of 50.7 bar at $t_{\text{ext}} = 41$ °C, showing an average value of 49.3 bar in transcritical operation conditions.

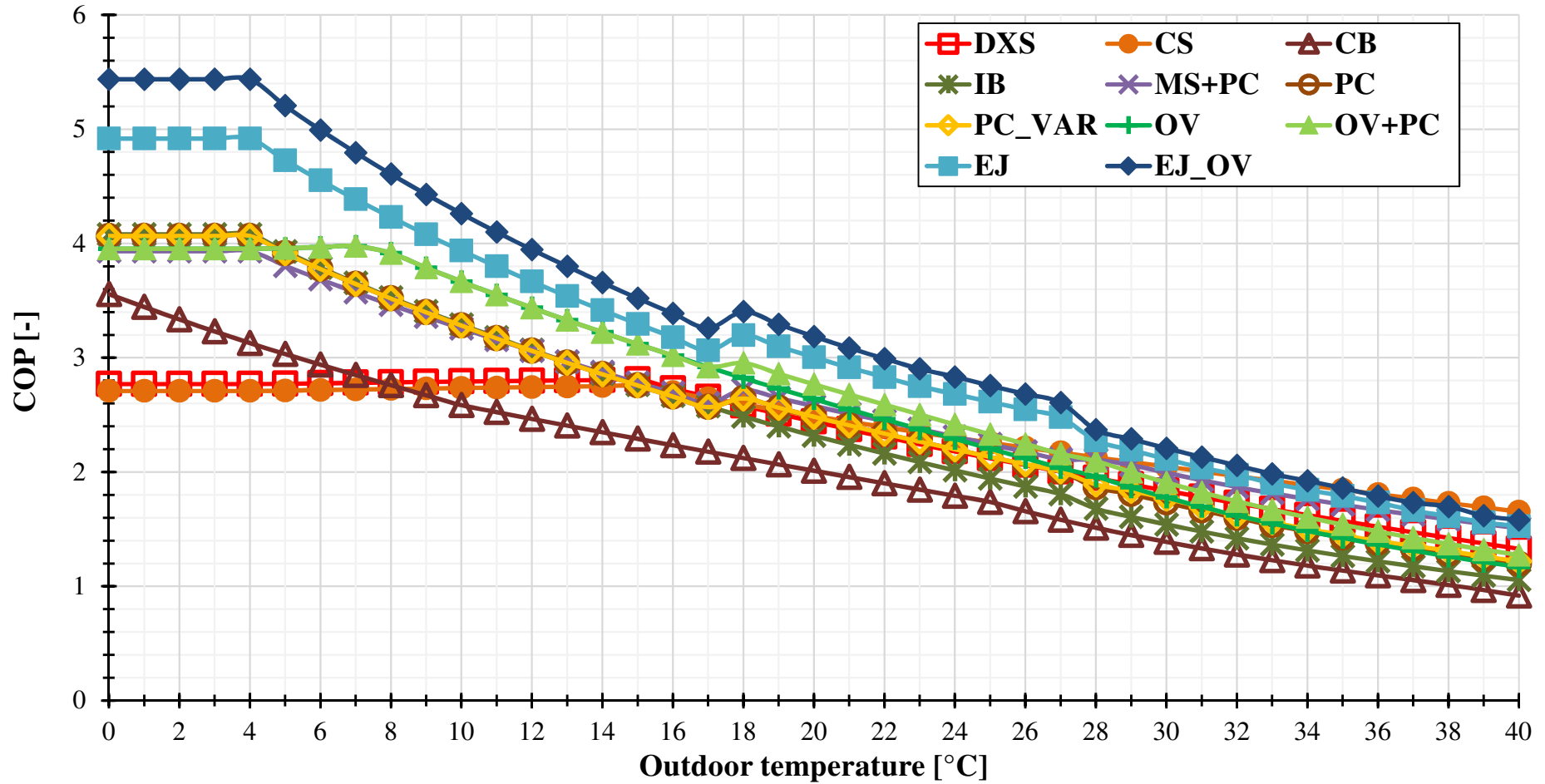


Fig. 5.2 - Comparison in terms of COP among all the investigated solutions as a function of the outdoor temperature.

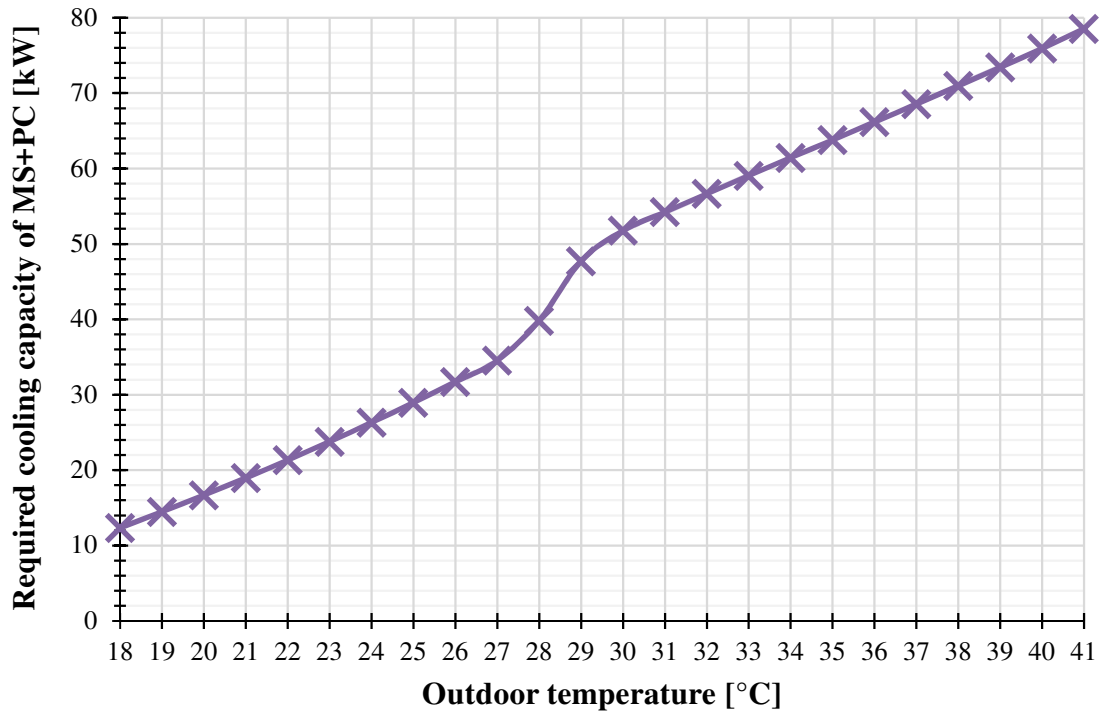


Fig. 5.3 - Cooling capacity required by the subcooling loop belonging to MS+PC as a function of the outdoor temperature.

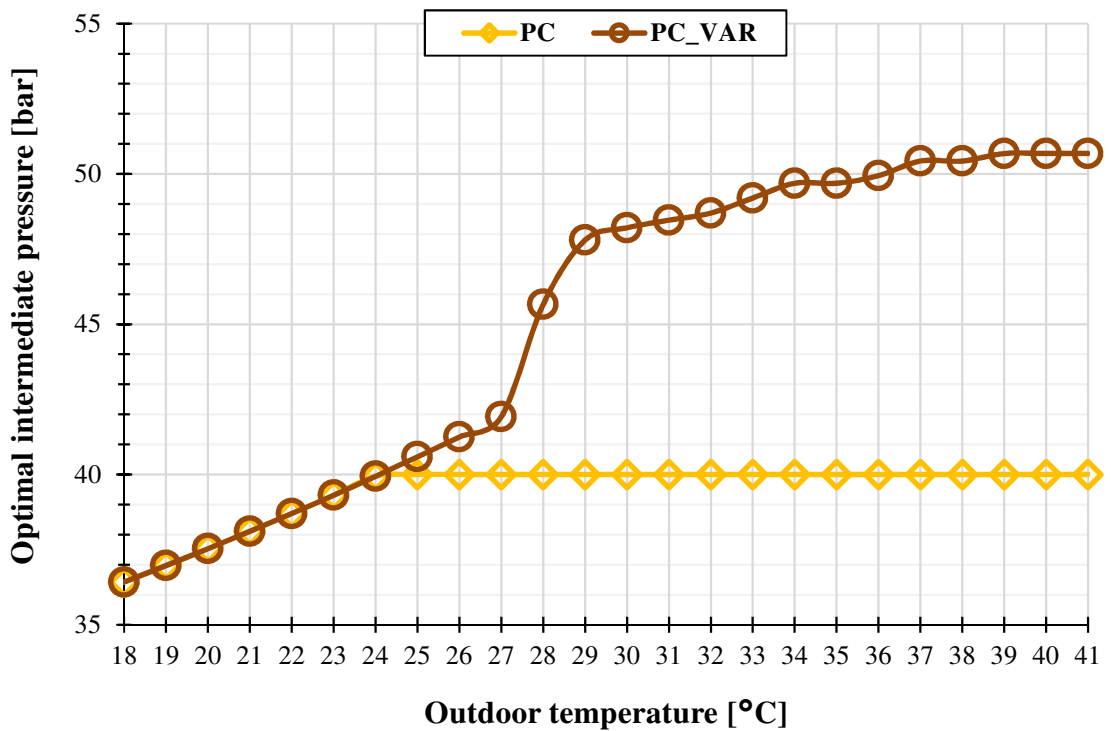


Fig. 5.4 – Optimal intermediate pressure for PC and PC_VAR as a function of the outdoor temperature.

5.1.1.3 Annual energy consumption for a typical supermarket

The annual electricity consumption of the solutions under investigated for a typical supermarket ($\dot{Q}_{MT,design} = 120 \text{ kW}$, $\dot{Q}_{LT,design} = 25 \text{ kW}$) are listed in Table 5.1, in which the energy saving over the selected baseline (DXS) are presented in brackets. Slightly lower energy savings can be associated with CS over the baseline, highlighting reduction in the required annual electricity from 1.2% (in Lisbon) up to 3.4% (in Seville). Significant enhancements over CB can be obtained by replacing the latter with IB. CB, in fact, presented from 16% (in Rome) up to 21.1% (in Seville) higher annual consumption than DXS. The reduction in the approach temperature of the gas cooler/condenser led to similar required power inputs between IB and the baseline in all the investigated locations. In comparison with the baseline, the adoption of the parallel compression was energetically justifiable mainly in Rome where an energy saving by about 6.3% could be accomplished. However, the integration of the R744 refrigerating system using parallel compression into the AC unit would have irreparably penalized this technology. In fact, as shown by Karampour and Sawalha (2015, 2016b), such a configuration is appropriate only for cold places. With respect to the other selected cities, reductions in the energy consumption ranging from 2.3% (in Seville) to 3.6% (in Valencia) were estimated. As previously mentioned, no noteworthy difference in terms of power input was noticed between PC and PC_VAR. The usage of a dedicated mechanical subcooling on the part of a CO₂ booster refrigerating plant with parallel compression (MS+PC) permitted increasing the energy savings over PC. In particular, these benefits reached values from 5.6% (in Lisbon) to 8.8% (in Rome) over DXS. The overfeeding of the MT evaporators allowed OV to accomplish interesting results. This configuration, in fact, attained reduction in energy consumption from 8.1% (in Seville) to 12.7% (in Rome). The outcomes also suggested that OV+PC was an appropriate alternative to the currently employed solutions in the investigated locations, especially in Rome. The energy savings associated with this technology were equal to 15.2% in Rome, 11.6% in Seville and about 13% in the other selected cities, respectively. The annual energy consumption could be dropped by 22.4% in Rome, 19.6% in Lisbon, 20.1% in Valencia, 20.2% in Athens and 19.4% in Seville over the baseline by employing EJ. Finally, the overfeeding of the LT evaporators led to consume from 24.1% (in Seville) to 27.3% (in Rome) less energy than DXS, which entailed a further energy conservation from 20.3 MWh·year⁻¹ (in Rome) to 21.3 MWh·year⁻¹ (in Seville).

Table 5.1 – Annual energy consumption [MWh·y⁻¹] of the investigated systems in five warm climates in Southern Europe ($\dot{Q}_{MT,design} = 120$ kW, $\dot{Q}_{LT,design} = 25$ kW).

<i>Configuration</i>	<i>Rome</i>	<i>Lisbon</i>	<i>Valencia</i>	<i>Athens</i>	<i>Seville</i>
DXS	415.4	422.8	437.9	450.1	459.6
CS	409.9	417.8	429.1	437.4	444.1
	(-1.3%)	(-1.2%)	(-2.0%)	(-2.8%)	(-3.4%)
CB	482.0	504.6	522.0	539.3	556.6
	(+16.0%)	(+19.3%)	(+19.2%)	(+19.8%)	(+21.1%)
IB	406.9	427.9	445.7	461.5	477.6
	(-2.0%)	(+1.2%)	(+1.8%)	(+2.5%)	(+3.9%)
MS+PC	378.8	399.1	408.9	417.0	426.8
	(-8.8%)	(-5.6%)	(-6.6%)	(-7.4%)	(-7.1%)
PC	389.3	410.2	423.1	435.4	449.3
	(-6.3%)	(-3.0%)	(-3.4%)	(-3.3%)	(-2.3%)
PC_VAR	388.8	409.9	422.5	434.1	447.4
	(-6.4%)	(-3.1%)	(-3.5%)	(-3.6%)	(-2.7%)
OV	362.6	378.2	394.1	408.3	422.4
	(-12.7%)	(-10.6%)	(-10.0%)	(-9.3%)	(-8.1%)
OV+PC	352.4	367.8	381.1	393.6	406.3
	(-15.2%)	(-13.0%)	(-12.9%)	(-12.6%)	(-11.6%)
EJ	322.3	340.0	350.1	359.4	370.3
	(-22.4%)	(-19.6%)	(-20.1%)	(-20.2%)	(-19.4%)
EJ_OV	302.0	319.3	329.2	338.3	349.0
	(-27.3%)	(-24.5%)	(-24.8%)	(-24.8%)	(-24.1%)

The energy savings related to each of the most interesting technologies were also compared with CS in some of the previously selected European locations in Fig. 5.5. The chosen cities for this investigation were Rome, Valencia and Seville so as to consider the least warm place, the site characterized by an intermediate weather trend and the warmest city among the previously selected places. Compared to CS, MS+PC consumed from 3.9% (in Seville) to 7.6% (in Rome) less electricity, whereas OV+PC had from 8.5% (in Seville) to 14% (in Rome) lower energy consumption. As regards PC, it was possible to notice that this solution was capable of appreciably reducing the energy consumption over CS only in Rome. The use of the multi-ejector pack (EJ) permitted bringing from 21.4% down to 16.6% (in Seville) the energy consumption in comparison with CS. The additional energy savings achievable by using EJ_OV ranged from 21.4% (in Seville) to 26.3% (in Rome).

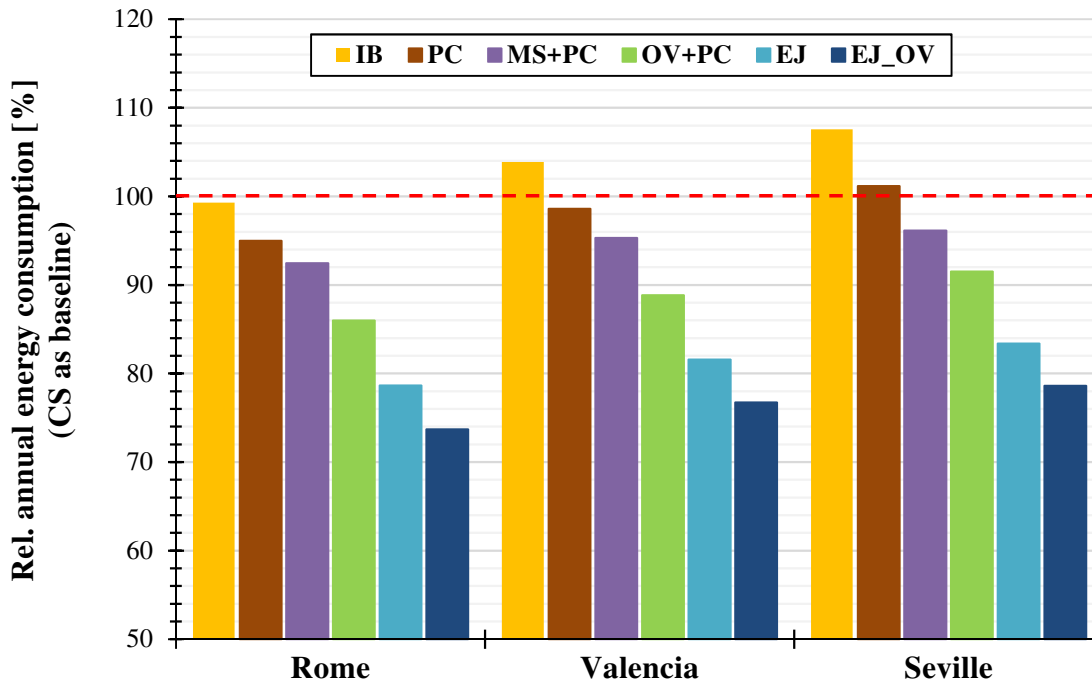


Fig. 5.5 - Energy saving over CS of some of the investigated solutions in different European locations.

In comparison with IB (Fig. 5.6), a reduction in the electricity consumption ranging from 4.1% (in Lisbon) to 5.9% (in Seville) for PC, from 6.7% (in Lisbon) to 10.6% (in Seville) for MS+PC and from 13.4% (in Rome) to 14.9% (in Seville) by OV+PC were estimated. With respect to the ejector-based solutions, the energy saving over IB ranged from 20.5% (in Lisbon) to 22.5% (in Seville) for EJ and from 25.4% (in Lisbon) to 26.9% (in Seville) for EJ_OV. These results led to the conclusion that the higher the average annual outdoor

temperature, the higher the energy savings achievable by adopting one of the investigated technologies over IB were. Furthermore, all these results are in agreement with the ones pointed out by Wiedenmann (2015).

The solution with auxiliary compressor at fixed intermediate pressure is the current benchmark when it comes to CO₂ refrigerating plants for supermarket applications (Javerschek et al., 2016). By adopting PC as the baseline (Fig. 5.7), it could be noticed that, due to the complicated control system of MS+PC and its cost, the usage of the latter was moderately justifiable only in Seville. The technology of the parallel compression needed, at least, to be combined with that of the overfed evaporators. The outcomes obtained, in fact, revealed that an energy saving by about 10% could be achieved in all the investigated locations. As for the configurations equipped with the multi-ejector rack, the reduction in annual consumption dropped approximately by 17% for EJ and by 22% for EJ_OV, respectively over PC.

It is important to remark that the results obtained were substantially influenced by the weather trend in the selected places. For instance, in Rome (Fig. 5.8) the aforementioned solutions mostly operated at external temperatures ranging from 8 °C to 14 °C at which even IB (see Fig. 5.2) could outperform DXS. This implied that, although interesting energy savings could be attributed to PC and MS+PC, the auxiliary compressors and dedicated mechanical subcooling could be employed for less than 40% of the time over the year. As a consequence:

- the reductions in the energy consumption related to both PC and MS+PC were mainly due to the low values of gas cooler/condenser approach temperature;
- the energy savings associated with OV+PC were mainly ascribable to the usage of overfed evaporators.

On the other hand, in Lisbon the “CO₂ only” refrigerating plants performed at outdoor temperatures ranging from 15 °C to 17 °C for most of the time over the year (Fig. 5.9). In these operating conditions and as previously described in Subsection 5.1.1.2, the performance of all the selected improved R744 systems tended to worsen as the auxiliary compressors and the dedicated mechanical subcooling were not employed.

Although Valencia is warmer than Lisbon, more promising results in terms of energy saving could be attained in the former. This is due to the fact that the CO₂-based solutions operated at the most favourable operating conditions for most of the time over the year (i.e. at outdoor temperatures below and above 15 °C÷17 °C), as shown in Fig. 5.10.

As for the results obtained in both Athens and Seville, they were justifiable by considering their higher average annual outdoor temperature in relation to other selected locations.

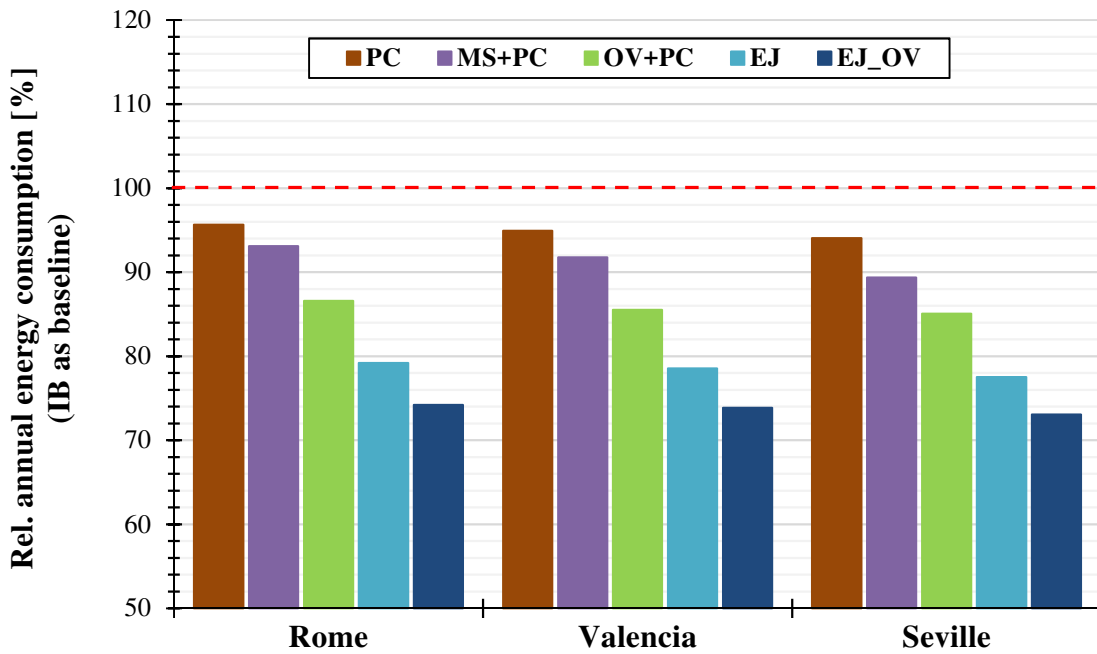


Fig. 5.6 - Energy saving over IB of some of the investigated solutions in different European locations.

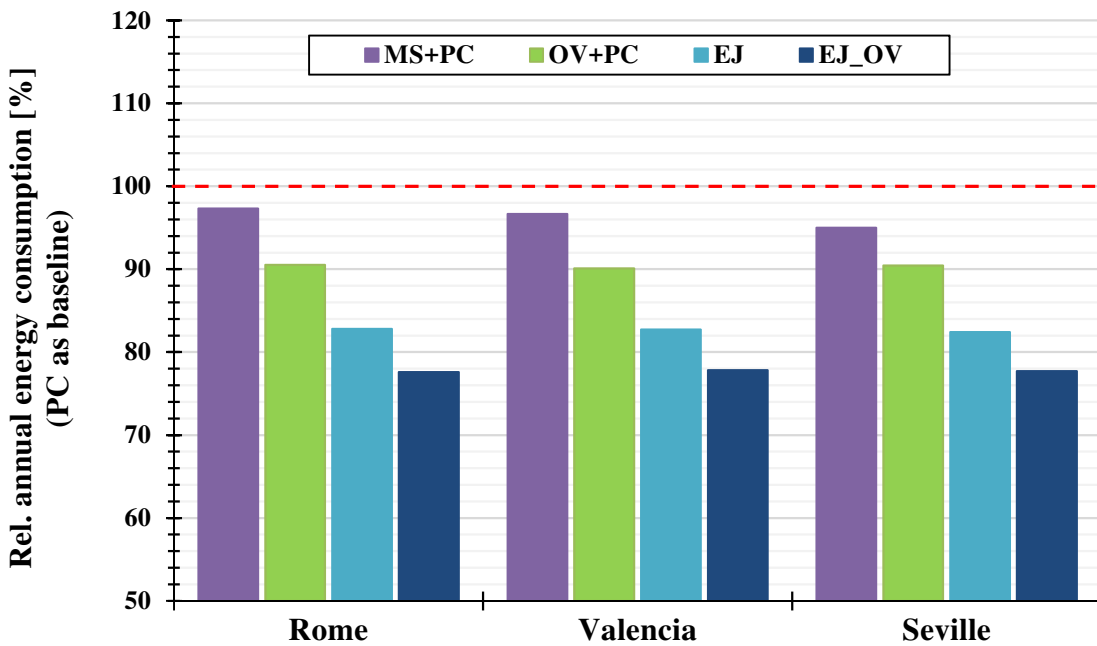


Fig. 5.7 - Energy saving over PC of some of the investigated solutions in different European locations.

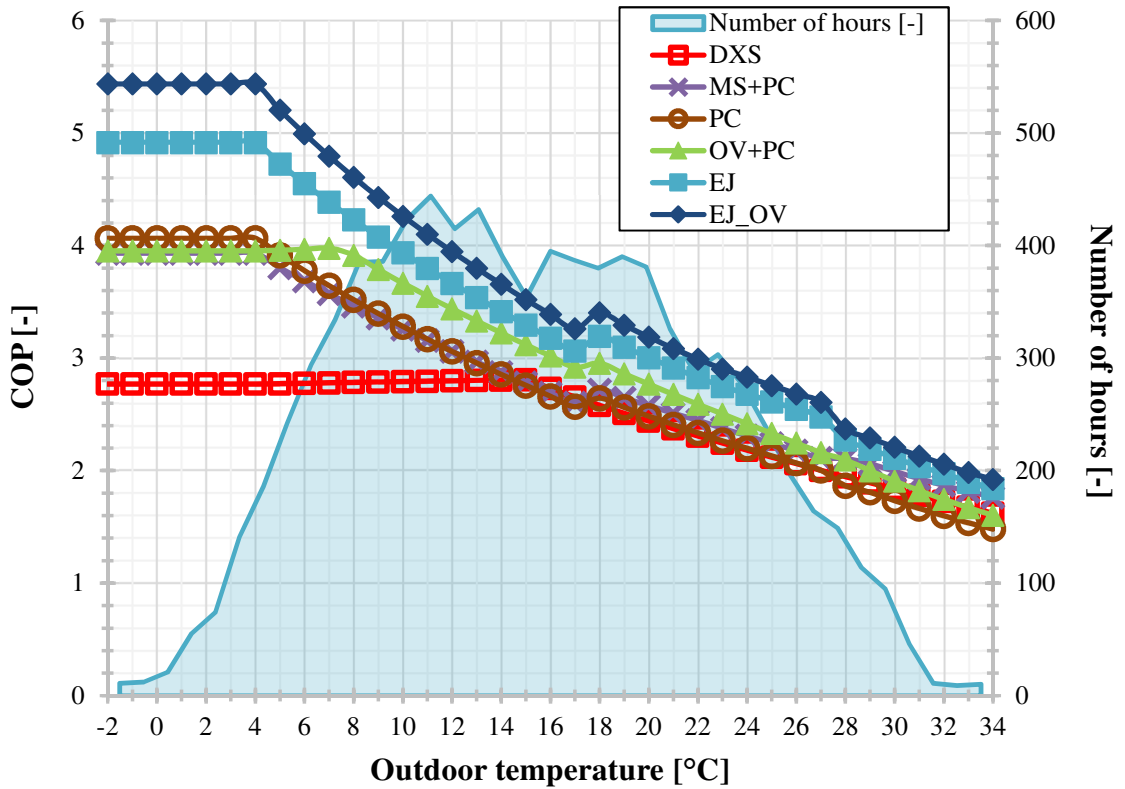


Fig. 5.8 - COP of some of the investigated solutions and number of hours per year at different outdoor temperatures in Rome.

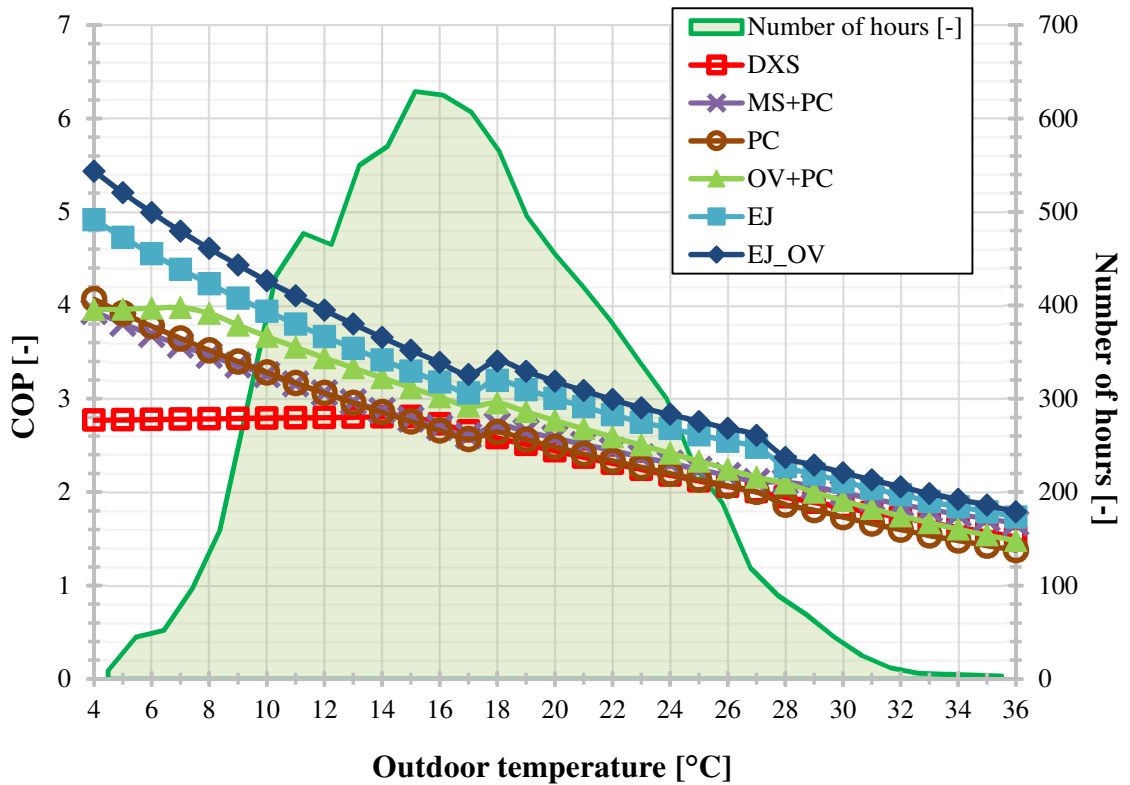


Fig. 5.9 - COP of some of the investigated solutions and number of hours per year at different outdoor temperatures in Lisbon.

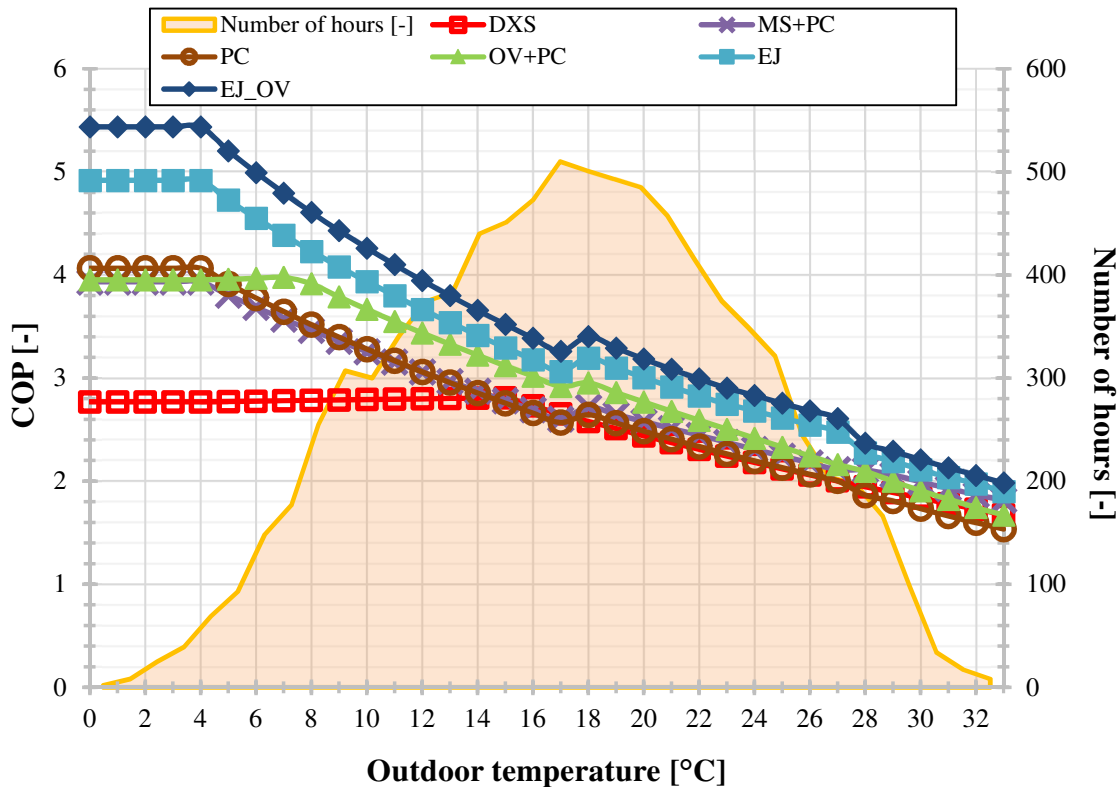


Fig. 5.10 - COP of some of the investigated solutions and number of hours per year at different outdoor temperatures in Valencia.

Fig. 5.11 and Fig. 5.12 are proposed to sum up the outcomes obtained. In Fig. 5.11, the energy savings related to the nowadays most promising solutions are sketched. The schematic suggests that the reduction in annual energy consumption associated with a solution with parallel compression and operating in Southern Europe was almost negligible ($-4\% \div -6\%$). This result would have been additionally confirmed for “only-in-one” configurations. The usage of MT overfed evaporators permitted bring the total electricity consumption down to about 10% over a booster unit employing parallel compression in Mediterranean Europe. The energy savings achievable in warm regions by EJ and EJ_OV were estimated to be equal to about 8% and 14% in comparison with the configuration employing both parallel compression and MT overfed evaporators, respectively. Considering a conventional R744 booster system (i.e. “old” benchmark for commercial R744 refrigeration units), the solution using the multi-ejector pack allowed reducing the electricity consumption by $21\% \div 27\%$ in Southern Europe (Fig. 5.12). Also, in comparison with the “current” benchmark for R744 supermarket refrigeration plants (i.e. “CO₂ only” configuration with auxiliary compressor), it could be noticed that in warm countries an energy saving by $17\% \div 22\%$ could be attained by employing the multi-ejector rack.

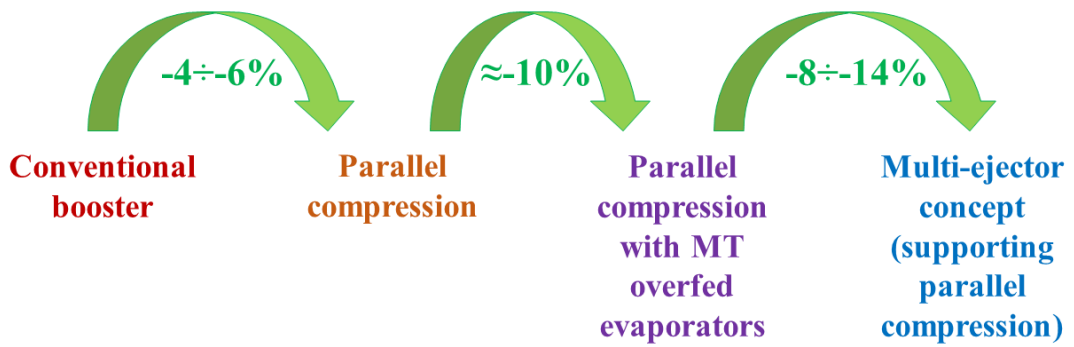


Fig. 5.11 - Evolution of the energy savings associated with the current state-of-the-art technologies for commercial R744 refrigeration systems operating in warm regions.

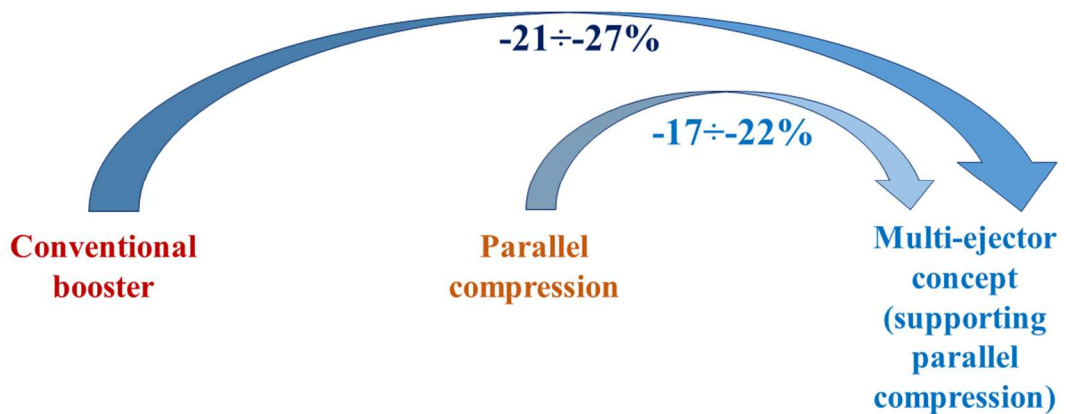


Fig. 5.12 - Energy savings achievable by the commercial R744 refrigeration systems equipped with multi-ejector rack and operating in warm regions over the “old” (conventional booster configuration) and the “current” benchmark (booster configuration with parallel compression).

As regards the economic perspective, it was also claimed that the configuration with ejectors is currently at worst about 10% as expensive as HFC systems (Shecco, 2016). The growing production and requests permitted increasing the efficiency of these solutions by 25% and, contemporary, dropping the equipment cost by 30% from 2008 to 2016 (Shecco, 2016).

5.1.1.4 Effect of the MT on the annual energy consumption of the booster systems with overfed evaporators

In Fig. 5.13 the influence of MT on the annual electric power consumption of OV and OV+PC are compared with that of DXS. The rise in MT allowed OV (MT = -4 °C) to save from 3.5% (in Rome) to 3.9% (in Seville) more electricity over OV (MT = -6 °C). In comparison with DXS, OV (MT = -6 °C) and OV (MT = -4 °C) consumed from 4.4% (in Seville) to 9.6% (in Rome) and from 8.1% (in Seville) to 12.7% (in Rome) less energy than DXS, respectively. With respect to OV+PC (MT = -6 °C) and OV+PC (MT = -4 °C), the removal of the flash gas via auxiliary compressor led to reduction in annual energy consumption ranging from 8.2% (in Seville) to 12.3% (in Rome) and from 11.6% (in Seville) to 15.2% (in Rome) over DXS, respectively. OV+PC (MT = -6 °C) had from 3% (in Rome) to 4.1% (in Seville) lower energy consumption than OV (MT = -6 °C). Furthermore, OV (MT = -6 °C) and OV+PC (MT = -6 °C) required from 0.1% (in Seville) to 2.5% (in Rome) and from 4.2% (in Seville) to 5.4% (in Rome) less electricity to be run over PC_VAR, respectively.

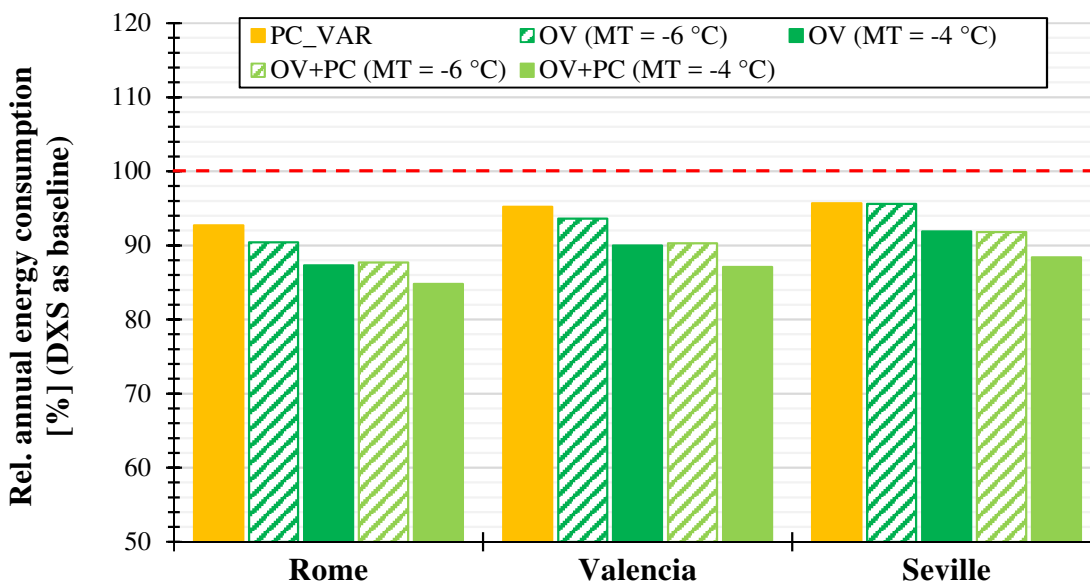


Fig. 5.13 - Effect of MT on the annual energy consumption of OV and OV+PC over DXS in different locations.

To conclude, the overfeeding of the MT evaporators is a more promising technology than that using parallel compression. In fact, even OV (MT = -6 °C) allowed achieving better energy savings than PC_VAR in all the investigated solutions. It was obvious that MT had to be as high as possible, as well as that greater energy benefits could be accomplished by combining these two technologies.

5.1.1.5 Effect of the adoption of the de-superheater on the annual energy consumption of some of the investigated booster systems

In this subsection, the energy saving related to the adoption of a de-superheater located downstream of the LS compressor rack are estimated. In fact, the discharge temperature of the LS compressors is usually very high (up to 90 °C). Due to the high intermediate pressure, the usage of such a technology is supposed to provide significant energy benefits to PC_VAR, (MT = -4 °C), OV+PC (MT = -4 °C) and OV+PC (MT = -6 °C) (Fig. 5.14). Also, the de-superheater can suitably be employed to produce DHW.

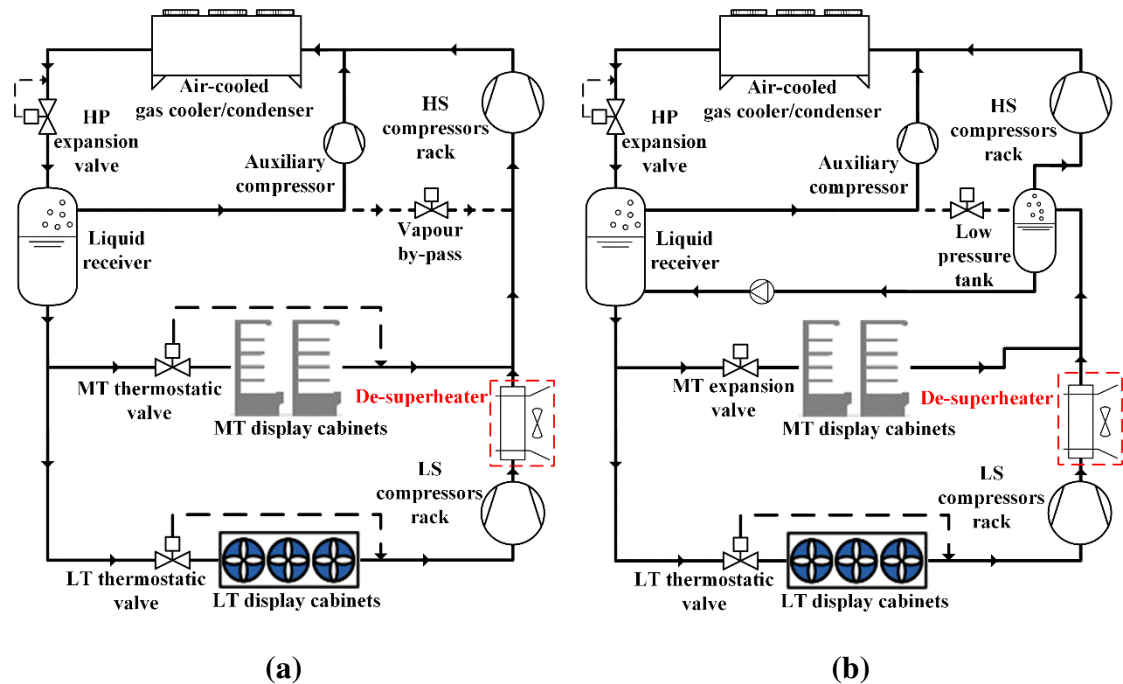


Fig. 5.14 – (a) Schematic of a R744 booster refrigeration system with parallel compression and de-superheater; (b) Schematic of a R744 booster refrigeration system with parallel compression, MT overfed evaporators and de-superheater.

Fig. 5.15 shows that the energy saving for PC_VAR+DES ranged from 5.9% in Seville to 9.1% in Rome over DXS. As for OV+PC, OV+PC (MT = -4 °C) and OV+PC (MT = -6 °C) brought the energy consumption from 14.5% (in Rome) down to 10.4% (in Seville) and from 17.7% (in Rome) down to 14% (in Seville) in relation to DXS.

The adoption of the de-superheater led to energy savings:

- from 2.7% (in Rome) to 3.1% (in Seville) on the part of PC in comparison with the corresponding solution without the de-superheater. The usage of such a heat exchanger on the part of this solution was more energy beneficial in “warmer” climates;

- from 2.6% (in Rome) to 2.3% (in Seville) on the part of OV+PC+DES (MT = -6 °C) in relation to the corresponding configuration without the de-superheater;
- from 3% (in Rome) to 2.7% (in Seville) on the part of OV+PC+DES (MT = -4 °C) in comparison with the corresponding system without the de-superheater. The usage of such a heat exchanger for the CO₂ refrigeration solutions with MT overfed evaporators was more energy beneficial in “less” warm climates.

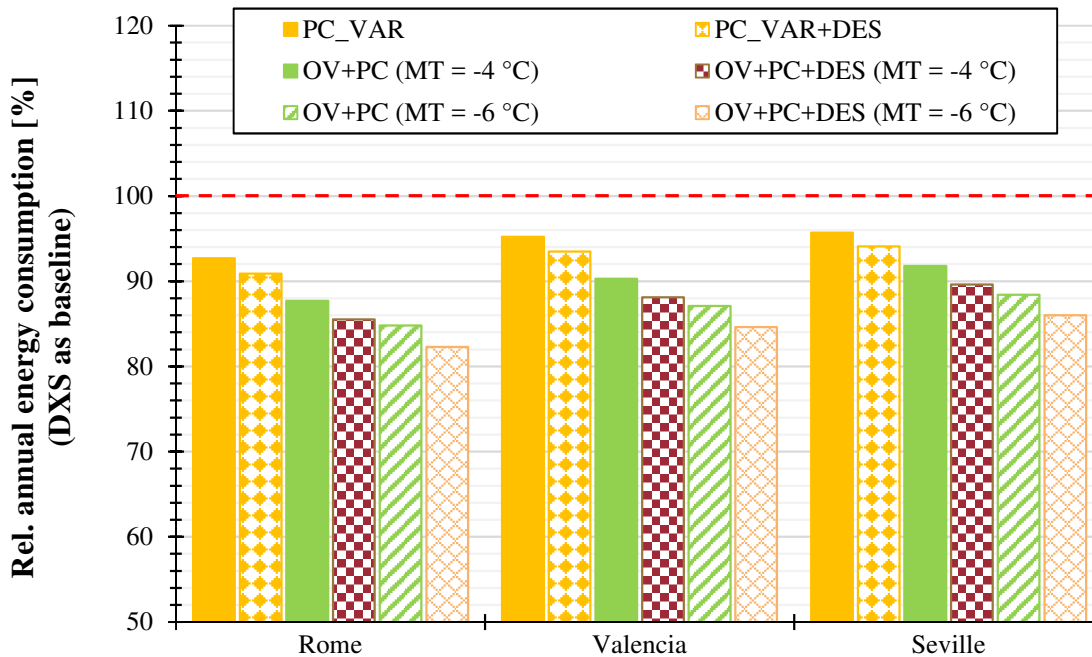


Fig. 5.15 - Energy saving on the part of PC_VAR, OV+PC (MT = -4 °C) and OV+PC (MT = -6 °C) over DXS in different locations.

5.1.1.6 Annual energy consumption of the integrated solution for a typical supermarket
 The annual energy consumption of the HFC-based solutions (i.e. DXS for refrigeration reclaim and R410A solutions for the demand of the AC unit) and that of EJ_OV_AC for the conventional supermarket application ($\dot{Q}_{MT,design} = 120$ kW, $\dot{Q}_{LT,design} = 25$ kW) are compared in Table 5.2. Only EJ_OV was assessed as it represents the most promising configuration among the ones selected in this study, as previously showed.

The outcomes obtained revealed that an annual energy saving ranging from 26% (in Rome) to 22% (in Seville) could be achieved over the separated HFC-based solutions in *Scenario I*. Furthermore, the latter consumed from 24.9% (in Rome) to 19.6% (in Seville) more electricity than the integrated CO₂ configuration over the year in *Scenario II*. Despite the large cooling capacity of AC in *Scenario III*, EJ_OV integrated with AC was

significantly more beneficial than the conventional solutions attaining a reduction in the annual consumption ranging from 23% (in Rome) to 16.6% (in Seville).

Table 5.2 – Annual energy consumption [MWh·y⁻¹] of DXS+AC and EJ_OV_AC ($\dot{Q}_{MT,design} = 120$ kW, $\dot{Q}_{LT,design} = 25$ kW).

<i>Scenario</i>	<i>Configuration</i>	<i>Rome</i>	<i>Valencia</i>	<i>Seville</i>
<i>Scenario I</i> (50% of $\dot{Q}_{MT,design}$)	DXS+AC	434.7	461.7	496.4
	EJ_OV_AC	320.9	352.4	387.4
<i>Scenario II</i> (100% of $\dot{Q}_{MT,design}$)	DXS+AC	453.9	485.5	532.6
	EJ_OV_AC	341.0	377.1	428.3
<i>Scenario III</i> (200% of $\dot{Q}_{MT,design}$)	DXS+AC	492.4	533.1	605.6
	EJ_OV_AC	378.9	423.8	504.8

Fig. 5.16 compares the power consumption related to PC, EJ_OV and EJ_OV_AC at some specific operating conditions. At $t_{ext} = 25$ °C, the HS and auxiliary compressors belonging to PC_VAR were responsible for 66.9% and 13.2% of the total required electric power input, respectively. When it comes to EJ_OV, they respectively consume 42.2% and 34.2% of the total electricity. The combination with the AC unit caused a significant unloading of the HS compressor. In fact, due to the large amount of vapour caused by the AC system, 55.4% of the consumption of EJ_OV_AC was owing to the auxiliary compressors. The energy consumption of the auxiliary compressor associated with PC_VAR ranged from 14.5% ($t_{ext} = 30$ °C) to 22.2% ($t_{ext} = 40$ °C) of the total required electricity. With respect to EJ_OV, a sharp increase in parallel compressor usage could be evaluated at $t_{ext} = 30$ °C because of the occurrence of the transcritical running modes. The auxiliary compressors, in fact, were accountable for 76.8% of the total consumption,

whereas the HS compressors resulted almost completely unloaded. This result was even more marked for EJ_OV_AC at outdoor temperatures ranging from 30 °C to 40 °C. These outcomes further support the need for more remarkably enhanced auxiliary compressors for multi-ejector based solutions.

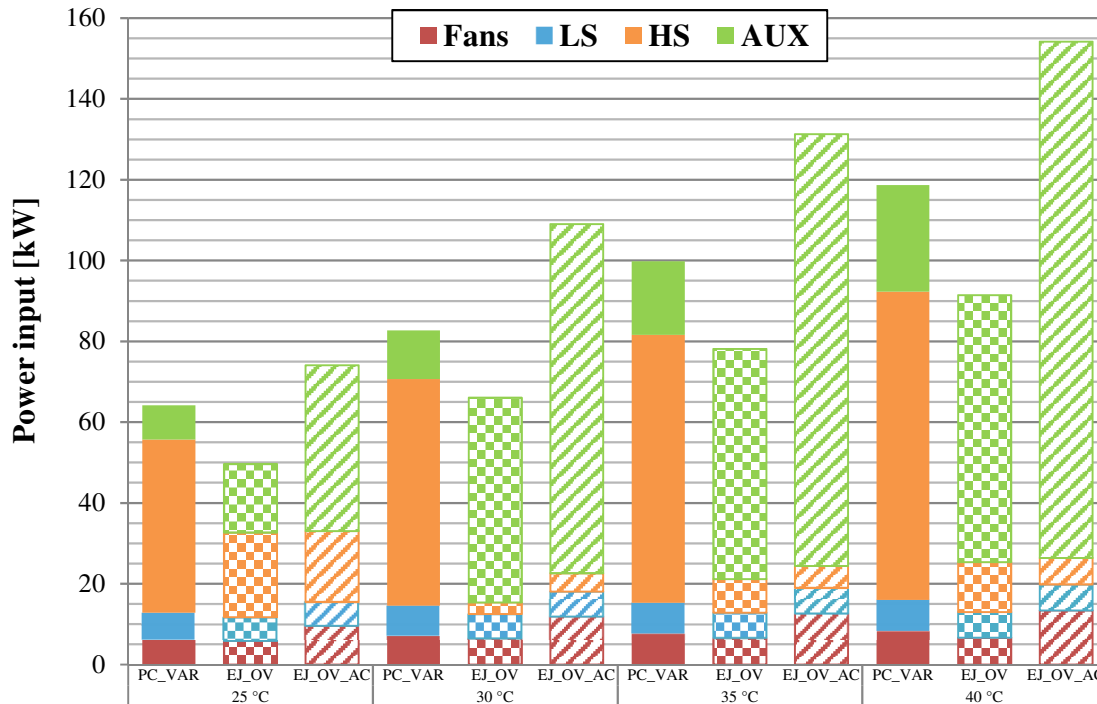


Fig. 5.16 - Total power input split into the compressor fractions for PC_VAR, EJ_OV and EJ_OV_AC.

The optimal value of pressure lift for multi-ejector based systems is a trade-off between the benefits associated with the increase in the suction pressure of the auxiliary compressors and those related to the amount of the vapour to be pre-compressed. The values of pressure lift reached by EJ, EJ_OV and EJ_OV_AC are compared at different transcritical running modes in Fig. 5.17. It was possible to notice that the pressure lift increased with rise in outdoor temperatures in all the investigated cases. In fact, the pressure lift for EJ_OV_AC was equal to 9.2 bar at $t_{\text{ext}} = 30$ °C, 11.2 bar at $t_{\text{ext}} = 35$ °C and 13.6 bar at $t_{\text{ext}} = 40$ °C. As regards EJ and EJ_OV, the pressure lift respectively added up to 6.6 bar at $t_{\text{ext}} = 30$ °C, about 8 bar at $t_{\text{ext}} = 35$ °C and 13.1 bar at $t_{\text{ext}} = 40$ °C. It could be concluded that the performance of the multi-ejector arrangement was mainly affected by the coupling with the AC system rather than LT.

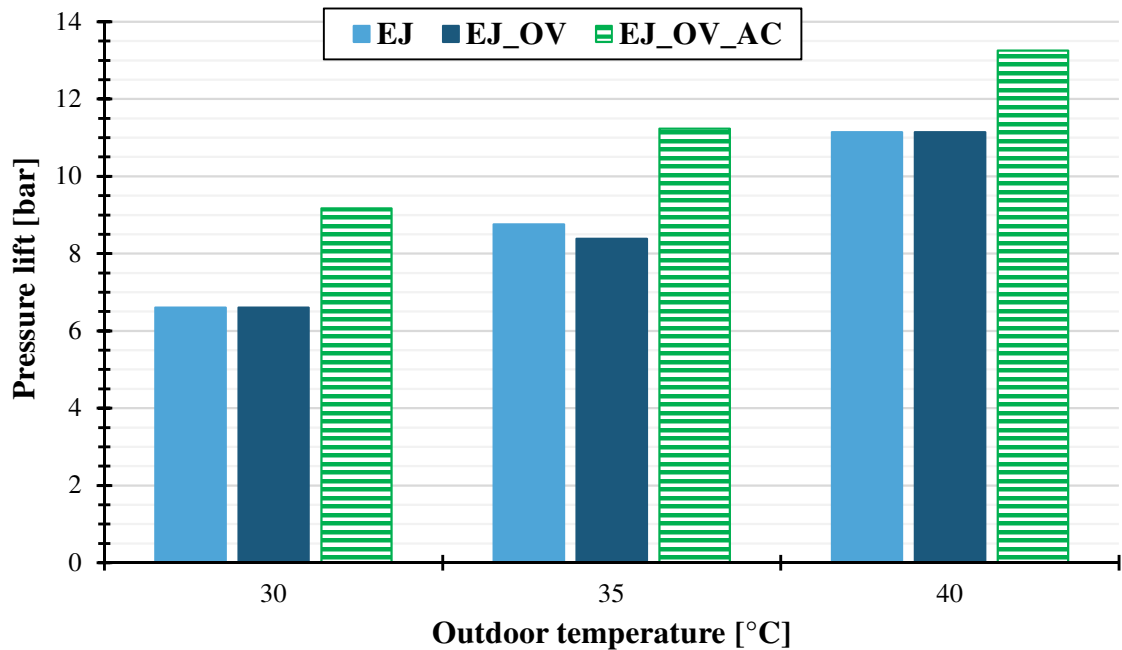


Fig. 5.17 - Values of pressure lift reached by the investigated multi-ejector based solutions.

5.1.1.7 Influence of size of AC unit, global efficiency of auxiliary compressors and size of supermarket on the annual energy consumption

According to Sharma et al. (2014), the ratio of \dot{Q}_{MT} to \dot{Q}_{LT} , defined as load factor (LF), usually ranges from 2 to 5. In this subsection, $\dot{Q}_{LT,design}$ was kept constant in all the evaluations, whereas two additional scenarios involving $\dot{Q}_{MT,design}$ equal to 65 kW (LF ~ 2.5) and to 200 kW (LF ~ 8, which represents a superstore application) were also taken into account. In addition to this, different sizes of the AC system were also assessed. All the results are summarized in Table 5.3, Table 5.4 and Table 5.5 in which “Improved” EJ_OV_AC stands for EJ_OV_AC having 10% higher efficiency of the auxiliary compressors than the previously assessed EJ_OV_AC. Also, the values in brackets for DXS+AC refer to the electricity consumption of the AC unit.

With respect to the results for LF ~ 2.5 (Table 5.3), it was noticed that energy savings ranging from 26.2% (*Scenario I*) to 23.7% (*Scenario III*) could be accomplished on the part of EJ_OV in Rome. The enhancement in the performance of the auxiliary compressors led to an additional reduction in the energy consumption from 2.4% (*Scenario I*) up to 3.4% (*Scenario III*). This expedient is particularly promising in very warm climate cities, such as Seville. In fact, in this location DXS+AC respectively consumed from 22.7% (*Scenario I*) to 18.2% (*Scenario III*) and from 25.1% (*Scenario I*) to 21.9% (*Scenario III*) more electricity than EJ_OV_AC and “Improved” EJ_OV_AC.

“Improved” EJ_OV_AC exhibited (Table 5.4) a further energy saving ranging from 2.6% (*Scenario I*) to 3.7% (*Scenario III*) in Rome, from 3% (*Scenario I*) to 4.2% (*Scenario III*) and from 3.6% (*Scenario I*) to 5% (*Scenario III*) in comparison with the outcomes presented in Subsection 5.1.1.6.

As regards the results with LF = 8 (Table 5.5), decrements in the annual electricity consumption over DXS ranging from 26.2% (*Scenario I*) to 22.7% (*Scenario III*) in Rome, from 23.5% (*Scenario I*) to 20% (*Scenario III*) in Valencia and from 21.5% (*Scenario I*) to 15.6% (*Scenario III*) in Seville could be obtained by EJ_OV_AC. On the other hand, “Improved” EJ_OV_AC was further able to reduce the energy consumption from 2.7% (*Scenario I*) to 3.9% (*Scenario III*) in Rome, from 3.1% (*Scenario I*) to 4.3% (*Scenario III*) in Valencia and from 3.8% (*Scenario I*) to 5.2% (*Scenario III*) in Seville compared to EJ_OV_AC.

As an example, the scenario without AC and thus based only on the performance of EJ_OV and “Improved” EJ_OV for LF ~ 5 was also investigated. The latter solution allowed dropping the annual energy consumption by 2.3% in Rome, 2.7% in Valencia and 3.3% in Seville over EJ_OV.

Table 5.3 – Annual energy consumption [MWh·y⁻¹] of DXS+AC, EJ_OV_AC and “improved” EJ_OV_AC for LF ~ 2.5 as a function of AC size.

<i>Scenario related to supermarket</i>	<i>Scenario related to AC</i>	<i>Configuration</i>	<i>Rome</i>	<i>Valencia</i>	<i>Seville</i>
LF ~ 2.5	<i>Scenario I</i> (50% of $\dot{Q}_{MT,design}$)	DXS+AC	297.2 (10.5)	314.5 (13.0)	336.2 (19.9)
		EJ_OV_AC	219.3	239.0	260.0
		Improved EJ_OV_AC	214.1	232.4	251.8
	<i>Scenario II</i> (100% of $\dot{Q}_{MT,design}$)	DXS+AC	307.6 (20.9)	327.3 (25.8)	355.9 (39.5)
		EJ_OV_AC	230.5	252.8	282.0
		Improved EJ_OV_AC	224.2	244.9	271.5
	<i>Scenario III</i> (200% of $\dot{Q}_{MT,design}$)	DXS+AC	328.4 (41.7)	353.2 (51.7)	395.4 (79.1)
		EJ_OV_AC	250.6	277.5	323.3
		Improved EJ_OV_AC	242.2	267.0	308.7

Table 5.4 – Annual energy consumption [MWh·y⁻¹] of DXS+AC, EJ_OV_AC and “improved” EJ_OV_AC for LF ~ 5 as a function of AC size.

<i>Scenario related to supermarket</i>	<i>Scenario related to AC</i>	<i>Configuration</i>	<i>Rome</i>	<i>Valencia</i>	<i>Seville</i>
LF ~ 5	<i>Scenario I</i> (50% of $\dot{Q}_{MT,design}$)	DXS+AC	434.7 (19.3)	461.7 (23.9)	496.4 (36.8)
		EJ_OV_AC	320.9	352.4	387.4
		Improved EJ_OV_AC	312.5	341.8	373.3
	<i>Scenario II</i> (100% of $\dot{Q}_{MT,design}$)	DXS+AC	453.9 (38.5)	485.5 (47.7)	532.6 (73.0)
		EJ_OV_AC	341.0	377.1	428.3
		Improved EJ_OV_AC	331.0	364.5	411.7
	<i>Scenario III</i> (200% of $\dot{Q}_{MT,design}$)	DXS+AC	492.4 (77.0)	533.1 (95.4)	605.6 (146.0)
		EJ_OV_AC	378.9	423.8	504.8
		Improved EJ_OV_AC	364.9	406.2	479.7

Table 5.5 – Annual energy consumption [MWh·y⁻¹] of DXS+AC, EJ_OV_AC and “improved” EJ_OV_AC for LF = 8 as a function of AC size.

<i>Scenario related to supermarket</i>	<i>Scenario related to AC</i>	<i>Configuration</i>	<i>Rome</i>	<i>Valencia</i>	<i>Seville</i>
LF = 8	<i>Scenario I</i> (50% of $\dot{Q}_{MT,design}$)	DXS+AC	634.8 (32.2)	675.9 (39.9)	729.4 (61.3)
		EJ_OV_AC	468.2	516.8	572.7
		Improved EJ_OV_AC	455.5	500.8	550.9
	<i>Scenario II</i> (100% of $\dot{Q}_{MT,design}$)	DXS+AC	666.7 (64.2)	715.5 (79.5)	789.8 (121.7)
		EJ_OV_AC	501.7	557.9	640.2
		Improved EJ_OV_AC	486.2	538.5	614.7
	<i>Scenario III</i> (200% of $\dot{Q}_{MT,design}$)	DXS+AC	730.9 (128.4)	795.0 (158.9)	911.5 (243.4)
		EJ_OV_AC	565.3	636.1	769.2
		Improved EJ_OV_AC	543.3	608.5	728.9

5.1.2 Results of exergy analyses

5.1.2.1 Conventional booster solution

The results of the conventional exergy analysis for CB at the design outdoor temperature (i.e. dead state temperature or t_0 or t_{ext}) of 40 °C are summarized with the aid of Fig. 5.18. The designer's attention had to be firstly focused on HS compr, which was accountable for 31.7% of $\dot{E}_{D,tot}$, secondarily to GC (28.7% of $\dot{E}_{D,tot}$) and then to HP exp (23.6% of $\dot{E}_{D,tot}$). The analysis suggested also considering some enhancements for both VB and MT evap, as they were respectively responsible for 7.3% and 4.4% of $\dot{E}_{D,tot}$. Since the total required power input (\dot{W}_{tot}) and the total exergy losses rate (\dot{E}_L) amounted respectively to 159 kW and to 2.49 kW, the exergy efficiency of CB was estimated to be 0.160 at $t_0 = 40$ °C.

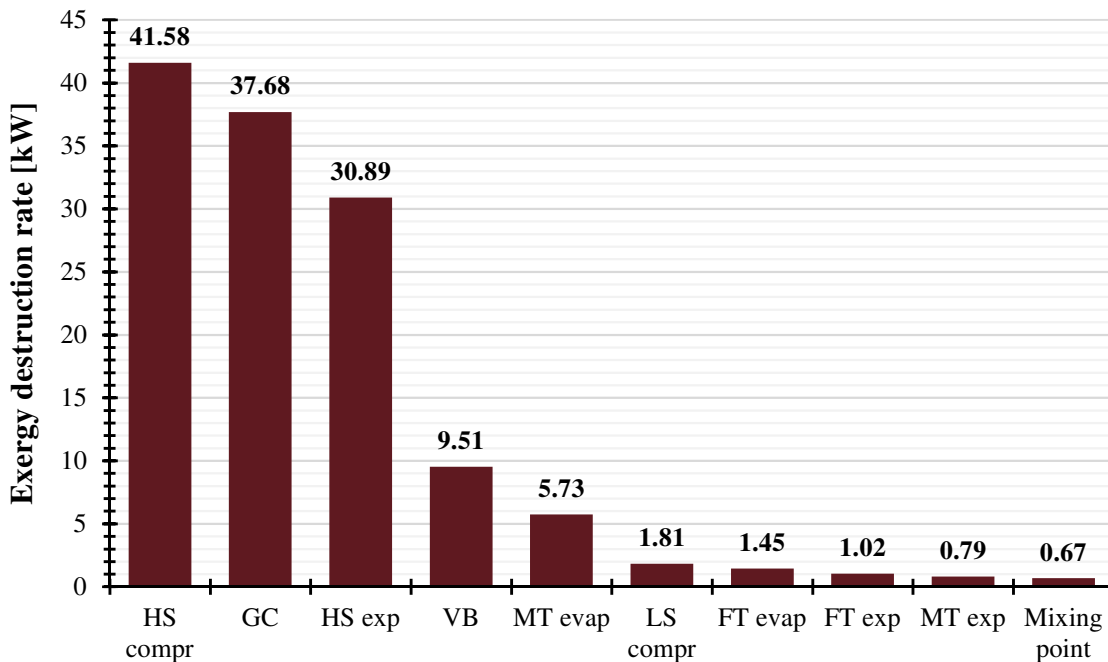


Fig. 5.18 – Results of the conventional exergy analysis for CB ($t_0 = 40$ °C).

As displayed in Fig. 5.19, more than 67% of the total exergy destruction taking place in the investigated system was avoidable. In particular, 44% of $\dot{E}_{D,tot}^{AV}$ was due to HS compr, while GC caused 28% of the total avoidable irreversibilities, as shown in Fig. 5.20. Also, 12%, 8% and 4% of $\dot{E}_{D,tot}^{AV}$ were respectively ascribable to HS exp, VB and MT evap. Unlike HS exp, the exergy destruction rates related to all these components were mainly preventable, being respectively equal to 92.2% of $\dot{E}_{D,HScompr}$ for HS compr, 66.6% of $\dot{E}_{D,GC}$ for GC, 77.3% of $\dot{E}_{D,VB}$ for VB and 60.5% of $\dot{E}_{D,MTevap}$ for MT evap (Fig. 5.21).

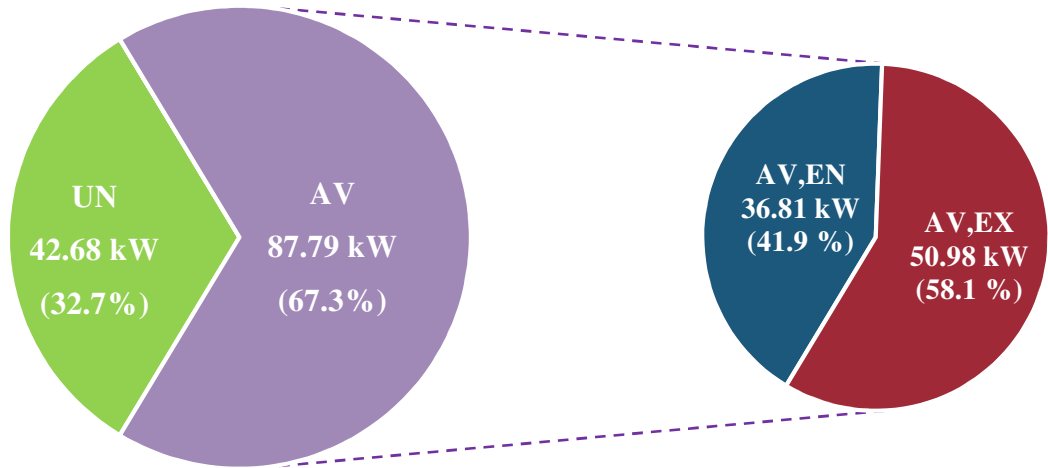


Fig. 5.19 – Breakdown of the avoidable exergy destruction rates of CB ($t_0 = 40\text{ }^\circ\text{C}$).

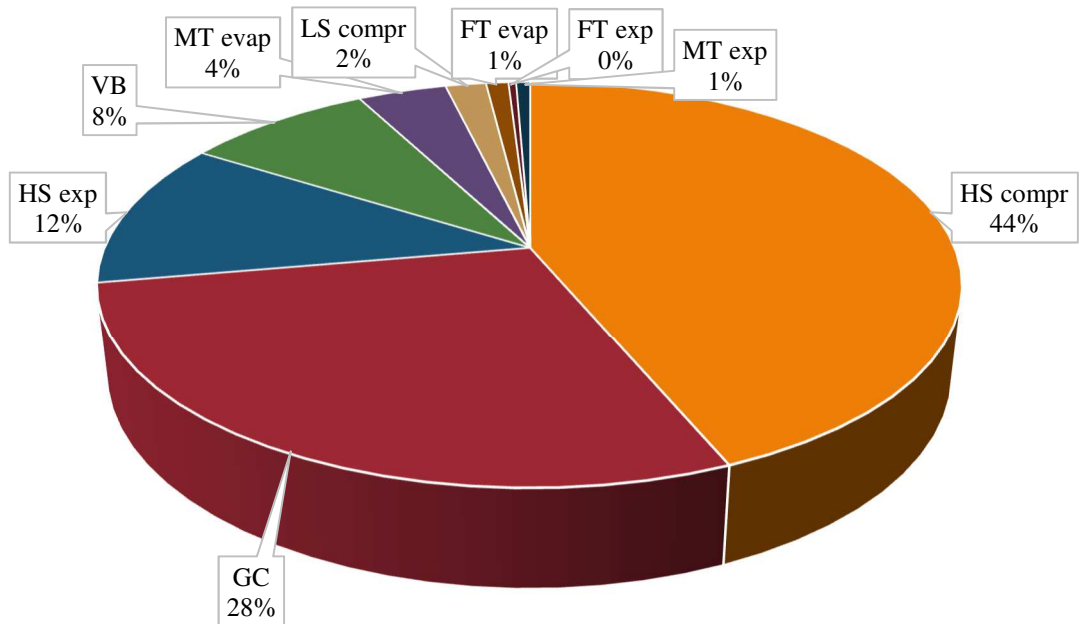


Fig. 5.20 – Contributions of each component belonging to CB to $\dot{E}_{D,tot}^{AV}$ ($t_0 = 40\text{ }^\circ\text{C}$).

The following splitting of the irreversibilities into their avoidable endogenous and exogenous parts can suggest the strategies which have to be adopted to enhance the evaluated system. Fig. 5.19 shows that about 58.1% of $\dot{E}_{D,tot}^{AV}$ was exogenous at $t_0 = 40\text{ }^\circ\text{C}$. In accordance with this result, 61.7% of \dot{E}_D^{AV} related to GC and the whole amount of avoidable irreversibilities for both HS exp and VB were exogenous (Fig. 5.21). This meant that at $t_0 = 40\text{ }^\circ\text{C}$ only 33% of the inefficiencies associated with HP exp could be actually avoided and uniquely by enhancing the other components. On the other hand, 56% of $\dot{E}_{D,HScompr}^{AV}$ was due to the component itself, whereas the irreversibilities related

to MT evap were completely endogenous (Chen et al., 2015; Morosuk et al., 2012; Morosuk and Tsatsaronis, 2009), as depicted in Fig. 5.21.

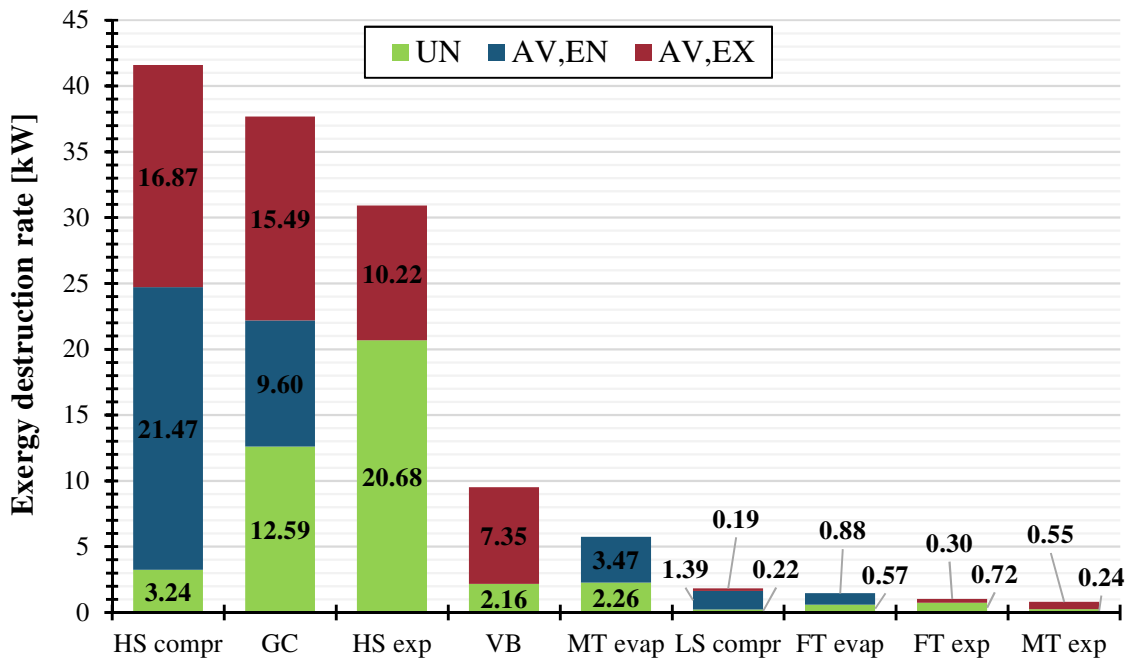


Fig. 5.21 – Results of the advanced exergy analysis for CB ($t_0 = 40\text{ }^\circ\text{C}$).

The effect of the system under investigation on the component being taken into account is discovered by evaluating its exogenous exergy destruction. Table 5.6 reveals that GC could be enhanced firstly by decreasing the exergy destruction of the investigated system and secondly by improving HS compr. The latter outcome was due to the fact that an enhancement in such a component would have led to a lessening in its discharge temperature and thus in a better matching between CO_2 and air temperature profiles in GC. Also, Table 5.6 suggests that a decrease in the irreversibilities associated with both CB and GC permitted substantially reducing the inefficiencies related to HS compr. Additional improvements could be accomplished by enhancing the HP expansion valve, as well as by reducing the temperature difference in MT evap. The latter measure would have increased HS compr suction pressure. A rise in MT evap would also have entailed a drop in the irreversibilities occurring in VB. In addition, the negative value of the exogenous exergy destruction rate associated with this component meant that a further enhancement in its performance could be attained by increasing the irreversibilities in the other components. Finally, a massive decrement in the irreversibilities of HP exp could be achieved by lowering the approach temperature of GC.

Table 5.6 – Splitting of the exogenous exergy destruction of the main components belonging to CB at the design outdoor temperature of 40 °C.

<i>k-th component</i>	$\dot{E}_{D,k}^{EX} [kW]$	<i>r-th component</i>	$\dot{E}_{D,k}^{EX,r} [kW]$
GC	17.53	HS compr	5.45
		HP exp	1.68
		MT evap	0.77
		VB	0.32
		LS compr	0.29
		LT evap	0.18
		LT exp	0.05
		MT exp	0.02
		<i>MX</i>	8.77
		HS compr	17.33
HP exp	2.88		
MT evap	3.55		
VB	0.12		
LS compr	0.16		
LT evap	0.09		
LT exp	0.10		
MT exp	0.03		
<i>MX</i>	5.91		
HP exp	11.06		
		MT evap	-0.18
		LT evap	-0.02
		LT exp	0.07
		MT exp	0.02

		<i>MX</i>	<i>0.11</i>
VB	8.17	GC	0.67
		HS compr	0.00
		HP exp	0.43
		MT evap	3.16
		LS compr	0.00
		LT evap	0.00
		LT exp	3.22
		MT exp	3.21
		<i>MX</i>	<i>-2.52</i>

In order to conduct an in-depth investigation, a sensitivity analysis was also implemented at design external temperatures ranging from 25 °C to 40 °C. Fig. 5.22 and Fig. 5.23 respectively show the effect of t_0 on the avoidable exergy destruction and on the avoidable endogenous and exogenous irreversibilities associated with some components of CB. It was important to highlight that the irreversibilities occurring in LS compr, FT evap, FT exp and MT exp were negligible compared to those taking place in the other components, even at t_0 between 25 °C and 40 °C. The avoidable inefficiencies related to MT evap weakly changed with respect to t_0 , as shown in Fig. 5.22. With increment in t_0 , the avoidable irreversibilities of VB and HP exp respectively doubled and tripled. A sharp increase in the avoidable exergy destruction rates related to HS compr and GC could be noticed as t_0 went up. In particular, GC showed that $\dot{E}_{D,GC}^{AV,EN}$ was on a par with $\dot{E}_{D,GC}^{AV,EX}$ in terms of contribution to $\dot{E}_{D,GC}^{AV}$ at $t_0 = 25$ °C, as depicted in Fig. 5.23. On the other hand, $\dot{E}_{D,GC}^{AV,EX}$ was about 1.6 times as high as $\dot{E}_{D,GC}^{AV,EN}$ at $t_0 = 40$ °C. As for HS compr, $\dot{E}_{D,HScompr}^{AV,EN}$ was roughly 1.5 times as great as $\dot{E}_{D,HScompr}^{AV,EX}$ at t_0 up to 35 °C, whereas its contribution to $\dot{E}_{D,HScompr}^{AV}$ was slightly lower at $t_0 = 40$ °C. It is worth remarking that HP exp, VB and MT evap were not included in Fig. 5.22, since their avoidable irreversibilities were respectively completely exogenous for both the expansion valves and totally endogenous for the heat exchanger, in accordance with the outcomes depicted in Fig. 5.21.

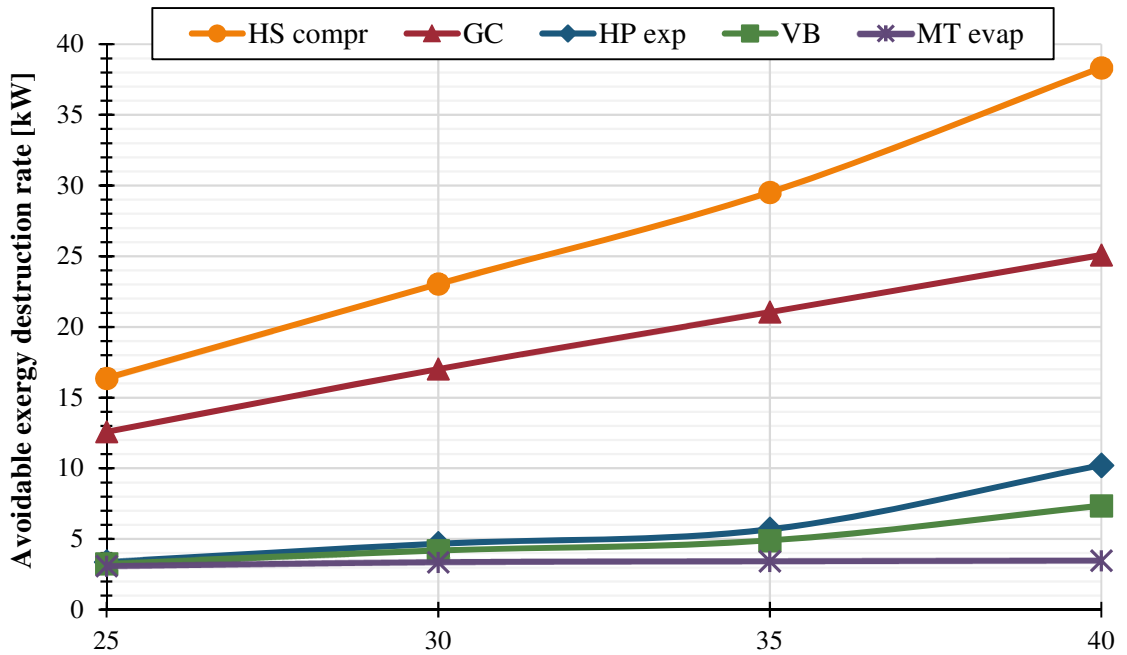


Fig. 5.22 – Influence of design outdoor temperature on avoidable exergy destruction related to main components belonging to CB.

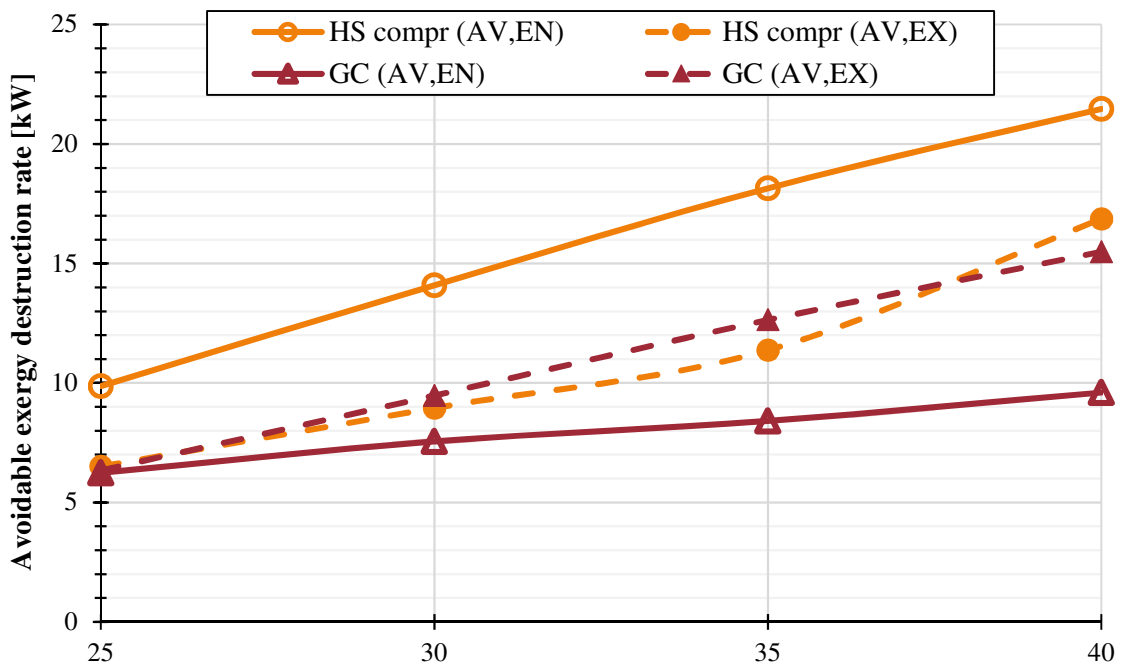


Fig. 5.23 – Influence of design outdoor temperature on endogenous and exogenous avoidable exergy destruction related to main components belonging to CB.

To sum up, the implementation of only the conventional exergy analysis would have led to misleading results as regards the appropriate design of booster refrigeration plants for high ambient temperature countries. In fact, such an assessment suggested paying close

attention to HS compr, followed by GC, then HP exp, VB and finally MT evap. The application of the advanced exergy analysis improved the understanding regarding the strategies to be adopted to enhance the performance of the system being investigated. First of all, it showed that even closer attention had to be focused on the main compressors, as these components were accountable for more than 40% of the total avoidable irreversibilities at $t_{\text{ext}} = 40$ °C. On the other hand, the contribution of $\dot{E}_{D,HScompr}^{AV,EN}$ to $\dot{E}_{D,HScompr}^{AV}$ was comparable to that of $\dot{E}_{D,HScompr}^{AV,EX}$ with rise in design outdoor temperatures. In addition, GC was mainly improvable by enhancing the other components at t_{ext} above 25 °C. This outcome was substantially more marked at $t_{\text{ext}} = 40$ °C. Also, the inefficiencies associate with the HP exp were actually mostly unavoidable, whereas their avoidable part was mainly reducible by enhancing the GC. Since the discharge of HS compr corresponds with the inlet at GC, a strong relation between the irreversibilities occurring in these components was revealed. In addition, the higher the design temperature, the higher the avoidable exogenous exergy destruction rates related to GC compared to its avoidable endogenous ones were. Finally, it could be claimed that further benefits could be associate with:

- the increment in MT, especially for the HS compr and VB;
- the enhancement of the whole investigated system, especially for the GC and HS compr.

5.1.2.2 Improvement strategy for conventional booster solution

Based on the outcomes discussed above, it could be concluded that, as for the components taken individually, very close attention had to be paid firstly to the HS compressors, the gas cooler and the HP expansion valve and, secondly, to MT evaporators.

As far as the HS compressors were concerned, their enhancement was mainly based on:

- an improvement of the components themselves so as to drop their avoidable endogenous irreversibilities, which were slightly higher than their avoidable exogenous inefficiencies. This expedient could also permit reducing the gas cooler inlet temperature and thus enhancing the HP heat exchanger performance;
- a drop in the exergy destruction associated with the whole system and then with the gas cooler, the MT evaporator and the HP expansion valve. This would have allowed decreasing the avoidable exogenous irreversibilities related to the HS compressors, as they also had a remarkable contribution to the preventable inefficiencies occurring in these components.

As regards the gas cooler:

- the main benefits could be achieved by improving the entire system and the HS compressors, as its avoidable irreversibilities were mainly exogenous;
- additional substantial enhancements could also be accomplished by improving its performance.

With respect to the HP expansion valve, it was important to remark that its inefficiencies were mainly unavoidable, meaning that the designer had to seriously take its substitution into consideration. However, some advantageous could be accomplished by improving the gas cooler. Furthermore, additional benefits could be obtained by enhancing the performance of the MT evaporators. Since noticeably advancements from the performance viewpoint, especially for the gas cooler and the HS compressors, could be achieved by improving the whole system, the adoption of some state-of-the-art technologies on the part of the investigated system also had to be properly assessed. At $t_0 = 40\text{ }^\circ\text{C}$, this result was further suggested by the fact that about 33% of the irreversibilities occurring in this system were actually unavoidable. Therefore, for the sake of the performance of R744 booster refrigerating plants, it was necessary to:

- reduce as much as possible the approach temperature of the gas cooler;
- significantly enhance the performance of the HS compressors. This purpose could be accomplished by both using more efficient components and enhancing the HS compressor operating conditions (e.g. drop in mass flow rate, increase in suction pressure);
- employ a device for expansion work recovery, such as a multi-ejector block, in place of the HP expansion valve;
- rise in the medium temperature, i.e. the usage of overfed evaporators;
- adopt a more sophisticated architecture.

As highlighted in this work, the improvements achievable by adopting only the first expedient is not sufficient to accomplish great enhancements for “CO₂ only” systems operating in warm climates. In addition, the last four conclusions stated above suggested the usage of a multi-ejector based system. In fact, besides properly replacing the HP expansion valve and increase the medium temperature, the usage of a multi-ejector module features the presence of some auxiliary compressors. This could be beneficial to both the gas cooler and the HS compressors.

5.1.2.3 Proposed layout: multi-ejector based solution

In this subsection, the real advantages related to EJ_OV compared to CB are revealed with the aid of the advanced exergy analysis. As depicted in Fig. 5.24, at $t_0 = 40\text{ °C}$ the enhanced architecture (i.e. EJ_OV) possessed half of the total exergy destruction rate attributed to the reference system (i.e. CB). With respect to the conventional exergy analysis, EJ_OV had an exergy efficiency of about 0.277. Furthermore, the avoidable irreversibilities was dropped from 42.68 kW to 38.05 kW, while the unavoidable exergy destruction went from 87.79 kW down to 25.08 kW. Also, approximately 60% of the irreversibilities occurring in EJ_OV can be avoided, suggesting that additional remarkable improvements can be accomplished by such a configuration.

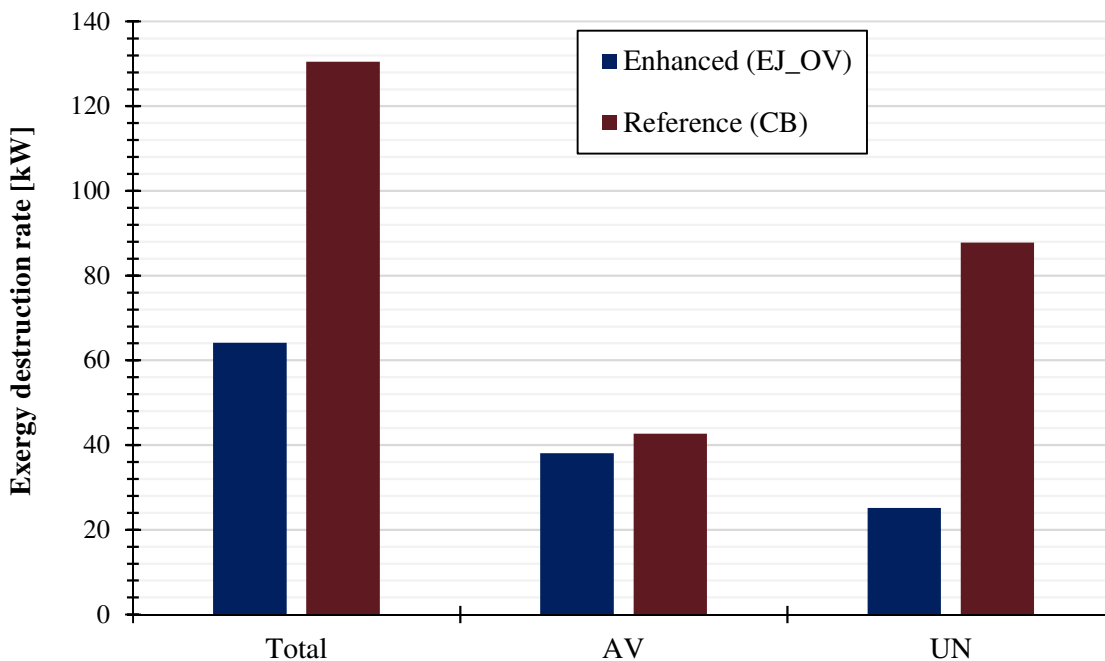


Fig. 5.24 – Comparison of the exergy destruction of the enhanced (EJ_OV) and reference (CB) systems ($t_0 = 40\text{ °C}$).

As it can be observed in Fig. 5.25, the designer's attention had to firstly addressed to AUX. This was due to the significant unloading of HS compr, which commonly takes place in such a technology at high outdoor temperatures. In particular, AUX was accountable for 45.6% of $\dot{E}_{D,tot}^{AV}$. A great contribution to $\dot{E}_{D,tot}^{AV}$ was also found for GC (32.7%), followed by VEJ (6.3%), LS compr (5.7%), MT evap (4.7%) and HS compr (3.4%). In particular, $\dot{E}_{D,GC}^{AV}$, $\dot{E}_{D,AUX}^{AV}$ and $\dot{E}_{D,VEJ}^{AV}$ added up to 60.7%, 89.8% and only to 17.3% of their corresponding total irreversibilities, respectively.

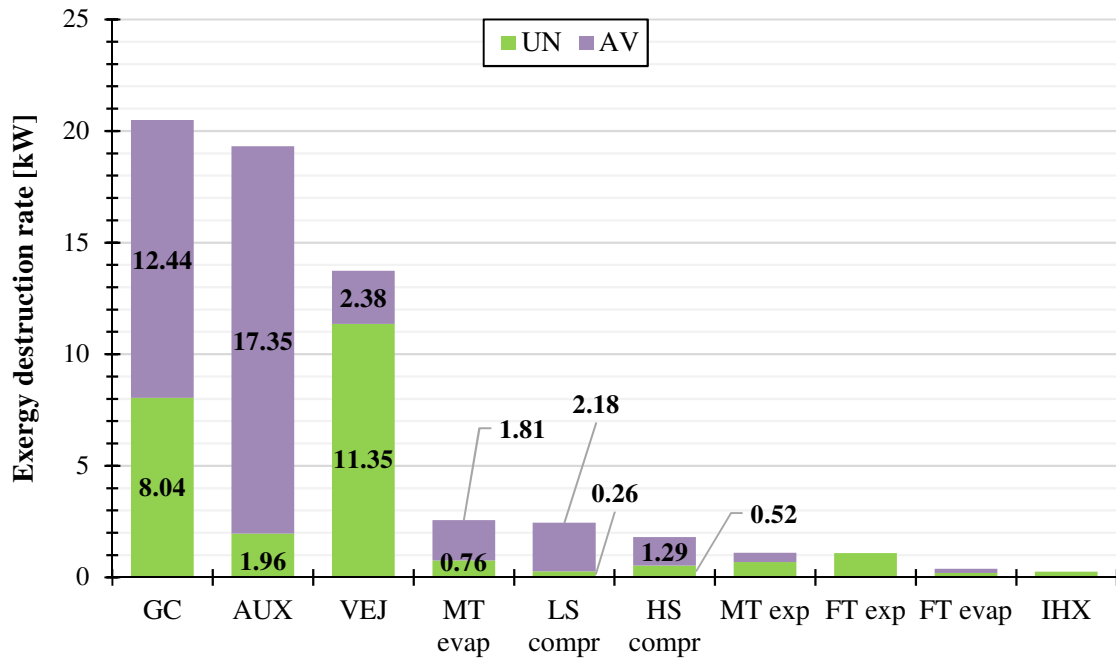


Fig. 5.25 – Results of the advanced exergy analysis for EJ_OV ($t_0 = 40\text{ }^{\circ}\text{C}$).

5.2 Results of environmental analysis

In this part of the present investigation the results in terms of TEWI were computed in five different warm cities for a conventional supermarket application. Furthermore, an assessment based on the TEWI was also implemented for the CO₂ refrigeration configurations integrated with the AC unit in three different warm places. This evaluation took into account different AC and refrigeration loads, as well as the influence of the auxiliary compressor efficiency on the environmental performance of a multi-ejector based configuration.

5.2.1 Results of TEWI for a typical supermarket

Fig. 5.26 depicts the results in terms of TEWI for DXS. Since the direct contribution to the greenhouse gas emissions is independent from the location, the estimated value of TEWI_{direct} amounted to 2066.9 $t_{CO_2,equiv}$ in all the selected cities. This implied that 55.3% in Rome, 61.7% in Lisbon, 66.2% in Valencia and 65.1% in Seville of the total environmental impact associated with DXS was caused by R404A leakages. On the other hand, only 38.9% of the TEWI in Athens could be attributed to the refrigerant leaks. This result could be justified by considering its significantly high value of indirect emission factor.

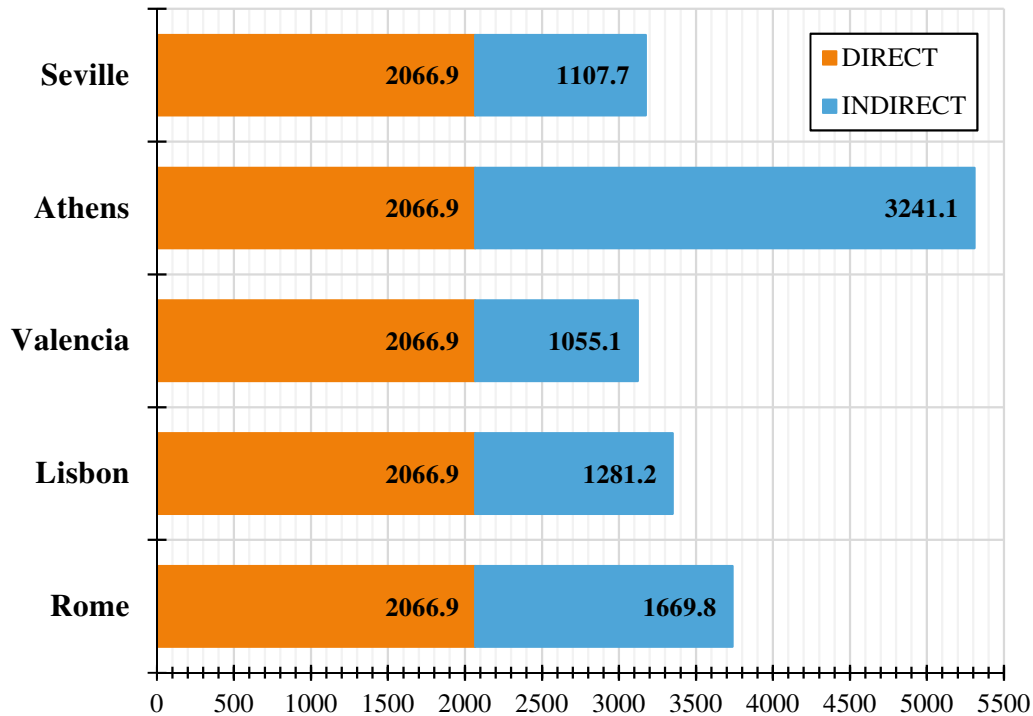


Fig. 5.26 – Splitting of TEWI related to DXS into its direct and indirect contributions.

Despite the usage of a high-GWP refrigerant (i.e. R134a), CS featured for a reduction in TEWI ranging from 30.6% (in Athens) to 49.8% (in Valencia) over DXS. The reason for this result lies in the fact that:

- the GWP of R134a is about one third of that of R404A, as well as the refrigerant charge associated with CS was much lower than that related to DXS;
- CS had slightly higher annual energy consumption than DXS in the evaluated locations.

As shown in Table 5.7, all the investigated “CO₂-only” refrigerating plants presented lower greenhouse gas emissions than DXS. In spite of the performance of CB and the high value of indirect emission factor in Athens, CB was capable of decrease TEWI by 26.9% in comparison with the R404A-based configuration in the above mentioned location. The largest reductions for CB were estimated in Valencia (-59.7%). By reducing the approach temperature of the gas cooler/condenser, TEWI could be dropped from 37.4% (in Athens) to 65.6% (in Valencia) over DXS.

Table 5.7 – TEWI [tonnes] and percent difference [%] in comparison with DXS.

<i>Configuration</i>	<i>Rome</i>	<i>Lisbon</i>	<i>Valencia</i>	<i>Athens</i>	<i>Seville</i>
CS	2179.7	1797.8	1566.0	3681.2	1602.2
	(-41.7%)	(-46.3%)	(-49.8%)	(-30.6%)	(-49.5%)
CB	1937.5	1528.8	1258.0	3882.7	1341.4
	(-48.1%)	(-54.3%)	(-59.7%)	(-26.9%)	(-57.7%)
IB	1635.8	1296.6	1074.1	3322.7	1151.0
	(-56.2%)	(-61.3%)	(-65.6%)	(-37.4%)	(-63.7%)
MS+PC	1523.0	1209.3	985.6	3002.3	1028.6
	(-59.2%)	(-63.9%)	(-68.4%)	(-43.4%)	(-67.6%)
PC	1564.9	1242.9	1019.5	3134.8	1082.7
	(-58.1%)	(-62.9%)	(-67.3%)	(-40.9%)	(-65.9%)
PC_VAR	1562.8	1241.9	1018.1	3125.6	1078.2
	(-58.2%)	(-62.9%)	(-67.4%)	(-41.1%)	(-66.0%)
OV	1457.7	1145.9	949.78	2939.8	1018.0
	(-61.0%)	(-65.8%)	(-69.6%)	(-44.6%)	(-67.9%)
OV+PC	1416.6	1114.4	918.45	2833.9	979.2
	(-62.1%)	(-66.7%)	(-70.6%)	(-46.6%)	(-69.2%)
EJ	1295.5	1030.3	843.5	2587.8	892.4
	(-65.3%)	(-69.2%)	(-73.0%)	(-51.2%)	(-71.9%)
EJ_OV	1214.1	967.6	793.2	2436.1	841.1
	(-67.5%)	(-71.1%)	(-74.6%)	(-54.1%)	(-73.5%)

In comparison with DXS, similar environmental impacts could be associated with MS+PC and OV, which ranged from 43.4% (by MS+PC in Athens) to 69.6% (by OV in Valencia). The usage of parallel compressor allowed bringing TEWI from 40.9% (by PC in Athens) down to 67.4% (by PC_VAR in Valencia). The total environmental impact in

relation to DXS could be dropped by employing OV+PC by 46.6% (in Athens), at least, and by 70.6%, at best (in Valencia). Great results in terms of reduction in TEWI could be associated with the ejector-based configurations. The adoption of such solutions permitted halving the value of TEWI in Athens and bringing the total greenhouse gas emissions down to approximately 70% over DXS in all the other evaluated locations. By selecting CS as the baseline (Fig. 5.27), it was possible to notice that CB and IB reduced TEWI by 19.7% and by 31.4% in Valencia, respectively. EJ and EJ_OV almost halved the greenhouse gas emissions over CS. Also, in comparison with the cascade arrangement, the drop in TEWI on the part of MS+PC, PC and OV+PC was estimated to be equal to 37.1%, 34.9% and 41.4%, respectively. In spite of R744 is characterized by a very low value of GWP, CB had a higher TEWI than CS (+5.5%) in Athens due to its large energy consumption. The reduction in approach temperature of the gas cooler/condenser (IB) led to reduction in TEWI by 9.7% over CS, despite its better performance and higher indirect emission factor. The adoption of MS+PC, PC and OV+PC permitted bringing TEWI down to 18.4%, 14.8% and 23% in comparison with CS, respectively. These reductions amounted to 29.7% and 33.8% for EJ and EJ_OV, respectively. All the enhanced solutions featured lower TEWI than that of both DXS and CS. This result could be associated with both a much lower direct environmental impact than the solutions using high-GWP refrigerants solutions and the energy savings achievable by employing them.

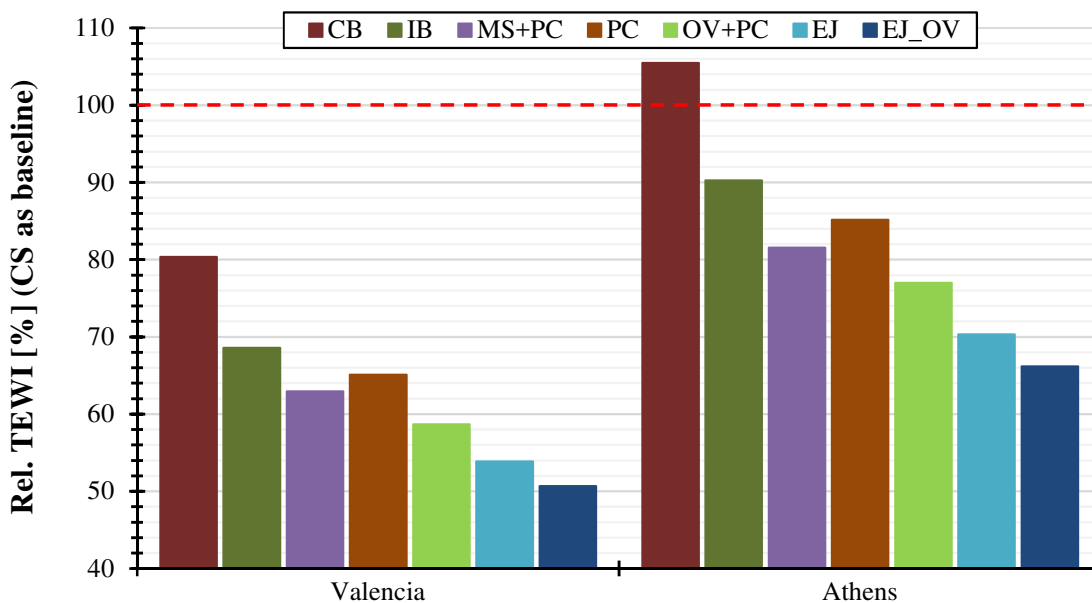


Fig. 5.27 - Reduction in TEWI over CS on the part of some of the investigated solutions in Valencia and in Athens.

5.2.2 Results of TEWI of the integrated solution

In this sub-section, the environmental impacts associated with DXS+AC, EJ_OV_AC and Improved EJ_OV_AC are compared in Rome, Valencia and Seville involving two different cases, ie. $LF \sim 2.5$ in *Scenario I* (50% of $\dot{Q}_{MT,design}$) (Case I, top part in Fig. 5.28) and $LF = 8$ in *Scenario III* (200% of $\dot{Q}_{MT,design}$) (Case II, bottom part in Fig. 5.28). The results are listed in Table 5.8.

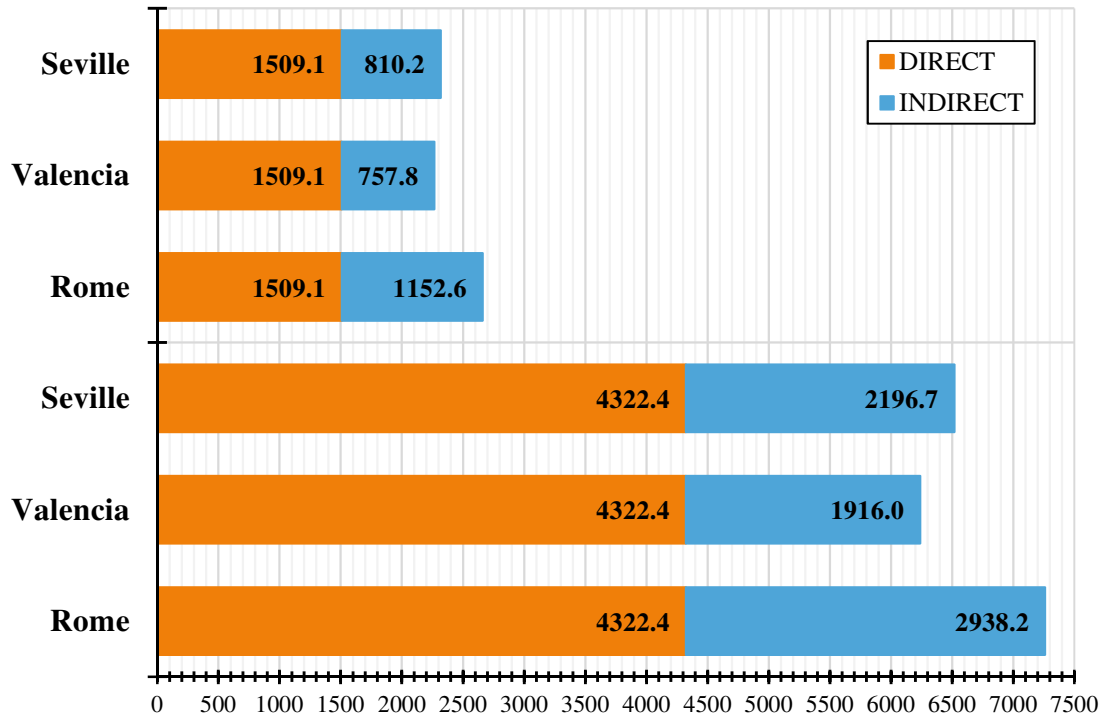


Fig. 5.28 - Splitting of TEWI related to DXS+AC into its direct and indirect contributions for Case I (at the top) and Case II (at the bottom).

In Fig. 5.28, TEWI for the two selected cases is split into its two components. It was possible to notice that the direct contribution to the greenhouse gas emissions outweighed, ranging from 56.7% in Rome (Case I) to 69.3% in Valencia (Case II). In particular, $TEWI_{direct}$ associated with AC was equal from 8.2% in Rome (Case I) to 11.9% in Valencia (Case II) of the total environmental impact related to DXS+AC.

In Case I, EJ_OV and Improved EJ_OV reduced TEWI by 66.9% and 67.7% in Rome, by 74.6% and 75.3% in Valencia and by about 73% in Seville over DXS+AC, respectively. As far as Case II was concerned, reductions by 68.7% and 69.9% in Rome, by 75.4% and 76.5% in Valencia and by 71.6% and 73.1% in Seville over DXS+AC were respectively accomplished.

Table 5.8 – TEWI [tonnes] and percent difference [%] in comparison with DXS+AC for the smallest and the largest AC unit size investigated in this study.

<i>Scenario related to supermarket</i>	<i>Scenario related to AC</i>	<i>Configuration</i>	<i>Rome</i>	<i>Valencia</i>	<i>Seville</i>
LF ~ 2.5	<i>Scenario I</i> (50% of $\dot{Q}_{MT,design}$)	DXS+AC	2661.7	2267.0	2319.4
		EJ_OV_AC	881.6	576.0	626.6
		Improved	860.7	560.1	606.8
		EJ_OV_AC	(-66.9%)	(-74.6%)	(-73.0%)
LF = 8	<i>Scenario III</i> (200% of $\dot{Q}_{MT,design}$)	DXS+AC	7260.6	6238.4	6519.1
		EJ_OV_AC	2272.5	1533.0	1853.8
		Improved	2184.1	1466.5	1756.6
		EJ_OV_AC	(-68.7%)	(-75.4%)	(-71.6%)
		EJ_OV_AC	(-69.9%)	(-76.5%)	(-73.1%)

5.3 Discussion

According to Subsection 5.1 and Subsection 5.2, transcritical R744 refrigerating solutions can efficiently replace both R404A direct expansion systems and R134a/R744 cascade configurations in supermarkets located in Mediterranean Europe from both the environmental and energy viewpoint.

The outcomes obtained have suggested that the combination of the parallel compression with MT overfed evaporators and, in particular, the usage of the multi-ejector concept are the best HFC-free technologies. These lead to energy savings ranging from 11.6% to 27.3% over a R404A unit in the selected locations. In comparison with a R134a/R744 cascade solution, they reveal reductions in the annual energy consumption ranging from 8.5% to 26.3% in the same cities. If the current benchmark (i.e. parallel compression) for CO₂ supermarket refrigeration systems is taken into account, the previously mentioned solutions show energy savings from 9.5% to 22.4% in the selected cities. The adoption of an auxiliary compressor allows consuming from 4% to 6% less electricity than a booster

system in high ambient temperature countries. The coupling with MT overfed evaporators permits further reducing the annual energy consumption by about 10% in warm regions, meaning that greater energy benefits can be obtained with rise in MT than with parallel compression. Also, the usage of the multi-ejector module decreases the annual electricity consumption from 8% to 14% in relation to the solution combining auxiliary compressor with MT overfed evaporators in Southern Europe. Finally, it can also be claimed that, due to the high investment cost and the complicated control system, the configuration with dedicated mechanical subcooling and parallel compression could be an acceptable solution in small applications. Next, although some energy benefits and the production of some DHW can be associated with the use of a de-superheater, its adoption would imply an increase in the total capital investment. Therefore, a suitable trade-off between the economic and the energetic aspects should be considered. Furthermore, the solution using a multi-ejector rack and MT and LT overfed evaporators and integrated with the AC system consumes from 16.6% to 26.2% less energy than a conventional HFC-based solution in warm countries. The results significantly depend on the climatic conditions, as well as on the size of both the AC unit and the food retail. As a consequence, “fully integrated” R744 refrigerating plants will become more economically convenient than separated high-GWP units in the near future. Also, this investigation has revealed that the enhancement of auxiliary compressor efficiency on the part of the manufacturers should be considered for such a configuration, especially for applications located in warm/hot places, large supermarkets and AC units. This argument is supported by the fact that the use of the auxiliary compressors is substantially extended in the configurations equipped with multi-ejector block, particularly in “all-in-one” units. It is important to remark again that “all-in-one” configurations will have a relevant role in the diffusion of transcritical R744 supermarket systems across Europe. For this reason, it is possible to claim that parallel compression is not sufficient to achieve this target in warm regions.

Although indirect arrangements are out of scope of this study, it is worth remarking that, conforming to the EU F-Gas Regulation 517/2014, R1234ze(E)/CO₂ refrigeration systems are also acceptable configurations for supermarket applications. HFO-1234ze(E) is a slightly flammable (A2L) and extremely expensive working fluid, having a negligible GWP. Purohit et al. (2016) compared the annual energy consumption of the aforementioned solutions with that of both some transcritical CO₂ booster refrigeration plants and a R404A direct expansion unit in different hot locations worldwide. In this work, the authors selected similar boundary conditions to those applied to this

investigation. The authors demonstrated that a pure CO₂ unit with parallel compressor offers an energy saving by 4.3% in Seville over a R404A system. In comparison with R1234ze(E)-based indirect configurations, the decrease in the annual energy consumption ranges from 2% up to 4.7% in the same city. This means that transcritical R744 systems using technologies such as overfed evaporators and multi-ejector rack have much better energy and environmental performance than R1234ze(E)/CO₂ indirect arrangements in Southern Europe. It is also important to stress that, according to Greenpeace (2016), HFOs are basically HFCs with a different name, as well as HFO blends possess a high GWP. Additionally, both the production and the decomposition into the atmosphere of these working fluids imply the creation of toxic by-products.

As regards the exergy evaluation, the application of the conventional analysis to a conventional booster refrigerating system has led to some deceptive results. A better understanding of the most beneficial enhancement strategies to be adopted can be obtained by applying the advanced exergy analysis, which is the most powerful thermodynamic tool to design any energy conversion system. This assessment has suggested that the most effective interventions to undertake are:

- a significant drop in the approach temperature of the gas cooler;
- a noticeably (direct or indirect) enhancement in the performance of the HS compressors;
- the replacement of the HP expansion valve with an expansion work recovery device, as well as an increase in the medium temperature;
- the usage of a more advanced layout.

The application of only the first measure among the ones listed above is not enough to allow transcritical CO₂ systems to substantially boost their performance in warm regions, as showed in this work on the energy perspective. As a consequence, a more state-of-the-art architecture, such as the one using a multi-ejector rack, has been investigated by applying the advanced exergy analysis. At the design temperature of 40 °C, the adoption of the multi-ejector concept enabling halving the exergy destruction rate related to the overall system compared to a conventional booster solution. Also, the avoidable exergy destruction and the unavoidable irreversibilities were respectively brought from 42.68 kW down to 38.05 kW and from 87.79 kW down to 25.08 kW. In addition, approximately 60% of these irreversibilities can be further avoided. In particular, the auxiliary compressors and the gas cooler are responsible for the largest contributions to total

avoidable irreversibilities (respectively equal to 45.6% and 32.7%), followed by the multi-ejector block (6.3%). In particular, the avoidable exergy destruction rate of the gas cooler, auxiliary compressors and vapour ejectors amount to 60.7%, 89.8% and only to 17.3% of their corresponding total exergy destruction rates, respectively. By making a comparison between the results related to the conventional booster unit and those associated with the multi-ejector based configuration, it can be concluded that the improvements of the enhanced system are accomplished by:

- a decrement by about 50% of the inefficiencies occurring in the gas cooler. This achievement has been derived firstly from the adoption of a more advanced configuration and then from the reduction in the discharge temperature of the compressors, as well as from the drop in its approach temperature;
- a reduction by approximately half on the part of the avoidable irreversibilities related to both compressors compared to HS compressors belonging to the conventional system;
- a fall by roughly 77% associated with the expansion device;
- a halving of the avoidable inefficiencies taking place in the MT evaporators thanks to rise in its operating temperature.

Gullo et al. (2016c) applied the advanced exergy analysis to a CO₂ booster refrigeration system with parallel compression. Although the selected boundary conditions were different from the ones adopted in this study, an interesting comparison between this solution and the multi-ejector based technology can be made. In both cases, close attention has to be paid firstly to the compressors and then to the gas cooler, whereas the contribution of the avoidable irreversibilities to total avoidable exergy destruction taking place in the expansion devices are modest. Also, unlike the case with ejectors, the MT evaporators have a remarkable avoidable exergy destruction rate as the configuration with parallel compressor is taken into account.

Finally, the state-of-the-art transcritical R744 solutions drops TEWI from 40.9% up to 74.6% over R404A-based systems in Mediterranean cities. In comparison with a R134a/R744 cascade configuration, the carbon footprint of supermarkets located in Valencia and in Athens falls from 14.8% to 49.3% by employing pure CO₂ systems. This implies that the usage of such technologies has to be avoided from the energy and the environmental perspectives. Also, in the case of the integration with the AC unit, these

technologies lead to reduction in TEWI ranging from 66.9% to 76.5% in Southern Europe over the solutions using HFCs.

6 CONCLUSIONS AND FUTURE WORK

In Chapter 6 the main conclusions are summed up and some directions for future work are pointed out.

6.1 Conclusions

In this paper, the state-of-the-art technologies for commercial R744 refrigeration systems have been theoretically compared from both the thermodynamic and environmental point of views. The energy assessments have been based on the operating conditions of supermarket applications operating in five warm climate European locations, i.e. Rome (Italy), Lisbon (Portugal), Valencia (Spain), Athens (Greece) and Seville (Spain). The advanced HFC-free solutions considered in the present work have included the dedicated mechanical subcooling, the parallel compression, the overfed evaporators and the multi-ejector concept. In addition, two R744 booster solution with different heat rejection control strategies, a R404A multiplex direct expansion refrigeration system and a R134a/R744 cascade refrigeration arrangement have also been taken into account. The efficiencies of all the selected compressors have been derived from some manufacturers' selection software as a function of the pressure ratio. Firstly, the assessment has been carried out by assuming the running modes of a typical food retail application. At a later time, the effect of the global efficiency of the parallel compressors on the annual energy consumption has also been examined for the most promising technology among the ones investigated (i.e. the configuration using the multi-ejector module and overfed LT and

MT evaporators). This parameter will play a crucial role in the near future in the diffusion of the “CO₂ only” refrigeration plants in warm climates. For this reason, the size of the supermarket, as well as the integration of AC units with different capacities into the R744 refrigerating system have also been examined. This sensitivity analysis represents one of the most interesting and innovative parts of the present study.

The main conclusions which can be drawn on the energy perspective are:

- no significant differences have been showed by the two chosen solutions with parallel compression. In addition, such a technology is energetically competitive with HFC-based solutions at outdoor temperatures up to about 27 °C. This implies that it is not a suitable technology for warm regions, especially in “fully integrated” systems;
- the use of overfed evaporators has no effects on the energy efficiency limit of pure CO₂ systems in relation to the configuration with parallel compression. However, unlike the latter, the former leads to relevant energy savings in the selected locations over R404A systems even in case of MT = -6°C rather than MT = -4 °C. As these two technologies are combined, “CO₂ only” systems can outperform the currently used solutions at outdoor temperatures up to 33 °C. Their energy savings over a R404A unit range from 11.6% to 15.2% in the investigated cities;
- it is also possible to claim that the dedicated mechanical subcooling is not a very promising technology. The reasons for this lie in the fact that modest energy savings can be attained in comparison with the investment cost. It is worth highlighting as the solutions with overfed evaporators and parallel compression are more affordable and energy beneficial than that with subcooling loop. In addition, its control strategy is complicated to be implemented. On the other hand, the life expectancy of its compressors is supposed to be longer than those employed in the other investigated R744 solutions;
- the common energy efficiency limit occurring for transcritical R744 units with rise in outdoor temperature in comparison with a R404A solution disappears by employing the multi-ejector concept. For a typical supermarket operating in warm climates, the adoption of the multi-ejector module leads to an annual energy saving by about 20%. If the LT display cabinets are also overfed, a decrease in the annual energy consumption by about 25% is attained. Both results are consistent with the ones available in the open literature. It is also possible to state

that, thanks to this technology, nowadays transcritical R744 supermarket refrigeration systems can be employed in any climate context with great results;

- the previously claimed conclusions can be extended to the case of the R134a/CO₂ arrangements, meaning that this solution, besides being unacceptable from the environmental viewpoint, consumes much more energy than the state-of-the-art transcritical R744 solutions in warm regions;
- the overfeeding of both the MT and the LT evaporators on the part of a R744 solution equipped with a multi-ejector pack and integrated with the AC unit leads to energy savings ranging from 16.6% to 26.2% in relation to the conventional HFC-based solutions. The outcomes obtained strongly depend on the size of both the AC system and the supermarket, as well as on the climatic conditions. This points out that “all-in-one” CO₂ refrigeration system will be able to become more affordable than typical solutions (several independent units) in the next few years;
- as the usage of the parallel compressors is enormously extended in ejector-based configurations, the manufacturability of more efficient auxiliary compressors is energetically justifiable, especially in the scenarios involving the integration with the AC unit. In particular, this could also be economically favourable for systems running in warm/hot locations, large food retail industries and large AC systems. Also, additional energy decreases ranging from 2.4% to 5.2% over the conventional system equipped with the multi-ejector rack could be achieved, according to the size of both the AC unit and the supermarket, as well as to the weather conditions.

As far as the advanced exergy analysis is concerned, the application of such an evaluation to a R744 booster supermarket system for warm regions confirms the need for the adoption of multi-ejector based configurations. At the design temperature of 40 °C, the usage of the multi-ejector module leads to a decrease in total irreversibilities by about 50% compared to a conventional booster system. Additionally, the avoidable inefficiencies fall from 42.68 kW down to 38.05 kW, while the unavoidable irreversibilities are decreased from 87.79 kW down to 25.08 kW. Significant enhancements can be attributed to the auxiliary compressors and the gas cooler, as they are accountable for the highest contributions to $\dot{E}_{D,tot}^{AV}$. The multi-ejector pack is responsible for 6.3% of the total avoidable irreversibilities, whereas only 17.3% of them can be actually avoided.

At last, it is also relevant to highlight that the usage of the R744 reduces TEWI from 14.8% up to 74.6% compared to HFC-based solutions in the investigated locations. As the AC unit is coupled with the refrigerating system, transcritical R744 configurations reduce the carbon footprint from 66.9% and 76.5% over separate HFC solutions. Consequently, the adoption of any synthetic refrigerant makes no sense from both the energy and the environmental viewpoint in commercial refrigeration sector.

The author do think that “all-in-one” CO₂ refrigeration systems will become extremely competitive in the near future even in terms of payback time in comparison with HFC-based solutions. As suggested by Shecco (2016), the achievement of this target is strongly related to the adoption of highly efficient solutions, meaning that the multi-ejector concept needs to be strongly encouraged. Furthermore, the total capital investment associated with these solutions will be reduced by promoting their spread, while the usage of more highly efficient devices (e.g. improved ejectors, smaller heat exchangers, more efficient compressors, etc.) will permit dropping the operating costs significantly. It is worth remarking that the coming into force of the EU F-gas Regulation 517/2014 was greeted with scepticism on the part of many industry members as it would have encouraged the use of the R744 in warm regions. On the other hand, as of when it was adopted this legislative act has substantially boosted many advances in HFC-free technologies, especially in high ambient temperature countries and penalize HFCs in terms of both cost and availability. This has been leading to an ever-growing trend of both their cost-effectiveness and their efficiency. Thus the entry into the market of the multi-ejector concept is already allowing an additional move of the “CO₂ efficiency equator” further south. Additionally, it will lead to its deletion in the near future and significant tracks of this are already visible. Next, compared to HFC-based systems, further significant energy (and cost) savings on the part of the multi-ejector based systems in relation to those computed in this study could be accomplished by completely integrating the refrigeration plant with the HVAC unit. Also, as already proved by Karampour and Sawalha (2015, 2016b), the parallel compression technology is not a suitable solution when it comes to “fully integrated” CO₂ booster solutions operating in warm climate contexts. This is an additional strong argument in favour of the multi-ejector concept in any climate condition, with particular emphasis on mild/warm regions.

To conclude. it can be asserted that the usage of R744 in commercial refrigeration sector is no longer open to dispute, as great performance can be attained even in high ambient temperature countries by adapting the system layout to the distinctive properties of such

a working fluid. In fact, nowadays the diffusion of transcritical R744 refrigerating systems in Southern Europe is mainly discouraged by some remaining non-technological barriers, such as shortage of service technicians, social and political factors. Therefore, enormous advantages will be taken by the manufacturers and the suppliers who will be able to successfully invest in commercial R744 refrigeration units.

6.2 Future work

As exhaustively explained in the above sections the multi-ejector concept and that related “all-in-one” solutions are the most promising technologies when it comes to R744 refrigerating plants for food retail industry. However, further and more thorough investigations need to be conducted so as to strengthen the confidence in the previously mentioned solutions, as well as fully exploit their potential. Additional efforts still need to be addressed to enhance the understanding of the achievable energy and economic savings. In order to attain this target, it is necessary to carry out various further experimental campaigns/field measurements and use these data to implement and validate some advanced thermodynamic simulation models. These future investigations should involve the typical running modes of supermarket applications and take into account the benefits related to the integration with the HVAC unit. A remarkable attention should be focused on the applications located in Mediterranean Europe and, at a later time, on those in hot climate contexts.

These aspects and the outcomes of this study point to some directions for future work with respect to “fully integrated” transcritical CO₂ refrigeration systems equipped with multi-ejector module:

- the implementation of a suitable control strategy for heat recovery, which, to the best of the author's knowledge, has never been investigated;
- the evaluation of a correct balance in terms of load and a suitable control for both the high-stage compressors and the parallel ones so as to avoid the degradation of their performance and further reduce the total energy consumption;
- the generation/improvement of the multi-ejector performance maps. This activity will allow developing advanced thermodynamic models of the aforementioned solutions, assessing their best operating conditions and predicting the energy savings achievable in commercial buildings;
- the fulfilment of appropriate economic evaluations based on the payback period calculation and, more suitably, on the life-cycle cost analysis (LCCA). This will

play a pivotal role in the diffusion of the transcritical R744 units in the next few years;

- an in-depth comparison of the energy and environmental performance of R744 ejector supported parallel systems with that of indirect configurations using ultra low-GWP refrigerants (i.e. R717, R1234ze(E)).

Also, the current knowledge regarding multi-ejector R744 supermarket refrigerating plants needs to be suitably transferred to heat pumping installations at the conventional working conditions of some key sectors. In addition, advanced energy, economic and environmental analyses will also have to be performed for these solutions. All the evaluations will have to be validated against some experimental data.

All these investigations will boost the confidence in R744 for both supermarket applications and heat pumping units. As a consequence, in the next few years a great diffusion of such technologies will take hold in highly energy-consumptive buildings, especially in the ones located in warm regions, and all the remaining non-technological barriers will be removed.

REFERENCES

- Açikkalp, E., Aras, H., Hepbasli, A., 2014. Advanced exergy analysis of a trigeneration system with a diesel-gas engine operating in a refrigerator plant building. *Energy and Buildings* 80, 268-275. DOI: [10.1016/j.enbuild.2014.05.029](https://doi.org/10.1016/j.enbuild.2014.05.029)
- Alternative Fluorocarbons Environmental Acceptability Study, 2006. AFEAS Data. – Available at: <<https://agage.mit.edu/data/afeas-data>> [accessed 01.12.2016].
- Aminyavaria, M., Najafi, B., Shirazi, A., Rinaldi, F., 2014. Exergetic, economic and environmental (3E) analyses, and multi-objective optimization of a CO₂/NH₃ cascade refrigeration system. *Applied Thermal Engineering* 65(1-2), 42-50. DOI: [10.1016/j.applthermaleng.2013.12.075](https://doi.org/10.1016/j.applthermaleng.2013.12.075)
- ASHRAE, 2013. ANSI/ASHRAE Standard 34-2013 Designation and Safety Classification of Refrigerants; Atlanta, USA. ISSN: 1041-2336.
- Bai, T., Yu, J., Yan, G., 2016. Advanced exergy analysis of an ejector expansion transcritical CO₂ refrigeration system. *Energy Conversion and Management* 126, 850-861. DOI: [10.1016/j.enconman.2016.08.057](https://doi.org/10.1016/j.enconman.2016.08.057)
- Banasiak, K., Hafner, A., Kriezi, E. E., Madsen, K. B., Birkelund, M., Fredslund, K., Olsson, R., 2015. Development and performance mapping of a multi-ejector expansion work recovery pack for R744 vapour compression units. *International Journal of Refrigeration* 57, 265-276. DOI: [10.1016/j.ijrefrig.2015.05.016](https://doi.org/10.1016/j.ijrefrig.2015.05.016)
- Banasiak, K., Hafner, A., Haddal, O., Eikevik, T. M., 2014. Test facility for a multiejector R744 refrigeration system. In: *Proceedings of the 11th IIR Gustav*

- Lorentzen Conference on Natural Refrigerants, 31 August-2 September; Hangzhou, China. ID: 70.
- Bansal, P., 2012. A review – Status of CO₂ as a low temperature refrigerant: Fundamentals and R&D opportunities. *Applied Thermal Engineering* 41, 18-29. DOI: [10.1016/j.applthermaleng.2011.12.006](https://doi.org/10.1016/j.applthermaleng.2011.12.006)
 - Bell, I., 2004. Performance increase of carbon dioxide refrigeration cycle with the addition of parallel compression economization. In: *Proceedings of the 6th IIR Gustav Lorentzen Conference on Natural Working Fluids*, 29 August-1 September; Glasgow, UK. ID: 1630.
 - Beshr, M., Bush, J., Aute, V., Radermacher, R., 2016. Steady state testing and modeling of a CO₂ two-stage refrigeration system with mechanical subcooler. In: *Proceedings of the 12th IIR Gustav Lorentzen Natural Working Fluids Conference*, 21-24 August; Edinburgh, UK. ID: 1146.
 - Bilir, N., Ersoy, H. K., 2009. Performance improvement of the vapour compression refrigeration cycle by a two-phase constant area ejector. *International Journal of Energy Research* 33, 469–480. DOI: [10.1002/er.1488](https://doi.org/10.1002/er.1488)
 - BITZER, 2015. BITZER Software Version 6.4.4.1464 – Available at: <https://www.bitzer.de/websoftware/> [accessed 01.12.2016].
 - Brown, J. S., Yana-Motta, S. F., Domanski, P. A., 2002. Comparative analysis of an automotive air conditioning systems operating with CO₂ and R134a. *International Journal of Refrigeration* 25(1), 19-32. DOI: [10.1016/S0140-7007\(01\)00011-1](https://doi.org/10.1016/S0140-7007(01)00011-1)
 - Cabello, R., Sánchez, D., Llopis, R., Catalán, J., Nebot-Andrés, L., Torrella, E., 2017. Energy evaluation of R152a as drop in replacement for R134a in cascade refrigeration plants. *Applied Thermal Engineering* 110, 972-984. DOI: [10.1016/j.applthermaleng.2016.09.010](https://doi.org/10.1016/j.applthermaleng.2016.09.010)
 - Campbell, A., Maidment, G. G., Missenden, J. F., 2007. A refrigerant system for supermarkets using natural refrigerant CO₂. *International Journal of Low Carbon Technologies* 2(1), 65-79. DOI: [10.1093/ijlct/2.1.65](https://doi.org/10.1093/ijlct/2.1.65)
 - Carr-Shand, S., Staafgard, L., Uren, S., Johnson, A., 2009. Sustainability trends in European retail.
 - Cavallini, A., Zilio, C., 2007. Carbon dioxide as a natural refrigerant. *International Journal of Low-Carbon Technologies* 2(3), 225-249. DOI: [10.1093/ijlct/2.3.225](https://doi.org/10.1093/ijlct/2.3.225)

- Cecchinato, L., Corradi, M., Minetto, S., 2012. Energy performance of supermarket refrigeration and air conditioning integrated systems working with natural refrigerants. *Applied Thermal Engineering* 48, 378-391. DOI: [10.1016/j.applthermaleng.2012.04.049](https://doi.org/10.1016/j.applthermaleng.2012.04.049)
- Cecchinato, L., Corradi, M., Minetto, S., 2010b. Energy performance of supermarket refrigeration and air conditioning integrated systems. *Applied Thermal Engineering* 30 (14-15), 1946-1958. DOI: [10.1016/j.applthermaleng.2010.04.019](https://doi.org/10.1016/j.applthermaleng.2010.04.019)
- Cecchinato, L., Corradi, M., Minetto, S., 2010a. A critical approach to the determination of optimal heat rejection pressure in transcritical systems. *Applied Thermal Engineering* 30(13), 1812-1823. DOI: [10.1016/j.applthermaleng.2010.04.015](https://doi.org/10.1016/j.applthermaleng.2010.04.015)
- Cecchinato, L., Chiarello, M., Corradi, M., Fornasieri, E., Minetto, S., Stringari, P., Zilio, C., 2009. Thermodynamic analysis of different two-stage transcritical carbon dioxide cycles. *International Journal of Refrigeration* 32(5), 1058-1067. DOI: [10.1016/j.ijrefrig.2008.10.001](https://doi.org/10.1016/j.ijrefrig.2008.10.001)
- Cecchinato, L., Corradi, M., Minetto, S., Chiesaro, P., 2007. An experimental analysis of a supermarket plant working with carbon dioxide as refrigerant. In: *Proceedings of the 22nd IIR International Congress of Refrigeration*, 21-26 August; Beijing, China. ID: ICR07-D1-1062.
- Chen, J., Havtun, H., Björn, P., 2015. Conventional and advanced exergy analysis of an ejector refrigeration system. *Applied Energy* 144, 139-151. DOI: [10.1016/j.apenergy.2015.01.139](https://doi.org/10.1016/j.apenergy.2015.01.139)
- Chen, Y., Gu, J., 2005. The optimum high pressure of CO₂ transcritical refrigeration systems with internal heat exchangers. *International Journal of Refrigeration* 28(8), 1238-1249. DOI: [10.1016/j.ijrefrig.2005.08.009](https://doi.org/10.1016/j.ijrefrig.2005.08.009)
- Chesi, A., Esposito, F., Ferrara, G., Ferrari, L., 2014. Experimental analysis of R744 parallel compression cycle. *Applied Energy* 135(C), 274-285. DOI: [10.1016/j.apenergy.2014.08.087](https://doi.org/10.1016/j.apenergy.2014.08.087)
- Chiarello, M., Giroto, S., Minetto, S., 2010. CO₂ supermarket refrigeration system for hot climates. In: *Proceedings of the 9th IIR-Gustav Lorentzen Conference on Natural Refrigerants*, 12-14 April; Sydney, Australia. ID: 39.

- Choi, K.-II, Pamitran, A. S., Oh, C.-Y., Oh, J.-T., 2007. Boiling heat transfer of R-22, R-134a, and CO₂ in horizontal smooth minichannels. International Journal of Refrigeration 30(8), 1336-1346. DOI: [10.1016/j.ijrefrig.2007.04.007](https://doi.org/10.1016/j.ijrefrig.2007.04.007)
- Da Ros, S., 2005. Optimisation of a Carbon Dioxide Transcritical Cycle with Flash-gas Removal. In: Proceedings of IIR International Conferences – Thermophysical properties and Transfer Processes of Refrigerants, 31 August-2 September; Vicenza, Italy.
- Danfoss, 2016b. Italy's Largest Hypermarket Opts for CO₂ Refrigeration. – Available at: [http://www.danfoss.com/newsstories/rc/italy-largest-hypermarket-opts-for-co2-refrigeration/?ref=17179879870#/>](http://www.danfoss.com/newsstories/rc/italy-largest-hypermarket-opts-for-co2-refrigeration/?ref=17179879870#/) [accessed 01.12.2016].
- Danfoss, 2016a. HFC Phase Down (F-Gas Regulation). – Available at: [http://refrigerants.danfoss.com/hfc/#/>](http://refrigerants.danfoss.com/hfc/#/) [accessed 01.12.2016].
- Danfoss, 2008. Transcritical Refrigeration Systems with Carbon Dioxide (CO₂). – Available at: [http://files.danfoss.com/TechnicalInfo/Rapid/01/Article/TranscriticalArticle/PZ000F102_ARTICLE_Transcritical%20Refrigeration%20Systems%20with%20Carbon%20Dioxide%20\(CO2\).pdf](http://files.danfoss.com/TechnicalInfo/Rapid/01/Article/TranscriticalArticle/PZ000F102_ARTICLE_Transcritical%20Refrigeration%20Systems%20with%20Carbon%20Dioxide%20(CO2).pdf) [accessed 01.12.2016].
- Dopazo, J.A., Fernandez-Seara, J., Sieres, J., Uhia, F.J., 2009. Theoretical analysis of a CO₂-NH₃ cascade refrigeration system for cooling applications at low temperatures. Applied Thermal Engineering 29(8-9), 1577-1583. DOI: [10.1016/j.applthermaleng.2008.07.006](https://doi.org/10.1016/j.applthermaleng.2008.07.006)
- Dorin, 2015. Dorin Software 15.07 – Available at: <http://www.dorin.com/en/Software/> [accessed 01.12.2016].
- Eikevik, T. M., Bertelsen, S., Haugsdal, S., Tolstorebrov, I., Jensen, S., 2016. CO₂ refrigeration system with integrated propane subcooler for supermarkets in warm climate. In: Proceedings of the 12th IIR Gustav Lorentzen Natural Working Fluids Conference, 21-24 August; Edinburgh, UK. ID: 1031.
- Elbel, S., Hrnjak, P., 2008. Experimental validation of a prototype ejector design to reduce throttling losses encountered in transcritical R744 system operate. International Journal of Refrigeration 31, 411-422. DOI: [10.1016/j.ijrefrig.2007.07.013](https://doi.org/10.1016/j.ijrefrig.2007.07.013)
- EMERSON Climate Technologies, 2010. Refrigerant Choices for Commercial Refrigeration – Finding the Right Balance. Technical Report No.: TGE124-091/E. – Available at: <http://www.emersonclimate.com/> [accessed 01.12.2016].

- EPEE, 2015. Achieving the EU HFC Phase Down: The EPEE “Gapometer” Project.
- Erbay, Z., Hepbasli, A., 2014. Application of conventional and advanced exergy analyses to evaluate the performance of a ground-source heat pump (GSHP) dryer used in food drying. *Energy Conversion and Management* 78, 499-507. DOI: [10.1016/j.enconman.2013.11.009](https://doi.org/10.1016/j.enconman.2013.11.009)
- European Commission, 2014. Regulation (EU) No 517/2014 of the European Parliament and of the Council of 16th April 2014 on fluorinated greenhouse gases and repealing Regulation (EC) No 842/2006.
- European Commission, 2008. Development and demonstration of a prototype transcritical CO₂ refrigeration system. Final Report of LIFE Project Number: LIFE05 ENV/DK/000156-CO2REF. – Available at: http://knudsenkoling.itide.dk/files/Final_report-kbm.pdf [accessed 01.12.2016].
- European Environment Agency, 2016. Fluorinated greenhouse gases 2015 - Summary of data reported by companies on the production, import and export of fluorinated greenhouse gases in the European Union. EEA Report No.: 33/2016. – Available at: www.eea.europa.eu/publications/fluorinated-greenhouse-gases [accessed 01.12.2016].
- EY, Arcadia International, Cambridge econometrics, 2014. The economic impact of modern retail on choice and innovation in the EU food sector. EU Report, ISBN: 978-92-79-40324-8. – Available at: <http://ec.europa.eu/competition/publications/KD0214955ENN.pdf> [accessed 01.12.2016].
- F-Chart Software, 2015b. Engineering Equation Solver Manual, Madison (USA) – Available at: http://www.fchart.com/assets/downloads/ees_manual.pdf [accessed 01.12.2016].
- F-Chart Software, 2015a. Engineering Equation Solver (EES), Academic Professional version 9.908 - Available at: <http://www.fchart.com/ees/> [accessed 01.12.2016].
- Fazelpour, F., Morosuk, T., 2014. Exergoeconomic analysis of carbon dioxide transcritical refrigeration machines. *International Journal of Refrigeration* 38, 128-139. DOI: [10.1016/j.ijrefrig.2013.09.016](https://doi.org/10.1016/j.ijrefrig.2013.09.016)

- Fredslund, K., Kriezi, E. E., Madsen, K. B., Birkelund, M., Olsson, R., 2016. CO₂ installations with a multi ejector for supermarkets, case studies from various locations. In: Proceedings of the 12th IIR Gustav Lorentzen Natural Working Fluids Conference, 21-24 August; Edinburgh, UK. ID: 1105.
- Frigo-Consulting LTD, 2015. Carrefour Timisoara: new technology successfully implemented. – Available at < http://www.frigoconsulting.ch/en/news/carrefour_timisoara_ejector.html > [accessed 01.12.2016].
- Frigo-Consulting LTD, 2014. Most southerly CO₂-refrigeration system in Spain now in operation. – Available at < http://www.frigoconsulting.ch/en/news/most_southerl_co2-refrigeration_system_in_spaien.html > [accessed 01.12.2016].
- Fritschi, H., Tillenkamp, F., Löhner, R., Brügger, M., 2016. Efficiency increase in carbon dioxide refrigeration technology with parallel compression. International Journal of Low-Carbon Technologies 0, 1-10. DOI: [10.1093/ijlct/ctw002](https://doi.org/10.1093/ijlct/ctw002)
- Ge, Y. T., Tassou, S. A., 2014. Control optimizations for heat recovery from CO₂ refrigeration systems in supermarket. Energy Conversion and Management 78, 245-252. DOI: [10.1016/j.enconman.2013.10.071](https://doi.org/10.1016/j.enconman.2013.10.071)
- Ge, Y. T., Tassou, S. A., 2011b. Performance evaluation and optimal design of supermarket refrigeration systems with supermarket model “SuperSim”. Part II: Model applications. International Journal of Refrigeration 34(2), 540-549. DOI: [10.1016/j.ijrefrig.2010.11.004](https://doi.org/10.1016/j.ijrefrig.2010.11.004)
- Ge, Y. T., Tassou, S. A., 2011a. Thermodynamic analysis of transcritical CO₂ booster refrigeration systems in supermarket. Energy Conversion and Management 52(4), 1868-1875. DOI: [10.1016/j.enconman.2010.11.015](https://doi.org/10.1016/j.enconman.2010.11.015)
- Ge, Y. T., Tassou, S. A., 2009. Control optimisation of CO₂ cycles for medium temperature retail food refrigeration systems. International Journal of Refrigeration 32(6), 1376-1388. DOI: [10.1016/j.ijrefrig.2009.01.004](https://doi.org/10.1016/j.ijrefrig.2009.01.004)
- Getu, H. M., Bansal, P. K., 2008. Thermodynamic analysis of an R744-R717 cascade refrigeration system. International Journal of Refrigeration 31, 45-54. DOI: [10.1016/j.ijrefrig.2007.06.014](https://doi.org/10.1016/j.ijrefrig.2007.06.014)
- Giroto, S., 2012. CO₂ refrigeration in warm climates, efficiency improvement. In: Proceedings of the ATMOsphere Europe 2012, 5-7 November; Brussels, Belgium.

- Girotto, S., Minetto, S., Neksa, P., 2004. Commercial refrigeration system using CO₂ as the refrigerant. *International Journal of Refrigeration* 27(7), 717-723. DOI: [10.1016/j.ijrefrig.2004.07.004](https://doi.org/10.1016/j.ijrefrig.2004.07.004)
- Gong, S., Goni Boulama, K., 2015. Advanced exergy analysis of an absorption cooling machine: Effects of the difference between the condensation and absorption temperatures. *International Journal of Refrigeration* 59, 224-234. DOI: [10.1016/j.ijrefrig.2015.07.021](https://doi.org/10.1016/j.ijrefrig.2015.07.021)
- Gong, S., Goni Boulama, K., 2014. Parametric study of an absorption refrigeration machine using advanced exergy analysis. *Energy* 76, 453-467. DOI: [10.1016/j.energy.2014.08.038](https://doi.org/10.1016/j.energy.2014.08.038)
- Greenpeace, 2016. HFOs: the new generation of F-gases. Greenpeace Position Paper. – Available at: < <http://www.greenpeace.org/international/en/publications/reports/HFOs/> > [accessed 01.12.2016].
- Gullo, P., Cortella, G., 2016b. Theoretical evaluation of supermarket refrigeration systems using R1234ze(E) as an alternative to high-global warming potential refrigerants. *Science and Technology for the Built Environment* 22(8), 1145-1155. DOI: [10.1080/23744731.2016.1223996](https://doi.org/10.1080/23744731.2016.1223996)
- Gullo, P., Cortella, G., 2016a. Comparative Exergoeconomic Analysis of Various Transcritical R744 Commercial Refrigeration Systems. In: *Proceedings of the 29th International Conference on Efficiency, Cost, Optimisation, Simulation and Environmental Impact of Energy Systems*, 19-23 June; Portorož, Slovenia. ID: 570.
- Gullo, P., Elmegaard, B., Cortella, G., 2016c. Advanced exergy analysis of a R744 booster refrigeration system with parallel compression. *Energy* 107, 562-571. DOI: [10.1016/j.energy.2016.04.043](https://doi.org/10.1016/j.energy.2016.04.043)
- Gullo, P., Cortella, G., Polzot, A., 2016b. Energy and environmental comparison of commercial R744 refrigeration systems operating in warm climates. In: *Proceedings of the 4th IIR Conference on Sustainability and the Cold Chain*, 7-9 April; Auckland, New Zealand.
- Gullo, P., Elmegaard, B., Cortella, G., 2016a. Energy and environmental performance assessment of R744 booster supermarket refrigeration systems operating in warm climates. *International Journal of Refrigeration* 64, 61-79. DOI: [10.1016/j.ijrefrig.2015.12.016](https://doi.org/10.1016/j.ijrefrig.2015.12.016)

- Gullo, P., Elmegaard, B., Cortella, G., 2015. Energetic, Exergetic and Exergoeconomic Analysis of CO₂ Refrigeration Systems Operating in Hot Climates. In: Proceedings of the 28th International Conference on Efficiency, Cost, Optimisation, Simulation and Environmental Impact of Energy Systems, 29 June-3 July; Pau, France. ID: 52577.
- Gungor, A., Erbay, Z., Hepbasli, A., Gunerhan, H., 2013. Splitting the exergy destruction into avoidable and unavoidable parts of a gas engine heat pump (GEHP) for food drying processes based on experimental values. *Energy Conversion and Management* 73, 309-316. DOI: [10.1016/j.enconman.2013.04.033](https://doi.org/10.1016/j.enconman.2013.04.033)
- Hafner, A., Banasiak, K., Fredslund, K., Giroto, S., Smolka, J., 2016. R744 ejector system case: Italian supermarket, Spiazzo. In: Proceedings of the 12th IIR Gustav Lorentzen Natural Working Fluids Conference, 21-24 August; Edinburgh, UK. ID: 1078.
- Hafner, A., Banasiak, K., 2016. Full scale supermarket laboratory R744 ejector supported and AC integrated parallel compression unit. In: Proceedings of the 12th IIR Gustav Lorentzen Natural Working Fluids Conference, 21-24 August; Edinburgh, UK. ID: 1159.
- Hafner, A., 2016. Natural refrigerants, a complete solution – Latest technological advancements for warm climates. In: Proceedings of the ATMOsphere Europe 2016, 19-20 April; Barcelona, Spain.
- Hafner, A., Fredslund, K., Banasiak, K., 2015. Next generation R744 refrigeration technology for supermarkets. In: Proceedings of the 24th IIR International Congress of Refrigeration, 16-22 August; Yokohama, Japan. ID: 768.
- Hafner, A., Hemmingsen, A.K., 2015. R744 refrigeration technologies for supermarkets in warm climates. In: Proceedings of the 24th IIR International Congress of Refrigeration, 16-22 August; Yokohama, Japan. ID: 168.
- Hafner, A., Hemmingsen, A.K., Nekså, P., 2014d. System configuration for supermarkets in warm climates applying R744 refrigeration technologies – Case studies of selected Chinese cities. In: Proceedings of the 11th IIR Gustav Lorentzen Conference on Natural Refrigerants, 31 August-2 September; Hangzhou, China. ID: 67.
- Hafner, A., Shönenberger, J., Banasiak, K., Giroto, S., 2014c. R744 ejector supported parallel vapour compression system. In: Proceedings of the 3rd IIR

- International Conference on Sustainability and Cold Chain, 23-25 June; London, UK. ID: 129.
- Hafner, A., Hemmingsen, A.K., Van de Ven, A., 2014b. R744 refrigeration system configurations for supermarkets in warm climates. In: Proceedings of the 3rd IIR International Conference on Sustainability and Cold Chain, 23-25 June; London, UK. ID: 127.
 - Hafner, A., Försterling, S., Banasiak, K., 2014a. Multi-ejector concept for R-744 supermarket refrigeration. *International Journal of Refrigeration* 43, 1-13. DOI: [10.1016/j.ijrefrig.2013.10.015](https://doi.org/10.1016/j.ijrefrig.2013.10.015)
 - Hafner, A., Poppi, S. Nekså, P., Minetto, S., Eikevik, T.M., 2012. Development of commercial refrigeration systems with heat recovery for supermarket building. In: Proceedings of the 10th IIR Gustav Lorentzen Conference on Natural Refrigerants, 25-27 June; Delft, The Netherlands.
 - Haida, M., Banasiak, K., Smolka, J., Hafner, A., Eikevik, T. M., 2016. Experimental analysis of the R744 vapour compression rack equipped with the multi-ejector expansion work recovery module. *International Journal of Refrigeration* 64, 93-107. DOI: [10.1016/j.ijrefrig.2016.01.017](https://doi.org/10.1016/j.ijrefrig.2016.01.017)
 - IEA, 2013. CO₂ emissions from fuel combustion *Highlights* (2013 Edition). OECD/IEA, Paris, France. – Available at: [<https://www.iea.org/>](https://www.iea.org/) [accessed 01.12.2016].
 - Javerschek, O., Reichle, M., Karbiner, J., 2016. Optimization of parallel compression systems. In: Proceedings of the 12th IIR Gustav Lorentzen Natural Working Fluids Conference, 21-24 August; Edinburgh, UK. ID: 1184.
 - Kaiser, H., Froschle, M., 2010. Latest developments in compressors and refrigeration systems using the refrigerant R744 (CO₂). In: Proceedings of 9th IIR Gustav Lorentzen Conference on Natural Working Fluids, 12-14 April; Sydney, Australia. ID: 28.
 - Karampour, M., Sawalha, S., 2016b. Integration of Heating and Air Conditioning into a CO₂ Trans-Critical Booster System with Parallel Compression. Part II: Performance analysis based on field measurements. In: Proceedings of the 12th IIR Gustav Lorentzen Natural Working Fluids Conference, 21-24 August; Edinburgh, UK. ID: 1050.
 - Karampour, M., Sawalha, S., 2016a. Integration of Heating and Air Conditioning into a CO₂ Trans-Critical Booster System with Parallel Compression. Part I:

- Evaluation of key operating parameter using field measurements. In: Proceedings of the 12th IIR Gustav Lorentzen Natural Working Fluids Conference, 21-24 August; Edinburgh, UK. ID: 1049.
- Karampour, M., Sawalha, S., 2015. Theoretical analysis of CO₂ trans-critical system with parallel compression for heat recovery and air conditioning in supermarkets. In: Proceedings of the 24th IIR International Congress of Refrigeration, 16-22 August; Yokohama, Japan. ID: 530.
 - Kauf, F., 1999. Determination of the optimum high pressure for transcritical CO₂-refrigeration cycles. *International Journal of Thermal Sciences* 38(4), 325-330. DOI: [10.1016/S1290-0729\(99\)80098-2](https://doi.org/10.1016/S1290-0729(99)80098-2)
 - Kim, M.-H., Pettersen, J., Bullard, C. W., 2004. Fundamental process and system design issues in CO₂ vapor compression systems. *Progress in Energy and Combustion Science* 30(2), 119-174. DOI: [10.1016/j.pecs.2003.09.002](https://doi.org/10.1016/j.pecs.2003.09.002)
 - Kornhauser, A. A., 1990. The Use of an Ejector as a Refrigerant Expander. In: Proceedings of the International Refrigeration and Air Conditioning Conference; West Lafayette, USA. ID: 82.
 - Lee, T-S., Liu, C-H., Chen, T-W., 2006. Thermodynamic analysis of optimal condensing temperature of cascade-condenser in CO₂/NH₃ cascade refrigeration systems. *International Journal of Refrigeration* 29, 1100-1108. DOI: [10.1016/j.ijrefrig.2006.03.003](https://doi.org/10.1016/j.ijrefrig.2006.03.003)
 - Liao, S.M., Zhao, T.S., Jakobsen, A., 2000. A correlation of optimal heat rejection pressures in transcritical carbon dioxide cycles. *Applied Thermal Engineering* 20(9), 831-841. DOI: [10.1016/S1359-4311\(99\)00070-8](https://doi.org/10.1016/S1359-4311(99)00070-8)
 - Llopis, R., Nebot-Andrés, L., Cabello, R., Sánchez, D., Catalán-Gil, J., 2016b. Experimental evaluation of a CO₂ transcritical refrigeration plant with dedicated mechanical subcooling. *International Journal of Refrigeration* 69, 361-368. DOI: [10.1016/j.ijrefrig.2016.06.009](https://doi.org/10.1016/j.ijrefrig.2016.06.009)
 - Llopis, R., Sanz-Kock, C., Cabello, R., Sánchez, D., Nebot-Andrés, L., Catalán-Gil, J., 2016a. Effects caused by the internal heat exchanger at the low temperature cycle in a cascade refrigeration plant. *Applied Thermal Engineering* 103, 1077-1086. DOI: [10.1016/j.applthermaleng.2016.04.075](https://doi.org/10.1016/j.applthermaleng.2016.04.075)
 - Llopis, R., Cabello, R., Sánchez, D., Torrella, E., 2015b. Energy improvement of CO₂ transcritical refrigeration cycles using dedicated mechanical subcooling.

- International Journal of Refrigeration 55, 129-141. DOI: [10.1016/j.ijrefrig.2015.03.016](https://doi.org/10.1016/j.ijrefrig.2015.03.016)
- Llopis, R., Sánchez, D., Sanz-Kock, C., Cabello, R., Torrella, E., 2015a. Energy and environmental comparison of two-stage solutions for commercial refrigeration at low temperature: Fluids and systems. Applied Energy 138, 133-142. DOI: [10.1016/j.apenergy.2014.10.069](https://doi.org/10.1016/j.apenergy.2014.10.069)
 - Lorentzen, G., 1995. The use of natural refrigerants: a complete solution to the CFC/HCFC predicament. International Journal of Refrigeration 18(3), 190-197. DOI: [10.1016/0140-7007\(94\)00001-E](https://doi.org/10.1016/0140-7007(94)00001-E)
 - Lorentzen, G., 1994. Revival of carbon dioxide as a refrigerant. International Journal of Refrigeration 17(5), 292-301. DOI: [10.1016/0140-7007\(94\)90059-0](https://doi.org/10.1016/0140-7007(94)90059-0)
 - Lorentzen, G., Pettersen, J., 1993. A new, efficient and environmentally benign system for car air-conditioning. International Journal of Refrigeration 16(1), 4-12. DOI: [10.1016/0140-7007\(93\)90014-Y](https://doi.org/10.1016/0140-7007(93)90014-Y)
 - Lundqvist, P., 2000. Recent refrigeration equipment trends in supermarkets: energy efficiency as leading edge. Bull. Int. Inst. Refrig. LXXX N°2000-5.
 - Matthiesen, O., Madsen, K., Mikhailov, A., 2010. Evolution of CO₂ systems design based on practical experiences from supermarket installations in Northern Europe. In: Proceedings of the 9th IIR Gustav Lorentzen Conference on Natural Working Fluids, 12-14 April; Sydney, Australia. ID: 81.
 - Mazzola, D., Sheehan, J., Bortoluzzi, D., Smitt, G., Orlandi, M., 2016. Supermarket application. Effects of sub-cooling on real R744 based trans-critical plants in warm and hot climate. Data analysis. In: Proceedings of the 12th IIR Gustav Lorentzen Natural Working Fluids Conference, 21-24 August; Edinburgh, UK. ID: 1089.
 - Messineo, A., 2012. R744-R717 Cascade Refrigeration System: Performance Evaluation compared with a HFC Two-Stage System. Energy Procedia 14, 56-65. DOI: [10.1016/j.egypro.2011.12.896](https://doi.org/10.1016/j.egypro.2011.12.896)
 - Minetto, S., Giroto, S., Rossetti, A., Marinetti, S., 2015. Experience with ejector work recovery and auxiliary compressors in CO₂ refrigeration systems. Technological aspects and application perspectives. In: Proceedings of the 6th IIR Ammonia and CO₂ Refrigeration Technologies Conference, 16-18 April; Ohrid, Macedonia.

- Minetto, S., Girotto, S., Salvatore, M., Rossetti, A., Marinetti, S., 2014b. Recent installations of CO₂ supermarket refrigeration system for warm climates: data from field. In: Proceedings of the 3rd IIR International Conference on Sustainability and Cold Chain, 23-25 June; London, UK. ID: 119.
- Minetto, S., Brignoli, R., Zilio, C., Marinetti, S., 2014a. Experimental analysis of a new method of overfeeding multiple evaporators in refrigeration systems. International Journal of Refrigeration 38, 1-9. DOI: [10.1016/j.ijrefrig.2013.09.044](https://doi.org/10.1016/j.ijrefrig.2013.09.044)
- Minetto, S., Cecchinato, L., Corradi, M., Fornasieri, E., Zilio, C., 2005. Theoretical and Experimental Analysis of a CO₂ Refrigerating Cycle with Two-Stage Throttling and Suction of the Flash Vapour by an Auxiliary Compressor. In: Proceedings of IIR International Conferences – Thermophysical Properties and Transfer Processes of Refrigerants, 31 August-2 September; Vicenza, Italy. ID: 37.
- Moran M. J., Shapiro H. N., Boettner D. D., Bailey M. B., 2011. Fundamentals of Engineering Thermodynamics. New York, USA: John Wiley and Sons Publisher.
- Morosuk, T., Tsatsaronis, G., Zhang, C., 2012. Conventional thermodynamic and advanced exergetic analysis of a refrigeration machine using a Voorhees' compression process. Energy Conversion and Management 60, 143-151. DOI: [10.1016/j.enconman.2012.02.021](https://doi.org/10.1016/j.enconman.2012.02.021)
- Morosuk, T., Tsatsaronis, G., 2009. Advanced exergetic evaluation of refrigeration machines using different working fluids. Energy 34(12), 2248-2258. DOI: [10.1016/j.energy.2009.01.006](https://doi.org/10.1016/j.energy.2009.01.006)
- Morosuk, T., Tsatsaronis, G., 2008. A new approach to the exergy analysis of absorption refrigeration machines. Energy 33(6), 890-907. DOI: [10.1016/j.energy.2007.09.012](https://doi.org/10.1016/j.energy.2007.09.012)
- Mosaffa, A. H., Garousi Farshi, L., Infante Ferreira, C. A., Rosen, M. A., 2014. Advanced exergy analysis of an air conditioning system incorporating thermal energy storage. Energy 77, 945-952. DOI: [10.1016/j.energy.2014.10.006](https://doi.org/10.1016/j.energy.2014.10.006)
- Nakagawa, M., Marasigan, A. R., Matsukawa, T., Kurashina, A., 2011. Experimental investigation on the effect of mixing length on the performance of two-phase ejector for CO₂ refrigeration cycle with and without heat exchanger. International Journal of Refrigeration 34(7), 1604-1613. DOI: [10.1016/j.ijrefrig.2010.07.021](https://doi.org/10.1016/j.ijrefrig.2010.07.021)

- Neksa, P., Hafner, A., Bredesen, A. M., Eikevik, T. M., 2016. CO₂ as working fluid - Technological development on the road to sustainable refrigeration. In: Proceedings of the 12th IIR Gustav Lorentzen Natural Working Fluids Conference, 21-24 August; Edinburgh, UK. ID: 1133.
- Neksa, P., Walnum H. T., Hafner, A., 2010. CO₂ – A refrigerant from the past with prospects of being one of the main refrigerants in the future. In: Proceedings of the 9th IIR Gustav Lorentzen Conference on Natural Working Fluids, 12-14 April; Sydney, Australia. ID: 154.
- Neksa, P., Rekstad, H., Zakeri, G., Schiefloe, P. A., 1998. CO₂-heat pump water heater: characteristics, system design and experimental results. International Journal of Refrigeration 21(3), 172-179. DOI: [10.1016/S0140-7007\(98\)00017-6](https://doi.org/10.1016/S0140-7007(98)00017-6)
- Ommen, T., Elmegaard, B., 2012. Numerical model for thermoeconomic diagnosis in commercial transcritical/subcritical booster refrigeration systems. Energy Conversion and Management 60, 161-169. DOI: [10.1016/j.enconman.2011.12.028](https://doi.org/10.1016/j.enconman.2011.12.028)
- Ozaki, Y., Takeuchi, H., Hirata, T., 2004. Regeneration of expansion energy by ejector in CO₂ cycle. In: Proceedings of the 6th IIR Gustav Lorentzen Conference on Natural Working Fluids, 29 August-1 September; Glasgow, UK.
- Palacz, M., Smolka, J., Fic, A., Bulinski, Z., Nowak, A. J., Banasiak, K., Hafner, A., 2015. Application range of the HEM approach for CO₂ expansion inside two-phase ejectors for supermarket refrigeration systems. International Journal of Refrigeration 59, 251-258. DOI: [10.1016/j.ijrefrig.2015.07.006](https://doi.org/10.1016/j.ijrefrig.2015.07.006)
- Pearson, A. B., 2014. CO₂ as a refrigerant. Paris, France: IIF-IIR International Institute of Refrigeration Publisher.
- Peñarrocha, I., Llopis, R., Tarrega, L., Sanchez, D., Cabello, R., 2014. A new approach to optimize the energy efficiency of CO₂ transcritical refrigeration plants. Applied Thermal Engineering 67(1-2), 137-146. DOI: [10.1016/j.applthermaleng.2014.03.004](https://doi.org/10.1016/j.applthermaleng.2014.03.004)
- Persistence market research, 2014. Frozen food market to rise 30% by 2020. – Available at: <http://www.coolingpost.com/world-news/frozen-food-market-to-rise-30-by-2020/> [accessed 01.12.2016].
- Polzot, A., Gullo, P., D'Agaro, P., Cortella, G., 2016c. Performance evaluation of a R744 booster system for supermarket refrigeration, heating and DHW. In:

- Proceedings of the 12th IIR Gustav Lorentzen Natural Working Fluids Conference, 21-24 August; Edinburgh, UK. ID: 1022.
- Polzot, A., D'Agaro, P., Gullo, P., Cortella, G., 2016b. Modelling commercial refrigeration systems coupled with water storage to improve energy efficiency and perform heat recovery. *International Journal of Refrigeration* 69, 313-323. DOI: [10.1016/j.ijrefrig.2016.06.012](https://doi.org/10.1016/j.ijrefrig.2016.06.012)
 - Polzot, A., D'Agaro, P., Cortella, G., Gullo, P., 2016a. Supermarket refrigeration and air conditioning systems integration via a water storage. In: Proceedings of the 4th IIR Conference on Sustainability and the Cold Chain, 7-9 April; Auckland, New Zealand.
 - Purohit, N., Gullo, P., Dasgupta, M. S., 2016. Comparative assessment of low-GWP based refrigerating plants operating in hot climates. In: Proceedings of the International Conference on Recent Advancement in Air Conditioning and Refrigeration, 10-12 November; Bhubaneswar, India. pp. 155-165.
 - Qureshi, B. A., Zubair, S. M., 2013. Mechanical sub-cooling vapor compression systems: Current status and future directions. *International Journal of Refrigeration* 36(8), 2097-2110. DOI: [10.1016/j.ijrefrig.2013.07.026](https://doi.org/10.1016/j.ijrefrig.2013.07.026)
 - Lemmon, E. W., Huber M. L., McLinden M. O., 2013. NIST Reference Fluid Thermodynamic and Transport Properties Database (REFPROP): Version 9.1. Gaithersburg, USA.
 - Reinholdt, L., Madsen, C., 2010. Heat recovery on CO₂ systems in supermarkets. In: Proceedings of the 9th IIR Gustav Lorentzen Conference on Natural Working Fluids, 12-14 April; Sydney, Australia. ID: 143.
 - Remund, J., Lang, R., Kunz, S., 2014. Meteonorm, Meteotest, Bern (Switzerland).
 - Reulens, W., 2009. Natural refrigerant CO₂. ISBN: 9789081346733. – Available at: http://www.khlim-inet.be/media/drupal/NaReCO2_manual_2009.pdf [accessed 01.12.2016].
 - Rezayan, O., Behbahaninia, A., 2011. Thermoeconomic optimization and exergy analysis of CO₂/NH₃ cascade refrigeration systems. *Energy* 36(2), 888-895. DOI: [10.1016/j.energy.2010.12.022](https://doi.org/10.1016/j.energy.2010.12.022)
 - Sánchez, D., Llopis, R., Cabello, R., Catalán-Gil, J., Nebot-Andrés, L., 2017. Conversion of a direct to an indirect commercial (HFC134a/CO₂) cascade refrigeration system: Energy impact analysis. *International Journal of Refrigeration* 73, 183-199. DOI: [10.1016/j.ijrefrig.2016.09.012](https://doi.org/10.1016/j.ijrefrig.2016.09.012)

- Sanz-Kock, C., Llopis, R., Sánchez, D., Cabello, R., Torrella E., 2014. Experimental evaluation of a R134a/CO₂ cascade refrigeration plant. *Applied Thermal Engineering* 73(1), 41-50. DOI: [10.1016/j.applthermaleng.2014.07.041](https://doi.org/10.1016/j.applthermaleng.2014.07.041)
- Sarkar, J., Joshi, D., 2016. Advanced exergy analysis of transcritical CO₂ heat pump system based on experimental data. *Sādhanā* 41(11), 1349-1356. DOI: [10.1007/s12046-016-0555-y](https://doi.org/10.1007/s12046-016-0555-y)
- Sarkar, J., Agrawal, N., 2010. Performance optimization of transcritical CO₂ cycle with parallel compression economization. *International Journal of Thermal Sciences* 49(5), 838-843. DOI: [10.1016/j.ijthermalsci.2009.12.001](https://doi.org/10.1016/j.ijthermalsci.2009.12.001)
- Sawalha, S., Piscopiello, S., Karampour, M., Manickam, L., Rogstam, J., 2017. Field measurements of supermarket refrigeration systems. Part II: Analysis of HFC refrigeration systems and comparison to CO₂ trans-critical. *Applied Thermal Engineering* 111, 170-182. DOI: [10.1016/j.applthermaleng.2016.09.073](https://doi.org/10.1016/j.applthermaleng.2016.09.073)
- Sawalha, S., Karampour, M., Rogstam, J., 2015. Field measurements of supermarket refrigeration systems. Part I: Analysis of CO₂ trans-critical refrigeration systems. *Applied Thermal Engineering* 87, 633-647. DOI: [10.1016/j.applthermaleng.2015.05.052](https://doi.org/10.1016/j.applthermaleng.2015.05.052)
- Sawalha, S., 2013. Investigation of heat recovery in CO₂ trans-critical solution for supermarket refrigeration. *International Journal of Refrigeration* 36(1), 145-156. DOI: [10.1016/j.ijrefrig.2012.10.020](https://doi.org/10.1016/j.ijrefrig.2012.10.020)
- Sawalha, S., 2008b. Theoretical evaluation of trans-critical CO₂ systems in supermarket refrigeration. Part II: System modifications and comparisons of different solutions. *International Journal of Refrigeration* 31(3), 525-534. DOI: [10.1016/j.ijrefrig.2007.05.018](https://doi.org/10.1016/j.ijrefrig.2007.05.018)
- Sawalha, S., 2008a. Theoretical evaluation of trans-critical CO₂ systems in supermarket refrigeration. Part I: Modeling, simulation and optimization of two system solutions. *International Journal of Refrigeration* 31(3), 516-524. DOI: [10.1016/j.ijrefrig.2007.05.017](https://doi.org/10.1016/j.ijrefrig.2007.05.017)
- Schönenberger, J., 2016. Experience with R744 refrigerating systems and implemented multi ejectors and liquid overfeed. In: *Proceedings of the 12th IIR Gustav Lorentzen Natural Working Fluids Conference*, 21-24 August; Edinburgh, UK. ID: 1107.
- Sharma, V., Fricke, B., Bansal, P., Zha, S., 2015. Evaluation of a transcritical CO₂ supermarket refrigeration system for the USA market. In: *Proceedings of the 6th*

- IIR Ammonia and CO₂ Refrigeration Technologies Conference, 16-18 April; Ohrid, Macedonia.
- Sharma, V., Fricke, B., Bansal, P., 2014. Comparative analysis of various CO₂ configurations in supermarket refrigeration systems. *International Journal of Refrigeration* 46, 86-99. DOI: [10.1016/j.ijrefrig.2014.07.001](https://doi.org/10.1016/j.ijrefrig.2014.07.001)
 - Shecco, 2016. F-Gas Regulation shaking up the HVAC&R industry. – Available at: <http://publication.shecco.com/publications/view/131> [accessed 01.12.2016].
 - Shecco, 2014. GUIDE 2014: Natural Refrigerants – Continued Growth & Innovation in Europe. – Available at: <http://publication.shecco.com/publications/view/2014-guide-natural-refrigerants-europe> [accessed 01.12.2016].
 - Shilliday, J. A., 2012. Investigation and optimisation of commercial refrigeration cycles using the natural refrigerant CO₂ [Ph.D. dissertation]. London, UK: Brunel University. – Available at: <http://bura.brunel.ac.uk/handle/2438/7454/> [accessed 01.12.2016].
 - SKM Enviros, 2012. Phase down of HFC consumption in the EU-Assessment of implications for the RAC sector – Available at: <http://www.epeeglobal.org/refrigerants/epee-studies/skm-envirosstudy/> [accessed 01.12.2016].
 - Smolka, J., Palacz, M., Bodys, J., Banasiak, K., Fic, A., Bulinski, Z., Nowak, A. J., Hafner, A., 2016. Performance comparison of fixed- and controllable-geometry ejectors in a CO₂ refrigeration system. *International Journal of Refrigeration* 65, 172-182. DOI: [10.1016/j.ijrefrig.2016.01.025](https://doi.org/10.1016/j.ijrefrig.2016.01.025)
 - Souza, L., Antunes, A., Mendoza, O., Bandarra Filho, E., 2015. Experimental evaluation of a cascade refrigeration system operating with R744/R134a. In: *Proceedings of the 24th IIR International Congress of Refrigeration*, 16-22 August; Yokohama, Japan. ID: 828.
 - Tambovtsev, A., Olsommer, B., Finckh, O., 2011. Integrated heat recovery for CO₂ refrigeration systems. In: *Proceedings of the 23rd IIR International Congress of Refrigeration*, 21-26 August; Prague, Czech Republic. ID: 361.
 - Tassou, S. A., Ge, Y. T., Hadawey, A., Marriott, D., 2011. Energy consumption and conservation in food retailing. *Applied Thermal Engineering* 31 (2-3), 147-156. DOI: [10.1016/j.applthermaleng.2010.08.023](https://doi.org/10.1016/j.applthermaleng.2010.08.023)

- The Australian Institute of Refrigeration, Air Conditioning and Heating, 2012. Methods of calculating Total Equivalent Warming Impact (TEWI) 2012. – Available at: <<http://www.airah.org.au/>> [accessed 01.12.2016].
- Thornton, J. W., Klein, S. A., Mitchell, J. W., 1994. Dedicated mechanical subcooling design strategies for supermarket applications. *International Journal of Refrigeration* 17(8), 508-515. DOI: [10.1016/0140-7007\(94\)90026-4](https://doi.org/10.1016/0140-7007(94)90026-4)
- Tsatsaronis, G., 2010. Minimization of Costs and Environmental Impact Using Exergy-Based Methods. In: *Proceedings of the Future for Sustainable Built Environments with High Performance Energy Systems Conference*; München, Germany.
- Tsatsaronis, G., 2008. Recent developments in exergy analysis and exergoeconomics. *International Journal of Exergy* 5(5/6), 489-499. DOI: [10.1504/IJEX.2008.020822](https://doi.org/10.1504/IJEX.2008.020822)
- Tsatsaronis, G., Moungh-Ho, P., 2002. On avoidable and unavoidable exergy destructions and investment costs in thermal systems. *Energy Conversion and Management* 43(9-12), 1259-1270. DOI: [10.1016/S0196-8904\(02\)00012-2](https://doi.org/10.1016/S0196-8904(02)00012-2)
- Wang, L., Yang, Y., Morosuk, T., Tsatsaronis, G., 2012. Advanced Thermodynamic Analysis and Evaluation of a Supercritical Power Plant. *Energies* 5(6), 1850-1863. DOI: [10.3390/en5061850](https://doi.org/10.3390/en5061850)
- Wiedenmann, E., 2015. Transcritical CO₂-booster with ejector and Liquid-Overfeed. In: *Proceedings of the International HPP Workshop*; Muttenz, Switzerland. – Available at: <http://www.heatpumpcentre.org/en/hptactivities/hppworkshops/Muttenz2015/Documents/08_2643_IEA_Wiedenmann_ewi_v31de_150418.pdf> [accessed 30.06.2016].
- Yang, L., Li, H., Cai, S-W., Shao, L-L., Zhang, C-L., 2015. Minimizing COP from optimal high pressure correlation for transcritical CO₂ cycle. *Applied Thermal Engineering* 89, 656-662. DOI: [10.1016/j.jrefrig.2015.05.016](https://doi.org/10.1016/j.jrefrig.2015.05.016)
- Yilmaz, B., Erdönmez, N., Ozyurt, A., Yilmaz, D., Mançuhan, E., Sevindir, M.K., 2015. Energy and exergy analysis and optimization studies of a CO₂/NH₃ cascade refrigeration system. In: *Proceedings of the 6th IIR Ammonia and CO₂ Refrigeration Technologies Conference*, 16-18 April; Ohrid, Macedonia.

References

- Zhang, M., 2006. Energy Analysis of Various Supermarket Refrigeration Systems. In: Proceedings of the 11th International Refrigeration and Air Conditioning Conference, 17-20 July; West Lafayette, USA. ID: 856.
- Zhang, W-J., Zhang, C-L., 2011. A correlation-free on-line optimal control method of heat rejection pressures in CO₂ transcritical systems. International Journal of Refrigeration 34, 844-850. DOI: [10.1016/j.ijrefrig.2011.01.014](https://doi.org/10.1016/j.ijrefrig.2011.01.014)

APPENDICES

APPENDIX A.1 – CORRELATIONS FOR MULTI-EJECTOR RACK

APPENDIX A.2 - GLOBAL EFFICIENCIES OF COMPRESSORS

APPENDIX A.1 – CORRELATIONS FOR MULTI-EJECTOR RACK

Table A.1.1 – Correlations used for simulating the multi-ejector rack.

<i>Correlations</i>	<i>Value of the coefficients</i>
$\omega = a + b \cdot P_{\text{lift}} + c \cdot P_{\text{lift}}^2 + d \cdot t_{\text{out,GC}} + e \cdot t_{\text{out,GC}}^2$ <p>for $t_{\text{ext}} \leq 17 \text{ }^\circ\text{C}$</p>	a = 0.6610985
	b = -0.2128984
	c = 0.0180093
	d = -0.0048173
	e = 0.0002467
$\omega = a + b \cdot t_{\text{out,GC}} + c \cdot t_{\text{out,GC}}^2 + d \cdot P_{\text{lift}} + e \cdot P_{\text{lift}}^2$ <p>for $17 \text{ }^\circ\text{C} < t_{\text{ext}} \leq 27 \text{ }^\circ\text{C}$</p>	a = 0.9807737
	b = -0.0461714
	c = 0.0015270
	d = -0.1303932
	e = 0.0064457

Appendices

$$\omega = a + b \cdot P_{\text{lift}} + c \cdot t_{\text{out,GC}}$$

for $t_{\text{ext}} > 27 \text{ }^{\circ}\text{C}$

$$a = -0.0147727$$

$$b = -0.0881130$$

$$c = 0.0336677$$

APPENDIX A.2 - GLOBAL EFFICIENCIES OF COMPRESSORS

Table A.2.1 - Global efficiencies of the compressors in subcritical and transition operating conditions.

<i>Configuration</i>	<i>Correlations</i>
	$\eta_{globHS,R744} = -0.1155 \cdot \left(\frac{P_{HP,R744}}{P_{MP,R744}}\right)^2 + 0.5762 \cdot \left(\frac{P_{HP,R744}}{P_{MP,R744}}\right) - 0.0404$
CB and MS+PC	$\eta_{globLS,R744} = -0.0012 \cdot \left(\frac{P_{MP,R744}}{P_{LP,R744}}\right)^2 - 0.0087 \cdot \left(\frac{P_{MP,R744}}{P_{LP,R744}}\right) + 0.6992$
	$\eta_{globAUX,R744} = -0.0507 \cdot \left(\frac{P_{HP,R744}}{P_{IP,R744}}\right)^2 + 0.2073 \cdot \left(\frac{P_{HP,R744}}{P_{IP,R744}}\right) + 0.4635$
R290 Subcooler loop	$\eta_{glob,R290} = -0.0939 \cdot \left(\frac{P_{HP,R290}}{P_{LP,R290}}\right)^2 + 0.4966 \cdot \left(\frac{P_{HP,R290}}{P_{LP,R290}}\right) - 0.0449$
	$\eta_{glob,HS} = -0.0245 \cdot \left(\frac{P_{HP}}{P_{MP}}\right)^2 + 0.1249 \cdot \left(\frac{P_{HP}}{P_{MP}}\right) + 0.5255$
IB	$\eta_{glob,LS} = -0.0114 \cdot \left(\frac{P_{MP}}{P_{LP}}\right)^2 + 0.0439 \cdot \left(\frac{P_{MP}}{P_{LP}}\right) + 0.5376$

PC and PC_VAR

$$\eta_{glob,HS} = -0.0323 \cdot \left(\frac{P_{HP}}{P_{MP}}\right)^2 + 0.1577 \cdot \left(\frac{P_{HP}}{P_{MP}}\right) + 0.4891$$

$$\eta_{glob,AUX} = -0.331 \cdot \left(\frac{P_{HP}}{P_{IP}}\right)^2 + 1.3131 \cdot \left(\frac{P_{HP}}{P_{IP}}\right) - 0.6074$$

$$\eta_{glob,LS} = -0.0114 \cdot \left(\frac{P_{MP}}{P_{LP}}\right)^2 + 0.0439 \cdot \left(\frac{P_{MP}}{P_{LP}}\right) + 0.5376$$

OV and OV+PC

$$\eta_{glob,HS} = -0.1656 \cdot \left(\frac{P_{HP}}{P_{MP}}\right)^2 + 0.764 \cdot \left(\frac{P_{HP}}{P_{MP}}\right) - 0.2108$$

$$\eta_{glob,AUX} = -0.2113 \cdot \left(\frac{P_{HP}}{P_{IP}}\right)^2 + 0.8213 \cdot \left(\frac{P_{HP}}{P_{IP}}\right) - 0.1133$$

$$\eta_{glob,LS} = -0.0114 \cdot \left(\frac{P_{MP}}{P_{LP}}\right)^2 + 0.0439 \cdot \left(\frac{P_{MP}}{P_{LP}}\right) + 0.5376$$

EJ

$$\eta_{glob,HS} = -0.1004 \cdot \left(\frac{P_{HP}}{P_{MP}}\right)^2 + 0.4359 \cdot \left(\frac{P_{HP}}{P_{MP}}\right) + 0.2334$$

$$\eta_{glob,AUX} = -0.3432 \cdot \left(\frac{P_{HP}}{P_{IP}}\right)^2 + 1.3625 \cdot \left(\frac{P_{HP}}{P_{IP}}\right) - 0.6324$$

$$\eta_{global,LS} = -0.0117 \cdot \left(\frac{P_{MP}}{P_{LP}}\right)^2 + 0.0439 \cdot \left(\frac{P_{MP}}{P_{LP}}\right) + 0.5496$$

EJ_OV

$$\eta_{glob,HS} = -0.1004 \cdot \left(\frac{P_{HP}}{P_{MP}}\right)^2 + 0.4359 \cdot \left(\frac{P_{HP}}{P_{MP}}\right) + 0.2334$$

$$\eta_{glob,AUX} = -0.3432 \cdot \left(\frac{P_{HP}}{P_{IP}}\right)^2 + 1.3625 \cdot \left(\frac{P_{HP}}{P_{IP}}\right) - 0.6324$$

$$\eta_{glob,LS} = -0.05 \cdot \left(\frac{P_{MP}}{P_{LP}}\right)^2 + 0.2116 \cdot \left(\frac{P_{MP}}{P_{LP}}\right) + 0.3715$$

Table A.2.2 - Global efficiencies of the compressors in transcritical operating conditions.

<i>Configuration</i>	<i>Correlations</i>
CB and MS+PC	$\eta_{globHS,R744} = -0.0021 \cdot \left(\frac{P_{HP,R744}}{P_{MP,R744}}\right)^2 - 0.0155 \cdot \left(\frac{P_{HP,R744}}{P_{MP,R744}}\right) + 0.7325$
	$\eta_{globLS,R744} = -0.0012 \cdot \left(\frac{P_{MP,R744}}{P_{LP,R744}}\right)^2 - 0.0087 \cdot \left(\frac{P_{MP,R744}}{P_{LP,R744}}\right) + 0.6992$
	$\eta_{globAUX,R744} = -0.0272 \cdot \left(\frac{P_{HP,R744}}{P_{IP,R744}}\right)^2 + 0.2117 \cdot \left(\frac{P_{HP,R744}}{P_{IP,R744}}\right) + 0.2476$
R290 Subcooler loop	$\eta_{glob,R290} = -0.0226 \cdot \left(\frac{P_{HP,R290}}{P_{LP,R290}}\right)^2 + 0.1816 \cdot \left(\frac{P_{HP,R290}}{P_{LP,R290}}\right) + 0.3701$
	$\eta_{glob,HS} = -0.0113 \cdot \left(\frac{P_{HP}}{P_{MP}}\right)^2 + 0.067 \cdot \left(\frac{P_{HP}}{P_{MP}}\right) + 0.557$
IB	$\eta_{glob,LS} = -0.0114 \cdot \left(\frac{P_{MP}}{P_{LP}}\right)^2 + 0.0439 \cdot \left(\frac{P_{MP}}{P_{LP}}\right) + 0.5376$

PC and PC_VAR

$$\eta_{glob,HS} = -0.0156 \cdot \left(\frac{P_{HP}}{P_{MP}}\right)^2 + 0.0847 \cdot \left(\frac{P_{HP}}{P_{MP}}\right) + 0.5407$$

$$\eta_{glob,AUX} = -0.0243 \cdot \left(\frac{P_{HP}}{P_{IP}}\right)^2 + 0.1324 \cdot \left(\frac{P_{HP}}{P_{IP}}\right) + 0.4741$$

$$\eta_{glob,LS} = -0.0114 \cdot \left(\frac{P_{MP}}{P_{LP}}\right)^2 + 0.0439 \cdot \left(\frac{P_{MP}}{P_{LP}}\right) + 0.5376$$

OV and OV+PC

$$\eta_{glob,HS} = -0.0058 \cdot \left(\frac{P_{HP}}{P_{MP}}\right)^2 + 0.0087 \cdot \left(\frac{P_{HP}}{P_{MP}}\right) + 0.6823$$

$$\eta_{glob,AUX} = -0.023 \cdot \left(\frac{P_{HP}}{P_{IP}}\right)^2 + 0.1209 \cdot \left(\frac{P_{HP}}{P_{IP}}\right) + 0.5365$$

$$\eta_{glob,LS} = -0.0114 \cdot \left(\frac{P_{MP}}{P_{LP}}\right)^2 + 0.0439 \cdot \left(\frac{P_{MP}}{P_{LP}}\right) + 0.5376$$

EJ

$$\eta_{glob,HS} = -0.0032 \cdot \left(\frac{P_{HP}}{P_{MP}}\right)^2 + 0.0164 \cdot \left(\frac{P_{HP}}{P_{MP}}\right) + 0.6472$$

$$\eta_{glob,AUX} = -0.0665 \cdot \left(\frac{P_{HP}}{P_{IP}}\right)^2 + 0.3569 \cdot \left(\frac{P_{HP}}{P_{IP}}\right) + 0.2108$$

$$\eta_{glob,LS} = -0.0117 \cdot \left(\frac{P_{MP}}{P_{LP}}\right)^2 + 0.0439 \cdot \left(\frac{P_{MP}}{P_{LP}}\right) + 0.5496$$

EJ_OV

$$\eta_{glob,HS} = -0.0032 \cdot \left(\frac{P_{HP}}{P_{MP}}\right)^2 + 0.0164 \cdot \left(\frac{P_{HP}}{P_{MP}}\right) + 0.6472$$

$$\eta_{glob,AUX} = -0.0665 \cdot \left(\frac{P_{HP}}{P_{IP}}\right)^2 + 0.3569 \cdot \left(\frac{P_{HP}}{P_{IP}}\right) + 0.2108$$

$$\eta_{glob,LS} = -0.05 \cdot \left(\frac{P_{MP}}{P_{LP}}\right)^2 + 0.2116 \cdot \left(\frac{P_{MP}}{P_{LP}}\right) + 0.3715$$

Table A.2.3 – Global efficiencies of the compressors for HFC-based solutions.

<i>Configuration</i>	<i>Correlations</i>
	$\eta_{glob,R134a} = -0.0053 \cdot \left(\frac{p_{HP,R134a}}{p_{MP,R134a}}\right)^2 + 0.0674 \cdot \left(\frac{p_{HP,R134a}}{p_{MP,R134a}}\right) + 0.4802$
CS	$\eta_{glob,R744} = 0.0111 \cdot \left(\frac{p_{MP,R744}}{p_{LP,R744}}\right)^2 - 0.0793 \cdot \left(\frac{p_{MP,R744}}{p_{LP,R744}}\right) + 0.803$
	$\eta_{glob,LTC} = -0.0004 \cdot \left(\frac{p_{HP}}{p_{LP}}\right)^2 - 0.0021 \cdot \left(\frac{p_{HP}}{p_{LP}}\right) + 0.6989$
DXS	$\eta_{glob,MTC} = -0.0075 \cdot \left(\frac{p_{HP}}{p_{MP}}\right)^2 + 0.0652 \cdot \left(\frac{p_{HP}}{p_{MP}}\right) + 0.5609$
AC	$\eta_{glob,R410A} = -0.0293 \cdot \left(\frac{p_{HP}}{p_{LP}}\right)^2 + 0.2008 \cdot \left(\frac{p_{HP}}{p_{LP}}\right) + 0.3549$